BMR JOURNAL of Australian Geology & Geophysics

VOLUME 1, NUMBER 4,

DECEMBER 1976

Department of National Resources, Australia

Minister: The Rt Hon. J. D. Anthony, M.P.

Secretary: J. Scully

Bureau of Mineral Resources, Geology and Geophysics

Director: L. C. Noakes

Editor, BMR Journal: J. F. Truswell

The BMR Journal of Australian Geology and Geophysics is a quarterly journal of research and related activities. Contributions are from officers of the BMR, from BMR officers working in collaboration with others, or requested work sponsored by the BMR. In addition to articles the Journal may include shorter notes and discussion of papers published in it. Discussion of papers is invited from anyone.

Annual subscription to the Journal is at the rate of $10 (Australian). Individual numbers, if available, cost $3. Subscriptions, etc., made payable to the Receiver of Public Moneys in Australian dollars, should be sent to the Director, Bureau of Mineral Resources, Geology & Geophysics, P. O. Box 378, Canberra, A.C.T. 2601, Australia. The Journal can also be obtained from the offices of the Department of National Resources in Sydney and Melbourne.

Other matters concerning the Journal should be sent to the Director, marked for the attention of the Editor, BMR Journal.

B M R JOURNAL

of Australian Geology and Geophysics

Volume 1, Number 4

December 1976

AUSTRALIAN GOVERNMENT PUBLISHING SERVICE
CANBERRA 1976

Cover design:
Contours from part of the 1976 1:5 000 000 Gravity Map of Australia. Illustration prepared in the gravity section of the Geophysical Drawing Office, BMR.

ISSN 0312-9608

Printed by Kerton Bros (S.A.) Pty Ltd, Edwardstown, S.A.

Editorial

The 25th International Geological Congress was held in Australia in August 1976. To coincide with this event the Bureau of Mineral Resources has published three major maps of the Australian continent: a new geological map in four sheets at a scale of 1:2 500 000, a four-sheet map at the same scale showing the available magnetic coverage, and a gravity map of Australia at 1:5 000 000.

To mark the release of the Gravity Map of Australia this issue of the Journal includes two special small-scale gravity maps in colour, and nine papers devoted to Australian gravimetry. These include: a history of gravimetry in Australia—dating back to 1819—a description of the methods used to produce the map, a selected bibliography, and six papers in which gravity observations are used in interpretation of the Earth's structure.

Gravity maps show only the anomalous component. These anomalies are expressed either as a *free-air anomaly*, which allows for the distance of the measurement from the centre of the Earth; or as a *Bouguer anomaly*—which also corrects for the attraction of the masses, relative to sea level, that make up the topography.

It is relevant to ask—what is the significance of these measurements of the variation in gravity? Answers to this lie in geodesy, in geophysics, and also in space physics. Bouguer anomalies reflect upper crustal density changes and so aid in the definition of sedimentary basins and in the search for minerals; while free-air anomalies, because they do not assume any Earth density distributions, are of value in defining the shape of the Earth, and in investigating the strength of the lithosphere, and presence of horizontal density variation in the core and mantle. In space physics some perturbations of the satellites' orbits are caused by the variations in the Earth's gravity field.

Australia becomes the first continent for which the gravity field has been determined completely on a regional scale. Three factors have contributed significantly to this coverage and the production of the resulting maps

1. the very flat topography, which has enabled the land surface to be covered on a systematic basis, and has minimized those errors that rugged terrain imparts to measurements of gravity anomaly.
2. the use of large computers which has enabled the half million measurements to be manipulated and analysed.
3. the willing co-operation of all institutions that have made gravity measurements in Australia to supply data to the National Gravity Repository at BMR. State Mines Departments, tertiary institutions and exploration companies have always assisted not only in providing data, but also in maintaining and controlling standards for observations.

Gravimetry in Australia, 1819-1976

J. C. Dooley and B. C. Barlow

The earliest known gravity measurements in Australia were made by French expeditions in 1819 and 1824, using pendulums at Sydney. Later in the 19th century, further pendulum measurements with an accuracy of about 10 mGal were made at various capital cities by observers from Britain, Bavaria, Austria-Hungary, Russia and Italy.

A very early gravity meter was designed and constructed at Sydney University during the last decade of the century, but was used only experimentally. Reasonably accurate gravity meter surveys started about 1947.

The Cambridge pendulums were used in 1950-51 to establish a national network of 59 stations with an accuracy of about 0.8 mGal; this was supplemented between 1950 and 1959 by gravity meter and pendulum measurements made as part of international surveys, which also helped to relate the Australian datum to the international network. Meanwhile, surveys, mainly for geophysical prospecting, were made by Government authorities, universities, and private companies; some of these surveys covered extensive areas and enabled compilation of a preliminary Bouguer anomaly map in 1959.

Early marine gravity surveys included observations in nearby oceans with Vening Meinesz' submarine pendulums, gravity measurements on offshore islands and reefs, and from 1956, underwater gravity meter surveys on the continental shelf.

Two factors stimulated regional gravity coverage in 1959—firstly the Petroleum Search Subsidy Act, which ensured that exploration data from subsidized surveys were publicly available, and secondly, use of helicopters for reconnaissance gravity coverage of the continent, which was completed in 1973. Gravity data at sea were obtained mainly from reconnaissance marine geophysical surveys carried out under contract to BMR between 1965 and 1973, but include also traverses by international survey vessels and exploration companies.

Gravity meter calibration ranges were established in the main cities in 1960-61. Gravity values at the Cambridge pendulum stations were revised in 1962 using all relevant data, to establish a more accurate control network with standard errors ranging from 0.2 to more than 0.4 mGal for compilation of data from many surveys. These values were superseded by the Isogal Project of 1964-67, which gave values with standard errors of 0.1-0.2 mGal, in which several gravity meters were transported by aircraft along trans-continental east-west traverses. Values at the eastern ends of the traverses, forming part of the Australian Calibration Line (ACL), were established by a US Air Force survey in 1965. The accuracy of the ACL was significantly improved by Soviet pendulum measurements in 1972-74, and joint Soviet-Australian gravity meter measurements in 1973—a precision of about 0.01 mGal being achieved.

Introduction

This paper describes briefly the history of gravimetry in Australia leading up to the production of a coloured gravity map at 1:5 000 000 scale in 1976. For convenience we discuss the history separately for three periods 1819-1949, 1950-1958, and 1959-1976.

The period 1819-1949 is mainly of historical interest. Only a few of the 12 000 gravity observations made during that period were sufficiently accurate to be included in modern compilations. Reports on various gravity observations are scattered throughout the scientific literature of the period; some references have been collated in this paper.

The Australian National Gravity Network (ANGN) was established during 1950-51 using the Cambridge pendulums and was later improved by pendulum and gravity meter measurements. Virtually all gravity surveys since 1950 were tied to that network and used gravity meters capable of accuracies of a few hundredths of a milligal. Data from most of the 50 000 stations observed during 1950-1958 can be included in modern compilations.

In 1959 the Australian Government accelerated the search for oil. A scheme for subsidising the cost of petroleum exploration conducted by private oil exploration companies was introduced, and additional funds were made available so that BMR could speed up its reconnaissance gravity coverage by using helicopter transport. Within a few years new gravity stations were being observed at the rate of 35 000 per year.

More than 500 000 gravity stations have now been observed to complete regional coverage of the continent of Australia (8 500 000 km²) and reconnaissance coverage over the continental margin.

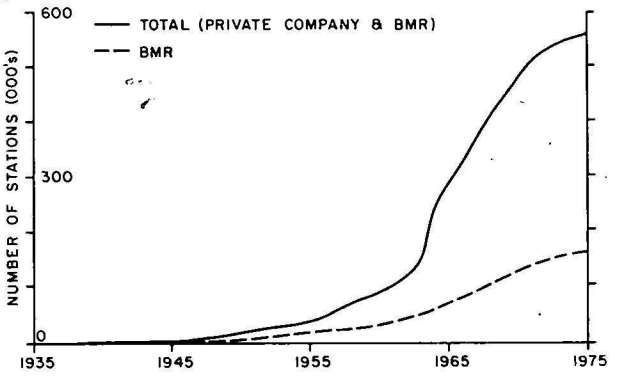

Figure 1. Cumulative totals of gravity stations observed in the Australian region. Annual production increased substantially in 1962 and remained high until 1972.

Figure 1 shows how the total number of observed stations has increased over the years. The improvement in the gravity coverage of Australia is shown progressively in Figure 2. The diagrams show that most of the gravity coverage has been obtained in recent years. That fact, together with the establishment of good control networks and free interchange of gravity data between organisations, has aided the compilation of a computer-based data storage system and the production of gravity maps of Australia.

The precision of the control network has been increased steadily in order to minimize systematic errors, which are of

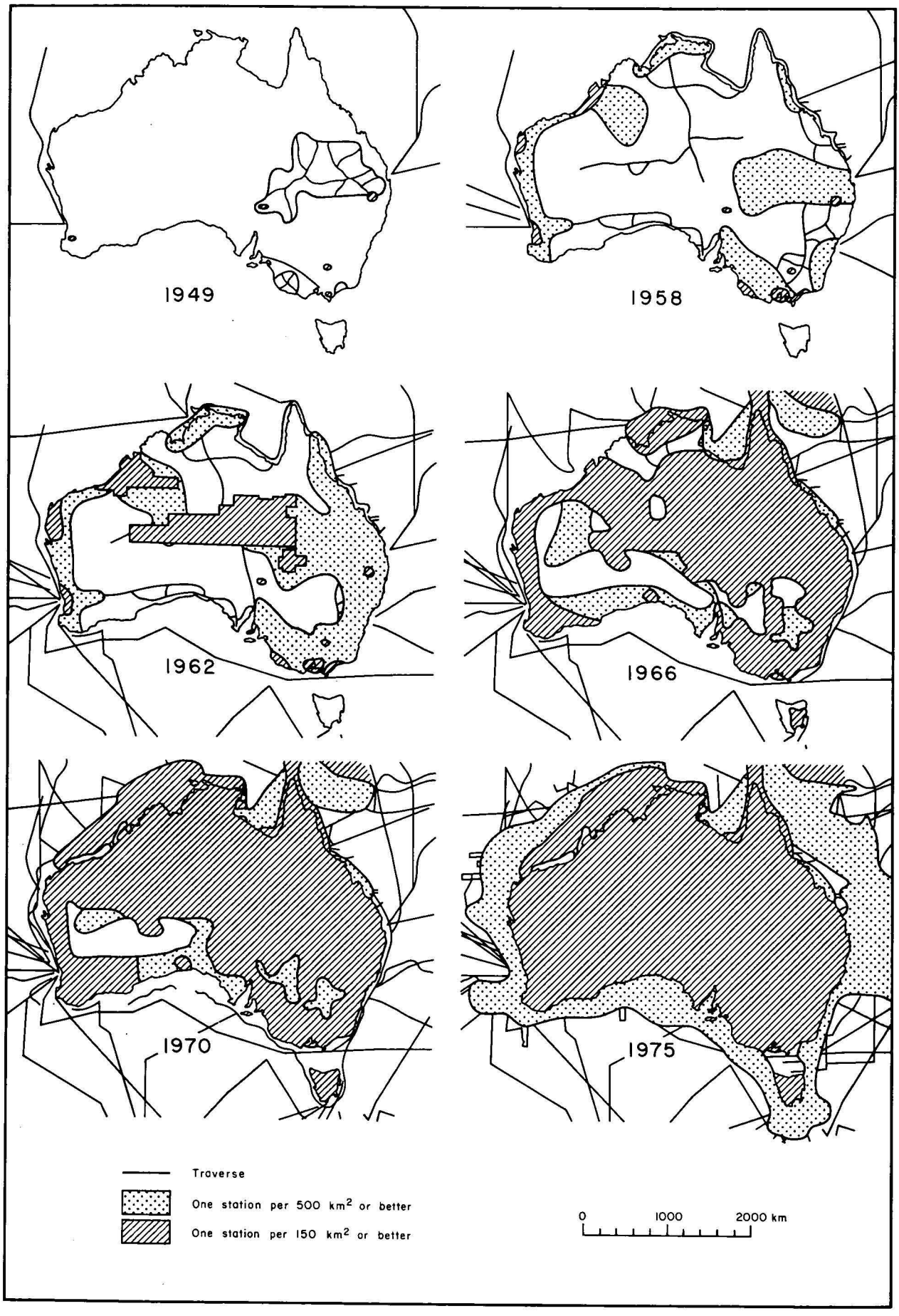

Figure 2. Progress of Australian gravity coverage.

primary importance in the use of gravity data banks for geodetic purposes (Mather *et al.*, 1971) and the production of gravity maps of continental extent. As an illustration of this improvement, Table 1 shows the precision of gravity values for base stations of the Australian Calibration Line (ACL) when corrected for scale (see later).

Table 1: Precision of gravity values at Australia Calibration Line base stations

Source	*Root mean square error (mGal)*
Pre-1940 pendulum observations	10
1950-51 pendulum observations	0.43
1962 network adjustment	0.16
1965-67 Isogal surveys	0.10
1970 ACL survey	0.04
1972-74 Soviet-Australian surveys	c. 0.01

Acknowledgement

The figures for this article were drawn by the gravity drafting group, Geophysical Drawing Office, BMR.

Gravity observations 1819-1949

International gravity ties

The geodetic need for a world-wide set of internally consistent gravity data was recognised by predecessors of the present International Association of Geodesy, but, until 1949, only a few ties had been made to Australia from overseas control stations. Pendulum apparatus was invariably used.

Ackerl (1932) catalogued gravity observations throughout the world for a spherical harmonic analysis; he listed 4165 gravity values, of which only 170 were in the southern hemisphere; and about 80 south of 10°S latitude. These included 10 measurements at Sydney, six at Melbourne, and one at each of Brisbane, Perth and Hobart; i.e. 19 measurements at five stations in the Australian area (Table 2). All the Australian observations in Ackerl's list were extracted from previous lists compiled by Borrass (1911, 1914). Borrass also refers mainly to tables in previous compilations in the same series of reports, but gives some details of the expeditions and equipment.

For the early French measurements at Sydney, invariable one-second pendulums were used. Neumayer was the founder of the Melbourne Observatory and Director from 1858 to 1864, and Baracchi was Director from 1892 to 1915 (Dooley, 1958). Neumayer used a German (Lohmeyer) absolute pendulum with accuracy assessed as ± .021 cm/s² (± 21 mGal). The British measurements of Pritchett (Table 2), and those of Baracchi, were made with invariable one-second Kater pendulums.

Elblein, Guberth, and Budik were officers of the Austro-Hungarian Navy; their measurements were part of a world-wide series of observations, with the base at the Hydrographischen Amtes at Pola (Kesslitz, 1902). Bernacchi's measurements, with a Stuckrath tripendular half-second

Place	*Year*	*Observer*	*Lat. (S)*	*Long. (E)*	*Elev. (m)*	*g*(Gal)*	*Reference*	*Modern value on Potsdam datum (Gal)*	*Correction to earlier value (mGal)*
Sydney City	1819	Freycinet	33°52′	151°13′	33	979.716	Ackerl (1932); Borrass (1911)	979.682	−34
Sydney Fort	1824	Duperrey	33°52′	151°13′	6	9.693	Ackerl (1932); Borrass (1911)	.688	− 5
Sydney Observatory	1882	Pritchett	33°52′	151°12′	43	9.687	Ackerl (1932); Borrass (1911)	.679	− 8
Sydney Observatory	1894	Pritchett	33°52′	151°12′	43	9.687	Ackerl (1932); Borrass (1911)	.679	− 8
Sydney Observatory	1893	Elblein	33°52′	151°12′	43	9.678	Ackerl (1932); Borrass (1911)	.679	+ 1
Sydney Observatory	1894	Guberth	33°52′	151°12′	43	9.698	Ackerl (1932); Borrass (1911)	.679	−19
Sydney Observatory	1896	Budik	33°52′	151°12′	43	9.686	Ackerl (1932); Borrass (1911)	.679	− 7
Sydney Observatory	1897	Budik	33°52′	151°12′	43	9.674	Ackerl (1932); Borrass (1911)	.679	+ 5
Sydney Observatory	1904	Hecker	33°52′	151°12′	43	9.681	Ackerl (1932); Borrass (1911)	.679	− 2
Sydney Observatory	1906	Alessio	33°52′	151°12′	43	9.679	Ackerl (1932); Borrass (1914)	.679	0
Melbourne Observatory	1863	Neumayer	37°50′	144°59′	18	980.032	Borrass (1911)	.988	−44
Melbourne Observatory	1893	Baracchi	37°50′	144°59′	26	979.993	Ackerl (1932); Borrass (1911)	.986	− 7
Melbourne Observatory	1893	Elblein	37°50′	144°59′	26	9.991	Ackerl (1932); Borrass (1911)	.986	− 5
Melbourne Observatory	1894	Guberth	37°50′	144°59′	26	9.997	Ackerl (1932); Borrass (1911)	.986	+11
Melbourne Observatory	1901	Bernacchi	37°50′	144°59′	26	9.971	Ackerl (1932); Borrass (1911)	.986	+15
Melbourne Observatory	1904	Hecker	37°50′	144°59′	26	9.985	Ackerl (1932); Borrass (1911)	.986	+ 1
Melbourne Observatory	1905	Alessio	37°50′	144°59′	26	9.989	Ackerl (1932); Borrass (1914)	.986	− 3
Melbourne Observatory	1912	Wright	37°50′	144°59′	26	9.991	Wright (1921)	.986	− 5
Brisbane Observatory	1896	Budik	27°28′	153°02′	40	979.148	Ackerl (1932); Borrass (1911)	.159	+11
Hobart Observatory	1897	Budik	42°54′	147°22′	58	980.441	Ackerl (1932); Borrass (1911)	980.451	+10
Perth	1905	Alessio	31°57′	115°51′	58	979.378	Ackerl (1932); Borrass (1914)	.384	+ 6
Perth University	1935	Vening Meinesz	31°59′	115°49′	11	9.390	Vening Meinesz (1941)	.393	+ 3
The Lakes Hostel	1935	Vening Meinesz	31°53′	116°19′	278	9.412	Vening Meinesz (1941)	.428	+16
York Town Hall	1935	Vening Meinesz	31°54′	116°46′	177	9.427	Vening Meinesz (1941)	.439	+12
Quairading T.H.	1935	Vening Meinesz	32°01′	117°24′	250	9.424	Vening Meinesz (1941)	.417	− 7
Bruce Rock Road Board	1935	Vening Meinesz	31°53′	118°09′	282	9.391	Vening Meinesz (1941)	.389	− 2
Merredin Court House		Vening Meinesz	31°29′	118°17′	320	9.354	Vening Meinesz (1941)	.344	−10
Northam C'wealth Bank	1935	Vening Meinesz	31°39′	116°40′	151	9.438	Vening Meinesz (1941)	.420	−18
Adelaide Old Observatory	1937	Kerr Grant	138°35′	34°56′	?	9.740	Vening Meinesz (1941)	.722	−18

Table 2: Early gravity observations at Australian stations.

* g given by Ackerl is reduced by 16 mGal to conform with the Potsdam standard (Jeffreys, 1941). g_{obs} listed by Vening Meinesz (Table II, p. 93-94) included the free-air correction; this has been removed to give observed gravity at the station.

apparatus, were made en route to Antarctica with the British National Antarctic Expedition of 1901-1904 (Bernacchi, 1908). Hecker, of the Royal Prussian Geodetic Institute of Potsdam, used a four-pendulum apparatus, with two Fechner pendulums and two Stuckrath pendulums; presumably these were used to establish base stations for his marine measurements (see below). Alessio's measurements were made with a tripendular apparatus of the R. Istitut Idrigrafico a Padova, during a circumnavigation of the world in the Italian ship 'Calabria'.

Jeffreys (1941), in another summary of world-wide gravity data, added an observation at Melbourne by Wright (1921) en route to Antactica; and also the results of Vening Meinesz' submarine cruise in the Indian Ocean in 1935, during which he made observations with the Vening Meinesz pendulums at Fremantle, and with Holweck-Lejay pendulums at Perth and six other stations in Western Australia up to about 250 km inland from Perth (Vening Meinesz, 1941).

Kerr-Grant carried out a series of measurements in and near Adelaide using the Cambridge pendulums in 1937; several stations were occupied, the furthest from Adelaide being at Whyalla.

Holweck-Lejay pendulums were used by Shell (Queensland) Development Pty Ltd in 1940-42 to tie a number of base control stations in southern Queensland.

Observations at Brisbane using the Vening Meinesz pendulums were made during submarine cruises in 1948-49 (see below).

Continental coverage

(a) *Gravity gradiometers.* Prior to about 1940, most gravity field surveys were carried out using gradiometers or Eotvos torsion balances. No attempt has been made to incorporate data from such surveys into modern gravity maps of Australia.

Small surveys were carried out at a number of places by the Imperial Geophysical Experimental Survey, including brown coal investigations at Gelliondale, Victoria, an attempt to trace a buried basement ridge and fault near Lakes Entrance, Victoria, and a deep lead near Gulgong, New South Wales (Broughton-Edge and Laby, 1931). The instruments needed to be set up in an insulated portable hut and only 3-4 gradiometer stations per day could be read; the torsion balance was even slower. It was also necessary to read levels out to a radius of about 60 m around each station for topographic corrections.

Gradiometers were also used by the Aerial Geological and Geophysical Survey of Northern Australia (AGGSNA), for example at Blair Athol coalfield, Queensland (AGGSNA, 1940). BMR carried out one such survey on the Leigh Creek coalfield, South Australia (Thyer & Dooley, 1946), successfully delineating the limits of two coal seams.

(b) *Pendulums.* Very little coverage resulted from pendulum observations such as those made by Vening Meinesz, Kerr-Grant and Shell mentioned above, although the Vening Meinesz measurements revealed the large gravity feature which we now know is due to the sediments of the Perth Basin.

(c) *Gravity meters.* One of the earliest, if not the first, gravity meters in the world was constructed at Sydney University (Threlfall & Pollock, 1900). Although this meter was used for very few observations, its development is historically interesting.

The sensing element consisted of a horizontal fused quartz fibre under torsion, with a gilded brass beam attached perpendicularly at the centre of the fibre. The beam was 53 mm long and had a mass of .018 g; its centre of gravity was displaced a small distance to one side of the thread. The torsion in the fibre could be altered by a lever at one end, the angle of rotation being measured on a graduated scale. The end of the beam was observed by a microscope, and was restored to a null position, near the point of instability a few degrees above horizontal.

Development started in 1888, the year following Boys' discovery of the properties of fused quartz, and field experiments started in 1893; however further modifications were made until 1897. During 1897-1898, observations were made at Springwood and Hornsby near Sydney, and at Armidale, Melbourne, Launceston and Hobart. Total weight was about 100 kg including a resistance box used for a platinum thermometer. An observation took about four minutes, but had to be made at daily maximum or minimum temperature for best results. An accuracy of a few milligals was claimed.

In 1898 Threlfall returned to England, and the gravity meter was not used again until 1923, when it was sent to England for further tests (Threlfall & Dawson, 1933).

The next known use of gravity meters was a survey in the Roma area by the German company Elbof about 1928. Shell (Queensland) Development Pty Ltd carried out extensive surveys in southern Queensland from about 1940-42 using Thyssen gravity meters with Holweck-Lejay pendulums for base control. Subsequent checks show that the accuracy of this survey was probably several milligals.

The Bureau of Mineral Resources (BMR) used a gravity meter (Humble-Truman) for the first time in 1946-47 in the Collie Coal Basin, Western Australia (Chamberlain, 1948). This was a cumbersome instrument, awkward to read because of post-release beam drift—readings had to be made at exactly sixteen seconds after release—and had an accuracy of about 0.2 mGal. The acquisition of a Heiland gravity meter in 1947 permitted more accurate gravity surveying; this was first used for the oil and gas search in the Frome Embayment area north of Broken Hill (Dooley, 1948), in a cooperative venture with Zinc Corporation and Vacuum Oil Co.; the latter used Carter gravity meters. A Western meter of similar construction was used in the Roma area in 1948-49 (Dooley, 1950).

Marine coverage

The first known gravity measurements at sea in the vicinity of Australia were those of Hecker about 1904 (Heiskanen, 1936; Daly, 1940), who used an apparatus in which a column of mercury was balanced against the pressure of an enclosed mass of air at constant temperature; the absolute atmospheric pressure was found from the boiling point of water. This method could be used on a surface ship with a claimed accuracy of about 30 mGal. Hecker discovered anomalies of the right sign over the Tonga Trench and Ridge, but with errors of 50 to 100 mGal by comparison with later work (Talwani *et al.*, 1961). An average positive free-air anomaly of over 200 mGal (Daly, *loc. cit.*, p. 253) between Sydney and Auckland is not confirmed by later work.

Vening Meinesz (1941) made measurements in the Indian Ocean off Western Australia as part of his gravity submarine pendulum cruise in 1935. Later surveys using Vening Meinesz pendulums were carried out by the United States submarines *Capitaine* in 1948 and *Bergall* in 1948-49 along traverses from Brisbane crossing the Coral Sea through New Guinea, Solomon Islands, New Hebrides and New Caledonia (Worzel, 1965).

Gravity observations 1950-1958

The first National Report presented to the International Gravity Commission (Dooley, 1959) summarizes work during this period.

International gravity ties

(a) *Pendulums.* The Cambridge pendulums were used to tie Melbourne to Cambridge in 1950-51 during establishment of the Australian control network A (see below). Sydney was tied to New York during a survey using the Vening Meinesz pendulums on board the submarine HM *Telemachus* (see below). Observers from G. P. Woollard's group at the University of Wisconsin, working under the auspices of the Woods Hole Oceanographic Institute (WHOI), made observations using the Gulf Oil. Co. pendulums. Ties from Madison, USA were made to Melbourne and a few other stations by Rose in 1957 and to Sydney by Iverson in 1958 (Woollard & Rose, 1963).

(b) *Gravity meters.* From 1950 onwards, geodetic gravity meters were used to establish or re-occupy base stations in Australia to strengthen the international network (Woollard & Rose, 1963). In 1950 Muckenfuss observed more than 100 stations throughout Australia and tied them to Washington using a geodetic Worden gravity meter (Woollard & Rose, 1963). Observers from WHOI made further ties from USA to Melbourne and a few other stations using Worden meters—Bonini in 1954, Rose in 1957 and Laudon in 1958. A geodetic La Coste & Romberg was used by Sparkman for a tie to Melbourne in 1958 en route to Antarctica. Expeditions Polaires Francaises made ties from Paris to Melbourne in 1952-53 and 1955-56 using Western meters en route to Antarctica (Stahl, 1954).

National control network

The pendulum stations established before 1950 provided a very poor control network because of uncertainties arising from datum inconsistencies at the overseas base stations and inaccuracies in the ties to Australia.

However in 1950 a National Gravity Base Station (NGBS) was established at BMR's laboratories at Footscray near Melbourne, and was the only Australian gravity station to be included in the First Order World Gravity Net (FOWGN). Observations were made at NGBS and at 58 other stations throughout Australia (Dooley *et al.*, 1960). The average accuracy of the measurements was estimated at ± 0.6 mGal, though comparisons with later work give a figure of ± 0.8 mGal. Mu-metal shielding was used to reduce the effects of the earth's magnetic field on the invar pendulums during the 1950-51 measurements. The question of what magnetic corrections, if any, should be applied to the results has never been resolved satisfactorily. The 59 Cambridge pendulum stations were designated the Australian National Gravity Network (ANGN). Most are still re-occupiable and are key stations in the present ANGN.

Continental coverage

From 1950 onwards gravity meter surveys were carried out by exploration companies, State Mines Departments, Universities, and BMR, at an increased rate. Some of these surveys covered extensive areas using vehicular transport. Examples were that in 1951-52 by Sydney University (Marshall & Narain, 1954) along more than 15 000 km of main roads in the eastern part of Australia, and those by BMR in East Gippsland in 1951 (Dooley & Mulder, 1953), the Perth Basin in 1951-52 (Thyer & Everingham, 1956), the Carnarvon Basin in 1950-53 (Chamberlain *et al.*, 1954), the Canning Basin in 1952-54 (Flavelle & Goodspeed, 1962), north-east Queensland in 1954 (Dooley, 1965a), and Western Victoria (unpublished data). A Norgaard gravity meter was used for part of the Perth Basin survey; as it depends on measuring an angle of tilt, it should not need any scale factor calibration; however high drift rates and temperature effects outweighed any advantage from this feature.

Helicopter transport was used experimentally in the Great Sandy Desert in 1957, and demonstrated its capacity for increasing the productivity of gravity surveys in areas with difficult access.

Marine coverage

The first BMR approach to a marine gravity survey was an 'island hopping' survey in the Great Barrier Reef in 1954; readings were taken with an Atlas gravity meter wherever it was possible to land on islands and reefs (Dooley, 1965a). This was undertaken partly in response to a request from the Great Barrier Reef Commission, and partly in relation to a projected visit to Australia of Vening Meinesz. The visit did not eventuate because Vening Meinesz fell off his bicycle and broke his leg, but the survey nevertheless went ahead!

In 1956, a joint survey was undertaken by Lamont Geological Observatory, BMR and the Royal Navy in the British submarine HM *Telemachus*, from Sydney across the Tasman Sea to Wellington, then zig-zagging northwards across the Kermadec and Tonga Trenches, and returning to Sydney via Fiji, Norfolk Island and Lord Howe Island (Dooley, 1963).

With the acquisition of a North American underwater gravity meter in 1957, surveys were conducted in the continental shelf areas—initially in Port Phillip Bay, Victoria (Gunson & Williams, 1965), and later in a long cruise around the north coast of Australia, covering areas from Wyndham, Western Australia, through Darwin, the Gulf of Carpentaria, Gulf of Papua, and the Great Barrier Reef as far south as Hervey Bay near Bundaberg.

In 1957 BMR invited oil companies, State Government Departments, universities and other institutions that had carried out gravity work in Australia, to contribute data on a regional basis for incorporation in a gravity data bank for the production of a gravity map of Australia. All of the organizations responded favourably and many went to considerable trouble to prepare their data in a suitable form. Compilation of the data and manual computation of mean anomalies prior to the advent of computers was a laborious task, but the map was completed and released in 1959 (see gravity observations 1959-1976, and Fig. 3).

Gravity maps of Australia

The earliest gravity map covering a substantial part of the Australian continent was made by Marshall and Narain (1954). Their map was based on gravity and barometric observations at about 10-mile intervals along some of the main roads in the eastern half of Australia (see Fig. 4). In spite of the wide spacing — sometimes hundreds of miles—between traverses, they were able to detect many of the principal features of the current gravity map; such as the negative anomalies north and south of Alice Springs, low values over granite batholiths, positive anomalies at Broken Hill and Mount Isa (which were hopefully joined together by the contour lines), and a correlation with structural high and low features in eastern Queensland.

Nearly all gravity data observed during the period 1950-58 were immediately computed to the datum and scale of the ANGN and the elevations of most stations were known relative to mean sea level.

Gravity observations 1959-1976

Gravity work during this period is summarized in the National Reports presented to the International Gravity

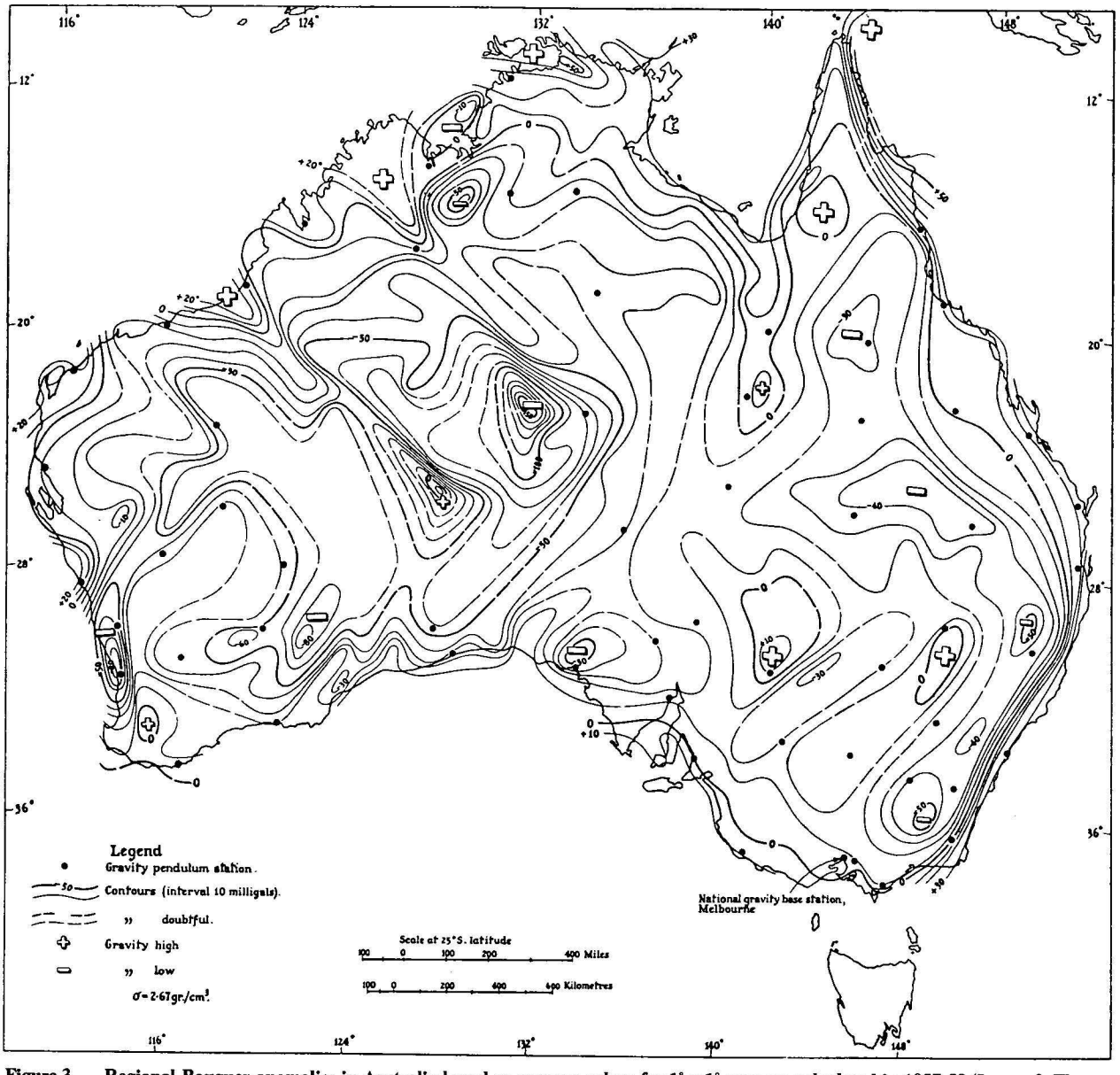

Figure 3. Regional Bouguer anomalies in Australia based on average values for 1° x 1° areas as calculated in 1957-59 (Jaeger & Thyer, 1960, Fig. 1).

Commission (Dooley, 1965b; Langron, 1966; Barlow, 1970; Wellman, 1974).

The first and, to date, only absolute determination of the acceleration due to gravity in Australia was made by Bell *et al.* (1973) at the National Standards Laboratory (NSL), Sydney. The experiment was of the rise and fall type, in which measurements were made of the vertical motion of a cube corner reflector in vacuo (Gibbings *et al.*, 1971). The result is compatible with the latest international ties within experimental error (0.14 mGal).

International gravity ties

(a) *Pendulums.* Inoue of the Geographical Survey Institute (GSI) of Japan tied Kyoto to Melbourne in 1959 (Inoue & Seto, 1961) using the GSI pendulums, and Jackson repeated the tie Cambridge to Melbourne using the Cambridge pendulums in the same year. In 1960-61, Strickholm of the University of Wisconsin repeated the tie Madison to Melbourne using the Gulf pendulums en route to and from Antarctica (Woollard & Rose, 1963). BMR took delivery of a set of GSI pendulums in 1962 and tied Tokyo to Melbourne (Langron, 1966). Cambridge University made pendulum observations at Melbourne in 1967 as part of measurements on the Western Pacific Calibration Line (Browne & Honkasalo, 1969) but the direct tie Teddington-Melbourne was weakened when repeat measurements at Melbourne had to be abandoned because of illness of the observer. GSI tied Tokyo to Sydney and Canberra in 1967, the BMR set of pendulums being used side-by-side with the GSI set in Sydney and Canberra. During 1970 GSI tied Tokyo to Brisbane.

The most accurate pendulum ties to Australia were made in 1972 and 1974 by the Soviet Geophysical Committee of the Academy of Sciences, USSR in co-operation with BMR (Gusev, 1973; Boulanger *et al.*, 1973; Wellman *et al.*, 1974; Gusev, 1975), and USSR Central Research Institute of Geodesy, Aerial Survey and Cartography (TsNIIGAiK), using a set of five Russian OVM pendulums from the base station at Ledovo (Moscow), which is accurately tied to Potsdam. In 1972 a tie was made to Sydney, and in 1974 ties were made to Port Moresby in Papua New Guinea, and Hobart. The results are in excellent agreement with other independent measurements.

(b) *Gravity meters.* In 1959, three Wordens were used to make measurements of the small gravity intervals between Melbourne-Auckland, Cairns-Johannesburg and Sydney-Hakone (Williams *et al.*, 1961).

Singly run ties each using a La Coste & Romberg gravity meter resulted from the cruise of the Scripps Institution vessel *Argo* in 1961, flights by the US Navy Hydrographic Office as part of Project Magnet, and flights by members of the University of Wisconsin during 1962. Similar ties were made by the United States Army Map Service, Far East, in 1964.

Very strong international ties were achieved by the United States Air Force in 1965-66 using four La Coste gravity meters in a series of measurements designed to strengthen the whole world network. Observations were made along the east coast of Australia in 1965 as part of a double run on the Western Pacific Calibration Line (WPCL) (Whalen, 1966; Shirley, 1966) and across southern Australia in 1966 as part of a run around the world.

The Dominion Observatory of Canada used two La Costes to make measurements on the WPCL and in Australia in 1966. The Australian Antarctic Division also used two La Costes to make a tie to Christchurch and the Antarctic in 1966.

In 1969 BMR made a double run using four La Costes along the WPCL, the northern part of the North American Calibration Line and the Japanese Calibration Line.

National Control Network

(a) *1962 network adjustment.* Results from international ties and Australian surveys were used in a readjustment of values at 52 of the Cambridge pendulum stations in 1962 (Dooley, 1965c). The standard error was estimated at ± 0.1 mGal for 14 stations, ± 0.2 mGal for 12, ± 0.3 for 16, and higher for the remaining 16 stations. Comparison with more accurate recent work suggests that these figures should have been increased to about ± 0.2, ± 0.3 and ± 0.4 mGal respectively.

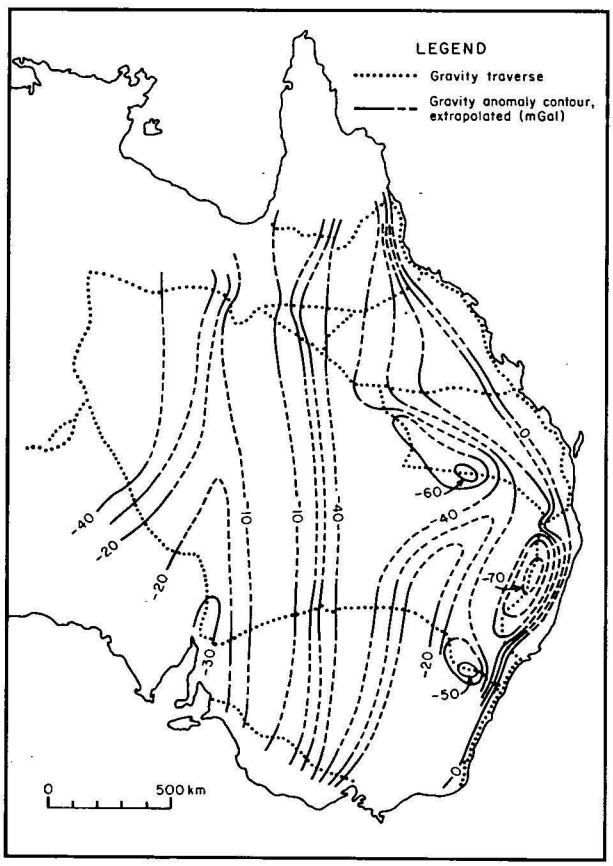

Figure 4. Bouguer anomalies in eastern Australia based on regional gravity traversing in 1951-52 (after Marshall & Narain, 1954, Fig. 20).

The adjustment was helped considerably by the establishment of local calibration ranges at the capital cities and other main towns in 1960-61 (Barlow, 1967). These facilitated adjusting gravity meter calibration factors to a common scale.

(b) *May 1965 Isogal values.* In order to establish a more accurate and denser ANGN, a series of surveys known collectively as the 'Isogal Project' was carried out in 1964-67 (Barlow, 1970). The principle was to establish gravity base stations at airfields along traverses roughly east-west across Australia, each traverse approximately following an 'isogal' of observed gravity values, thus minimising gravity difference between stations on the same traverse and the calibration problem. At least three dissimilar meters (La Coste & Romberg, Worden, World-Wide, Sharpe) were used to measure gravity intervals between successive base stations, and between each base and its excentres. Drift control was of the conventional ABAB (AB. . . .) type for all measurements, obtained between bases by repeated direct flights using a chartered aircraft over distances which were generally 150-250 km.

Each of the east-west traverses has as its observed gravity datum a station of the north-south Australian Calibration Line (ACL), which generally follows the east coast of Australia. The 1962 adjustment of the ANGN (see above) had given small standard errors for stations of the ACL, which had been observed during several international and Australian control surveys; more precise interval values became available in 1965 from the United States Air Force/BMR control survey, which used five La Costes along the ACL (Whalen, 1966; Shirley, 1966).

The 1962 value of 979 979.0 mGal for the National Gravity Base Station (NGBS), Melbourne, was retained as the Australian datum in the Potsdam system.

To determine scale a 'mean Australian milligal' was defined as the average given by the two intervals Melbourne-Cairns and Melbourne-Darwin as calculated from the 1962 values.

From this, a scale correction factor of 0.997 was determined and applied to the 1965 USAF/BMR gravity intervals which had been calculated using the manufacturer's calibration tables. The corrected intervals were used to determine values at base stations on the ACL, which were used as datum values for the east-west traverses.

Except for determination of datum and scale as outlined above all measurements prior to 1964 were disregarded in fixing 'May 1965 Isogal values' for the ANGN. The comparatively weak results obtained on north-south lines along the west coast and through the centre of Australia during the Isogal project were also disregarded at this stage.

A standard error of 0.1 milligal was estimated in the gravity value at a station relative to its east-west traverse, and a standard error of 0.2 milligal in the value relative to the network as a whole.

Fifty-seven of the 59 Cambridge pendulum stations were reoccupied as Isogal stations, and the new observed gravity values show that the 'mean Australian milligal' is consistent with that defined by the Cambridge pendulum results computed *without* magnetic corrections. Recent work has shown that the 'mean Australian milligal' is too small by 5 parts in 10^4, but that the Australian datum at NGBS, Melbourne was correct on the Potsdam datum (Wellman *et al.*, 1974).

(c) *Absolute values—IGSN71.* During the last few decades it became clear that values of observed gravity

based on the Potsdam datum are about 14 mGal greater than the true (or absolute) values which are needed for purposes such as force standards. Use of the 1930 normal gravity formula in calculating gravity anomalies more or less compensates for that error, but leaves an error in the anomalies which ranges from +3.2 mGal at the equator through 0 mGal at 29° latitude to −10.4 mGal at the poles, and is due to an error in the flattening coefficient in the 1930 ellipsoid.

In 1971 the International Union of Geodesy and Geophysics adopted a new international gravity reference system, the International Gravity Standardization Net 1971 (IGSN71). The IGSN71 datum and scale is defined by the gravity values for 1854 stations (including 18 stations in Australia) obtained from a single least squares adjustment of reliable absolute, pendulum and gravimeter data (Morelli *et al.*, 1974). The IGSN71 correction *at Potsdam* is −14.0 mGal. It should be noted that a new normal gravity formula, the Geodetic Reference System 1967 (GRS67), must be used when calculating gravity anomalies from observed gravity values based on IGSN71.

In 1973 the IGSN71 station 45331 A in Sydney was adopted as the new National Gravity Base Station for Australia together with its IGSN71 values (Boulanger *et al.*, 1973).

Boulanger *et al.* (1973) also adopted a new gravity scale for Australia, which was determined from Soviet GAG2 gravity meter measurements in 1973 (Wellman *et al.*, 1974). The new scale was confirmed by OVM pendulum observations in 1974 (Gusev, 1975).

Except for the Sydney value, IGSN71 values at stations along the ACL and elsewhere in Australia were not adopted by Australia because the scale determined by the IGSN71 along the ACL is in error by 15 parts in 10^5, as shown by the more accurate results obtained during 1973-74.

Values of observed gravity relative to May 1965 Isogal datum values can be adjusted to the 1973 datum and scale by the provisional formula:

$$g_{1973} = 979\,671.86 + 1.000\,511\,8(g_{1965} - 979\,685.74)$$

to give values with an estimated standard error of less than 0.2 mGal throughout Australia.

The correction in observed gravity ranges from about −15.0 mGal in PNG through −13.95 mGal at Sydney to about −13.5 mGal in Tasmania.

It should be noted that gravity anomalies based on 1973 values of observed gravity, and normal gravity values given by GRS67, differ from anomalies based on May 1965 observed gravity values, and the 1930 normal gravity formula, by an amount which ranges from about +2.5 mGal in PNG through 0 mGal at about latitude 28°S to about −2.6 mGal in Tasmania.

Continental coverage

The search for oil in Australia was accelerated from 1959 and resulted in a greatly increased rate of gravity coverage of the continent.

By far the largest single contribution to regional coverage of the continent was made by the BMR's reconnaissance gravity surveys using helicopter transport, which gave a minimum station density of 1 station per 130 km² over all parts of the continent not covered by other surveys. The techniques used were developed during 1959-62 and are described by Vale (1962) and by Hastie & Walker (1962). Since 1963 the surveys have been carried out by geophysical firms under contract to BMR. The accuracy of anomalies is limited by the necessary use of barometric levelling of the gravity stations, but third order control traverses and a special 'cell pattern' of helicopter flights ensures an RMS error of better than 5 m in the station elevations, and 1 mGal in the station anomalies. Apart from a number of very small gaps reconnaissance coverage of the whole continent was completed in 1975 (Fraser *et al.*, 1976).

A large contribution to the gravity coverage has been made by private exploration companies, mostly operating under the Petroleum Search Subsidy Acts, under which approved oil-search geophysical surveys were subsidised by the Australian Government. Some companies (and institutions) used helicopters to obtain reconnaissance coverage. In other areas where there was little or no existing gravity information ground transport was used, frequently in conjunction with seismic surveys.

Important contributions were also made by State Mines Departments. Notably those of South Australia (e.g. Kerr-Grant, 1951; Hall & Townsend, 1969) and New South Wales (e.g. McIntyre. 1972), and by Universities, notably that of Tasmania. About half of South Australia was surveyed by the SA Mines Department, who co-operated with BMR in the completion of the coverage of that state at a station density of at least 1 station per 42 km².

Regional road traverses, semi-detailed and detailed surveys by various organisations, have all contributed to the total coverage.

Marine coverage

Contract marine gravity surveys carried out for BMR have provided nearly all of the reconnaissance gravity coverage on the Australian continental margin, although contributions have been made in some areas by surveys conducted by exploration companies and overseas institutions (e.g. Gulf Oil Syndicate, 1964).

The continental shelf off north-west Australia was covered at a line spacing of 16 km during 1965-68. Various surface-ship gravity meters and navigational equipment were used. On these surveys surface gravity measurements were made along with continuous seismic and magnetic profiling at a compromise ship's speed of about 9 knots. Smith (1966), Jones (1969), and Whitworth (1969) describe the 1965, 1967 and 1968 surveys respectively.

Most of the continental shelf and slope was covered during 1970-73 by a surface marine geophysical survey by Compagnie Generale de Geophysique (1975) under contract to BMR. The objectives of that survey were to determine the extent of the Australian continental margin and to obtain regional information on the geological structure (Symonds & Willcox, 1976). A total of 186 000 km was traversed in the offshore areas of Australia and Papua New Guinea in waters between 50 m and 5000 m deep, at a line spacing which ranges from 37 km off the east coast of Australia to 56 km off the west coast. Preliminary hourly values, which are spaced at intervals of about 15 km along the traverses, are available at this time. Final values are being computed.

Surface marine gravity surveys were completed by Geophysical Service International for Wapet in their search for oil in the offshore Perth, Carnarvon and Canning Basins. A sea-bottom gravity survey was carried out in the Shark Bay (central West Coast) area by Layton Geophysical Associates for Oceania. The only other example of a sea-bottom gravity survey during the period 1959-76 was a novel survey of St Vincents Gulf, South Australia, by Beach Petroleum N.L. (Sprigg & Stackler, 1965). A diving bell containing a normal land gravity meter and an observer was lowered to the sea bottom in depths as great as 50 m.

The US Navy observed gravity along a number of traverses in the Gulf of Carpentaria and other waters north of Australia using USNS *Shoup* in 1963-64.

Lamont-Doherty Geological Observatory (LGO) of Columbia University read gravity traverses in the Coral Sea between the Australian mainland and TPNG. Observations

were made on the research vessels *Conrad* in 1964 and *Vema* in 1962. LGO also read regional gravity traverses to the south of Australia on USNS *Eltanin* in 1969. The University of NSW participated with LGO in the gravity work in both these areas.

Hawaii Institute of Geophysics made surface gravity meter observations along traverses to the north of TPNG and in waters around the Bismarck Archipelago in the Royal Navy vessel HMS *Dampier* during 1965. The US Coast & Geodetic Survey read a gravity traverse down the west coast of Australia, across the Great Australian Bight, along the south-east coast of Australia, and across the Tasman Sea in the vessel USCGSS *Oceanographer* during 1967; Australian observers participated in this cruise.

The Soviet Geophysical Committee of the Academy of Sciences of the USSR made gravity observations east of Australia during 1970-71 in the *Vitiaz*. Isolated traverses have also been run by the Japanese research vessel *Umitaka-maru* in 1963-65.

An index covering all known marine geophysical work in the offshore Australia area up until 1970 has been compiled by Riesz & Moss (1971).

Gravity maps of Australia

A gravity map was compiled from all available data in 1959 (Dooley, 1959). All Bouguer anomalies in each $1° \times 1°$ square were averaged; averages were obtained for about 470 squares out of a total of about 830 land and coastal squares; for some of these squares the only gravity observation available was the Cambridge pendulum measurement. Some marine data were included from underwater gravity meter surveys. The map was presented with the average value written in each square, and also in contoured form; the latter version was later published in a review paper by Jaeger and Thyer (1960) and is reproduced here as Fig. 3.

In 1965 a preliminary Bouguer anomaly map was produced. All major surveys in Australia were approximately adjusted to a common datum, but no attempt was made to recompute individual surveys to a common Bouguer density (discontinuities, mostly minor but up to 7 mGal, occur at survey boundaries). The map was presented on the same scale (40 miles to 1 inch) and projection as the 1960 Tectonic Map of Australia. Successive editions were issued as further areas were covered. (Vale, 1965; Darby & Vale, 1969). The contour interval is 5 mGal where sufficient data are available.

Two coloured maps, showing gravity data of Australia and its surroundings available to 1966, were published at a scale of 1:5 000 000 by the Ministry of Geology of USSR (1971); one map shows Bouguer anomalies on land and at sea, and the other shows Bouguer anomalies on land and free-air anomalies at sea.

In 1976, BMR published a coloured map at a scale of 1:5 000 000 showing Bouguer anomalies (calculated for a Bouguer density of 2.67) on land and free-air anomalies at sea. A mean free-air contour map at a scale of 1:2 500 000 was also prepared. Reductions of both maps are included in this issue and production of the 1:5 000 000 map is discussed by Anfiloff *et al.*(1976). Data for the preparation of these maps was compiled from the Australian National Gravity Repository (Murray, 1974).

References

ACKERL, F., 1932—Die Schwerkraft am Geoid, Abschnitt I. Verzeichnis der relativen Messungen der Schwerkraft mit Pendelapparaten bis Ende Juli 1931. *Akademie der Wissenschaften in Wien, Mathematische-naturwissenschaftliche Klasse.* Sitzungsberichte, Abteilung IIa.

AGGSNA, 1940—Geophysical survey at Blair Athol coal-field, Queensland. *Aerial Geological and Geophysical Survey of Northern Australia Report* (1939), 48-54.

ANFILOFF, W., BARLOW, B. C., MURRAY, A. S., DENHAM, D., & SANDFORD, R., 1976—Compilation and production of the 1976 Gravity Map of Australia. *BMR Journal of Australian Geology & Geophysics, 1,* 273-276.

BARLOW, B. C., 1967—Gravity meter calibration ranges in Australia. *Bureau of Mineral Resources, Australia—Report* **122.**

BARLOW, B. C., 1970—National report on gravity in Australia, July 1965 to June 1970. *Bureau of Mineral Resources, Australia—Record* **1970/62.**

BELL, G. A., GIBBINGS, D. L. H., & PATTERSON, J. B., 1973—An absolute determination of the gravitational acceleration at Sydney, Australia. *Metrologia,* **9,** 47-61.

BERNACCHI, L. C., 1908—NATIONAL ANTARCTIC EXPEDITION 1901-4: PHYSICAL OBSERVATIONS WITH DISCUSSION BY VARIOUS AUTHORS. PART II, PENDULUM OBSERVATIONS. *Royal Society of London.*

BORRASS, E., 1911—Bericht uber die relativen Messungen der Schwerkraft mit Pendelapparaten in der Zeit von 1808-1909; *in* Verhandlungen der XVI allgemeinen Konferenz der internationalen Erdmessung, 1909, *London,* 1911.

BORRASS, E., 1914—Bericht uber die relativen Messungen der Schwerkraft mit Pendelapparaten in der Zeit von 1909-1912; *in* Verhandlungen der XVII allgemeinen Konferenz der internationalen Erdmessung, 1912, **III** Teil. *Berlin,* 1914.

BOULANGER, Yu. D., SHCHEGLOV, S. N., WELLMAN, P., COUTTS, D. A., & BARLOW, B. C., 1973—Soviet-Australian gravity survey along the Australian Calibration Line. *Bulletin Geodesique,* **110,** 355-66.

BROUGHTON-EDGE, A. B., and LABY, T. H., 1931—THE PRINCIPLES AND PRACTICE OF GEOPHYSICAL PROSPECTING. *Cambridge University Press.*

BROWNE, B. C., & HONKASALO, T., 1969—Cambridge pendulum measurements of gravity differences on the West Pacific Calibration Base (unpublished). (Reference in Morelli *et al.* 1974).

CHAMBERLAIN, N. G., 1948—Preliminary report on the geophysical survey of the Collie coal basin. *Bureau of Mineral Resources, Australia—Report* **1.**

CHAMBERLAIN, N. G., DOOLEY, J. C., and VALE, K. R., 1954—Geophysical investigation in the Carnarvon Basin, W.A. *Bureau of Mineral Resources, Australia—Record* **1954/44.**

COMPAGNIE GENERALE DE GEOPHYSIQUE, 1975—Marine geophysical survey of the continental margins of Australia, Gulf of Papua and the Bismarck Sea 1970-73: Operations and Techniques. *Bureau of Mineral Resources, Australia—Record* **1975/151** (unpublished).

DALY, R. A., 1940—STRENGTH AND STRUCTURE OF THE EARTH. *Prentice Hall, N.Y.*

DARBY, F., & VALE, K. R., 1969—Progress of the reconnaissance gravity survey of Australia. *ECAFE Conference, Canberra, Australia, 1969,* and *Bureau of Mineral Resources, Australia—Record* **1969/110** (unpublished).

DOOLEY, J. C., 1948—Preliminary report on geophysical survey in the Frome Embayment. *Bureau of Mineral Resources, Australia—Record* **1948/17** (unpublished).

DOOLEY, J. C., 1950—Gravity and magnetic reconnaissance, Roma district, Queensland. *Bureau of Mineral Resources, Australia—Bulletin* **18.**

DOOLEY, J. C., 1958—Centenary of Melbourne—Toolangi Magnetic Observatory. *Journal of Geophysical Research,* **63,** 731.

DOOLEY, J. C., 1959—National report on gravity in Australia and Australian territories, May 1959. *Bureau of Mineral Resources, Australia—Record* **1959/7** (unpublished).

DOOLEY, J. C., 1963—Results of south-west Pacific submarine gravity survey 1956. *Bureau of Mineral Resources, Australia—Record* **1963/43** (unpublished).

DOOLEY, J. C., 1965a—Gravity surveys of the Great Barrier Reef and adjacent coast, North Queensland, 1954-60. *Bureau of Mineral Resources Australia—Report* **73.**

DOOLEY, J. C., 1965b—National report on gravity in Australia to June, 1965. *Bureau of Mineral Resources, Australia—Record* **1965/142** (unpublished).

DOOLEY, J. C., 1965c—Australian gravity network adjustment, 1962—*Bureau of Mineral Resources Australia—Report* **72.**

DOOLEY, J. C., MCCARTHY, E., KEATING, W. D., MADDERN, C. A., and WILLIAMS, L. W., 1961—Pendulum measurements of gravity in Australia 1950-51, *Bureau of Mineral Resources, Australia—Bulletin* **46.**

DOOLEY, J. C., and MULDER, H. J., 1953—Discussion of gravity results, East Gippsland, Victoria. *Bureau of Mineral Resources, Australia—Record* **1953/77** (unpublished).

FLAVELLE, A. J., & GOODSPEED, M. J., 1962—Fitzroy and Canning Basin reconnaissance gravity survey, Western Australia, 1952-60. *Bureau of Mineral Resources, Australia—Record* **1962/105** (unpublished).

FRASER, A. R., MOSS, F. J., & TURPIE, A., in press—Reconnaissance gravity survey of Australia. *Geophysics*, **41.**

GIBBINGS, D. L. H., PATTERSON, J. B., & BELL, G. A., 1971—The absolute determination of the gravitational acceleration at Sydney, Australia. *Bulletin Geodesique* **100,** 147-57.

GULF OIL SYNDICATE, 1964—Bonaparte Gulf gravity survey, Western Australia, 1959. *Petroleum Search Subsidy Act unpublished company report,* (BMR file number 47).

GUNSON, S., & WILLIAMS, L. W., 1965—Gravity surveys of Port Phillip Bay and adjacent areas, Victoria, 1957-8. *Bureau of Mineral Resources, Australia—Record* **1965/64** (unpublished).

GUSEV, N. A., 1973—Determination of gravity acceleration at Sydney with pendulum apparatus. *Central Research Institute of Geodesy, Aerial Survey and Cartography, Moscow, USSR Report* **1973** (in Russian). English version *Bureau of Mineral Resources, Australia—Record* **1973/115** (unpublished).

GUSEV, N. A., 1975—Determination of gravity acceleration at Port Moresby (Papua New Guinea) and Hobart (Australia) with OVM pendulum apparatus. *Bureau of Mineral Resources, Australia—Record* **1975/106** (unpublished).

HALL, J. McG., & TOWNSEND, I. J., 1969—Helicopter gravity survey of areas marginal to the western Great Artesian Basin. Department of Mines, *South Australia, Geological Survey—Mining Review.* **130,** 70-9.

HASTIE, L. M., & WALKER, D. G., 1962—Two methods of gravity traversing with helicopters. *Bureau of Mineral Resources, Australia—Record* **1962/134** (unpublished).

HEISKANEN, W. A., 1936—Handbuch der Geophysik 1 (editor B. Gutenburg), Part 4, Section 12, 878-951.

INOUE, E., & SETO, T., 1961—Pendulum determinations of the gravity differences between Tokyo and Melbourne. *Bulletin of the Geographical Survey Institute, Japan.* **6,** 201-211.

JAEGER, J. C., & THYER, R. F., 1960—Geophysics in Australia. *Geophysical Journal of the Royal Astronomical Society,* **3,** 450-461.

JEFFREYS, H., 1941—The determination of the Earth's gravitational field. *Geophysical Supplement, Monthly Notices of the Royal Astronomical Society,* **5,** 1-22.

JONES, B. F., 1969—Timor Sea gravity, magnetic and seismic survey, 1967. *Bureau of Mineral Resources Australia—Record* **1969/40** (unpublished).

KERR-GRANT, C., 1951—Geophysical survey of parts of counties Gawler, Stanly and Daly. *Department of Mines, South Australia, Geological Survey—Mining Review,* **91,** 164-7.

KESSLITZ, W., 1902—Resultate aus den Schwerebestimmungen durch Pendelbeobachten; ausgefuhrt von K.u.K. See-Offizieren in den Jahren 1892-1901: *in* Relative Schwerebestimmungen durch Pendelbeobachten **III** Heft, *Pola.*

LANGRON, W. J., 1966—National report on gravity in Australia, January 1960 to December 1962. *Bureau of Mineral Resources, Australia—Record* **1966/108** (unpublished).

MARSHALL, C. E., & NARAIN, H., 1954—Regional gravity investigations in the eastern and central Commonwealth. *University of Sydney, Department of Geology and Geophysics Memoir* **1954/2.**

MATHER, R. S., BARLOW, B. C., & FRYER, J. G., 1971—A study of the earth's gravitational field in the Australian region. *XV General Assembly, IAG, Moscow* 1971. *University of New South Wales UNISURV Report* **22,** 1-41.

MCINTYRE, J. I., 1972—Gravity values at bench marks along main roads in New South Wales. *Geological Survey of New South Wales Report, GS* **1972/440** (unpublished).

MINISTRY OF GEOLOGY OF USSR, 1971—Gravimetric map of Australia, 1:5 000 000 (two variants each of four sheets in colour).

MORELLI, C., GANTAR, C., HONKASALO, T., MCCONNELL, R. K., TANNER, J. C., SZABO, B., UOTILA, U., & WHALEN, T., 1974—The International Gravity Standardization Net 1971 (I.G.S.N. 71). *International Association of Geodesy, Special Publication* 4.

MURRAY, A. S., 1974—The Australian national gravity repository computer system. *Bureau of Mineral Resources, Australia—Record* **1974/68** (unpublished).

RIESZ, E. J., & MOSS, F. J., 1971—Regional marine geophysical surveys in the Australian region. *Bureau of Mineral Resources, Australia—Record* **1971/119** (unpublished).

SHIRLEY, J. E., 1966—Gravity meter measurements in connection with the Western Pacific Calibration Line (Australian segment), 1965. *Bureau of Mineral Resources, Australia—Record* **1966/160** (unpublished).

SMITH, E. R., 1966—Timor Sea/Joseph Bonaparte Gulf marine gravity and seismic "spark array" survey, North-west Australia, 1965. *Bureau of Mineral Resources, Australia—Record.* **1966/72** (unpublished).

SPRIGG, R. C., & STACKLER, W. F., 1965—Submarine gravity surveys in St. Vincent's Gulf, South Australia. *APEA Journal,* **5,** 168-178.

STAHL, P. 1954—Expeditions Terre Adelie, 1951-53. Extrait des Rapports Preliminaires 24, Gravimetrie. *Expeditions Polaires Francaises, Mission Paul-Emile Victor.*

SYMONDS, P. A., & WILCOX, J. B., 1976—The gravity field of offshore Australia. *BMR Journal of Australian Geology & Geophysics,* **1,** 303-14.

TALWANI, M., WORZEL, J. L., & EWING, M., 1961—Gravity anomalies and crustal section across the Tonga Trench. *Journal of Geophysical Research,* **66,** 1265-78.

THRELFALL, R., & POLLOCK, J. A., 1900—On a quartz thread gravity balance. *Philosophical Transactions of the Royal Society of London, Series A,* **193,** 215-257.

THRELFALL, R., & DAWSON, A. J., 1933—Further history of a quartz thread gravity balance. *Philosophical Transactions of the Royal Society of London, Series A.* **231,** 55-73.

THYER, R. F., & DOOLEY, J. C., 1947—A gravity survey over the northern basin of the Leigh Creek coalfield. *South Australian Mining Research* **84,** 146-150.

THYER, R. F., & EVERINGHAM, I. B., 1956—Gravity survey of the Perth Basin, W.A. *Bureau of Mineral Resources, Australia—Bulletin* **33.**

VALE, K. R., 1962—Reconnaissance gravity surveys, using helicopters, for oil search in Australia. *Bureau of Mineral Resources, Australia—Record.* **1962/130** (unpublished).

VALE, K. R., 1965—Progress of the reconnaissance gravity survey of Australia. *ECAFE Conference, Tokyo, Japan, 1965, and Bureau of Mineral Resources, Australia—Record* **1965/197** (unpublished).

VENING-MEINESZ, F. A., 1941—GRAVITY EXPEDITIONS AT SEA, 1934-39, Volume **III.** *Mulder, Delft.*

WELLMAN, P., BOULANGER, Yu. D., BARLOW, B. C., SHCHEGLOV, S. N., & COUTTS, D. A., 1974—Australian and Soviety gravity surveys along the Australian Calibration Line. *Bureau of Mineral Resources, Australia—Bulletin* **161.**

WELLMAN, P., 1974—National report on gravity in Australia, July 1970 to June 1974. *Bureau of Mineral Resources, Australia—Record* **1974/114** (unpublished).

WHALEN, C. T., 1966—The Western Pacific Calibration Line survey, 1964-65. *United States Air Force, ACCS Oflan 503, Phase Report No. 3* (unpublished).

WHITWORTH, R., 1969—Marine geophysical survey of the Northwest Continental Shelf, 1968. *Bureau of Mineral Resources, Australia—Record* **1969/99** (unpublished).

WILLIAMS, L. W., GOODSPEED, M. J., & FLAVELLE, A. J., 1961—International gravity meter ties 1959. *Bureau of Mineral Resources, Australia—Record* **1961/24** (unpublished).

WOOLLARD, G. P., & ROSE, J. C., 1963—INTERNATIONAL GRAVITY MEASUREMENTS. *University of Wisconsin, Madison.*

WORZEL, J. L., 1965—PENDULUM GRAVITY MEASUREMENTS AT SEA 1936-59. *Wiley, New York.*

WRIGHT, C. S., 1921—BRITISH (TERRA NOVA) ANTARCTIC EXPEDITION 1910-1913, DETERMINATIONS OF GRAVITY. *Harrison & Sons, London for the Committee of the Captain Scott Antarctic Fund.*

Compilation and production of the 1976 1:5 000 000 Gravity Map of Australia

W. Anfiloff, B. C. Barlow, A. Murray, D. Denham and R. Sandford

In 1976 a coloured 1:5 000 000 Gravity Map of Australia was published by BMR. At that stage the systematic reconnaissance gravity coverage of Australia, initiated by BMR in 1959, was complete, and preliminary gravity values were available from marine coverage of the continental shelf and margins. The map was based on approximately 260 000 gravity observations obtained by various organisations at a cost of about $12 000 000 from 300 surveys. It was produced using a CDC Cyber 76 computer system, Calcomp plotters and cartographic techniques. The computer processing phase took about four months and the cartography about three months. The coloured 1:25 000 000 Bouguer and free-air anomaly maps contained in this issue were also produced from the same data bank.

Sources of data

The data bank used to produce the 1976 1:5 000 000 gravity map of Australia (BMR, 1976) was compiled from the BMR gravity repository (Murray, 1974). This contains information on approximately 600 surveys, comprising more than 500 000 stations, which have been carried out in the Australian region.

All the surveys necessary to provide a complete regional coverage of Australia were processed so that the principal gravity facts were available in computer-compatible format. This process involved punching and digitizing the observations, checking for errors, and adjusting the values to tie in with the Australian Map Grid, the Australian Height Datum and the May 1965 values on the Australian National Gravity Network (Dooley & Barlow, 1976).

Observations from BMR surveys were processed in-house and those from other sources by a private contractor engaged especially for this task. Some surveys were too small or detailed to be used for the 1:5 000 000 scale map and were not processed. Data for surveys carried out in South Australia by the Mines Department and in Tasmania by the University of Tasmania were supplied in computer-compatible format and required only minimum processing.

About 85 percent of the contoured area was covered by surveys carried out either by BMR or private companies under contract to BMR. The remaining areas were covered by surveys carried out by State Mines Departments, private companies, tertiary institutions and the US Navy.

The BMR reconnaissance land surveys used helicopters for transport, microbarometers to determine heights, and Worden or La Coste and Romberg gravity meters (see for example, Fraser, 1973). These surveys were carried out between 1959 and 1974. The average station spacing over Australia is 11 km, except in South Australia and Tasmania where it is 7 km. Land areas surveyed by other organizations have station spacing ranging from 1 to 10 km.

Most of the marine data were obtained during a reconnaissance survey of the Australian continental margins completed for BMR during 1970-73, when about 185 000 km of systematic traversing were completed (Compagnie Generale de Geophysique, 1975). The line spacing varied from 30 to 50 km and the gravity values were based on preliminary hourly values representing an average station spacing of about 15 km along each traverse. Three other BMR surveys over the northwest continental shelf (1965, 1967 and 1968) covered about 59 000 km with a line spacing of 17 km. Values sampled at intervals of 11 km along the traverses were included in the data bank.

There are only three areas where the data coverage is poor (Fig. 1): the Gulf of Carpentaria/Arafura Sea, the Great Barrier Reef, and Bass Strait; elsewhere the coverage is considered adequate for the 1:5 000 000 map.

In some small areas of South Australia and in the eastern part of the Coral Sea, synthetic principal facts were prepared from published gravity anomaly maps because the real principal facts were not available in time. The synthetic stations are not shown in Figure 1, which shows only the locations of real observations. The synthetic principal facts were produced by digitizing the gravity anomaly contours at reasonable intervals and adding these values to the data bank.

Reduction of observations

The anomalies on the maps are based on the Potsdam datum for observed gravity values, and the 1930 International Gravity Formula.

The values of observed gravity are relative to May 1965 Isogal values at stations of the Australian National Gravity Network, which consists of a series of east-west traverses (Isogal traverses) between airports of nearly equal gravity, joined by three north-south traverses (see Fig. 2). This network of some 200 base stations spaced at about 300 km was established over Australia and Papua New Guinea during 1964-1967.

The positions of the helicopter stations were determined using aerial photographs to tie to the Australian Geodetic Datum, and heights by barometer ties to third-order levelling traverses, which in turn are tied to the Australian Height Datum.

A variety of navigation techniques were used on the marine surveys. These were a 'Toran' radio location system in 1965 (~50 m accuracy); a VLF/Omega system in 1967 integrated with dawn and dusk star fixes, radar, and navigation buoys (2-4 km accuracy); and for the remaining surveys a satellite/sonar-Doppler system, with the ship's velocity logs and a VLF/Omega system as backups (1-2 km accuracy).

The observed gravity values at sea have been reduced to free-air anomalies (FAA) in milligals, according to the formula:

$$FAA = g_o - g_n + 7.5\,Ve\cos\phi \qquad \ldots . (1)$$

where g_o is the observed gravity, g_n the normal value of gravity depending on latitude ϕ, and obtained from the 1930 International Gravity Formula:

$$g_n = 978\,049.0\,(1 + 0.005\,288\,4\sin^2\phi - 0.000\,005\,9\sin^2 2\phi) \qquad \ldots . (2)$$

and Ve is the eastward component of the ship's speed in knots used to calculate the Eotvos correction.

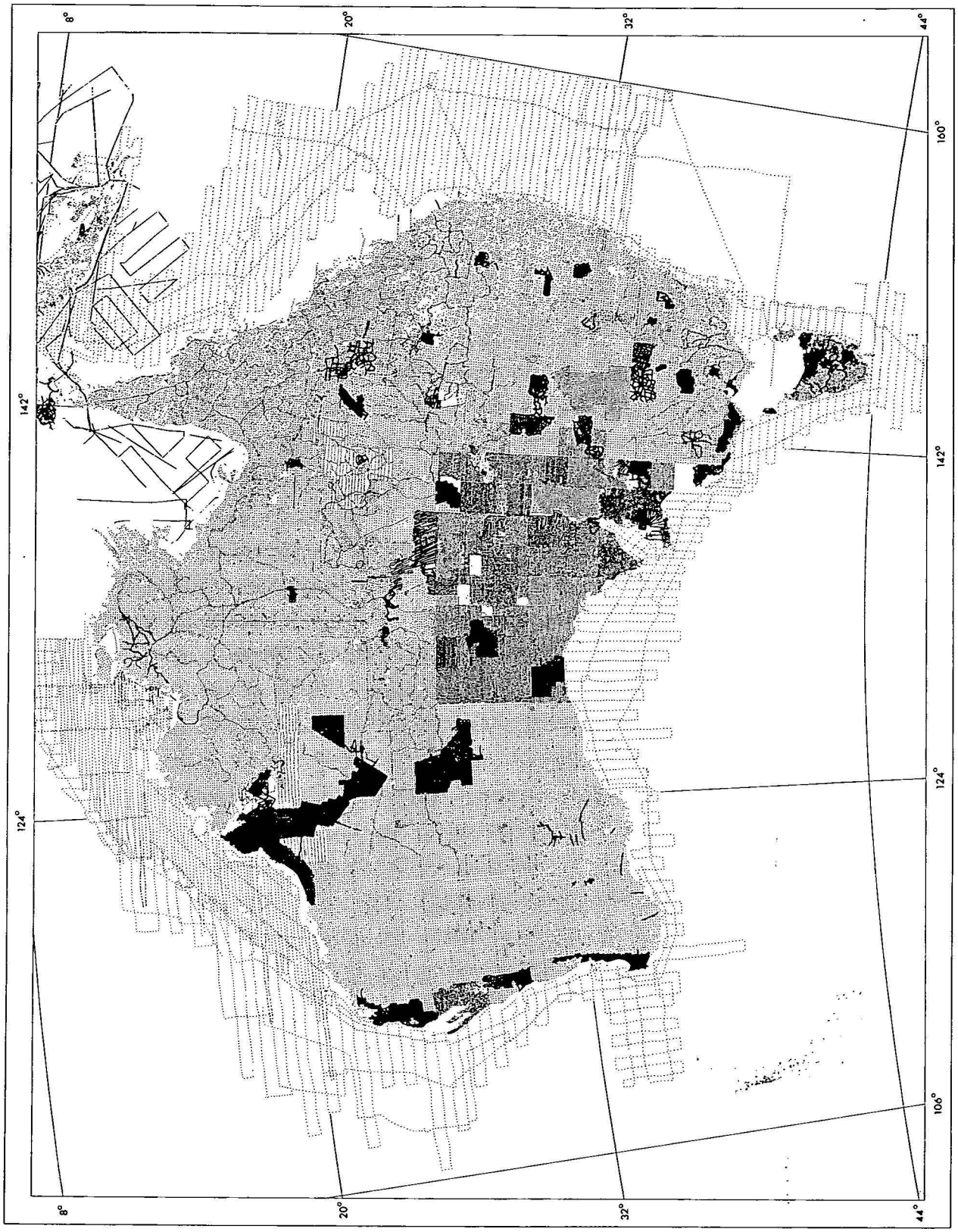

Figure 1. Distribution of data used to produce the 1:5 000 000 gravity map.

For land stations the simple Bouguer anomaly (BA) is used:

$$BA = g_o - g_n + 0.3086h - 0.0419\varrho h \quad \ldots . (3)$$

where h is the altitude in metres and ϱ is taken as 2.67 t/m³. No terrain corrections have been applied.

Accuracy of anomalies

The usual precision within each helicopter land gravity survey is better than 0.3 mGal for observed gravity differences, better than 5 m for altitude, and about 0.1 minutes of arc for latitudes and longitudes, resulting in

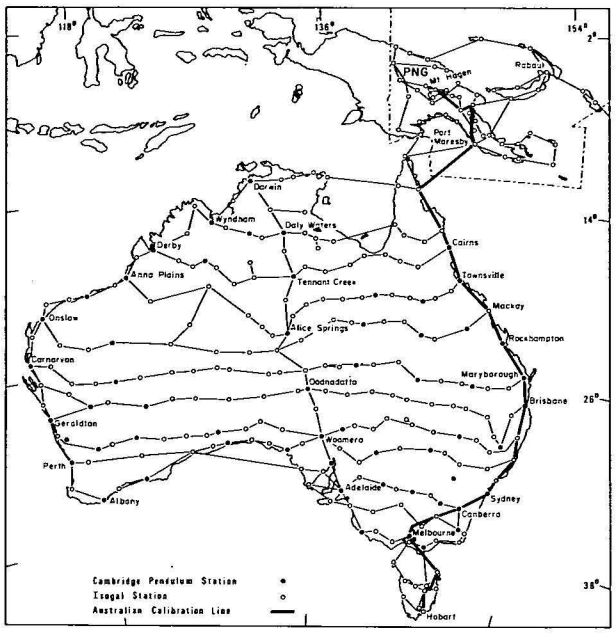

Figure 2. Australian Gravity Network.

Bouguer anomalies with a relative precision of about 1 mGal. The precision of ties between surveys is better than 0.5 mGal and 10 m, or about 2 mGal in Bouguer anomaly. Gravity values of the national network are estimated to have a standard error of 0.2 mGal relative to the network as a whole.

Terrain corrections within mainland Australia are less than 0.2 mGal over 80 percent of the area, and less than 2 mGal for the remainder of the area except in small areas of very steep topography, where the corrections may reach 10 mGal.

For the marine surveys the precision of the free-air anomalies can be estimated from the root-mean-square deviation (rms) of the differences of the gravity misties at line intersections. For the regional surveys over the north-west shelf the rms values varied from about 4 mGal in 1965 to about 2 mGal in 1968. On the survey of the continental margins the rms differences were about 6 mGal. The lower precision of this survey is largely due to a decrease in the precision with which the parameters affecting gravity could be measured in deep water (for instance, unknown ocean currents reduce the positioning accuracy).

There are two known small systematic errors in the anomalies:

1. the mean Australian milligal scale is now known to be smaller than the absolute scale by about 5 parts in 10^4, and
2. anomalies on the Potsdam system using the 1930 normal gravity formula differ from anomalies on present world standards because of an improved reference ellipsoid, which was adopted in 1967; and a revised international datum for observed gravity, which was adopted in 1971.

The correction C in milligals to the mapped anomaly at any point X is given by:

$$C = \text{Anomaly}(1967/71) - \text{Anomaly}(1930/65) \quad \ldots (4)$$

where Anomaly (1967/71) is calculated with 1971 datum and scale, and the 1967 ellipsoid; and Anomaly (1930/65) is calculated with the 1930 ellipsoid and the 1965 datum and scale.

Since the free-air and Bouguer corrections are the same in both systems we can write:

$$C = [g_o(1971) - g_n(1967)] - [g_o(1965) - g_n(1930)] \quad \ldots . (5)$$

$$= [g_o(1971) - g_o(1965)] - [g_n(1967) - g_n(1930)] \quad \ldots . (6)$$

$$\text{Now } g_n = \gamma_e (1 + A \sin^2\phi + B \sin^2 2\phi) \quad \ldots . (7)$$

where γ_e = equatorial gravity
= 978 049.0 (1930) or 978 031.8 (1967)
A = 0.005 288.4 (1930) or 0.005 302.4 (1967)
B = 0.000 005.9 (1930 and 1967)
the values for the coefficients are taken from Coron (1972).

Hence

$$g_n(1967) - g_n(1930) = -17.2 + 13.6 \sin^2\phi \quad \ldots . (8)$$

Also

$$[g_o(1971) - g_o(1965)] \text{ at } X = [g_o(1971) - g_o(1965)] \text{ at Sydney} + [\Delta g(1971) - \Delta g(1965)] \text{ for } X - \text{Sydney}$$
$$= -13.88 - b.\Delta g(1971) \quad \ldots . (9)$$

Where 1 + b is the scale correction factor
and $b = -5.08 \times 10^{-4}$ (Wellman *et al.*, 1974)

Neglecting differences in g_o caused be elevation and geological differences we get

$$g_o \approx g_n = \gamma_e (1 + A \sin^2\phi + B \sin^2 2\phi) \quad \ldots . (10)$$

$$\Delta g \text{ for } (X - \text{Sydney}) = \gamma_e A (\sin^2\phi_X - \sin^2\phi_{\text{Sydney}}) \quad \ldots . (11)$$

Neglecting the terms in $b\gamma$, and $_eB$ we get

$$g_o(1971) - g_o(1965) = -13.88 + 2.63 \sin^2\phi_X - 0.82 \quad \ldots . (12)$$

$$= -14.70 + 2.63 \sin^2\phi_X \quad \ldots . (13)$$

Substituting **(8)** and **(13)** in **(6)** we finally get

$$C = 2.5 - 11.0 \sin^2\phi \quad \ldots . (14)$$

Processing the data

The programs used to compile the map are based on those described by Murray (1974). These search several files for data in specified areas; sort the data into an appropriate form, and then plot the station positions and contour the gravity values. Editing facilities are available in the sort package to add, remove or amend the data. These programs have been modified and improved since a Cyber 76 computer system became available late in 1973. The Cyber system provided the capacity for large on-line data storage and fast processing (1.2 million characters of central processor core memory and 32.5 million characters of on-line disc memory), which was essential for the production of the map.

The first stage of processing involved extracting data from the computer files, survey by survey, and checking the station locations, the elevation, observed gravity, and Bouguer anomaly values. Each survey was then stored separately pending the accumulation of sufficient data to form an aggregate file. Aggregate files of up to 50 000 observations were then formed by concatenating several surveys. Next, they were plotted to ascertain the station coverage.

During the second processing stage four files corresponding to a four-fold division of Australia along 24°S and 132°E were created; each file had a manageable size of less than 100 000 observations.

During the third stage, data in each sector file was checked to eliminate errors. The files were first sorted to eliminate duplicates, and then plotted to check the final station coverage. Each sector was then contoured using a program which did not smooth the data, and errors thus detected were rectified. The final checking involved contouring and listing principal facts in 1:1 000 000 map areas; these maps provide a complete gravity coverage of the Australian region at the same scale and projections as the World Aeronautical Charts, ICAO series. The final data bank used for the 1:5 000 000 map consisted of about 260 000 land and marine gravity observations as shown on Figure 1.

Smoothing and contouring gravity anomalies

The first step in preparing the contours was to generate an approximately square reference grid, over the whole map area, with a spacing of about 6 minutes of arc. Each grid point was assigned a value equal to the average of all observations lying within the grid square centred on the point. Grid points having no observations within their grid square were assigned a value equal to that of the nearest grid point based on observations. The extrapolation of grid values to areas without data extended to one degree to enable small offshore gaps to be contoured.

The values on the grid were then smoothed to produce a surface of minimum curvature using the iterative method described by Briggs (1974). The method of drawing contour lines from the gridded values involved a four-point cubic interpolation between grid points to find contour cuts, and then a cubic spline to fit the cuts. Because the contour lines were based on the computed grid values and not directly on the anomaly values, they were precise to only about half a grid spacing, or about 3 minutes of arc.

The base map was scribed on a flatbed plotter using data provided by Division of National Mapping, Department of National Resources. The gravity contours were produced in several sections on a drum plotter; map compilation, final hand-scribed contours, and colour-separation masks were prepared in the Geophysical Branch Drawing Office.

The completed map is at the same scale and projection as the Tectonic Map of Australia and New Guinea 1971, and the Geological Map of the World—Australia and Oceania, 1965-1967—prepared on behalf of the Commission for the Geological Map of the World.

To produce the coloured 1:25 000 000 Bouguer and free-air maps presented in this issue, observations from the Gulf Rex were added to the data bank to fill gaps in the Coral and Arafura Seas. The free-air map was prepared from an unpublished 1:2 500 000 map and the Bouguer/free-air map was prepared from the 1:5 000 000 gravity map.

Acknowledgements

We would like to thank the following organisations for contributing data without which this map could not have been completed.

Flinders University
New South Wales Mines Department
Ocean Research Institute, Hawaii Institute of Geophysics
Oil companies operating under Petroleum Search Subsidy Acts
South Australian Mines Department
Tasmanian Mines Department
United States Navy
University of New South Wales
University of Tasmania
West Australian Petroleum Pty Ltd.

References

BMR, 1976—Gravity Map of Australia, 1:5 000 000 *Australian Bureau of Mineral Resources, Canberra.*

BRIGGS, I. C., 1974—Machine Contouring using Minimum Curvature; *Geophysics,* **39,** 39-48.

COMPAGNIE GENERALE DE GEOPHYSIQUE, 1975—Marine geophysical survey of the continental margins of Australia, Gulf of Papua and the Bismarck Sea 1970-1973: Operations and Techniques. *Bureau of Mineral Resources, Australia—Record* **1975/151** (unpublished).

CORON, S., 1972—Carte d'Anomalies Moyennes a l'Air Libre par 5° x 5°. Bulletin d'Information, **29,** *Bureau Gravimetrique Internationale, Paris.*

DOOLEY, J. C., & BARLOW, B. C., 1976—Gravimetry in Australia 1819-1976. *BMR Journal of Australian Geology & Geophysics,* **1,** 261-271.

FRASER, A. R., 1973—Reconnaissance helicopter gravity survey, W.A., 1971-72. *Bureau of Mineral Resources, Australia—Record* **1973/130** (unpublished).

MURRAY, A. S., 1974—The Australian National Gravity Repository Computer System. *Bureau of Mineral Resources, Australia—Record* **1974/68** (unpublished).

WELLMAN, P., BOULANGER, Yu. D., BARLOW, B. C., SHCHEGLOV, S. N., & COUTTS, D. A., 1974—Australian and Soviet Gravity Surveys along the Australian Calibration Line, *Bureau of Mineral Resources, Australia—Bulletin* **161.**

Relation of Bouguer anomalies to crustal structure in southwestern and central Australia

S. P. Mathur

An analysis of the gravity field in two largely Precambrian metamorphic rock areas of Australia, one in the southwestern and the other in the central part, indicates that the regional Bouguer anomalies may be explained by models of the crust and upper mantle consistent with the other geophysical and geological observations.

In the southwestern part, the longer wavelength component of the anomalies is consistent with a crust which has been determined by seismic measurements to be greater than normal in thickness and density in the west owing to the presence of a high-velocity basal layer that thins out eastwards. The shorter wavelength components show excellent correlation with the near-surface geology.

In central Australia, where no comparable seismic measurements have been made, the Bouguer anomaly field, which is dominated by large amplitude (up to 150 mGal) and long wavelength (about 150 to 200 km) components, is interpreted in terms of thickness and structure of a two-layer crust. The derived crustal model is based on the concept of folding and faulting that involves the entire crust and upper mantle, and is compatible with the broad aspects of surface geology and structure. The crustal upwarps in the model, with the intermediate and Mohorovicic discontinuities at depths as shallow as 15 and 27 km, are associated with the Arunta and Musgrave Blocks, where deep crustal rocks are exposed against large thrust faults. The crustal downwarps, with the discontinuities as deep as 31 and 43 km, are associated with basins containing substantial thicknesses of sediments. Depths to these discontinuities are in agreement with those estimated from the only two isolated deep seismic reflection probes in the basin areas.

Introduction

Studies of Bouguer anomalies, and the crustal structure as determined by seismic refraction measurements on both continents and oceans in other than the Australian region, strongly suggest that gravity values are controlled primarily by the mass variations associated with changes in crustal thickness (Woollard, 1959; Kesminskaya, *et al.*, 1969). Furthermore, they indicate that the areas where the crust is greater than normal in thickness and density are characterized by a well-defined high-velocity (6.8-7.3 km/s) basal crustal layer, a higher than normal mantle velocity, an excess in gravity, and an association with a basin; whereas the areas in which the crust is less than normal in thickness and density are characterized by a subnormal mantle velocity, a deficiency in gravity, and an evidence of uplift (Woollard, 1968). Similar studies made in southwestern Australia (Mathur, 1974a) are briefly reviewed here to show that the above relationships are valid for Australia as well, and that the regional Bouguer gravity field is consistent with the structure and composition of the entire crust and upper mantle as determined by regional seismic measurements. In view of these empirical relationships a model of the crust in central Australia, which is compatible with the geological and other geophysical information, is derived from the regional Bouguer anomalies. Although it lacks adequate seismic control, the model is considered very probable.

Acknowledgement

The figures were prepared by B. Holden, Geophysical Drawing Office, BMR.

Southwestern Australia

Geologic setting

The generalized geology and structure of the southern part of the Yilgarn Block, the largest and oldest part of the West Australian shield, are shown in Figure 1. The block is made up mainly of Archaean gneiss, and lenticular masses of greenstones and metasediments, and is intruded by massive granites. On the west, the block is bounded by the Perth Basin, a narrow elongate depression which is filled with Palaeozoic and Mesozoic sediments and shows graben structure in the south; on the south and southwest it is girded by a belt of Proterozoic granites and metamorphic rocks of the Albany-Esperance Block, and granites and granulites of the Fraser Range Block.

Seismic studies

The results of deep crustal seismic investigations made in the southern part of the Yilgarn Block (Mathur, 1974a) are reproduced here in Figure 2 as crustal sections along three traverses across the shield. The structural section in Figure 2a is based on both refraction and reflection data, and in Figure 2b on refraction data alone. The section in Figure 2c is based on dubious reflection data, but is considered to be consistent with the section in the Coolgardie area shown in Figure 2a, and with the major geological features observed across the Fraser Fault.

The crust is of normal continental type in the east, but becomes abnormal toward the Perth Basin in the west. It consists of two layers with average velocities of 6.1 and 6.7 km/s, and is 34 km thick near Jubilee Mine (Kalgoorlie); whereas near Perth it is 44 km thick and includes an extra basal layer of average velocity 7.4 km/s. In the Perth Basin, about 7.5 km of sediments overlie a block of crust which has been thrown down to the west along the Darling Fault. Southeast of Coolgardie, the high-velocity basal layer is shown to be thin and the southeastern part of the crustal block is assumed to be upthrust to the northwest along the Fraser Fault. The average velocity of the material under the thicker than normal crust is measured to be 8.3 km/s.

Gravity studies

The shorter wavelength features of the Bouguer anomaly map (Fig. 3) show excellent correlation with the geology and tectonics in southwestern Australia: the narrow extensive low along the western coast correlates with the Perth Basin, the low in the south with the Albany granite, the narrow zone of high positive anomalies in the southeast with the denser basic mass in the Fraser Range Block, the small circular highs in the northeast with the greenstones of the

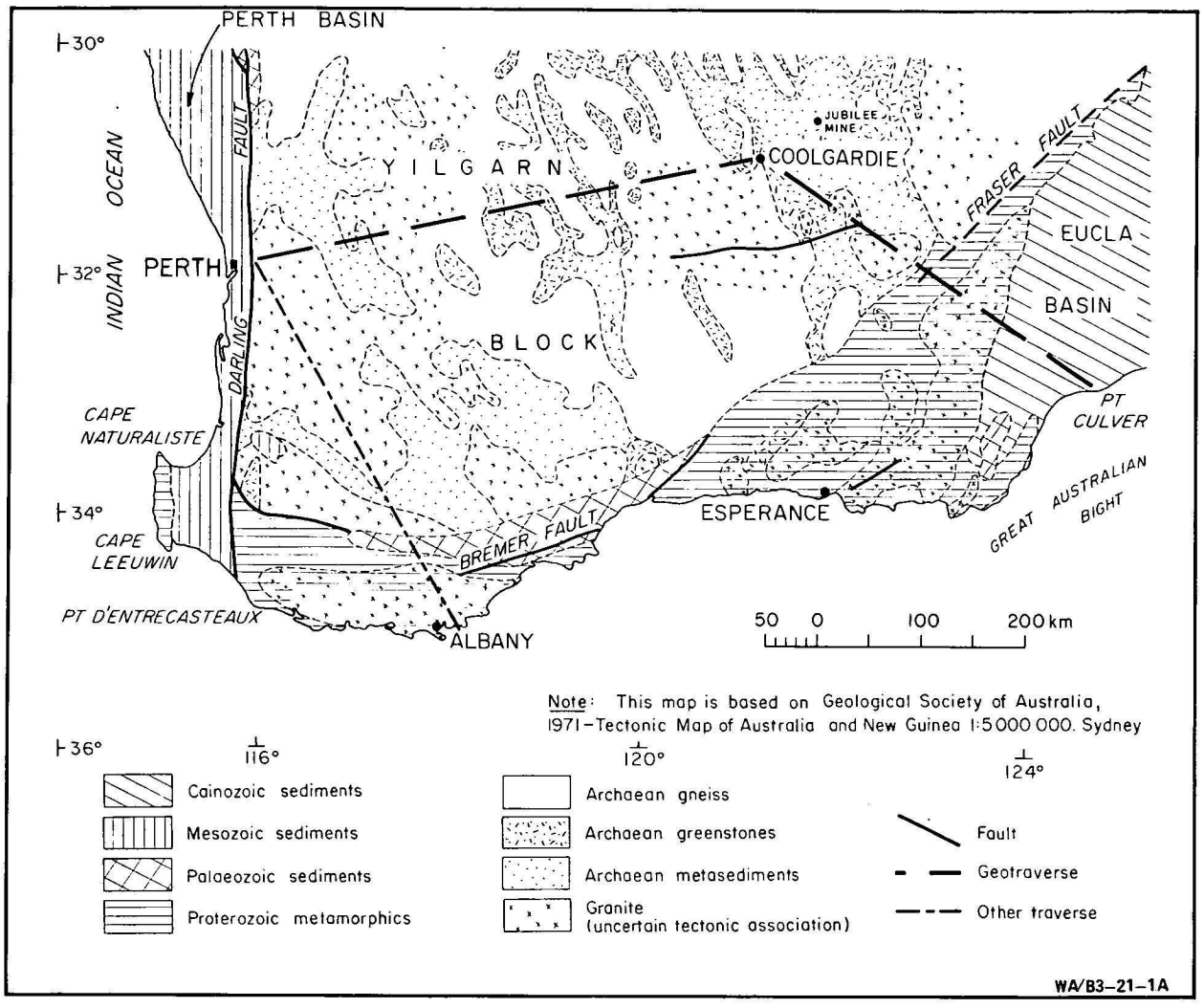

Figure 1. Generalized geological map of southwestern Australia, showing the Yilgarn Block of the Archaean shield bounded by the Proterozoic Albany-Esperance and Fraser Fault mobile zones, and the Phanerozoic Perth Basin.

Kalgoorlie area. The mean, i.e., the longer wavelength component, of the observed Bouguer anomalies show good agreement with the gravity values computed for the crustal structure shown in Figure 2. The densities of the lower crustal layers and the upper mantle material have been derived from a value of 2.78 t/m^3 assumed for the upper crustal layer, largely made up of gneisses, granites and greenstones, and from the density contrasts required for a good agreement between the computed and mean observed gravity anomalies. These densities are also compatible with the measured seismic velocities of the various layers. The analysis of the gravity data and the assumptions involved have been discussed in detail by Mathur (1974a).

An alternate interpretation of gravity anomalies across the Fraser Fault has been made by Anfiloff & Shaw (1973) who explained the anomaly features solely in terms of mass variations within the upper 12 km of the crust, suggesting flat Conrad and Mohorovicic discontinuities at 20 and 35 km depths respectively, and no dislocations in the lower crust. Although the seismic data are inadequate and inconclusive in this area, the model in Figure 2c is favured here because it is considered likely that the entire crust was involved in the tectonism which brought the deep crustal rocks (granulites) to the surface along the Fraser Fault zone.

Central Australia

Geologic setting

The generalized geology and structure of the region studied is shown in Figure 4. The prominent geological features are the easterly trending series of anticlinoria of Precambrian metamorphic rocks, the Arunta and Musgrave Blocks, and the intracratonic depressions filled with late Precambrian and Palaeozoic sediments of the Ngalia, Amadeus and Officer Basins. In the Arunta and Musgrave Blocks, the metamorphic rocks consist of gneiss, schist, and several sequences of metamorphosed sedimentary and volcanic rocks which are intruded by granite and other igneous rocks. The region had been subjected to at least three major orogenies: Arunta in the Precambrian, Petermann Ranges in the Late Adelaidean, or Early Cambrian, and Alice Springs in the Carboniferous. The orogenies caused reactivation of metamorphic rocks and resulted in complex structures and zones of deformation along the northern margin of the Ngalia Basin, and the northern and southern margins of the Amadeus Basin. Forman and Shaw (1973) believe that these zones pass through the crust into the mantle beneath, and that the crust and mantle in each deformed zone have been upthrust, bringing granulite facies rocks to the surface.

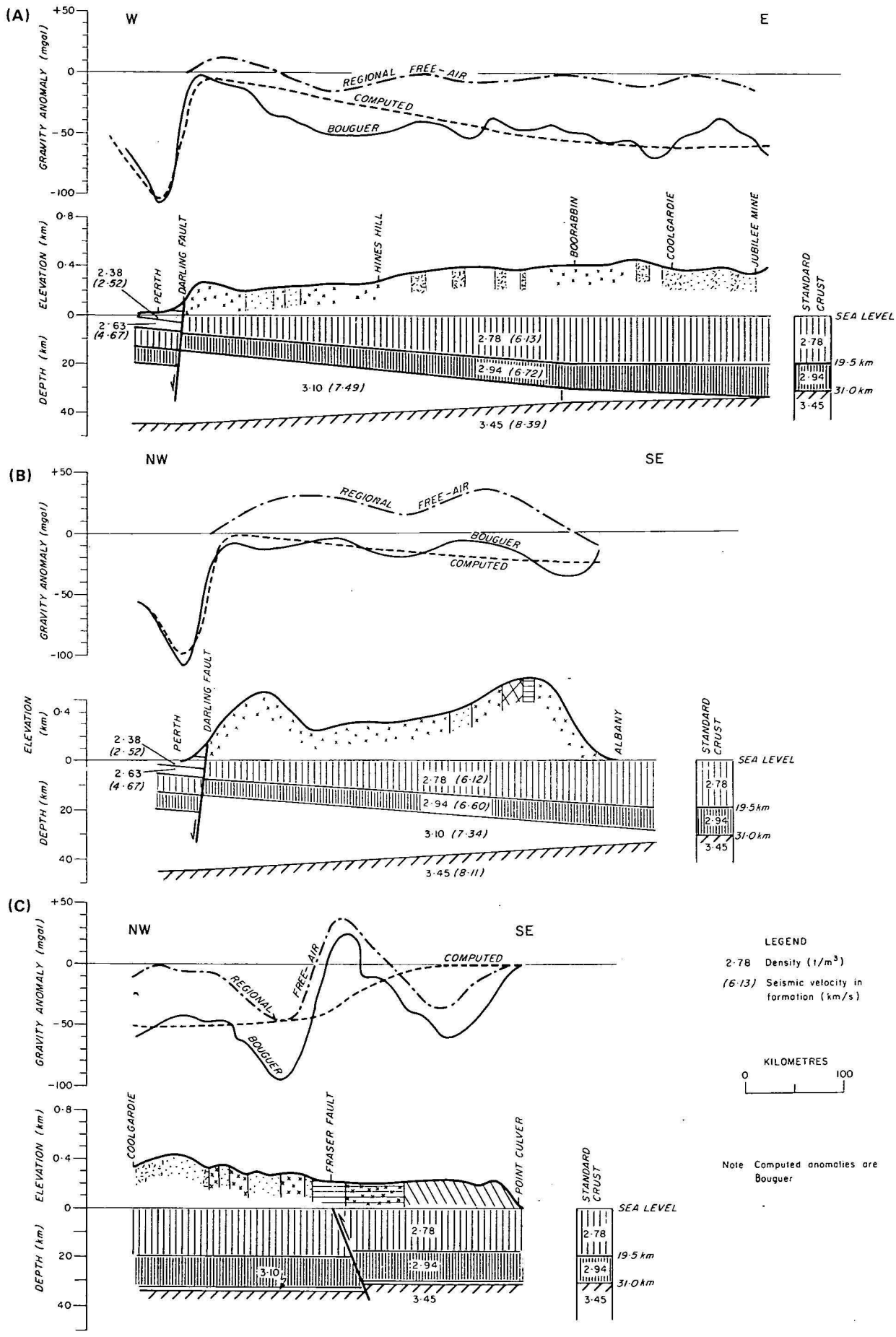

Figure 2. **Crustal structure and gravity profiles along three traverses across the southwestern Australian shield (after Mathur, 1974a). The gravity anomalies computed for the structure based on seismic refraction/reflection data show good agreement with the mean observed Bouguer anomalies; the shorter wavelength components relate to the near-surface geology. Surface geology as in Figure 1.**

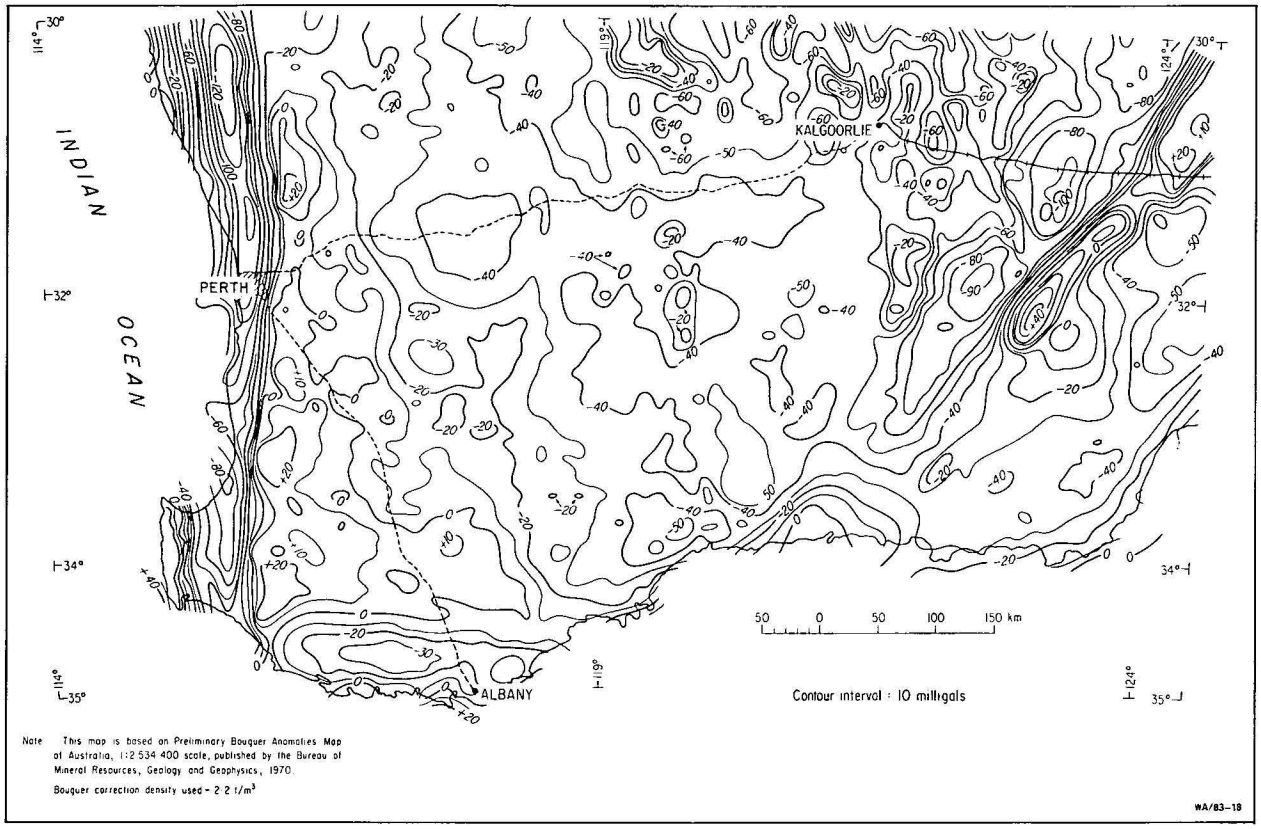

Figure 3. Bouguer anomaly map of southwestern Australia. The shorter-wavelength highs in the northeast relate to the greenstone bodies; the broad region of positive anomalies in the southwest reflects the excess mass in the denser basal layer in the crust.

Seismic studies

Seismic studies in the area have been restricted mainly to the investigation of thickness and structure of sediments in the basin areas. The results have confirmed the shapes of the basins suggested by the magnetic data (Fig. 5) and indicated the thickness of sediments to be about 5 km in the western and deeper part of the Ngalia Basin (Wells, Moss & Sabitay, 1972), about 10 km in the north-central part of the Amadeus Basin (Moss, 1964) and about 5 km in the northeastern part of the Officer Basin (Milton & Parker, 1973). The presence of reflections below crystalline basement rocks along the northern margin of the Ngalia Basin and the northeastern margin of the Officer Basin suggest major overthrusting. Such overthrusting along the Ngalia Basin margin is clearly illustrated in the seismic section in Figure 6, which is reproduced here from Wells *et al.* (1972).

Deep crustal reflections have been recorded at only two isolated sites in the area, one in the Amadeus Basin, about 160 km west of Alice Springs, and the other near the northern margin of the Ngalia Basin (Brown, 1970) (Fig. 4). Under the Amadeus Basin sediments, two deep events with large amplitudes stand out at about 8.5 and 12.0 seconds (Fig. 7). Using average velocities of 5.0 km/s for the sediments, 6.1 for crustal layer I and 6.7 for crustal layer II, these reflections yield depths of 24 and 36 km for the intermediate crustal and Mohorovicic discontinuities. In the Ngalia Basin, a depth of 38 km is suggested for a strong reflection event at 12.7 s believed to originate from the Mohorovicic discontinuity.

Gravity data

Overall the region shows a largely negative Bouguer anomaly field, a prominent feature on the Gravity Map of Australia. The most striking characteristic of the anomalies in central Australia (Fig. 8) is the series of slightly arcuate, easterly elongate gravity lows separated by similarly trending highs. The lows reach a minimum of about −155 mGal in the Amadeus Basin, whereas the highs reach a maximum of about +50 mGal in the Musgrave Block south of the basin. The main highs, the Papunya and Blackstone Ridges, are centred over areas of metamorphic rocks, the Arunta and Musgrave Blocks. But on the other hand the lows, namely the Yuendumu, Amadeus, Ayers Rock and Purndoo Lows, are larger in extent than, and slightly offset from, the exposed basin areas.

The main highs are separated from the lows by steep gravity gradients. The gradients on the south flank of the Papunya Ridge and on the north flank of the Blackstone Ridge coincide approximately with the deformed zones on the northern and southern margins of the Amadeus Basin. The areas of the Amadeus and Purndoo Lows roughly coincide with the thickest parts of the Amadeus and northeast Officer Basins as indicated by the magnetic basement depths in Figure 5, and the gravity patterns over the major part of these basin areas are in qualitative agreement with the magnetic basement configuration. However, the Ngalia Basin lies on the southern flank of the Yuendumu Low, and its northern margin, a thrust fault, along the axis of the low. The southeastern margin of the Amadeus Basin lies roughly along the axis of the Ayers Rock Low.

Interpretation

Before the areal gravity coverage of central Australia was obtained, Marshall & Narain (1954) interpreted a north-south reconnaissance traverse in the area in terms of crustal deformation caused by compression in the crust. These authors also showed, from theoretical considerations of the elastic theory of bending of beams, that a crustal folding with wavelengths of 200 to 400 km and fractures about 85 km apart was possible. Forman (in Wells *et al.*, 1970)

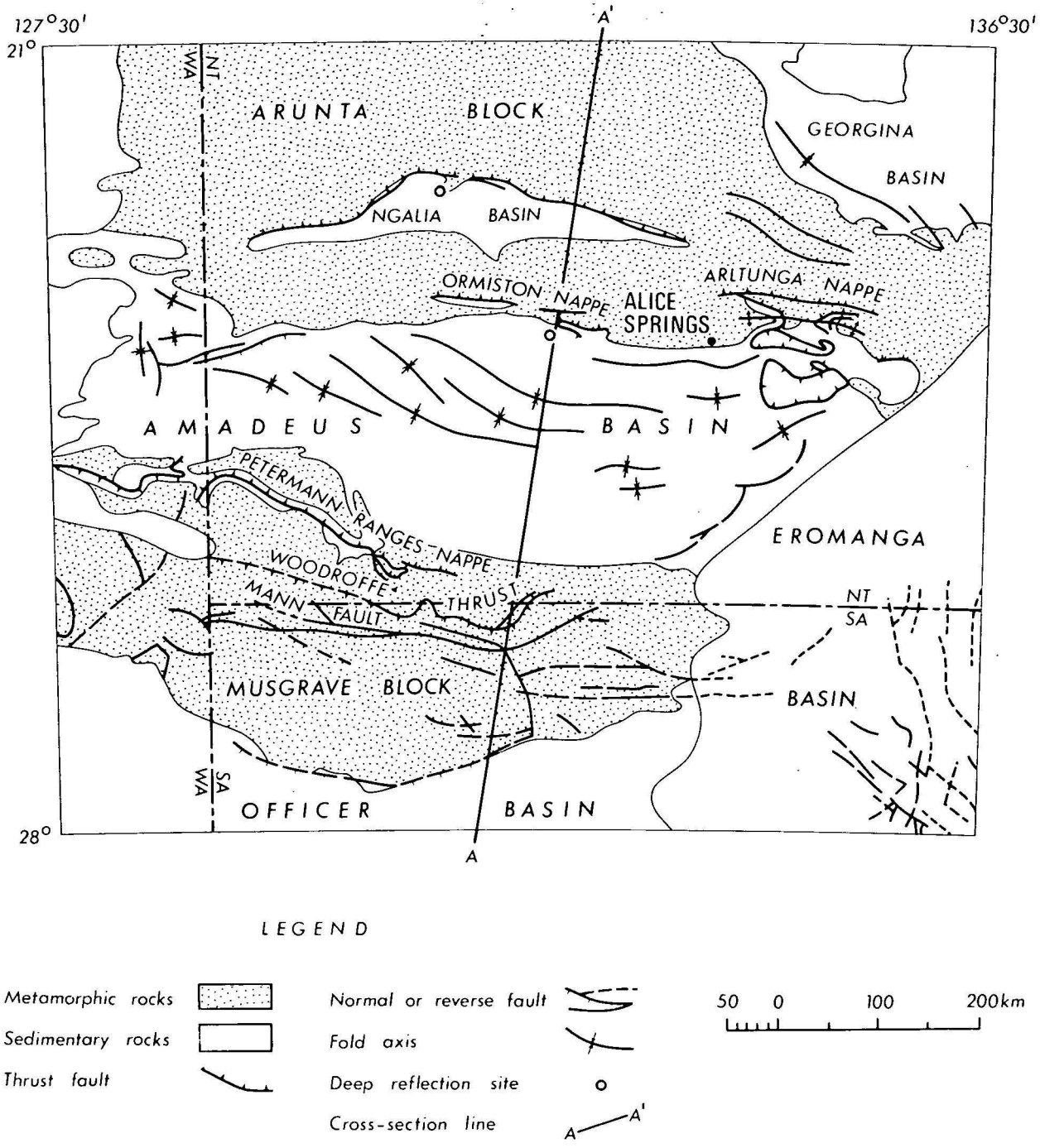

Figure 4. Simplified geological map of central Australia (after Geological Society of Australia, 1971). The prominent feature is the easterly trending series of anticlinoria of Precambrian metamorphic blocks and the intracratonic depressions filled with later sediments.

showed that the density contrast between the sedimentary rocks of the Amadeus Basin and the basement metamorphic rocks in the Arunta Block, assuming their densities to be 2.5 and 2.7 t/m^3 respectively, would produce an anomaly difference of only 50 mGal compared to the observed difference of 160 mGal. He showed also that the observed anomaly profile across the northern margin of the basin could be interpreted in terms of folding of a two-layer crust with densities of 2.7 and 3.0 overlying a mantle of density 3.3. An analysis of the Papunya Regional Gravity Ridge over the Arunta Block by Whitworth (1970) indicated that the source of the anomaly could be an uplifted block of denser crustal rocks, the top of which might not be deeper than 13 km. The distribution of granulite facies rocks in the Arunta Block suggested to Forman & Shaw (1973) that these lower crustal rocks might have been brought to the surface by major thrusts along the Ormiston and Arltunga Nappe Complexes at the northern margin of the Amadeus Basin. They therefore proposed that the folding and faulting in central Australia involved the entire crust and the upper mantle. However, the extent of folding and faulting proposed in their model is too intense, as the

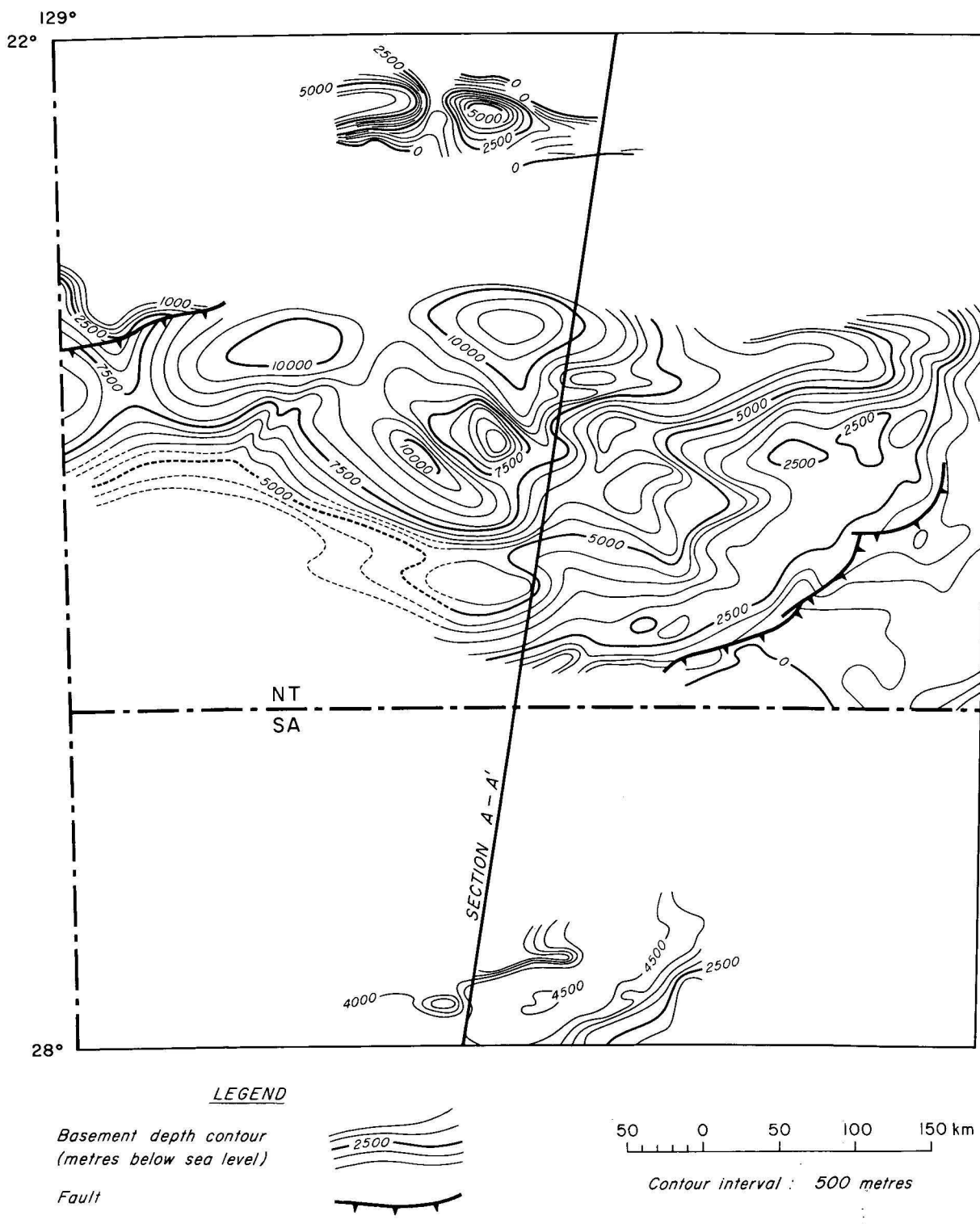

Figure 5. Magnetic basement depth map of central Australia (after Milton & Parker, 1973; Wells *et al.*, 1970; Wells *et al.*, 1972. Shallow seismic surveys have confirmed the basin shape and sediment thickness derived from magnetic data.

gravity anomalies computed for this model are about 200-300 mGal more than those observed in the metamorphic rock areas. Additional support for the hypothesis of folding and faulting involving the entire crust and upper mantle comes from the studies by Goode & Moore (1975), who estimated that the depths of primary crystallization of high pressure intrusive rocks found within the granulite terrain of the Musgrave Block are 35-40 km, and suggested that the uplift of these rocks to the surface was accompanied by sub-surface uplift of the upper mantle.

The contribution of near-surface variations in lithology to the gravity anomalies is assumed to be relatively small. This assumption is supported by the results of the detailed gravity survey across the Arltunga Nappe Complex in the eastern part of the Arunta Block (Anfiloff, 1975); the gravity profile obtained at 1 km spacing is essentially similar to that obtained from the regional survey at 11 km spacing, and the maximum difference between the measured values and those interpolated from the regional data is 10 mGal. The smoothness of the detailed gravity

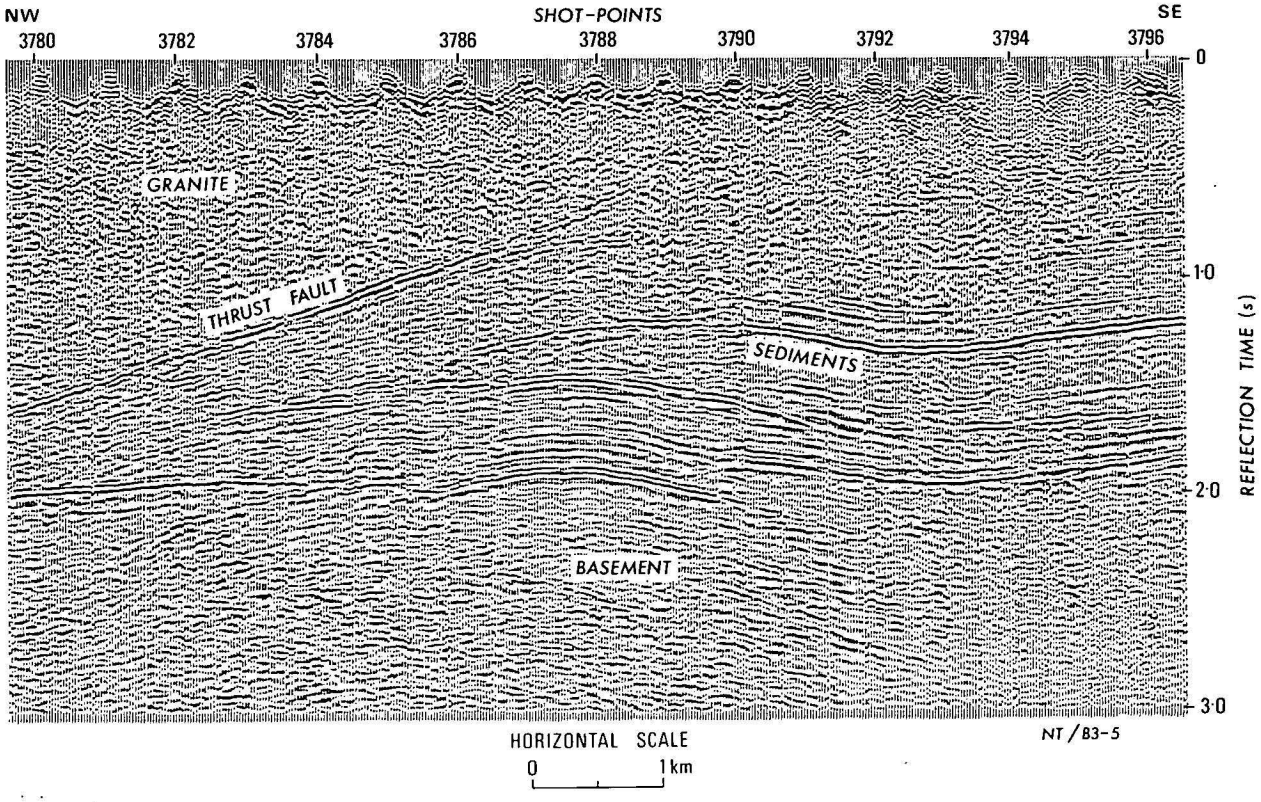

Figure 6. Seismic reflection section across the northern margin of the Ngalia Basin showing major overthrusting of granitic rocks on to the basin sediments (after Wells *et al.*, 1972). The overthrust fault shows a vertical displacement of about 5 km and a horizontal displacement of about 11.5 km.

profile implies that density variations are either deep-seated, or near-surface but gradual. As a wide variety of rocks—from acid to basic—and several faults, have been mapped in the area, the surface density changes are not gradual. It follows that most of the gravity anomaly is caused by density changes deeper in the crust. This conclusion is also supported by the long wavelength—about 150 to 200 km—of the main anomaly features (Fig. 8).

The relationships between the major features of the Bouguer anomalies and of the surface geology, as discussed above, suggest that both the anomalies and the geology are related to the structure of the crust down to the Mohorovicic discontinuity.

The predominant trend of the Bouguer anomaly and the main geological features is easterly. The relations between the anomalies, the geology and the crustal structure can therefore be studied meaningfully in a profile at right angles to them (AA', Figs. 4, 8 & 9). The surface geology, gravity anomalies and the interpreted structure of the crust along this profile are shown in Figure 9. The information shown in this figure was obtained from the following sources: the observed Bouguer anomalies from the Bouguer anomaly map (Fig. 8); the surface geology and structure incorporating results of recent geological mapping (R. D. Shaw, pers. comm.); the shapes of the Ngalia and Amadeus Basins from the depth to magnetic basement map (Fig. 5). In addition the shapes of the Officer Basin and its northern margin were assumed to be similar to that suggested by new seismic work and a re-interpretation of magnetic data (Milton & Parker, 1973).

Based on a density contrast of 0.15 t/m^3 between the granitic gneisses of crustal layer I and the sediments of the basins which are mainly lower Palaeozoic and Upper Proterozoic, the gravity effects for the basins were computed and subtracted from the observed values. The depths to the second crustal layer and the mantle were then derived from the remaining anomalies, assuming that most of the remaining anomaly was of deep crustal origin; that the thickness of the second crustal layer of basic granulites was constant; that the standard crust parameters found suitable for a similar analysis in southwestern Australia (Mathur, 1974a) were applicable; and that the upper mantle density in central Australia was 3.30 t/m^3.

No specific shapes and densities of the near-surface rocks, i.e. those mapped at the surface, are proposed in the model, nor are gravity effects computed for them because the knowledge of their subsurface distribution is inadequate. The contribution of the near-surface effects is however considered to be relatively small and is therefore not included in the computed anomalies shown in Figure 9. In the observed Bouguer anomaly profile, the shorter wavelength, i.e. the near-surface components, may also be attenuated because of the 11 km spacing of the original observations and because the profile has been interpolated from the contour map in Figure 8.

The match between the computed and the observed anomaly profiles is considered good everywhere except in the metamorphic block areas. For ease of computation, the density of the rocks in the uplifted blocks has been assumed to be 2.78 t/m^3, the same as that of the crustal layer I in other areas. If, however, the average density of these blocks, which contain a high proportion of denser granulite and amphibolite facies rocks, is assumed to be 2.83, the computed anomalies would show a better match with the observed values.

The lack of uniqueness inherent in the gravity interpretation and the poor knowledge of the lithological and density variations with depth make it possible to propose other subsurface models to explain the observed anomalies. One such model for central Australia has been proposed

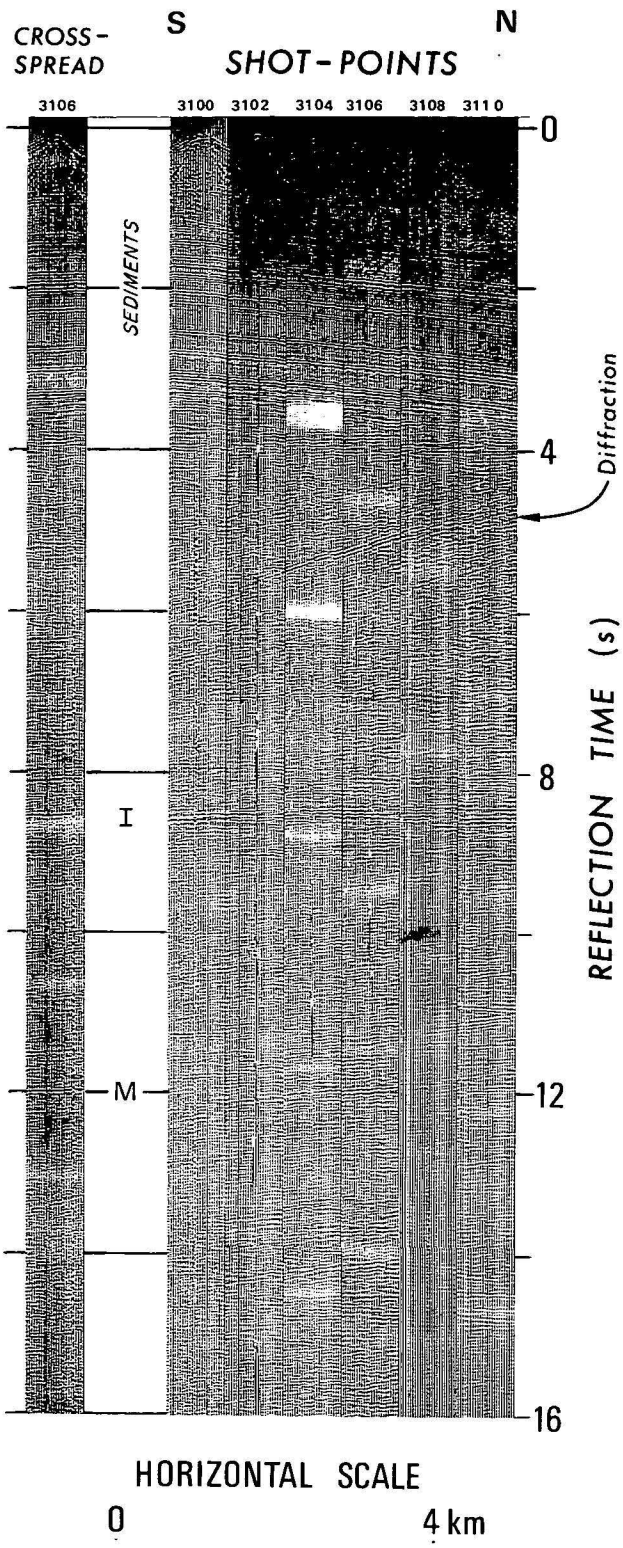

Figure 7. Seismic section in the north-central Amadeus Basin (after Brown, 1970). The two strong reflection events suggest depths of 24 and 36 km to the intermediate (I) and Mohorovicic (M) discontinuities.

by Anfiloff & Shaw (1973). The main assumptions made in their model are that all the major gravity low areas are underlain by huge granite masses of density 2.65, that most of the anomalies are caused by density variations within only the upper 20 km of the crust, and that the Conrad and Mohorovicic discontinuities at 20 and 35 km depths are flat interfaces, implying no structural or density variations in the lower crust. These assumptions are based on a theory that after each orogeny the stresses which caused the deformations in central Australia were released and the irregularities below 20 km in the crust, produced by the deformations, were annulled by a process of density equilibration consisting of diffusion, vertical separation of elements, and phase changes in minerals as a result of adjustment to new conditions of pressure and temperature. The plausibility of this model is therefore dependent on that of the theory of stress release and the process of density equilibration, as proposed by the authors, and not on deductions from the gravity analysis as the authors imply. A proper discussion of density equilibration is beyond the scope of this paper and requires a detailed study of the petrological and geochemical implications of the process in the context of the geological and tectonic history of the region. Nevertheless, seismic measurements in southwestern Australia (discussed above) as well as in other parts of Australia (Dooley, 1970), in Europe (Sollogub *et al.*, 1974), in USSR (Belyaevsky *et al.*, 1974) and in USA (Warren & Healy, 1974), indicate that the continental crust in tectonic areas shows up to 25 km of structural relief at the Mohorovicic discontinuity, and similar variation in its thickness, and is therefore not homogeneous below 20 km depths.

The results from the two deep reflection probes in the area provide support for the crustal model presented in Figure 9. The depths to the deep crustal interfaces are within 2 km of those estimated from the deep seismic data, namely 24 and 36 km respectively for the intermediate and Mohorovicic discontinuities under the northern Amadeus Basin and 38 km for the Mohorovicic discontinuity under the northern Ngalia Basin.

Conclusions

In southwestern Australia the longer wavelength component of the Bouguer anomalies is consistent with the shield crust, which is shown by seismic investigations to be greater than normal in thickness and density in the western part owing to the presence of a high-velocity basal layer. Positive gravity anomalies and a major tectonic feature, the Perth Basin, are associated with this abnormal crust.

The simple crustal model proposed for central Australia is considered to represent gross structure and composition which is consistent with the major features of the available geological and geophysical information.

The crustal folding and faulting shown in the model is compatible with the geological evidence in the area. Deep crustal rocks associated with large thrust faults, including high-pressure granulites, have been mapped in the Arunta and Musgrave Blocks; these are areas of crustal uplift. Sedimentary basins containing substantial thicknesses of sediments are present in the areas of crustal downwarp. The amplitude of uplift in the Arunta Block is of the same order as the displacement observed along the thrust faults at the northern margin of the Amadeus Basin.

The structural model is in general agreement with the hypothesis of crustal folding and faulting proposed earlier by Marshall & Narain (1954) on the basis of a reconnaissance gravity traverse; and by Forman & Shaw (1973) on the basis of the surface geology and structure mapped at the surface. However, the degree of folding and faulting inferred from the present analysis is not as high as that suggested by Forman & Shaw.

The shapes of the basins in the model have been derived primarily from the magnetic data, and the configuration of the intermediate and Mohorovicic discontinuities from the

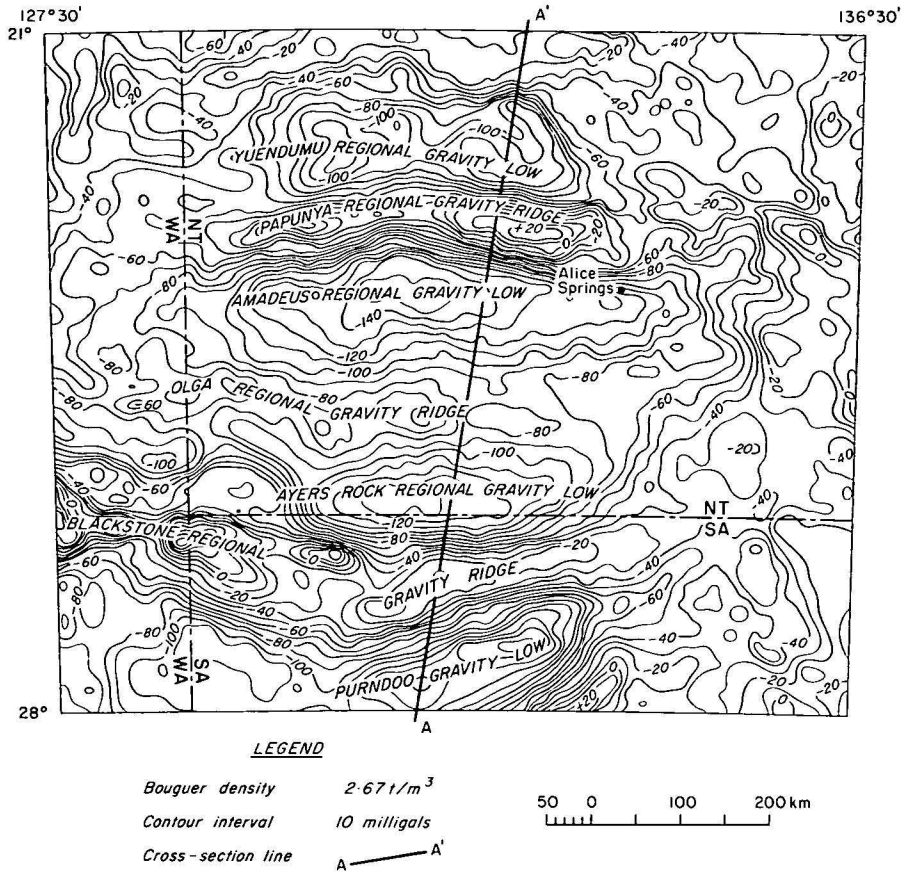

Figure 8. **Bouguer anomaly map of central Australia, showing the easterly trending series of regional gravity highs and lows; the highs are centred over metamorphic blocks and the lows are over, but slightly offset from, the basin areas (cf. Fig. 4).**

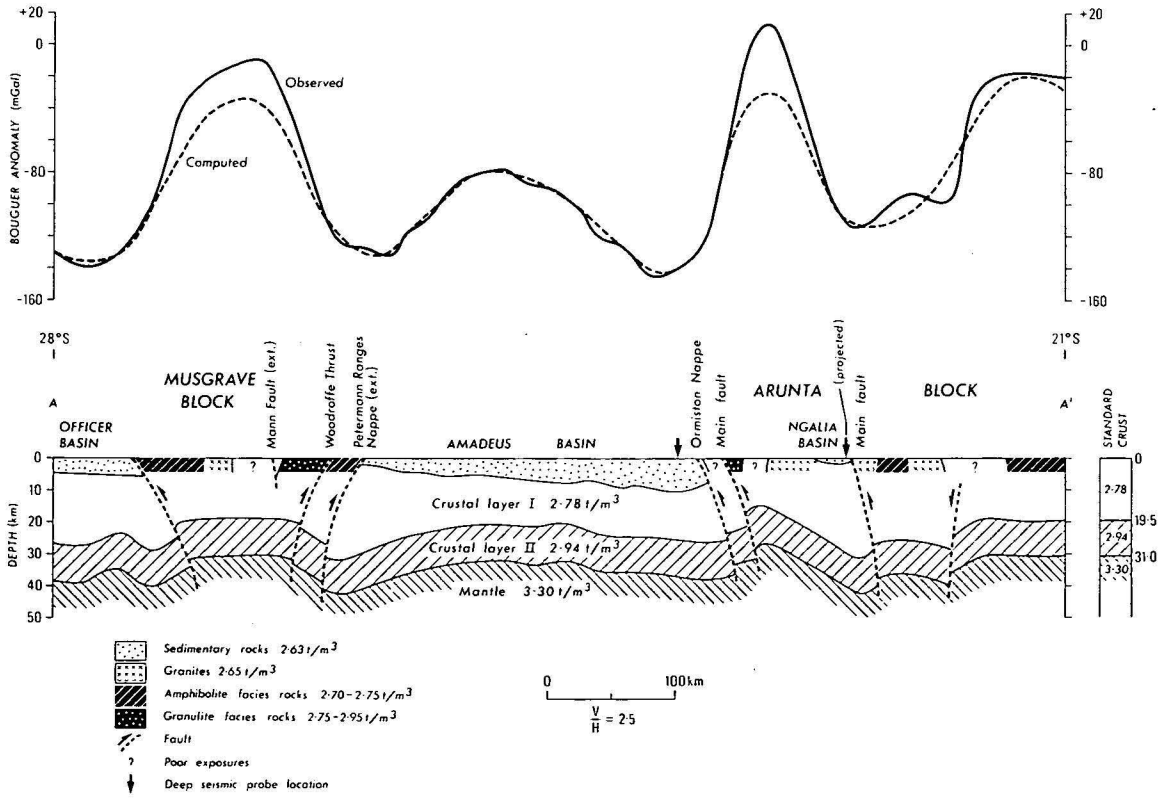

Figure 9. **Gravity profiles and a gross crustal structure model across central Australia interpreted from the Bouguer anomalies. The shorter-wavelength discrepancies between the computed and the observed anomalies are related to the near-surface geology. Geology after Shaw (pers. comm.). The depths to the crustal discontinuities in the northern Amadeus and Ngalia Basins are in agreement with the deep seismic reflection measurements.**

gravity data. The thickness of the sediments, and the depths to the intermediate crustal layer and the mantle in the northern parts of the Amadeus and Ngalia Basins are in agreement with those estimated from the seismic reflection data available in the area.

In order to test the validity of the proposed model systematic deep seismic sounding surveys, as suggested by Mathur (1974b), are required to investigate the structure at the intermediate and Mohorovicic discontinuities in detail.

References

ANFILOFF, W., 1975—Arltunga Nappe detailed gravity survey, N.T. 1973 *Bureau of Mineral Resources, Australia—Record* **1975/178** (unpublished).

ANFILOFF, W., & SHAW, R. D., 1973—The gravity effects of three large uplifted granulite blocks in separate Australian shield areas. *Proceedings Symposium on Earth's Gravitational Field & Secular Variations in Position, Sydney.* 173-289.

BELYAEVSKY, N. A., BORISOV, A. A., FEDYNSKY, V. V., FOTIADI, E. E., SUBBOTIN, S. I. & VOLVOVSKY, I. S., 1974—Structure of the earth's crust on the territory of the U.S.S.R.; *in* Stephan Mueller (Editor) THE STRUCTURE OF THE EARTH'S CRUST BASED ON SEISMIC DATA. *Developments in Geotectonics,* **8,** 35-45, *Elsenier, Amsterdam.*

BROWN, A. R., 1970—Deep crustal reflection studies, Amadeus and Ngalia Basins, N.T., 1969. *Bureau of Mineral Resources, Australia—Record* **1970/94** (unpublished).

DOOLEY, J. C., 1970—Seismological studies of the upper mantle in the Australian region. *Proceedings of the Second Symposium on Upper Mantle Project, December 1970, Hyderabad,* 113-146.

FORMAN, D. J., & SHAW, R. D., 1973—Deformation of the crust and mantle in central Australia. *Bureau of Mineral Resources, Australia—Bulletin* **144.**

FRASER, A. R., DARBY, F., & VALE, K. R., in preparation—A qualitative analysis of the results of the reconnaissance gravity survey of Australia. *Bureau of Mineral Resources, Australia—Record.*

GOODE, A. D. T. & MOORE, A. C., 1975—High pressure crystallization of the Ewarara, Kalka and Gosse Pile intrusions, Giles Complex, Central Australia. *Contributions to Mineralogy and Petrology,* **51,** 77-97.

GEOLOGICAL SOCIETY OF AUSTRALIA, 1971—Tectonic map of Australia and New Guinea, 1:5 000 000. *Sydney.*

KOSMINSKAYA, I. P., BELYAEVSKY, N. A., & VOLVOVSKY, I. S., 1969—Explosion seismology in the U.S.S.R.; *in* P. J. Hart (Editor), THE EARTH'S CRUST AND UPPER MANTLE. *Geophysical Monograph* **13,** 195-208, *American Geophysical Union, Washington, D.C.*

MARSHALL, C. E., & NARAIN, H., 1954—Regional gravity investigations in the eastern and central Commonwealth. *University of Sydney, Department of Geology & Geophysics—Memoir* **1954/2.**

MATHUR, S. P., 1974a—Crustal structure in southwestern Australia from seismic and gravity data. *Tectonophysics,* **24,** 151-182.

MATHUR, S. P., 1974b—A proposal for a deep seismic sounding and associated gravity survey in central Australia. *Bureau of Mineral Resources, Australia—Record* **1974/69** (unpublished).

MILTON, B. E., & PARKER, A. J., 1973—An interpretation of geophysical observations on the northern margin of the eastern Officer Basin. *Quarterly Geological Notes, Geological Survey of South Australia,* **46,** 10-14.

MOSS, F. J., 1964—Gosses Bluff seismic survey, Amadeus Basin, Northern Territory, 1962. *Bureau of Mineral Resources, Australia—Record* **1964/66** (unpublished).

SOLLOGUB, V. B., PROSEN, D., & CO-WORKERS, 1974—Crustal structure of central and southeastern Europe by data of explosion seismology; *in* Stephan Mueller (Editor), THE STRUCTURE OF THE EARTH'S CRUST BASED ON SEISMIC DATA. *Developments in geotectonics,* **8,** 1-33, *Elsevier, Amsterdam.*

WARREN, D. H., & HEALY, J. H., 1974—Structure of the crust in the conterminous United States; *in* Stephan Mueller (Editor), THE STRUCTURE OF THE EARTH'S CRUST BASED ON SEISMIC DATA. *Developments in Geotectonics,* **8,** 203-213, *Elsevier, Amsterdam.*

WELLS, A. T., FORMAN, D. J., RANFORD, L. C., & COOK, P. J., 1970—Geology of the Amadeus Basin, central Australia. *Bureau of Mineral Resources, Australia—Bulletin* **100.**

WELLS, A. T., MOSS, F. J., & SABITAY, A., 1972—The Ngalia Basin, Northern Territory,—Recent geological and geophysical information upgrades petroleum prospects. *APEA Journal,* **12,** 144-151.

WHITWORTH, R., 1970—Reconnaissance gravity survey of parts of Northern Territory and Western Australia, 1967. *Bureau of Mineral Resources, Australia—Record* **1970/15** (unpublished).

WOOLLARD, G. P., 1959—Crustal structure from gravity and seismic measurements. *Journal of Geophysical Research,* **64,** 1521-1544.

WOOLLARD, G. P., 1968—The interrelationship of the crust, the upper mantle and isostatic gravity anomalies in the United States; *in* L. Knopoff, C. Drake & P. Hart (Editors), THE CRUST AND UPPER MANTLE OF THE PACIFIC AREA. GEOPHYSICAL MONOGRAPH **12,** 312-341, *American Geophysical Union, Washington, D.C.*

The gravity field of the Australian basement

Peter Wellman

The Australian gravity field is analysed to determine whether the basement differs between regions of exposed basement and of covered basement (sedimentary basins). When the thickness of cover is allowed for, there is no systematic change in gravity variability from exposed to covered basement regions and the pattern of density differences is inferred to be similar in the two basement types. With one exception the trends of the gravity anomalies are continuous from covered to exposed basement regions; therefore geological structure and rock formations in the basement are considered to be continuous between the two kinds of regions. After making allowance for altitude and the effects of cover beds, the covered basement is calculated to have gravity anomalies that average 5 mGal less than the exposed basement. This gravity difference is probably caused by the two kinds of basement not being isostatically balanced relative to each other, rather than the basements having a different average density. No major differences between exposed and covered basement are apparent. It is likely that the two basement types have a similar history of formation, and consequently similar mineral potential.

Introduction

Continental crust consists mainly of basement with a thin layer of covering beds in the regions that are known as basins. The basement is thus partly covered and partly exposed. For Australia about 60 percent of the basement is covered. Covering beds are essentially undeformed and at places contain minor amounts of volcanic rock. The basement consists of metamorphic and intrusive rocks, together with some strongly deformed sedimentary rocks. In most places the division between the covering beds and basement is clearly defined, but the cover beds are of different ages in different parts of Australia.

The basins are major geological features, but their mode of origin is not fully understood. A point of major importance is the nature of the basement itself. Is it different where it is hidden below the basins from where it is exposed between the basins? Gravity observations provide limited information on this point. For Australia there is complete gravity coverage with a maximum distance between observations of 11 km. These observations are analysed below in terms of mean anomaly, variability and trend with respect to the covered and exposed basement.

Mean gravity anomalies

Gravity anomalies above exposed basement have been compared with those above covered basement, using mean values for one-degree areas. The values have been reduced to a common altitude by plotting free-air anomalies against altitude separately for areas of exposed basement and of covered basement. Values in eastern Australia have been treated separately because they have a different gravity/altitude relation (Wellman, 1976b); the boundary between the two areas is shown as a dashed line in Figure 1. A least-squares straight line has been determined for each of the four sets of data; it is found that within each area the lines for exposed and covered basement regions do not differ significantly in slope. The mean gravity difference between exposed and covered basement regions is the gravity difference between the least-squares lines at the mean altitude of the observations. This is found to be 9.6 ± 1.7 mGal in eastern Australia, and 10.6 ± 1.7 mGal over the remainder, the exposed basement having higher gravity values.

If the cover thickness varies gradually, if cover is much wider than the depth of compensation, and if the crust is in isostatic equilibrium, then there will be almost no free-air anomaly expression of the cover region. In the other extreme, if the cover is very narrow relative to the depth of compensation then compensation can be ignored, and the free-air anomalies will express the full gravity attraction of the cover. The Australian cover areas are intermediate between these two extreme examples. Taking the known cover geometry, and the most likely density distribution, the cover is estimated to contribute about 5 mGal in both eastern and the remainder of Australia, so in both regions there is about 5 mGal to be explained.

This 5 mGal could be explained if there was a density difference between the covered and exposed basement. If the density difference is assumed to extend down to the base of the crust then it needs to be about 0.01 t/m^3; if the density difference does not extend so far down then it will be correspondingly greater.

However this explanation assumes perfect isostatic equilibrium, and it is known that the cover areas have a history of movement downward relative to the exposed basement areas (legend of Geological Society of Australia, 1971), even though erosion tends to make the surface levels of the two regions equal. It is likely therefore that the areas are not in isostatic equilibrium, and there is no density difference between them. The explanation for the gravity difference I prefer is to assume that the two types of basement have the same density, and that the covered basement is being pulled down, or that the exposed basement is being pushed up beyond an isostatic position. The isostatic imbalance of 5 mGal is equal to the gravitational attraction of a thickness of about 35 m of basement rock. It is thus suggested that the 5 mGal gravity difference is caused by relative vertical movement taking place between the two different types of areas at the present day.

Gravity variability

Variations in crustal density are caused by mafic and felsic intrusions, and faulting and folding of igneous, metamorphic and sedimentary rocks. These lateral variations in crustal density are the main cause of the variability of gravity anomalies. The gravity variability mapped in Figure 1 is the standard deviations of 0.1° x 0.1° Bouguer anomalies within a one-degree area, where each 0.1° x 0.1° Bouguer anomaly is the mean of the simple Bouguer anomalies of stations in that area. Because of the station distribution there are only about 90 available 0.1° x 0.1° values in each one-degree area; however this is sufficient for standard deviations to be well determined. Gravity variability is generally small in eastern Australia relative to the rest of Australia, and is generally smaller over covered basement than over exposed basement. Within about 2° of the continental edge the gravity variability reflects principally the gradient of the continental edge gravity anomaly.

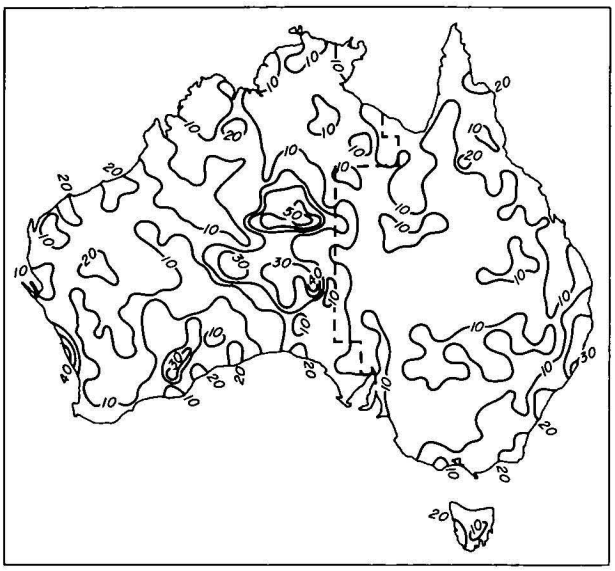

Figure 1. Gravity variability in milligal—standard deviation of 0.1° x 0.1° area Bouguer anomaly values in one degree areas. The dashed line is the boundary between regions with different free-air anomaly-altitude relations.

Figure 2 shows the gravity variability plotted against cover thickness for eastern and western Australia, omitting areas within 200 km of the continental edge. The cover thicknesses are the mapped depth from sea level to basement (Geological Society of Australia, 1971) corrected for ground height. In eastern Australia cover thicknesses are known from geology, seismic reflection and drilling; strongly deformed sedimentary areas are considered as basement. In western Australia cover thicknesses are approximated by depth to aeromagnetic basement; the sedimentary area where these depths are not available has been omitted. The gravity variability in central Australia is not plotted, because cover thicknesses are not known in the north, and the rest of the area is dominated by anomalously high amplitude anomalies with long wavelength, where the gravity variability is thought to be dominated by variations in crustal thickness (Wells *et al.*, 1970).

A gravity anomaly caused by basement density variation has its amplitude attenuated if it is measured above an appreciable thickness of cover. For a gravity anomaly with a peak-to-peak wavelength w, then

$$A_z/A_o = \exp(-2\pi z/w),$$

where A_o and A_z are the anomaly amplitudes on exposed basement and on a thickness z of cover. Gravity variability is assumed to be similarly attenuated with increased cover thickness, the degree of attenuation depending on the wavelength as described above. The dominant wavelength on exposed basement in eastern Australia is 50 to 80 km. Figure 2a shows that for an assumed dominant wavelength of 65 km the observed attenuation is consistent with the predicted attenuation for high and low values of gravity variability. The dominant wavelength over exposed basement in the western part of Australia ranges from 50 to 200 km. Because of the longer mean wavelength the attenuation should be smaller than in eastern Australia, and this is apparent in Figure 2. When attenuation is allowed for, the mean gravity variability on covered basement is not significantly different from that on exposed basement both in eastern and western Australia. The surface topography is on the average rougher over exposed basement than over covered basement, so on exposed basement the effect of terrain is higher, leading to a higher gravity variability. The gravity variability on covered basement due to density changes within the basement itself is increased because of the gravity effects due to abrupt changes in cover thickness. This effect is considerable in narrow, deep basins with faulted margins such as those in central and southwest Australia. Elsewhere both these increases in gravity variability over covered and exposed basement will be relatively minor. Hence in both eastern and western Australia the measured distribution of gravity variability is consistent with the density variability of the exposed basement rocks being the same as the variability of the covered basement rocks.

Gravity trend lines

Over the exposed basement the gravity trend lines, axes of elongate highs and lows, agree in position and direction with the structural trend lines defined by geological mapping and represented by elongate intrusions, major folds, and major faults. The gravity trend lines, unlike the geological ones, can be delineated over almost the whole of Australia, including areas where the basement is covered (Wellman, 1976a). Structural basement trend lines may thus be inferred over almost the whole of Australia, and can be used to find whether the covered and exposed basements differ.

At the line of contact between exposed and covered basement there are three observed situations: two sets of trend lines parallel to each other and parallel to the line of contact; two sets of trend lines at an angle to each other, one set being parallel to the line of contact; and two sets of trend lines that are parallel and continuous across the line of contact. The last is the critical situation. It is assumed to indicate that structural trends extend across the boundary between exposed and covered basement, and hence that the two basements are the same structurally, have the same history of formation, and, almost certainly, the same

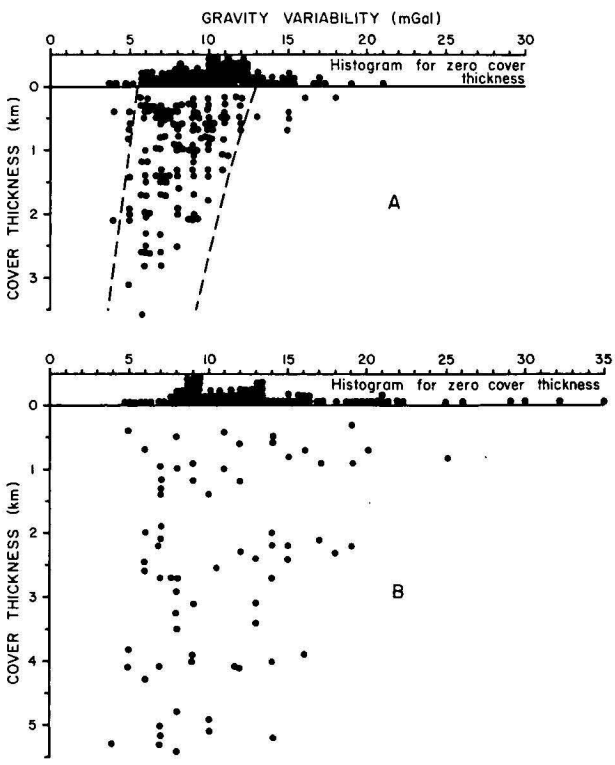

Figure 2. Relation between gravity variability and cover thickness in (A) eastern Australia and (B) western Australia. The dashed lines show the shape of attenuation predicted for 65 km wavelength anomalies.

Figure 3. Relation between the gravity trend pattern and the region of covered basement (clear) and exposed basement (stippled).

density and overall composition. Figure 3 shows that this critical situation exists for some parts of almost all the contacts between exposed and covered basement. The area of covered basement in north-western Australia known as the Kimberley Basin is the sole exception.

Harrington, Burns and Thompson (1973) have postulated that the Officer, Canning and Great Artesian Basins were formed in the late Proterozoic to middle Cambrian by the break up of Australia into four sub-plates. The break up was about poles in the Officer and Eucla Basins with marginal seas forming between the sub-plates (Harrington, 1974), the marginal seas subsequently becoming continental crust, presumably without changing in area. However the gravity trend pattern is continuous from much of the postulated marginal sea area into adjacent postulated sub-plates, and gravity trends are not in the expected directions either at right angles or parallel to the small circle of opening. Since the gravity trends, and presumably the geological trends, are not consistent with the marginal sea model this origin for the basin areas seems unlikely. The unity of the Australian continent through time is also indicated by the palaeomagnetic results from Australian Precambrian rocks (McElhinny & Embleton, 1976).

Discussion

For Australia the gravity observations provide data on two related matters of major geological importance: 1. The degree of uniformity of the basement in Australia, and in particular whether the covered basement is significantly different from the exposed basement; and 2. The method by which some basement is continually uplifted and eroded, while elsewhere it is continually depressed and covered by layers of sedimentary strata. Considered together the two are simply the problem of the difference between uplift areas and basins.

How basins form depends on the degree of isostatic balance that exists and has existed throughout time. If balance is not assumed to be perfect, then basement can move up and down to a limited extent; the causes of the movement being unknown forces beneath the basement, and not changes in the density of the basement itself. On the other hand if isostatic balance is assumed to be perfect, then the basement of what is to become a basin must become denser relative to the other basement, and no unknown forces are needed. Similarly there are two possible modes of origin of uplift areas.

The Australian gravity field is consistent with there being no appreciable difference between adjacent exposed and covered basement in mean density, density variability, or history of formation. Hence unknown forces acting after the basement was formed and stabilized are required to explain the formation of basins and uplift areas and explain their continued existence. Exposed and covered basement are interpreted to have a similar history until after stabilization, so it is inferred that they have a similar mineral potential.

Acknowledgements

I am grateful for the help given by Dr H. W. Wellman and Mr F. J. Moss in the preparation of this paper. The illustrations were drawn by the gravity drafting group of the Geophysical Drawing Office, BMR.

References

GEOLOGICAL SOCIETY OF AUSTRALIA, 1971—Tectonic map of Australia and New Guinea, 1:5 000 000. *Sydney*.

HARRINGTON, H. J., 1974—The Tasman Geosyncline in Australia; *in* DINMEAD, A. K., TWEEDALE, G. W., & WILSON, A. F. (Editors, THE TASMAN GEOSYNCLINE, A SYMPOSIUM IN HONOUR OF PROFESSOR DOROTHY HILL, 383-407. *Queensland Division of the Geological Society of Australia, Brisbane*.

HARRINGTON, J. M., BURNS, K. L., & THOMPSON, B. R., 1973—Gambier-Beaconsfield and Gambier-Sorell Fracture Zones and the movement of plates in the Australia-Antarctica-New Zealand region. *Nature Physical Science*. **245,** 109-12.

MCELHINNY, M. W., & EMBLETON, B. J. J., 1976—Precambrian and early Palaeozoic palaeomagnetism in Australia. *Philosophical Transactions of the Royal Soceity of London*, **A280,** 417-31.

WELLMAN, P., 1976a—Gravity trends and the growth of Australia—tentative correlation. *Journal of the Geological Society of Australia*, **23,** 11-4.

WELLMAN, P., 1976b—Regional variation of gravity, and isostatic equilibrium of the Australian crust. *BMR Journal of Australian Geology & Geophysics*, 1, 297-302.

WELLS, A. T., FORMAN, D. J., RANFORD, L. C., & COOK, P. J., 1970—Geology of the Amadeus Basin, Central Australia. *Bureau of Mineral Resources, Australia—Bulletin* **100**.

BMR Journal of Australian Geology & Geophysics, 1 (1976), 291-296

Variation of crustal mass over the Australian region

J. C. Dooley

Seismic refraction surveys in Australia and nearby marine areas provide data on crustal velocities and layer thicknesses. The averages of these at various places have been used to estimate a density-depth structure. By applying corrections for average elevation and free-air gravity, a crustal mass deficiency (CMD) is calculated for each site; this characterizes a standard crustal column with zero elevation and zero free-air anomaly, which is considered to be in isostatic equilibrium over a mantle of uniform density 3.32 t/m³.

The CMD ranges from about 13 kt/m² in the south-west of the continent, to about 21 in parts of Queensland; marine values range from 15 to 17 kt/m². The variations imply that isostasy on a broad scale is not complete at the base of the crust. As the gravity field indicates that departures from isostasy are comparatively small, compensation must occur partly in the mantle.

Introduction

The existence of gravity anomalies is evidence that lateral density variations occur in the earth's crust and mantle. The deeper density variations tend to produce anomalies of longer wavelength; however this property cannot be used to separate, uniquely, anomaly sources at various depths. Free-air anomalies averaged over large enough areas are relatively small, and hence the near-surface mass variations are to a large degree isostatically compensated; however the depth of compensation, or the degree to which compensation occurs in the crust or the lithosphere cannot be determined uniquely from the gravity field alone.

Wellman (this volume) models crustal density and thickness variations on the basis of assumptions that one degree squares are isostatically compensated at the base of the crust, and that residual free-air anomalies result from lateral variations in crustal density. In the present paper isostasy at the base of the crust is not assumed; variations in crustal mass are calculated from a combination of gravity and seismic refraction measurements, with a view to studying to what extent departures from isostasy can be attributed to crustal mass distribution, and whether significant lateral density variations must be attributed to the uppermost mantle; and whether the crustal and mantle mass variations form a pattern which can be used in interpreting other geophysical results.

The approach adopted starts with seismic refraction evidence for crustal layering from surveys in Australia and surrounding marine areas. A mean velocity-density curve is used to convert the refraction velocities to densities. These are used, in conjunction with elevation and gravity data, to establish a standard crustal mass deficiency (CMD) with respect to a hypothetical mantle of uniform density extending to sea level. The CMD is found to vary considerably over Australia, so that in order to achieve approximately isostatic balance, either mantle density variations or undetected crustal layers (e.g. low velocity, or thin 'hidden layers'), or both, are required.

The standard crustal mass deficiency

Many authors have estimated standard sea-level crustal models: generally defined by the parameters standard depth to the base of the crust H_s, average density of crust ϱ_s, and density of mantle ϱ_m. It is generally assumed that isostatic compensation occurs at the crust/mantle boundary. For different elevations, isostasy may be maintained by varying either crustal thickness T, or average crustal density ϱ_c. The actual parameters used are generally derived from seismic data, often by statistical analysis.

The essential feature of such models is the CMD, the deficiency of mass of the crustal column by comparison with the hypothetical situation with mantle material present up to sea-level, i.e. $M = (\varrho_m - \varrho_s) H_s$. It is this quantity which is kept constant for local isostasy when T or ϱ_c is varied. Thus we define M as the 'standard crustal mass deficiency'; if crustal isostasy were true, it should be constant everywhere.

However, since isostatic anomalies calculated on any of the standard hypotheses (Pratt-Hayford, Airy-Heiskanen, or Vening-Meinesz) are not zero everywhere, the possibility must be admitted of departures from isostatic equilibrium, maintained either by finite strength in the crust or mantle, or by tectonic forces. On a broad scale, free-air anomalies indicate such departures. For a uniform slab or disc of crust covering an area several times as wide as its thickness, with an excess mass above that required for isostatic equilibrium, the excess pressure on the mantle is proportional to the excess mass per unit area; the free-air gravity anomaly is also proportional to the excess mass per unit area of the slab.

In the following calculations, it is assumed that the crustal layers are of sufficient lateral extent so that their average attraction approximates that of an infinite horizontal slab, i.e. $2\pi k\varrho T$, where k is the gravitational constant, ϱ is density in t/m³ and T is thickness in km; for anomalies in mGal, the factor $2\pi k$ is 41.85. Calculations using simple models such as rectangular prisms of infinite strike and vertical cylinders, show that for widths of about 10 T the average anomalies are about 0.9 of the infinite slab effect.

Thus the approach is applicable to stable areas of low relief, where the crustal layers may be expected to have reasonably constant properties over distances of several times the crustal thickness. It is not recommended for active tectonic areas, where local changes in topography and crustal structure are common.

In order to establish the CMD for an actual layered crust, a series of hypothetical crustal columns is depicted in Figure 1, and the gravity changes are calculated for successive replacement of the columns from (1) to (6). The hypothetical 'observed' gravity over column 1, corrected for normal gravity but not for elevation, is represented by g_i ($i = 1, \ldots . 6$)

Column (1) represents a standard crust; as the surface elevation is zero, its free-air gravity anomaly is

$$g_i = g_s \qquad \ldots . (1)$$

where g_s is a standard regional gravity field, supposed to be due to very broad or deep density variations below the 'level of compensation'.

In column (2), the standard crust is replaced by mantle material of density ϱ_m giving

$$g_2 = g_1 + 41.85\ H_s\ (\varrho_m - \varrho_s) \qquad \ldots . (2)$$

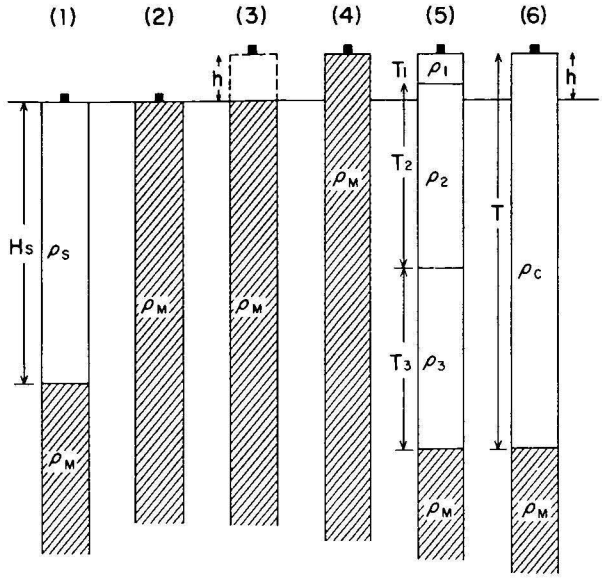

Figure 1. Derivation of formulae for crustal mass deficiency.

In column (3), the gravity meter is raised to the height of the topography h above sea level; the free-air effect gives

$$g_3 = g_2 - 308.6\,h \qquad \ldots . (3)$$

In column (4), material of mantle density is added between the gravity meter and sea level, giving

$$g_4 = g_3 + 41.85\,\varrho_m h \qquad \ldots . (4)$$

Next, the mantle material is replaced by the actual crustal layers of thickness T_i and density ϱ_i (i = 1, 2, ...), giving

$$g_5 = g_4 - 41.85\,\Sigma\,T_i\,(\varrho_m - \varrho_i) \qquad \ldots . (5)$$

Alternatively, this may be expressed in terms of total crustal thickness T and average density ϱ_c:

$$g_6 = g_5 = g_4 - 41.85\,T\,(\varrho_m - \varrho_c) \qquad \ldots . (6)$$

where $T = \Sigma\,T_i$ and $\varrho_c = \Sigma\,T_i\varrho_i/T$

Free-air and Bouguer anomalies g_F and g_B are calculated as usual:

$$g_F = g_6 + 308.6\,h \qquad \ldots . (7)$$

$$g_B = g_F - 41.85\,h\varrho_B \qquad \ldots . (8)$$

where ϱ_B is the Bouguer density.

Substituting from equations (3) to (6), we get

$$g_F = g_2 + 41.85\,[\varrho_m h - T\,(\varrho_m - \varrho_c)] \qquad \ldots . (9)$$

We assume that the residual free-air anomaly $g_F - g_s$ is due to crustal mass departing from that required for isostasy. The equivalent standard CMD for isostasy is then given by eliminating g_2 from (2) and (9):

$$M = H_S(\varrho_m - \varrho_S) = (g_F - g_S) / 41.85 + T(\varrho_m - \varrho_C) - h\varrho_m \qquad \ldots . (10)$$

If Bouguer anomalies are used, the expression becomes

$$M = (g_B - g_S) / 41.85 + T(\varrho_m - \varrho_c) - h(\varrho_m - \varrho_b) \qquad \ldots . (11)$$

For oceanic sites, h = 0, T_1 is taken as the ocean depth, and $\varrho_1 = 1.03$ t/m³; for sedimentary basins whose thickness and density can be estimated, appropriate values can be included in the summation.

Equations (9), (10) and (11) are equivalent to those derived previously by many authors, e.g. Frolov (1964), Woollard (1969). With slight modification they can be expressed in terms of depth to mantle H instead of thickness of crust T, where H = T − h. In (11), the Bouguer density ϱ_B is arbitrary, and need not be the same as ϱ_c or the near surface density, although it is obviously advantageous for it to be close to actual densities.

In the present paper equation (10) is used, because of the relation of free-air anomalies to crustal load and attraction, and also because the assumption of a value for ϱ_B is avoided. The use of T rather than H facilitates assigning densities for layers from the surface downwards, without any special significance at sea level.

Refraction data

The next step is to calculate the CMD M from (10) for the various models derived from refraction experiments in Tables 1 and 2, and Figures 2 and 3; a standard mantle density of 3.32 has been adopted for the calculations, based on Clark & Ringwood (1964).

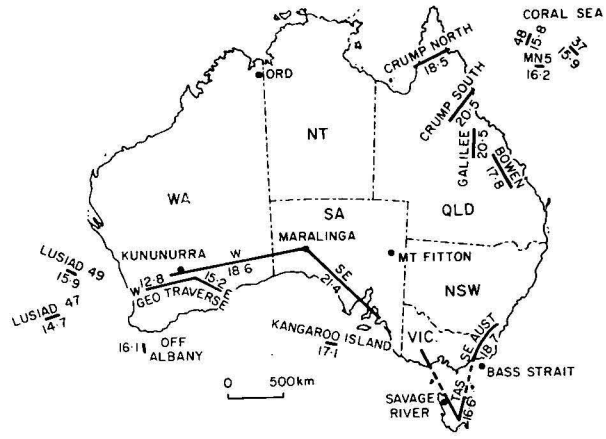

Figure 2. Location of seismic refraction surveys and values of crustal mass deficiency.

The refraction data are those reported in review papers by Dooley (1972), and Cleary (1973), with the following additions or modifications.

(a) A reinterpretation of the data in the West Australian shield area (the 'Geotraverse') by Mathur (1974).

(b) A single-ended spread in the Galilee Basin of northern Queensland (Cull and Riesz, 1972).

(c) A reversed profile using quarry blasts in the Bowen Basin of Central Queensland (Collins, pers. comm.).

(d) Marine profiles in the Indian Ocean offshore from Western Australia, being part of the *Lusiad* cruise (Francis & Raitt, 1967).

(e) A modification of the previous model of a single layer crust with average thickness of 25.6 km in Tasmania, by insertion of a lower crustal layer of 6.7 km/s below 21 km, as determined by Cameron (1971) from Savage River mine explosions.

Mantle velocities have been corrected for curvature (Mereu, 1967) where it appeared that this had not been done.

Other large explosions which have been recorded since 1971 include those at the Ord River damsite, Western Australia (Denham *et al.*, 1972), and the Trans-Australia seismic survey with three shots near Kununurra, Western Australia, Mount Fitton, South Australia, and in Bass

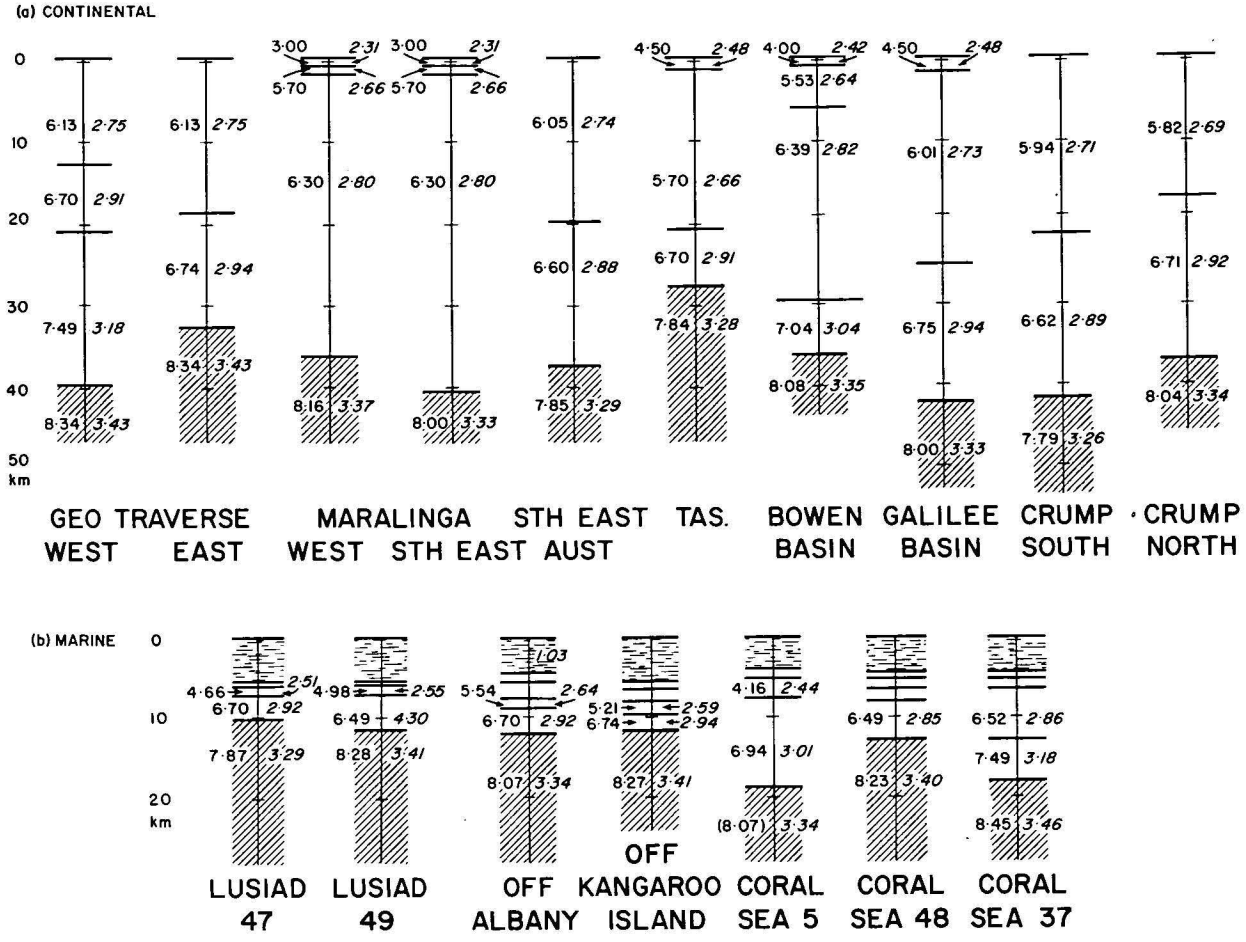

Figure 3. **Crustal columns from seismic refraction data—(a) Continental; (b) Marine. The numbers on the left of the columns give P wave velocities in km/s and those on the right densities in t/m³. Values for the thin layers at the top of the marine columns are given in table 2.**

Strait off the coast of Victoria (Finlayson *et al.*, 1974; Muirhead *et al.*, in press). However, as the recording equipment was set at large distances from the shot points in order to take full advantage of the large explosive charges used, these surveys contributed valuable information about the velocities and layering in the upper mantle, but little direct information on the crust; in fact the authors in general assume a crustal structure as a basis for interpreting the deeper layering.

The locations of the refraction lines are shown in Figure 2, and the models derived for them are summarized in Tables 1 and 2, and Figure 3a and b. For most lines, an average model near the centre of the line is used, unless conditions change along the line to such a degree that a separate model is warranted near each end of the line (e.g. Geotraverse), or in two parts of an area (e.g. CRUMP).

Estimation of densities from velocities

Many authors have published empirical curves showing a relation between seismic velocity and density for crust and mantle rocks, e.g. Woollard (1959, 1968), the Nafe-Drake curve (Talwani *et al.*, 1959), Birch (1961).

Most of these curves give the mean relations for igneous and metamorphic rocks with velocities greater than about 5.5 km/s and densities greater than about 2.6 t/m³; the Nafe-Drake curve continues into lower velocities and densities, using information for marine sediments; it does not apply for continental sediments.

The curve used here is a compromise between several of the published curves in the higher velocity-density region as shown in Figure 4. (A similar curve was used by Mathur (1974)). The Nafe-Drake curve has been used for marine sediments. For continental sediments, a curve has been drawn based on a limited amount of field data and laboratory measurements; a more reliable curve could no doubt be drawn from analysis of the large amount of data now available, but the results of the present investigation would be unlikely to be affected significantly as the sedimentary corrections are generally small. Tables 1 and 2,

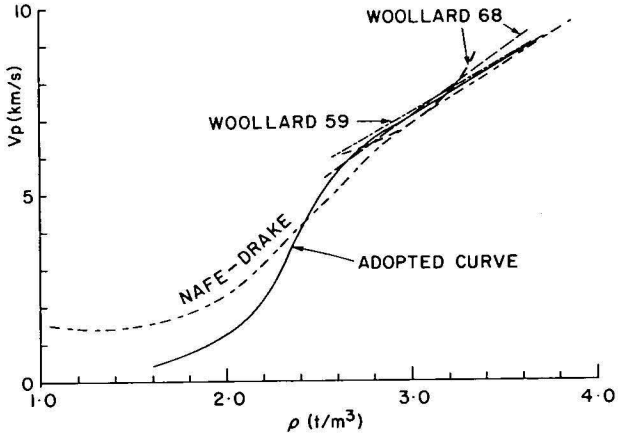

Figure 4. **Empirical velocity-density relations.**

Traverse	M(kt/m²)	Approx. location (°S, °E)	h(km) M_h	g_F g_s M_g	Shallow Layers V_i km/s	T_i km	ϱ_i t/m³	M_i ΣM_i	Deep Layers V_j km/s	T_j km	ϱ_j t/m³	M_j ΣM_j	Mantle V H	ϱ
Geotraverse West		31.6	0.30	0					6.13	13.0	2.75	7.40	8.34	3.43
		119.0		−20					6.70	8.0	2.91	3.28		
									7.49	19.0	3.18	2.66	39.7	
	12.8		−1.00	0.48								13.34		
Geotraverse East		32.0	0.36	−12					6.13	19.0	2.75	10.82	8.34	3.43
		123.0		−23					6.74	14.0	2.94	5.31	32.6	
	15.2		−1.20	0.26								16.13		
Maralinga West		30.5	0.25	−20	3.00	0.5	2.31	.50	6.30	35.0	2.80	18.20	8.16	3.37
		126.0		−21	5.70	1.0	2.66	.66					36.2	
	18.6		−0.83	0.02				1.16				18.20		
Maralinga Southeast		32.5	.10	0	3.00	0.5	2.31	.50	6.30	39.0	2.80	20.28	8.00	3.33
		135.5		−14	5.70	1.0	2.66	.66					40.4	
	21.4		−0.33	0.33				1.16				20.28		
Southeast Australia		36.0	0.50	40					6.05	20.0	2.74	11.60	7.85	3.29
		148.8		3					6.60	18.0	2.88	7.92	37.5	
	18.7		−1.66	0.88								19.52		
Tasmania		42.0	0.37	35	(4.50)	(1.5)	2.48	1.26	5.70	19.5	2.66	12.87	7.84	3.28
		147.0		−2					6.70	7.0	2.91	2.87	27.6	
	16.6		−1.23	0.88				1.26				15.74		
Bowen Basin		23.3	0.20	24	4.00	1.0	2.42	0.90	5.53	5.0	2.64	3.40	8.08	3.35
		149.0		10					6.39	24.0	2.82	12.00	36.3	
									7.04	6.5	3.04	1.82		
	17.8		−0.69	0.33				0.90				17.22		
Galilee Basin		21.3	0.30	27	4.50	1.5	2.48	1.26	6.01	24.0	2.73	14.17	8.00	3.33
		146.3		10					6.75	17.0	2.94	6.46	42.2	
	21.3		−1.00	0.41				1.26				20.63		
Crump South		18.5	0.60	30					5.94	22.0	2.71	13.41	7.79	3.26
		145.0		12					6.62	20.2	2.89	8.69	41.4	
	20.5		−1.99	0.43								22.10		
Crump North		14.8	0.10	23					5.82	17.0	2.69	10.70	8.04	3.34
		142.7		17					6.71	20.0	2.92	8.00	36.9	
	18.5		−0.33	0.14								18.70		

Table 1 Summary of Refraction Data—Land

and Figure 3a and b show the refraction velocities at each location, and the derived densities for the various crustal layers and the mantle.

The reason for adopting a standard density ϱ_m, rather than a different value derived from the measured velocity for the upper mantle at each locality, needs discussion. It is inconsistent to talk about complete crustal isostasy if we admit lateral density variations in the mantle, since if the pressure at a level corresponding to the deepest part of the crust were everywhere equal, then the pressure would increase with depth at different rates corresponding to the different densities below this level, and hence non-isostatic conditions would prevail at deeper levels.

If isostasy were complete at the base of the crust, M would be constant, and the free-air anomalies would be nearly zero (apart from 'edge' effects associated with compensated lateral density and thickness variations). It is now generally accepted that lateral density variations do occur in the uppermost mantle; the variation in P_n velocities in Tables 1 and 2 is one line of evidence for this. Thus M is not expected to be constant. The variation in M is inferred to be associated with compensating density variations in the mantle. If the variation follows a reasonably regular pattern, approximate values of M may be interpolated and used as parameters in interpreting crustal structure in conjunction with the gravity field and other geophysical data. Alternatively, the variation in M could be interpreted in terms of upper mantle structure.

The regional free-air anomaly field g_s was determined from the global satellite field of spherical harmonics to order 16, based on figure 1 of Anderson *et al* (1973); this is shown for the Australian region by Dooley (1974, fig. 8). As the continental crust is about 30 to 40 km thick, g_F should be taken as the average free-air anomaly over about 3° to 5° areas. Maps showing average free-air anomalies for 3° and 5° areas for the Australian region were given by Dooley (op. cit., figs. 4, 5). Averages of g_F over areas of different sizes in this range do not change greatly. The values given in Table 1 were estimated from the 3° map, over the appropriate traverse (or portion thereof). For the marine data in Table 2, g_F was estimated from the nearest available data on the 1:2 500 000 map, together with additional data for the *Lusiad* traverses; because of the thinner crust, average values for smaller areas are appropriate.

Discussion

The pattern of CMD shown in Tables 1 and 2, and Figure 2, indicates low values in the southwest of the continent, with an increase eastwards through the Maralinga traverses, high values in northeastern and southeastern Australia, and a low value in Tasmania. Marine CMD appear to be more consistent; they range between about 15 and 17 kt/m², whereas the continental CMD vary from about 13 to 21 kt/m². Marine values average 15.8 kt/m², and land values 18.0 kt/m².

The variation in CMD, in general increasing from southwest to northeast, corresponds broadly with the regional trend of g_s, particularly over the continent; the range in g_s is about 40 mGal, corresponding to about 1 kt/m² in CMD, so

Traverse		*Approx. location*	*depth*	g_F	*Shallow Layers*				*Deep Layers*				*Mantle*	
	M(kt/m²)	(°S, °E)	km M_d	g_s M_s	V_i km/s	T_i km	ϱ_i t/m³	M_i ΣM_i	V_j km/s	T_j km	ϱ_j t/m³	M_j ΣM_j	V H	ϱ
Lusiad 47		32.8	5.35	−25	2.15	0.60	2.21	0.67	6.70	3.00	2.92	1.20	7.87	3.29
		108.7		−13	4.66	1.10	2.51	0.89					10.0	
	14.7		12.25	−0.29				1.56				1.20		
Lusiad 49		29.8	5.35	−40	2.15	0.35	2.21	0.39	6.49	4.30	2.85	2.02	8.28	3.41
		111.5		−11	4.98	1.30	2.55	1.00					11.30	
	15.0		12.25	−0.69				1.39				2.02		
Off Albany		36.2	4.72	−25	1.89	1.03	1.85	1.51	5.54	1.37	2.64	0.93	8.07	3.34
		116.2		−24	3.87	1.76	2.35	1.71	6.70	2.96	2.92	1.18	11.90	
	16.1		10.81	−.02				3.22				2.11		
Off Kangaroo Island		37.0	5.48	(−30)	2.00	0.08	1.90	0.11	5.21	1.67	2.59	1.22	8.27	3.41
		134.2		−21	2.51	0.85	2.06	1.07	6.74	1.82	2.94	0.69	11.50	
					3.47	1.60	2.28	1.66						
	17.1		12.56	−.22				2.84				1.91		
Coral Sea MN5		14.9	4.01	+5	2.11	1.14	1.93	1.58	6.95	1.15	3.01	3.46	(8.07)	(3.34)
		151.0		17	4.16	2.50	2.41	2.28					18.80	
	16.2		9.20	−.29				3.86				3.46		
Coral Sea 48		12.9	4.53	−2	2.11	.82	1.93	1.14	4.59	1.30	2.50	1.07	8.23	3.40
		149.8		21	3.26	1.34	2.23	1.46	6.49	4.88	2.85	2.30	12.87	
	15.8		10.37	−.55				2.60				3.37		
Coral Sea 37		14.2	4.56	9	2.00	0.46	1.90	0.65	4.92	0.84	2.54	0.66	8.45	3.46
		154.5		17	3.92	0.58	2.26	0.61	6.52	6.44	2.86	2.97	18.00	
									7.49	5.12	3.18	0.72		
	15.9		10.45	−.19				1.26				4.35		

Table 2. Summary of Refraction Data—Marine

Notes on Tables 1 and 2. $M_h = 3.32h$ $M_d = 2.29 \times \text{depth}$ $M_s = (g_F - g_s)/41.85$ $M_i = (3.32 - \varrho_i)T_i$ $M = M_h \text{ (or } M_d) + M_s + \Sigma M_i + \Sigma M_j$

any reasonable change in g_s would not affect the CMD pattern significantly. If g_s was taken as zero everywhere, CMD would become higher in the northeast and lower in the southwest, i.e. the range of CMD variations would be greater.

The values of $g_F - g_S$, taken as representing 'local' departures from isostasy (i.e. on the scale of three degree areas), range from −29 to +37 mGal, a range of 1.6 kt/m². This is much less than the total range of CMD, and hence lateral density variations must occur in the mantle, to compensate for CMD variations and achieve the nearly isostatic conditions indicated by the gravity field. It is of interest to note that the gravity corrections are positive for all continental surveys in Table 1, and negative for all marine surveys in Table 2; the averages are +0.4 and −0.3 kt/m² respectively. As the surveys are generally close to either the continental margin or the edge of a submarine plateau, this may indicate that the effect of the continent-ocean transition on the free-air anomalies has not been completely removed by the averaging process.

There are several reasons why the CMD values may not be very accurate; these include the possibility of low-velocity layers, high velocity layers which may be difficult to detect because they appear only as late arrivals, and vertical velocity gradients; the empirical and not highly accurate nature of the velocity-density correlation; and the difficulty in determining whether gravity anomalies are associated with anomalous masses in the crust or the mantle.

The CMD pattern established here will serve as a basis for further discussions of crustal and mantle mass variations to be presented in subsequent papers.

Acknowledgements

Helpful discussions with Dr P. Wellman, Mr F. J. Moss, and Dr D. Denham were much appreciated. The figures were prepared by Gil Clarke of the Geophysical Drawing Office, BMR.

References

ANDERSON, R. N., MCKENZIE, D. P., & SCLATER, G. P., 1973—Gravity, bathymetry and convection in the Earth, *Earth and Planetary Science Letters*, **18**, 391-407.

BIRCH, F., 1961—The velocity of compressional waves in rocks to 10 kilobars, Part 2. *Journal of Geophysical Research*, **66**, 2199-224.

CAMERON, P. J., 1971—Crustal seismic velocities in Tasmania. B.Sc. (Hons) thesis, University of Tasmania.

CLARK, S. P., & RINGWOOD, A. E., 1964—Density distribution and constitution of the mantle. *Reviews of Geophysics*, **2**, 35-88.

CLEARY, J. R., 1973—Australian crustal structure. *Tectonophysics*, **20**, 241-8.

CULL, J. P., & RIESZ, E. J., 1972—Deep crustal seismic reflection/refraction survey between Clermont and Charters Towers, Queensland, 1971. *Bureau of Mineral Resources, Australia—Record* **1972/97** (unpublished).

DENHAM, D., SIMPSON, D. W., GREGSON, P. J., & SUTTON, D. J., 1972—Travel times and amplitudes from explosions in Northern Australia. *Geophysical Journal of the Royal Astronomical Society*, **28**, 225-35.

DOOLEY, J. C., 1972—Seismological studies of the upper mantle in the Australian region. *Proceedings of the Second Indian Symposium on the Upper Mantle Project, December 1970.* National Geophysical Research Institute, Hyderabad, 113-46.

DOOLEY, J. C., 1974—The gravity anomalies of Central Australia and their significance for long-term tectonic movements. *Proceedings of Symposium on Earth's Gravitational Field and Secular Variations in Position*, (Editors), R. S. Mather and P. V. Angus-Leppan, University of New South Wales, Sydney, 248-260.

FINLAYSON, D. M., CULL, J. P., & DRUMMOND, B. J., 1974—Upper mantle structure from the Trans-Australia seismic survey (TASS) and other seismic refraction data. *Journal of the Geological Society of Australia* **21**, 447-58.

FRANCIS, T. J. G., & RAITT, R. W., 1967—Seismic refraction measurements in the southern Indian Ocean. *Journal of Geophysical Research* **72**, 3015-41.

FROLOV, A. I., 1964—Gravitatsionne pole Antarktidi i isostaziya. *Communications of the National Astronomical Institute, Moscow University* 135.

MATHER, R. S., 1968—The free-air geoid in South Australia and its relation to the equipotential surfaces of the earth's gravitational field. *University of New South Wales, Sydney, UNISURV Rep.* **6.**

MATHUR, S. P., 1974—Crustal structure in southwestern Australia from seismic and gravity data. *Tectonophysics,* **24,** 151-82.

MEREU, R. F., 1967—Curvature corrections to upper mantle seismic refraction surveys. *Earth and Planetary Science Letters,* **3,** 469-75.

MUIRHEAD, K. J., CLEARY, J. R., & FINLAYSON, D. M., 1976—A long range seismic profile in southeastern Australia (in press).

TALWANI, M., SUTTON, G. H., & WORZEL, J. L., 1959—Crustal section across the Puerto Rico Trench. *Journal of Geophysical Research,* **64,** 1545-55.

WELLMAN, P., 1976—Regional variation of gravity and isostatic equilibrium of the Australian crust. *BMR Journal of Australian Geology & Geophysics, 1,* 297-302.

WOOLLARD, G. P., 1959—Crustal structure from gravity and seismic measurements. *Journal of Geophysical Research,* **64,** 1521-44.

WOLLARD, G. P., 1968—The interrelationship of the crust, the upper mantle, and isostatic gravity anomalies in the United States, *in* The crust and upper mantle of the Pacific area. (L. Knopoff, C. L. Drake, and P. J. Hart, Editors) *American Geophysical Union Monograph 12,* Washington, 312-41.

WOOLLARD, G. P., 1969—Regional variations in gravity, *in* The Earth's crust and upper mantle (P. J. Hart and V. V. Beloussov, Editors), *American Geophysical Union Monograph.* **13,** Washington, 320-41.

BMR Journal of Australian Geology & Geophysics, 1 (1976), 297-302

Regional variation of gravity, and isostatic equilibrium of the Australian crust

Peter Wellman

In eastern Australia free-air anomalies and altitudes averaged over 1° x 1° areas show a positive correlation of +0.059 ± .004 mGal. m^{-1}. Isostatic compensation of topography and crustal masses is thought to be mainly at the base of the crust, but partly deeper in the mantle, and to be almost complete for 1° x 1° areas. In central and western Australia free-air anomalies and altitudes have a zero or slightly negative correlation with a larger scatter; isostatic compensation is thought to be complete only for 3° x 3° areas and to be predominantly at the base of the crust. The deeper compensation in eastern Australia is thought to be related in some way to the youth of the crust and the presence of a low velocity zone at about 130 km. Elsewhere in the world Phanerozoic areas have a positive free-air anomaly altitude correlation, and Precambrian areas a negative correlation; so the different modes of isostatic compensation found in Australia may apply to crust of similar age elsewhere in the world.

In Australia the residual 1° × 1° area anomalies found by removing altitude, long wavelength and sedimentary effects generally have an amplitude of 30 mGal and a wavelength of 6°; they are thought to be due to isostatically compensated variations in crustal density. Using these anomalies, variations in crustal thickness are predicted.

Introduction

Isostatic equilibrium is the crustal and upper mantle process whereby the variations in the crustal load are compensated at the base of the crust and in the upper mantle, so that there is a depth in the mantle where the pressure of the overlying material is everywhere constant. Variations in the crustal load are caused by areal variations in both surface elevation and mean crustal density. These variations are compensated by variations in the thickness of the crust, compensating masses in the mantle, and by crustal strength spreading the affects of a crustal load over a wider area.

Regions in isostatic equilibrium have all anomalous crustal masses underlain by equal compensating masses, and hence the free-air anomalies average zero when taken over a large enough area. However the anomalous and compensating masses are at different depths, so that areal variations of the anomalous and compensating masses will be reflected in variations in the free-air anomalies. These variations in free-air anomaly are useful in studying the isostatic process. The depth(s) of isostatic compensation, and the maximum size of bodies that are uncompensated, can be inferred from the wavelength and amplitude of the free-air anomalies and from the correlation between free-air anomalies and altitude (for 1° × 1° or larger areas). Free-air anomalies corrected for their correlation with altitude are a type of isostatic anomaly, and give information on the regional variation of mean crustal density.

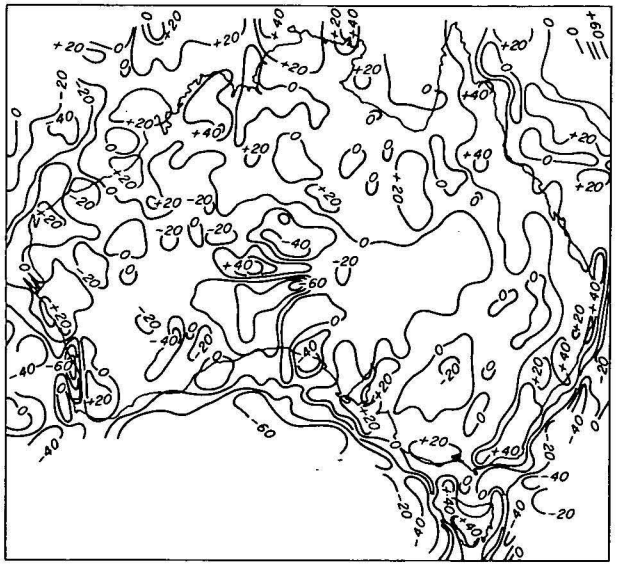

Figure 1. Free-air anomaly map of Australia from 1° x 1° area means. Contour interval 20 mGal.

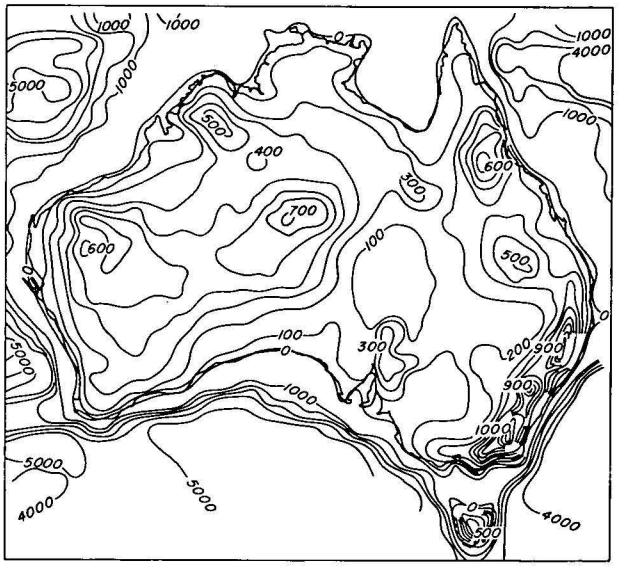

Figure 2. Altitude map of Australia from 1° x 1° area means. Contour interval 100 m on land, 1000 m at sea.

The relation between free-air anomaly and altitude

The relations between free-air anomaly and altitude provide a simple method of investigating the mechanism of isostatic equilibrium. The variation in altitude represents a known anomalous mass, while a major component of mean free-air anomalies is the difference in gravitational attraction between this anomalous mass and its compensating mass.

The continent can be divided by trial and error into areas within which there is a constant linear relation between gravity anomalies and altitude (Woollard, 1969a; Wilcox, 1971). Within each of these areas the isostatic mechanism is

likely to be the same, and the isostatic mechanism must be consistent with the linear relation. This is the technique used in this study. In each sufficiently large area of constant isostatic mechanism a Fourier analysis of gravity and altitude is used to derive the attraction of the compensating masses for a unit surface load, and from this attraction either the depths of isostatic compensation can be calculated (Lewis & Dorman, 1970, 1972) or lithospheric flexure parameters calculated (Walcott, 1976). Previously Woollard (1962), part 7, p. 12; 1969a, Fig. 6; 1972, p. 501) had shown using preliminary gravity data that the relations of gravity with altitude were different in eastern and central Australia.

The gravity anomalies have been calculated as free-air anomalies (rather than Bouguer anomalies) because this calculation does not involve the assumption of a crustal density. The free-air anomalies and the associated altitudes have been averaged over 1° x 1° areas; this suppresses noise from local changes in geology, but does not significantly smooth the basic gravity anomaly pattern due to large crustal masses (Woollard, 1969a, p. 469).

Means for each 1° x 1° area were calculated by averaging the known 0.1° x 0.1° area values; the means are well determined because there were usually over eighty such values in each 1° x 1° area. The altitudes used were those of the gravity observation points, so the calculated mean altitudes will be a systematically slightly low estimate of the true mean altitude in areas of rough topography. No terrain corrections have been applied to the gravity observations, but terrain corrections should be negligible in most parts of Australia. Figures 1 and 2 are maps of mean free-air anomaly and mean altitude.

The relation between altitude and free-air gravity anomalies was investigated in 22 tectonic areas, most corresponding to units on the Tectonic Map of Australia and New Guinea (Geological Society of Australia, 1971). The areas are, with one exception, either almost wholly sedimentary or wholly non-sedimentary; this division is made so that any differences between the two types of areas can be identified. Figure 3 shows the extent of the areas, and for each area a scatter diagram of the relation between altitude and free-air anomaly.

Within eastern Australia (areas 12, to 22, Figure 3) free-air anomalies have an overall significant positive correlation with altitude:

$$FAA = -(2.1 \pm 1.2) + (.0585 \pm .0042) \times h,$$

where h is the altitude in metres.

This gives a regression coefficient of 0.0585 ± 0.0042 mGal. m^{-1}. There is a root mean square deviation of a single observation from the regression line (RMSE) of

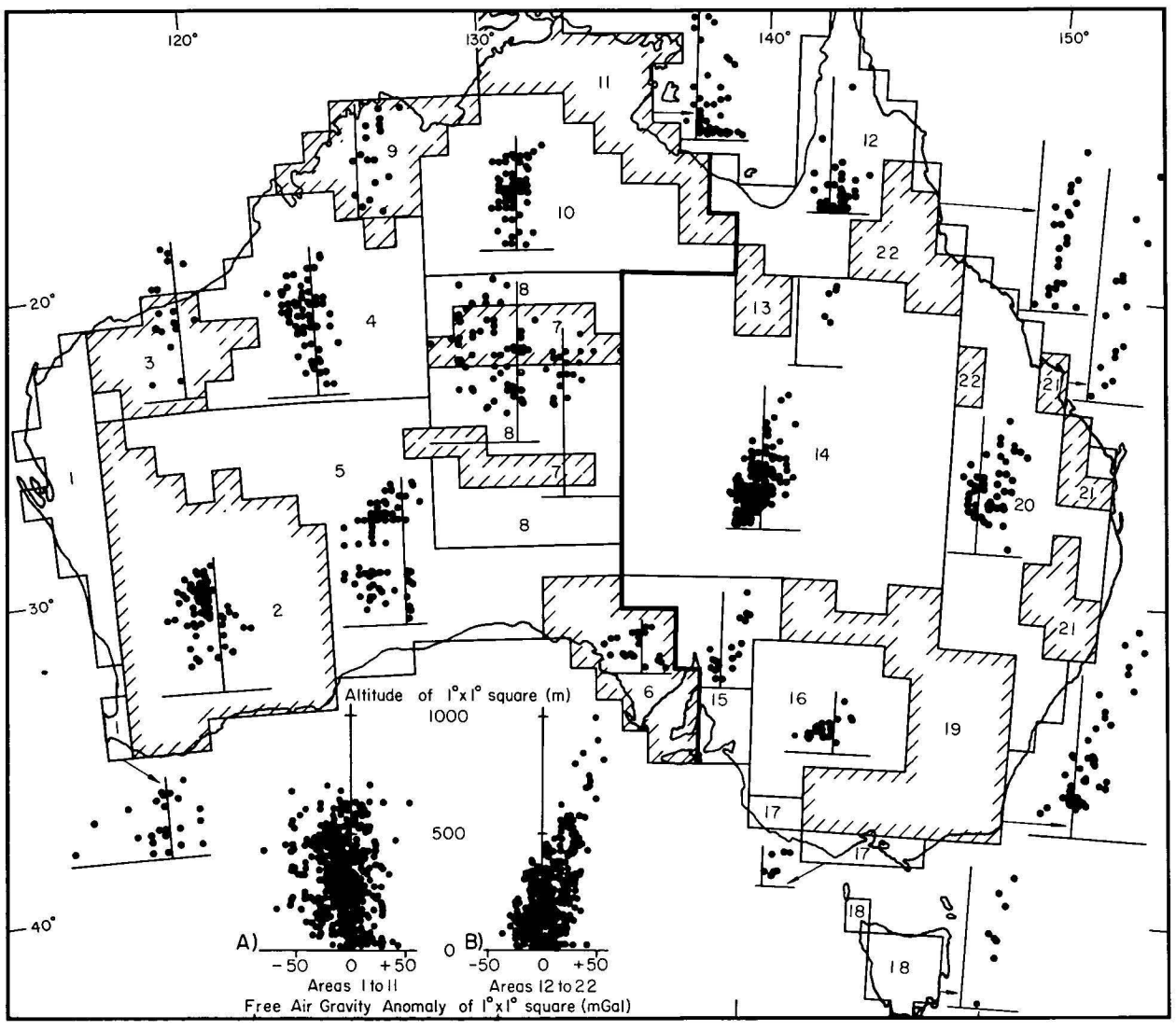

Figure 3. Relation between free-air anomalies and altitude for twenty two tectonic areas. Non-sedimentary areas are shown with shaded margins. Inset A shows relation for western and central Australia (areas 1-11), and inset B for eastern Australia (areas 12-22).

13.4 mGal. Most individual areas in eastern Australia also show this significant positive correlation. For central plus western Australia there is a significant overall negative correlation

$$FAA = (4.8 \pm 1.8) - (.0241 \pm .0055) \times h,$$
$$RMSE = 19.5 \text{ mGal.}$$

However most individual areas do not show a significant correlation, and neither do the larger areas of northern Australia (areas 9 + 10 + 11):

$$FAA = (12.1 \pm 2.4) - (.0051 \pm .0094) \times h,$$
$$RMSE = 13.6 \text{ mGal,}$$

central Australia (areas 7+8)

$$FAA = (-16.4 \pm 7.8) + (.0145 \pm .0175) \times h,$$
$$RMSE = 23.8 \text{ mGal,}$$

or western Australia (areas, 1, 2, 3, 4, and 5 west of 125°E)

$$FAA = (-4.62 \pm 2.75) - (.0057 \pm .0076) \times h,$$
$$RMSE = 16.7 \text{ mGal.}$$

For areas that are thought to be completely isostatically compensated at the base of the crust Woollard (1969a) showed empirically that the average relation of 2° x 2° free-air anomaly (FAA) and altitude in metres (h) is: FAA = 13 − 0.102 x h from 0 to 200 m, and FAA = −6 + 0.0075 x h from 200 m to 1700 m. The correlation of free-air anomaly and altitude would be expected to be zero or weakly positive if complete isostatic compensation was achieved at a level close to the surface such as within or at the base of the crust. A strong positive correlation would be expected if complete compensation was at a considerable distance from the topography, such as vertically below deep in the upper mantle, or laterally away such as at the base of the crust but over a large area. There would be a positive correlation of free-air anomaly and altitude if there was a positive correlation of upper crustal density and altitude, and a negative correlation if there was a negative correlation of upper crustal density and altitude.

The strongly positive free-air altitude correlation in eastern Australia is inferred to be due to topographic compensation being partly deep in the mantle. The relatively small residuals (RMSE = 13 mGal) suggest that 1° x 1° areas are close to isostatic equilibrium. The zero to slightly negative free-air altitude correlation found in northern, central and western Australia is explained by compensation being mainly at the base of the crust. The relatively large residuals (RMSE = 24, 17 mGal) in central and western Australia are thought to be due to both greater variation in mean crustal density compared with eastern Australia, and greater lithospheric strength, leading to isostatic equilibrium applying for larger areas.

The contrast between eastern, and central plus western Australia shown by the free-air anomaly—altitude relationships is also evident in other geological and geophysical data. Central and western Australia has, relative to eastern Australia, older crust (Compston and Arriens, 1968; Geol. Soc. Aust., 1971), higher upper crustal velocities (Cleary, 1973), higher mantle seismic velocities (Dooley, 1972, Cleary, 1973), lower station residuals for seismic P waves (Cleary, 1967; Cleary *et al.*, 1972), and no low velocity zone at 130 km depth according to Rayleigh wave studies (Gonez and Cleary, 1976). The low velocity layer in eastern Australia may represent a layer of low strength. This would allow smaller areas of crust to reach isostatic equilibrium in eastern Australia relative to central and western Australia, and if there was a density contrast across the top of the layer some isostatic compensation at this level would also result.

The Australian data can be compared with published gravity-altitude relations for other continents (Woollard, 1969a, b; Wilcox, 1971). Only areas with a linear relation from sea level to 1000 m have been used because areas with more complicated relations are probably composed of several sub-areas with different isostatic compensation mechanisms. Bouguer anomalies (density 2.67 $t.m^{-3}$) have been transformed to free-air anomalies using:

$$\text{free-air anomaly} = \text{Bouguer anomaly} + 0.1118 \text{ mGal.m}^{-1} \times h.$$

Figure 4 shows an unexpected result—in both Australia and elsewhere the free-air anomaly relation is negative over areas of Precambrian basement, and positive over areas of Phanerozoic (post Proterozoic) basement. This is interpreted as indicating that Precambrian and Phanerozoic areas have different modes of isostatic compensation.

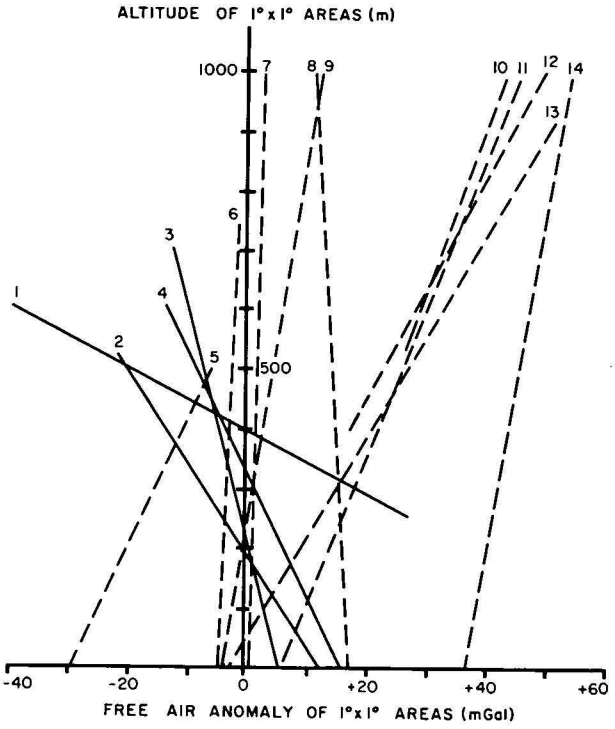

Figure 4. Correlation between free-air anomaly and altitude for 1° x 1° areas on Precambrian basement (solid lines) and on Phanerozoic basement (dashed lines). 1, central west USA; 2, Peninsula India; 3, western Australia; 4, central Canada; 5, eastern Canada; 6, Appalachians USA; 7, Mexico; 8, central Spain; 9, west coast USA; 10, European Alps; 11, Argentine and Andes; 12, Alaska; 13, eastern Australia; 14, central America. Data from Woollard, 1969b; Wilcox, 1971; and this paper.

Residuals from free-air-altitude correlations

The residuals from the free-air anomaly-altitude correlations for eastern Australia, and central plus western Australia, are shown in Figure 5. The anomalies are due in part to short wavelength crustal effects and in part to the following long wavelength effects from both the crust and mantle: (a) At the continental margin the depth of the base of the crust changes from 35-40 km under the continent to about 10 km under the oceans. The gravitational effect of this change is approximately +22 mGal at 100 km inland from the continental edge, +10 mGal at 200 km, +6 mGal at 300 km, and +3 mGal at 500 km. (b) Relative to basement areas the residuals over basin areas are systematically lower because of the underlying light sedimentary

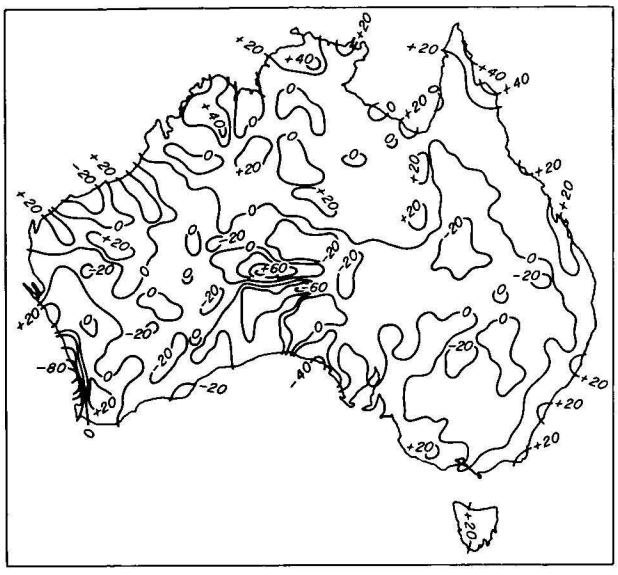

Figure 5. Residual gravity anomalies for 1° x 1° areas in Australia: observed anomaly minus altitude effect of Figure 3A, B. Contour interval 20 mGal. These anomalies are independent of altitude and can be regarded as a type of 'pure' isostatic anomaly.

rocks. The gravity effect varies with the geometry of the sedimentary basin, with large negative anomalies expected for narrow deep basins. The average gravity difference between basement and basin 1° x 1° areas after allowing for altitude effects is 9.6 ± 1.7 mGal in eastern Australia and 10.6 ± 1.7 mGal in central plus western Australia. These values are not significantly different, so a value of 10 mGal has been adopted for the whole of Australia. (c) There is a regional variation of free-air anomalies over Australia due to long wavelength lateral density variation in the crust and mantle. This regional effect has been mapped in Figure 6 by contouring the smoothed mean free-air values for the areas of Figure 3. The mean anomalies range from more than +25 mGal in northeastern Australia to less than −10 mGal on the south coast of Australia.

When these three long wavelength effects are removed from the residual anomalies (Figure 5) the short wavelength residuals of Figure 7 are obtained. In eastern Australia, most of northern Australia, and some of western Australia, these residuals have peak to peak amplitudes of 30 mGal and wavelengths of 6 to 7°; however in central and western Australia there are regions with residual anomalies amplitudes up to 60 mGal for wavelengths of 3-4°. The residuals of Figure 7 are thought to be due partly to variations in the mean crustal density and partly to the 1° × 1° areas not being in complete isostatic equilibrium. However this last effect is difficult to evaluate. In the following section the variation in crustal thickness over Australia is predicted on the assumption that 1° x 1° areas are completely compensated at the base of the crust. Earlier it was inferred that in western and central Australia isostatic equilibrium applied only to areas larger than 1° x 1°, and in eastern Australia some compensation was at a level deeper than the base of the crust.

If the mean crustal density of a 1° x 1° area differs from the average mean crustal density the mass difference will be compensated at depth. However because the crust is closer to the observation level than the compensating mass, the observed free-air anomaly will differ from zero, the gravity residual being positive in areas of high density crust, and negative in areas of low density crust. The regional variation in residual gravity can therefore be used to estimate the regional variation of mean crustal density. At isostatic equilibrium the mean crustal density (dc) is related to the thickness of the crust below sea level (H) by:

$$H = \frac{Ho(dm\text{-}ds) + h.dc,}{dm\text{-}dc}$$

where h is surface altitude, ds is the assumed standard crustal density, Ho is the assumed thickness of standard sea level crust, and dm is the assumed constant mantle density.

The variation of mean crustal density has been calculated from short wavelength gravity anomaly residuals as follows: the mean crustal and mantle densities are likely to be about 2.9 and 3.3 $t.m^{-3}$, and the mean crustal thickness at sea level about 35 km (Woollard, 1970; Sazhina & Grushinsky, 1971). If two adjacent dimensional crustal strips differ in density by 0.1 $t.m^{-3}$ (0.1 gm cm^{-3}) then their thicknesses will differ by about 9.4 km, assuming that the crust is in isostatic equilibrium. The resultant residual anomaly will vary with the wavelength of the density variation. A value of 36 mGal has been adopted, the mean of 38 mGal for a 4° wavelength and 35 mGal for a 6° wavelength density variation. Adjacent blocks with smaller density contrasts will give approximately proportional gravity anomalies. Hence for most of Australia the changes in crustal density and thickness can be calculated using 0.1 $t.m^{-3}$/36 mGal and 9.4 km/36 mGal = 0.26 km/mGal.

The increase in crustal thickness due to topography in Australia is not large, generally being less than 3 km, because altitudes are generally less than 0.5 km above sea level. It is therefore not critical what ratio dH/dh is used. A value of 6 has been adopted, the average of 7.5 derived by Woollard (1970) from seismic work mainly of American origin, and 5 derived by Sazhina & Grushinsky (1971) from seismic work mainly of Soviet origin. These values have been determined from the correlation of seismic crustal thickness and surface altitude, and so are independent of the isostatic compensation model.

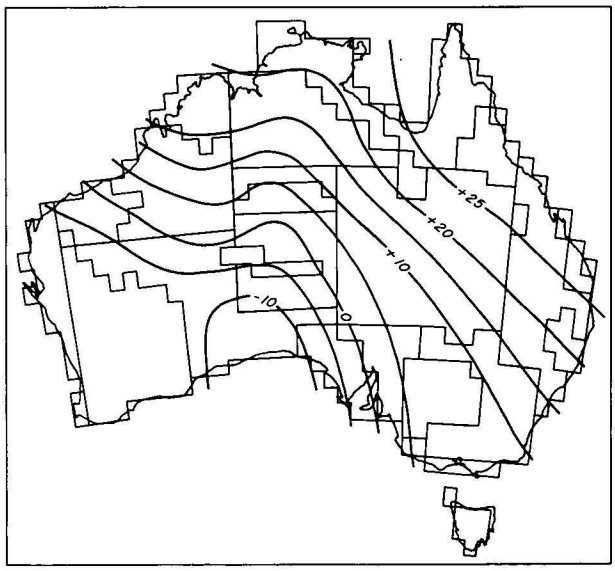

Figure 6. Regional free-air anomaly in Australia (mGal).

The thickness of the crust for each 1° x 1° area has been calculated using the free-air anomaly residuals (RG) of Figure 7, altitudes (h) of Figure 2, assuming that 1° x 1° areas are in complete isostatic equilibrium and using the relations derived above. The equation used is crustal thickness (depth of mantle below sea level) H = 35 + 6h + 0.26 RG, where H and h are in kilometres and RG in

Figure 7. Short wavelength residual anomaly in Australia. Contour interval 10 mGal.

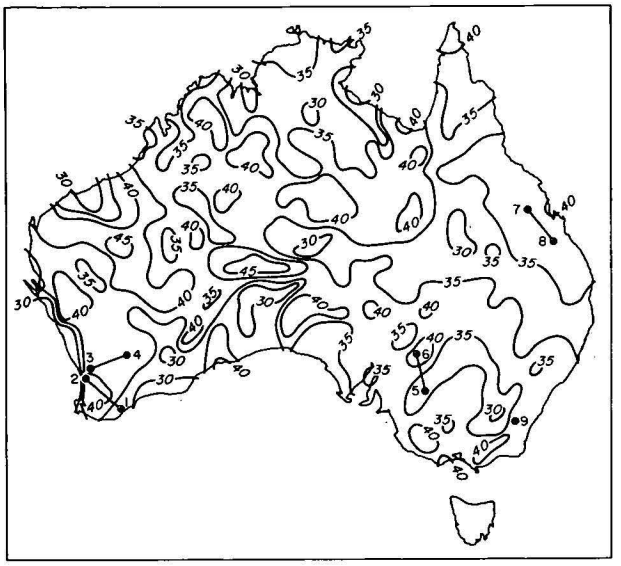

Figure 8. Predicted crustal thickness for Australia assuming 1° x 1° areas are in complete isostatic equilibrium. Contour interval 5 km. The numbered refer to seismic traverses of Fig. 9.

milligal. This method of relating gravity to crustal thickness is similar to that used by Strange & Woollard (1964). The inferred crustal thicknesses are mainly between 30 and 45 km (Figure 8). The absolute value of the predicted thicknesses have a large uncertainty due to the simplicity of the model relating crustal thickness to regional gravity values. Relative thicknesses over distances of 300 to 600 km are likely to be more accurate than absolute values because of the smaller effect of regional variation of crustal and mantle properties.

If isostasy is largely complete for 1° x 1° areas there should be a positive correlation of slope 45° between predicted and measured crustal thickness. If isostasy is complete only for much larger areas, then the 1° x 1° anomaly will reflect the attraction of the uncompensated masses, so there should be a lower or negative correlation between 1° x 1° residual gravity and crustal thickness for anomaly wavelengths of 3° to 6°, and hence a lower or negative correlation between predicted and measured crustal thickness.

In Figure 9 the inferred crustal thicknesses are compared with crustal thickness measured by seismic surveys. The crustal thicknesses are from seismic refraction profiles in southwestern Australia (points 1-4, Mathur, 1974, Figs. 8, 9), in the Bowen Basin (points 7, 8; C. D. Collins, pers. comm.) and in the Snowy Mountains (point 9; Doyle *et al.*, 1966); and seismic reflection points at Mildura and Broken Hill (points 5, 6; Branson *et al.*, 1970), the crustal velocities determined at these reflection points using expanded spreads. The measured and inferred crustal thicknesses show a positive correlation in three profiles out of four, the mean error of the predicted thicknesses being 3 km. Elsewhere in Australia the inferred crustal thicknesses show a non significant positive correlation with the time term analysis seismic thicknesses for the Cape York Peninsula area of Queensland (Finlayson, 1968), a non significant positive correlation with interpreted seismic reflection results for southeastern Queensland and western New South Wales, but a non significant negative correlation with interpreted seismic reflection results for central Australia (Dooley & Moss, in prep.). These correlations are consistent with the 1° x 1° areas being largely in isostatic equilibrium in eastern Australia, and possibly in the Yilgarn area of southwestern Australia, but not in isostatic equilibrium in central Australia. Figure 9 can therefore be used directly to infer relative crustal thicknesses in eastern Australia, but relative thicknesses in central and western Australia should be obtained after averaging over about a 3° x 3° area.

The dominant origin of the 1° x 1° free-air anomaly variation appears to be different in eastern Australia, compared with central plus western Australia. The variation in 1° x 1° free-air anomalies can be expressed as a variance (the square of the standard deviation). The origin of this variance can be determined using the correlation of gravity with altitude, with latitude and longitude, with position over basin or basement, and using the average variation of 0.1° x 0.1° anomalies about the 1° x 1° mean

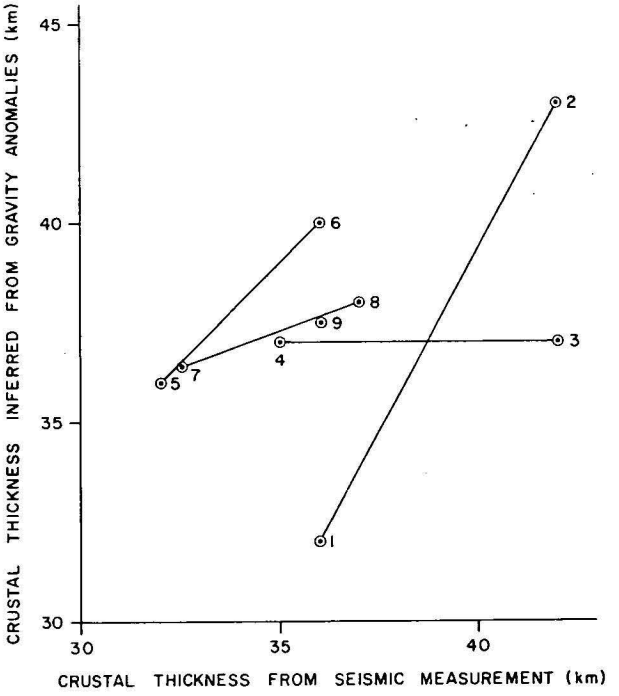

Figure 9. Relation between predicted and measured crustal thickness. The seismic line positions are given in Fig. 8, and references in the text.

anomaly. In eastern Australia the total variance is 281 mGal² per 1° x 1° area; this consists of 102 mGal² variance (36%) due to the difference in attraction of topography and isostatically compensating masses, 42 mGal² (15%) to regional variation in free-air anomalies, about 14 mGal² (6%) to the difference in upper crustal density between basins and basement, 10 mGal² (4%) to density variation within the 1° x 1° area influencing the mean value, and the remaining 112 mGal² (39%) to variations in mean crustal density and the associated compensating masses. Over the remainder of Australia the total variance is 393 mGal² per 1° x 1° area, and of this 16 mGal² (4%) is due to the difference in attraction of topography and isostatically compensating masses, 108 mGal² (27%) to regional variation in free-air anomalies, about 14 mGal² (4%) to the difference in upper crustal density between basins and basement, 19 mGal² (5%) to density variation within each 1° x 1° area influencing the mean value, and the remaining very large 236 mGal² (60%) to variations in crustal density and crustal thickness.

Acknowledgements

I am grateful for the help of Mr J. C. Dooley and Mr J. B. Connelly in the preparation of this paper. The figures were drawn by the gravity drafting group, Geophysical Drawing Office, BMR.

References

BRANSON, J. C., MOSS, F. J., & TAYLOR, F. J., 1972—Deep crustal reflection seismic test survey, Mildura, Victoria and Broken Hill, New South Wales, 1968. *Bureau of Mineral Resources, Australia—Record* **1972/127** (unpublished).

CLEARY, J. R., 1967—P times to Australian stations from nuclear explosions. *Bulletin of the Seismological Society of America*, **57**, 773-81.

CLEARY, J. R., 1973—Australian crustal structure. *Tectonophysics*, **20**, 241-48.

CLEARY, J. R., SIMPSON, D. W., & MUIRHEAD, K. J. 1972—Variations in Australian upper mantle structure from observations of the Cannikin explosion. *Nature*, **236**, 111-12.

COMPSTON, W., & ARRIENS, P. A., 1968—The Precambrian geochronology of Australia. *Canadian Journal of Earth Sciences*, **5**, 561-83.

DOOLEY, J. C., 1972—Seismological studies of the upper mantle in the Australian region. *Proceedings of the Second Symposium on Upper Mantle Project*, December 1970, *Hyderabad*. 113-44.

DOYLE, H. A., UNDERWOOD, R., & POLAK, E. J., 1966—Seismic Velocities from explosions off the central coast of New South Wales. *Journal of the Geological Society of Australia*, **13**, 355-72.

FINLAYSON, D. M., 1968—First arrival data from the Carpentaria Region Upper Mantle Project (CRUMP). *Journal of the Geological Society of Australia*, **15**, 33-50.

GEOLOGICAL SOCIETY OF AUSTRALIA, 1971—Tectonic Map of Australia and New Guinea 1:5 000 000. *Sydney*.

GONCZ, J. H., & CLEARY, J. R., 1976—Variations in the structure of the upper mantle beneath Australia from Rayleigh wave observations. *Geophysical Journal of the Royal Astronomical Society*, **44**, 507-16.

LEWIS, B. T. R., & DORMAN, L. M., 1970—Experimental Isostasy, 2. An isostatic model for the U.S.A. derived from gravity and topographic data. *Journal of Geophysical Research*, **75**, 3367-86.

LEWIS, B. T. R., & DORMAN, L. M., 1972—Experimental Isostasy, 3. Inversion of the isostatic Green function and lateral density changes. *Journal of Geophysical Research*, **77**, 3068-77.

MATHUR, S. P., 1974—Crustal structure of southwestern Australia from seismic and gravity data. *Tectonophysics*, **24**, 151-82.

SAZHINA, N., & GRUSHINSKY, N., 1971—GRAVITY PROSPECTING. *MIR Publishers, Moscow*.

STRANGE, W. E., & WOOLLARD, G. P., 1964—The use of geologic and geophysical parameters in the evaluation, interpolation and prediction of gravity. *Hawaiian Institute of Geophysics—Report*, **HIG-64-17.**

WALCOTT, R. I., 1976—Lithospheric flexure, analysis of gravity anomalies and the propagation of seamount chains: *in* THE GEOPHYSICS OF THE PACIFIC OCEAN BASIN AND ITS MARGIN, G. H. Sutton, M. H. Manghnani, & R. Moberly (Editors), *American Geophysical Union Monograph*, **19**, 431-8, *Washington, D.C.*

WILCOX, L. E., 1971—An investigation of areal gravity-elevation relations using covariance and empirical techniques. *Hawaiian Institute of Geophysics Report* **HIG-71-10.**

WOOLLARD, G. P., 1962—The relation of gravity anomalies to surface elevation, crustal structure and geology. *University of Wisconsin, Geophysical and Polar Research Centre—Report* **62-9.**

WOOLLARD, G. P., 1969a—Regional variations in gravity; *in* THE EARTH'S CRUST AND UPPER MANTLE. P. J. Hart & V. V. Beloussov (Editors) 320-41. *American Geophysical Union Monography* **13**, *Washington, D.C.*

WOOLLARD, G. P., 1969b—A study of the problems associated with the prediction of gravity in Europe. *Hawaiian Institute of Geophysics Report* **HIG-69-12,** part 2.

WOOLLARD, G. P., 1970—Evaluation of the isostatic mechanism and the role of mineralogic transformations from seismic and gravity data. *Physics of the Earth and Planetary Interiors*, **3**, 484-98.

WOOLLARD, G. P., 1972—Regional variations in gravity; *in* THE NATURE OF THE SOLID EARTH, E. C. Robertson (Editor), 463-505. *McGraw-Hill, New York*.

BMR Journal of Australian Geology & Geophysics, 1 (1976), 303-314

The gravity field of offshore Australia

P. A. Symonds and J. B. Willcox

The free-air anomaly field of offshore Australia has been divided into about fifty regional gravity provinces, each of which is characterized by uniformity of trend, free-air anomaly level, or degree of disturbance. These are discussed in relation to structural and/or bathymetric features in each region. The Bouguer anomalies are used as a rough guide to variations in crustal thickness.

On the continental shelf the free-air anomaly provinces generally correlate with the main structural elements. The Precambrian shields are associated mainly with regional gravity lows, and the peripheral mobile belts mainly with gravity ridges. On the northwest and southern margins these mobile belts cut across the continental shelf and appear to be truncated at the shelf-break. On the marginal plateaus and terraces the free-air anomaly pattern largely reflects the relative elevation of basement and the thickness of sediment. The well-defined gravity highs on the Lord Howe Island and Tasmantid seamount chains are caused by the combined effects of sea-floor topography and high-density igneous bodies.

Regional positive free-air anomaly values over the broad continental shelves of the Northwest and Southern Margins, and negative values on the adjacent abyssal plains, indicate that slight readjustment of the crust/mantle interface must occur in these regions if isostatic equilibrium is to be attained. However, the well-defined free-air anomaly ridges and troughs which correspond to the top and foot of the continental slope respectively, are largely a 'gravity edge effect' caused by abrupt changes in water depth and crustal thickness. This can reach ±70 mGal over steep slopes, such as that bordering the Tasman Basin. Regional positive free-air anomaly values over the Queensland and Marion Plateaus indicate that slight subsidence of these features is necessary if they are to attain isostatic equilibrium.

The Bouguer anomaly values indicate that the crust thins oceanward except in the Timor Sea area where crustal thickening occurs, probably due to interaction of lithospheric plates along the Inner Banda Arc. Crust of typically oceanic thickness (10-15 km) is confined to the lower part of the continental slopes and the abyssal plains, generally oceanward of the 4000 m isobath.

Introduction

Marine gravity observations used to prepare the 1:5000000 Gravity Map of Australia (BMR 1976a, and maps in this volume) were gathered largely during marine surveys completed between 1965 and 1973. Anfiloff *et al.* (1976) describe the method of data collection and reduction.

The observed gravity values at sea have been reduced to free-air anomalies (FAA) in milligals for presentation on the Gravity Map of Australia, according to the formula:

$$FAA = g_o - g_n + 7.5\ Ve \cos \phi$$

where g_o is the observed gravity, g_n the normal value of gravity depending on latitude ϕ and obtained from the 1930 International Gravity Formula, and Ve is the eastward component of ship's speed in knots used to calculate the Eötvös correction (Glicken, 1962). 'Marine Bouguer anomalies' (BA) were derived from the formula:

$$BA = FAA + 2\pi G \Delta\varrho d$$

where G is the universal gravitational constant, $\Delta\varrho$ is the difference in density between water and sediment (assumed to be 1.2 $t.m^{-3}$), and d is the water depth in metres. This approximates to the replacing of the water layer with a sediment layer, and theoretically removes the gravity effect of sea-floor topography.

On the continental shelf and on most of the marginal plateaus and terraces where the gradient of the seabed is relatively small, the Bouguer and free-air anomalies show a similar pattern. However, in places where the water depth varies abruptly, principally on the continental slopes, the free-air anomalies show a local correlation with water depth, and the Bouguer anomalies generally exhibit a steep monoclinal gradient which is attributed to crustal thinning, and which obscures the effects of near-surface geology.

Knowledge of densities in the crust and mantle, and the depths to the crust/mantle interface, would enable this Bouguer anomaly gradient to be removed. However, such information is rarely available in sufficient detail. Ideally then, for Bouguer anomalies to be of value over a continental slope, corrections for changes in crustal thickness are required.

The free-air anomalies provide more useful information than Bouguer anomalies over the continental slope—provided they are interpreted with caution. Free-air anomalies theoretically average zero over regions in isostatic equilibrium, and can be used as a measure of isostatic compensation. The minimum area found to be compensated is generally 100-200 km across; the local features being supported by the crust. Free-air anomalies combine the opposing gravity effects of increasing water depth and associated crustal thinning, and hence regional gradients tend to be less intense than for Bouguer anomalies.

On the continental slopes the free-air anomalies show a marked 'edge effect', which is made up of a gravity ridge along the top of the slope and a trough along its foot. It arises from differences in the rates of change of two opposing influences on free-air anomaly values as the continental margin is crossed; namely the gravity effects at sea level due to variations in depth to the sea floor, and to variations in crustal thickness (for example, see Bott, 1971, fig. 2.14). As an example, Figure 1 shows the predicted free-air anomaly edge effect from the continental shelf to the Tasman Basin and from the Eyre Terrace to the Southern Ocean, based on schematic two-dimensional models. Each model is in perfect isostatic equilibrium according to the Airy hypothesis, with a standard crustal thickness of 33 km. In the absence of edge effect the free-air anomalies would be zero; however, they deviate by as much as ±70 mGal over the change in slope, and by about ±20 mGal 100 km beyond it (dot-dash curve). The marine Bouguer anomalies (dashed curve) show much less evidence of edge effect. This is because they are computed by approximating the water layer to an infinite slab, and the approximation has the effect of undercorrecting for the water layer at the top of the slope and overcorrecting at its foot, and is thus opposite in sign to the edge effect. For comparison, the solid curve shows the total gravity effect of the models when the water

layer is replaced precisely with a sediment layer of density 2.2 t.m^{-3}, rather than with a Bouguer slab. In this case the edge effect is again apparent.

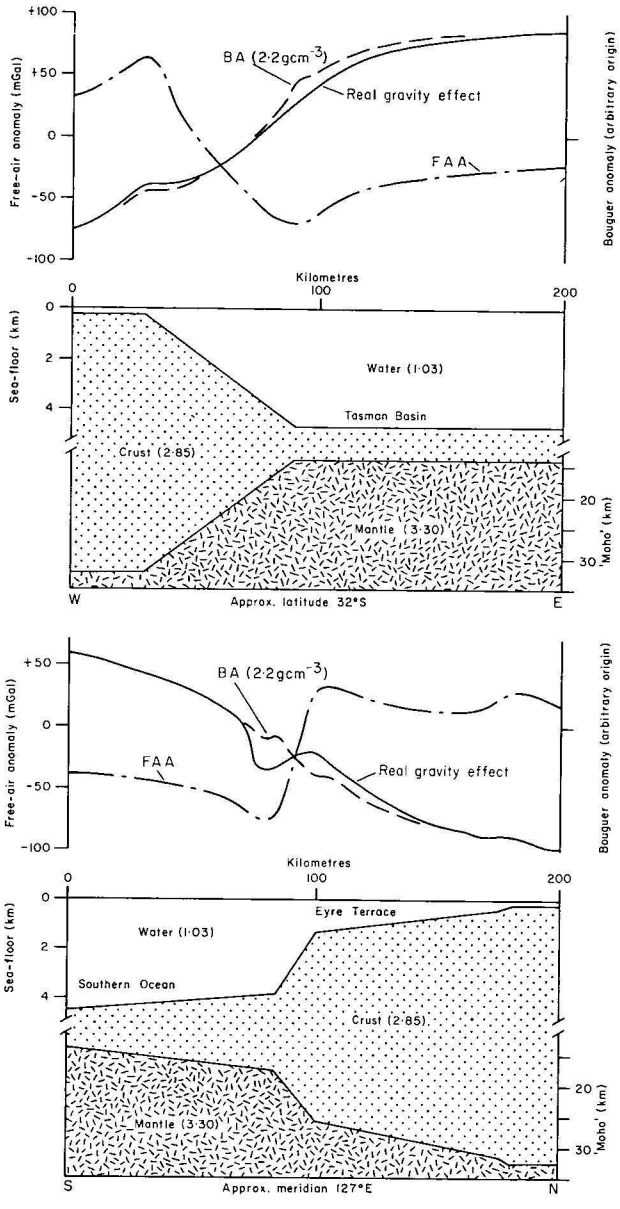

Figure 1. Edge effects over two-dimensional schematic models of the continental shelf—Tasman Basin and the Eyre Terrace—Southern Ocean. Models in isostatic equilibrium according to the Airy hypothesis. (Dot-dash curve shows computed free-air anomaly. Dashed curve shows marine Bouguer anomaly for Bouguer density 2.2 t.m^{-3}. Solid curve shows total gravity effect when water layer is replaced by sediment of density 2.2 t.m^{-3}).

The interpretation presented in this paper is based on the Gravity Map of Australia (showing Bouguer anomalies on land and free-air anomalies at sea; this volume) subdivided into provinces which are identified by numbers (Fraser, 1976, page 352). This subdivision follows the method adopted by authors writing on the results of Australian reconnaissance gravity surveys on land. Reference is also made to the Australian free-air anomaly map (showing free-air anomalies on land and at sea; this volume) and a 'marine Bouguer anomaly' map (Figure 4). The gravity results are discussed in relation to bathymetric and/or structural features in each region (Figures 2 & 3).

In this paper the continental margin is divided into five regions—the Northwest Margin, the Western Margin, the Southern Margin, Tasmania and the Tasman Sea, and the Coral Sea and Gulf of Papua (Fig. 2). Bass Strait and the Gulf of Carpentaria have not yet been systematically surveyed and are therefore excluded from consideration. For each region, a province by province interpretation is preceded by a discussion in which the main points are summarized.

The discussion relies partly upon a series of BMR interpretation reports of the offshore areas (Smith, 1966; Jones, 1969; Whitworth, 1969; Watt, 1975; Hogan & Jacobson, in press; Petkovic, 1975b; Willcox, 1974; Cameron & Pinchin, 1974; P. A. Symonds, unpublished data; Mutter, 1974; Tilbury, 1975) and for the Northwest Shelf upon the summary given by Fraser, Darby & Vale (in prep). More detailed discussions of the gravity field on the Exmouth and Naturaliste Plateaus and in the Great Australian Bight are given by Exon *et al.* (1975), P. J. Cameron & P. Petkovic (unpublished data) and Willcox (in press).

Regional gravity field based on satellite observations

Geodetic parameters describing the earth's gravity field have been computed by Gaposchkin & Lambeck (1971) using satellite and terrestrial gravity data. These results indicate that the height of the geoid ranges linearly from about +100 m over Papua New Guinea to about −40 m off southwest Australia. The regional free-air anomaly field has values of about +10 mGal over northern and eastern Australia; −10 mGal over Tasmania, the Tasman Sea and Lord Howe Rise; and −40 mGal over the southwest quadrant of the continent. The Australian free-air anomaly map (this volume) is consistent with this regional pattern in as much as it shows a preponderance of negative features in the southwest, flanked in the north and east by more positive features. It is generally considered that these regional gravity variations result from density differences within the mantle, and as such have little bearing on the shorter wavelength gravity features discussed herein. However, they must be considered when average free-air anomaly values are used as an indication of the degree of isostatic compensation.

Northwest Margin

The Northwest Margin is considered to extend from the Exmouth Plateau to the Arafura Sea (Figure 2). Its southwest boundary lies within the Cuvier Regional Gravity

Ashmore Reefs	2
Cata Trough	12
Dampier Ridge	8
Eastern Plateau	18
Gulf of Papua	19
Kangaroo Island	6
Lord Howe Basin	9
Lord Howe Is. Seamount Chain	10
Louisiade Archipelago	22
Mellish Rise	15
Middleton Basin	11
Montebello Trough	4
Moresby Trough	20
Osprey Basin	16
Papuan Plateau	21
Portlock Trough	17
Queensland Trough	14
Tasmantid Seamount Chain	7
Timor Trough	13
Townsville Trough	13
Wombat Plateau	3
St. Vincent's Gulf	5

Numbered features on Figure 2—Bathymetry

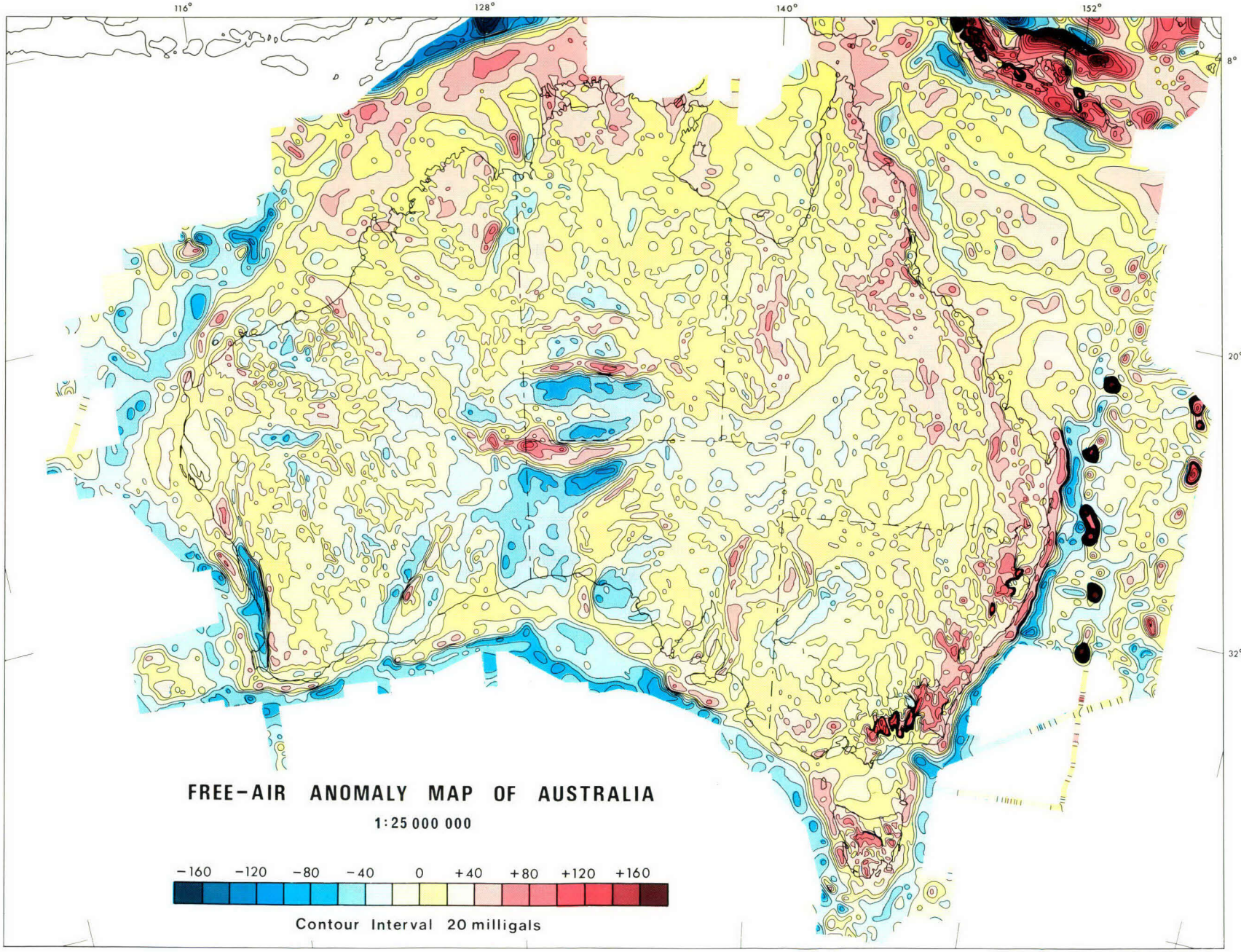
116°
128°
140°
152°
8°
20°
32°
FREE-AIR ANOMALY MAP OF AUSTRALIA
1:25 000 000
−160 −120 −80 −40 0 +40 +80 +120 +160
Contour Interval 20 milligals

On the following pages are a Free-air Anomaly Map of Australia and a Gravity Map of Australia (showing Bouguer anomalies on land and free-air anomalies at sea), both at a scale of 1:25 million.

The Free-air Anomaly map is a smaller version of an unpublished map prepared as an overlay to the 1:2.5 million 1976 Geological Map of Australia; its projection is Simple Conic. The Gravity Map is a smaller version of the 1:5 million 1976 Gravity Map of Australia; its projection is Lambert Conformal.

Both maps were prepared from the same data bank as the 1:5 million Gravity Map of Australia with the addition of some marine observations by the "Gulf Rex" which fill a large gap at the southern end of the Great Barrier Reef.

Details of the sources of data, reduction of observations, accuracy of the anomalies, and techniques used for smoothing and contouring are contained in Anfiloff et al. (this issue).

The maps were drawn by P. Moffat and A.J. Maxwell of BMR's Geophysical Drawing Office and printed by the Division of National Mapping, Department of National Resources.

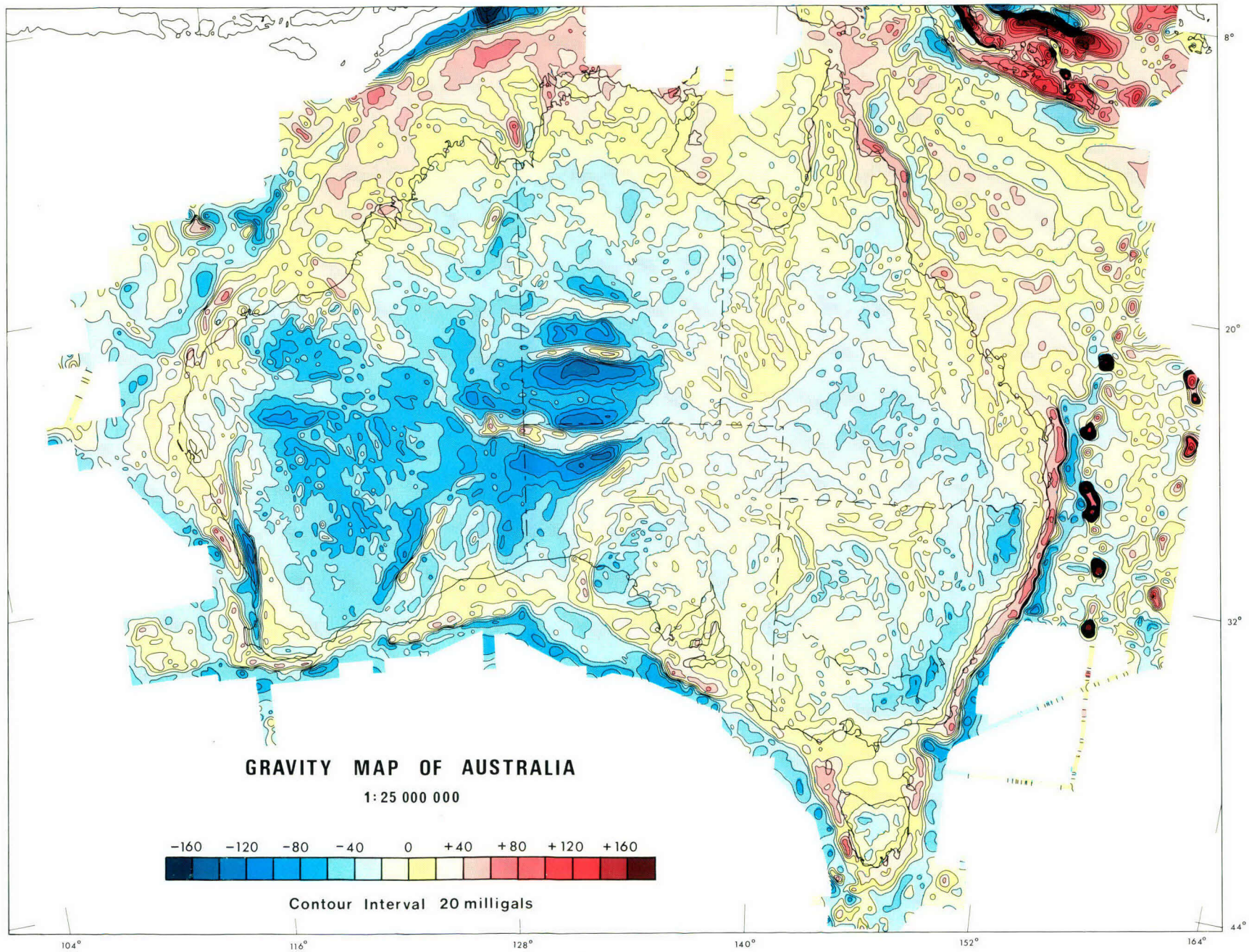
8°
20°
32°
44°
104°
116°
128°
140°
152°
164°
GRAVITY MAP OF AUSTRALIA
1:25 000 000
−160 −120 −80 −40 0 +40 +80 +120 +160
Contour Interval 20 milligals

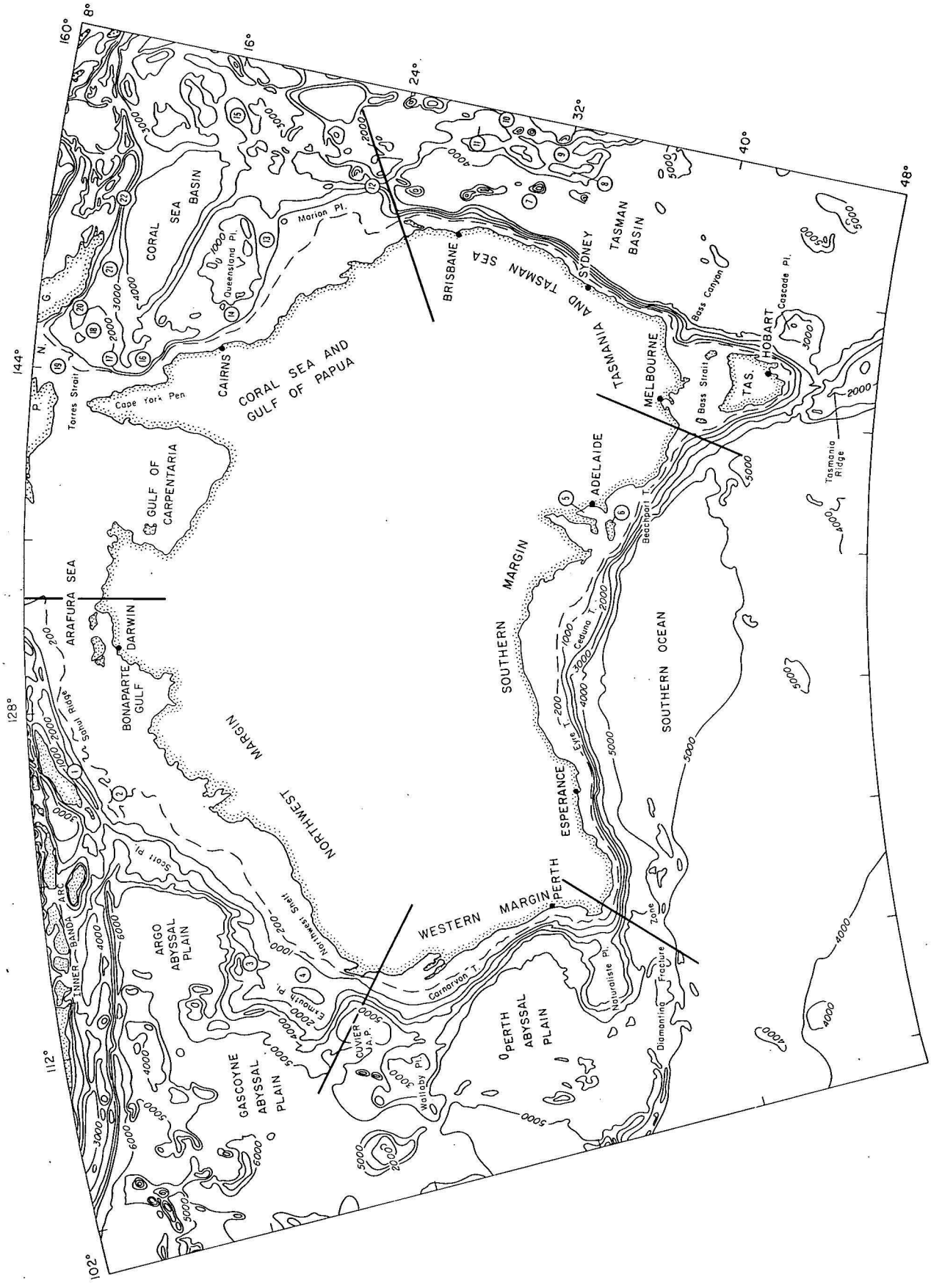

Figure 2. **Bathymetry. Contours in metres based on Continental Margin Survey data (BMR) and General Bathymetric Chart of the Oceans Sheet A111 prepared by the Hydrographic Office, R.A.N., Sydney. Shows regional subdivision of the margin.**

Complex (20), the description of which is included in this section for convenience. Until Jurassic time it probably lay along the northern shores of Gondwanaland, adjacent to the Tethyan Ocean (Veevers, 1976). Northeast-trending structures which are predominant along the margin formed in the late Middle Jurassic, probably as a result of sea-floor spreading about northeast-trending ridges, within and adjacent to Gondwanaland (Veevers & Heirtzler, 1974). Formation of the Timor Trough probably occurred in the Pliocene (Veevers, Heirtzler *et al.*, 1974) in response to either subduction beneath Timor (Fitch, 1972; Warris, 1973) which has since ceased; or subduction further north along the Inner Banda Arc (Chamalaun *et al.*, 1974).

Varying degrees of isostatic compensation are indicated by the average values of the free-air anomalies. The most significant departure from equilibrium probably occurs over the Timor Trough. The Bouguer anomalies in that area exhibit a steep gradient, with values decreasing northward, and probably reflect crustal thickening due to downwarping beneath the Trough (Audley-Charles *et al.*, 1972; Heirtzler, Veevers *et al.*, 1973). A preponderance of positive free-air anomalies on the continental shelf, possibly resulting from rapid accumulation of carbonate sands since the Miocene, indicate that slight subsidence is necessary if isostatic equilibrium is to be attained. The Exmouth and Scott Plateaus appear to be regionally compensated, although the presence of free-air anomaly features of up to 60 mGal magnitude indicates that individual structural elements, generally 100 to 200 km across, remain supported by the crust. The Bouguer anomaly values suggest that crust under the Exmouth Plateau has about the same thickness as that under the continental shelf and that crust of oceanic thickness (about 10-15 km) is confined to the lower continental slope and abyssal plains, generally beyond the 4000 m isobath (Branson, 1974; Figure 3).

Along the coast and inner continental shelf the gravity field is dominated by north to northwest-trending ridges, separated by broad gravity lows. Over the outer continental shelf these features are truncated or obscured by a northeast-trending band, made up of gravity ridges and flanking troughs. The gravity pattern results largely from crustal fragmentation which commenced in the Proterozoic (Powell, 1976), led to formation of the intracratonic Canning and Bonaparte Gulf Basins (Figure 3) in the Palaeozoic, and largely terminated with the breakup of eastern Gondwanaland in the late Middle Jurassic. A number of Permian to Tertiary epicontinental basins associated with breakup and formation of the continental margin lie beneath the inner continental slopes and give rise to a series of gravity lows.

Gravity provinces along the Northwest Margin are grouped according to the ages of the structural elements which give rise to them: namely, Proterozoic blocks and basins, Palaeozoic basins, and Mesozoic and Tertiary basins.

The Kimberley Regional Gravity Platform (41) corresponds with the Kimberley Block, which consists of flat-lying early Proterozoic sediments and volcanics. Offshore, shallow basement of the Londonderry Arch and Leveque Platform, is probably also part of the Kimberley Block. Sediments of similar age probably extend further west beneath the Browse Basin and underlie a Jurassic sequence on the Scott Plateau (Powell, 1976, figure 3). However, the gravity data cannot be used to confirm or refute this idea, since the Kimberley Block is associated with an almost featureless gravity field, which would be masked by the gravity effect of younger post-breakup structures within the Browse Basin and Scott Plateau areas.

The Fortescue Regional Gravity Complex (27) encompasses a partly buried Archaen craton, of which the Pilbara Block is the only exposed part. The northwest edge of the province corresponds with a fault separating the Pilbara Block from the Dampier Sub-basin (Geological Society of Australia, 1971); however, Archaean Pilbara Block basement probably extends beneath the Dampier Sub-basin. The Montebello Regional Gravity Ridge (23), which lies along the western margin of the Dampier Sub-basin, has the characteristics of the Anketell (29) and Ashburton (26) Regional Gravity Ridges on land; these are expressions of Proterozoic mobile belts on the northwest and southwest flanks of the Pilbara Block. The nature of the Precambrian basement inferred to exist beneath the Exmouth Plateau is unknown (Exon *et al.*, 1975).

The Bonaparte Regional Gravity Complex (45) covers part of the Bonaparte Gulf Basin, which consists of up to 15 000 m of Phanerozoic sediment (Laws & Kraus, 1974). The structural configuration of the area is essentially the result of Middle Jurassic fragmentation and Miocene folding of a once relatively simple Cambrian-Triassic Basin. Contrary to expectations, the free-air anomalies show a north-trending ridge over the central zone where the sediment is thickest, suggesting that dense material is present within the sedimentary section or that the basement density is anomalously high. The latter could be the result of an offshore extension of the Halls Creek Mobile Belt which flanks the Kimberley Block (Geological Society of Australia, 1971) since this gives rise to a gravity ridge of similar amplitude onshore. The Sahul Bank Regional Gravity Ridge (44) to the north of the Bonaparte Gulf Basin corresponds to a basement high known as the Sahul Ridge, which is bounded by northeast-trending Plio-Pleistocene faults. Southeasterly trending folds which cut across the area are believed to reflect a Permo-Triassic fault pattern (Laws & Kraus, 1974). The Cartier Regional Gravity Shelf (42) to the northwest corresponds to the Northeast Londonderry Ridge, which separates the Bonaparte Gulf and Browse Basins (Figure 3). The Northeast Londonderry Ridge resulted from northeast-trending en echelon faulting in the mid-Jurassic, rejuvenated in the Late Tertiary. Further to the northwest, the northeastern extremity of the Scott Regional Gravity Complex (38) reflects an uplifted area of thick Triassic sediment known as the Ashmore-Sahul Block. This lies

Abrolhos Sub-basin	18
Ashmore Sahul Block	1
Aure Trough	44
Barrow Sub-basin	11
Beagle Ridge	19
Beagle Sub-basin	7
Bedout Sub-basin	6
Bernier Platform	13
Bremer Fault	26
Bunbury Trough	25
Cape York/Oriomo Ridge	43
Clarence/Moreton Basin	36
Coen Inlier	42
Dampier Sub-basin	10
Darling Fault	22
Denman Basin	28
Dundas Trough	34
Dunborough Fault	23
Duntroon Embayment	30
Easter Ridge	16
Exmouth Sub-basin	12
Fraser Fault	27
Gascoyne Sub-basin	14
Halls Creek Mobile Belt	5
Hardabut Fault	15
Hodgkinson Basin	40
Kangaroo Syncline	9
Kanmantoo Trough	31
King Island High	32
Laura Basin	41
Leveque Platform	4
Londonderry Arch	3
Lord Howe Is. Seamount Chain	38
Lord Howe Rise	39
Maryborough Basin	37
Naturaliste Block	24
Northeast Londonderry Ridge	2
Northampton Block	17
Polda Trough	29
Rankin Platform	8
Rocky Cape Geanticline	33
Turtle Dove Ridge	20
Tyenna Geanticline	35
Vlaming Sub-basin	21

Numbered features on Figure 3—Structural elements

Figure 3. Structural elements (based on Tectonic Map of Australia and New Guinea, Geological Society of Australia, 1971).

within a zone of basement highs along the northwest Australian continental shelf forming the seaward margin of a series of Mesozoic sedimentary basins.

The Browse Regional Gravity Low (40) is associated with a broad depression in aeromagnetic basement (Geological Society of Australia, 1971) and the main depocentre of the Browse Basin, which consists of up to 10 000 m of Mesozoic to Tertiary sediments overlying a Palaeozoic sequence (Powell, 1976). The gravity ridge along its western margin is related to the Scott Reef Trend which is a structural high composed of block-faulted rocks of pre-Middle Jurassic age. Further west, a gravity low within the Scott Regional Gravity Complex (38) and the D'Artagnan Regional Gravity High (39), broadly reflect the structure of the basement surface on the Scott Plateau, as interpreted on BMR seismic profiles.

The Munro Regional Gravity Platform (37) and Fitzroy Regional Gravity Complex (36) extend over parts of the Canning Basin and its principal sub-basin, the Fitzroy Graben. Onshore, the Canning Basin and Fitzroy Graben have a northwesterly elongation, and consist of about 2000 m and possibly up to 19 000 m respectively, of mainly flat-lying Palaeozoic sediment with a Mesozoic cover. The gravity field broadly reflects variations in depth of magnetic basement, presumably Precambrian, but is caused partly by density contrasts within it. Offshore, the gravity contours have an east to northeast trend which reflects structures within a much thicker Mesozoic sequence in the Bedout Sub-basin (Challinor, 1970). However, this sub-basin has little gravity expression, probably because it is underlain by dense rocks which onshore give rise to the Anketell Regional Gravity Ridge (29).

The Barrow Regional Gravity Low (28) is attributed to the Barrow, Dampier and Beagle Sub-basins of the northern Carnarvon Basin. These sub-basins are Upper Triassic to Cretaceous downwarps between the Pilbara Block and the Rankin Platform; this platform is a fault-controlled ridge along the edge of the continental shelf. The Rankin Platform and a possible Proterozoic mobile belt, discussed above, jointly contribute to the Montebello Regional Gravity Ridge (23). Minor gravity lows between the Munro Regional Gravity Platform (37) and the Barrow Regional Gravity Low (28), reflect the continuity of thick Mesozoic sediments between the Bedout and Beagle Sub-basins.

Gravity features on the Exmouth Plateau can be related broadly to the relief of the Middle Jurassic unconformity surface and variations in water depth (Exon *et al.*, 1975). The sedimentary section in the area is up to 10 000 m thick and is considered by Exon *et al.* (1975) to be an extension of the northern Carnarvon Basin (Thomas & Smith, 1974). The northern end of the Petrel Regional Gravity Trough (18) coincides with the Montebello Trough (Falvey & Veevers, 1974), a saddle between the Northwest Shelf and the crest of the Exmouth Plateau, but low free-air anomaly values are attributed largely to relatively mass-deficient sediments of the underlying Kangaroo Syncline, which began to form in the Middle Jurassic. The eastern margin of the syncline underlies prograded carbonate sands forming the continental shelf in this area. Continuity of Bouguer anomalies from the continental shelf to the Montebello Trough, noted by Branson (1974), supports the concept of a depositional, rather than a structurally controlled, shelf-break. The Exmouth Plateau Regional Gravity Ridge (21) follows the crest of the Exmouth Plateau Arch, an area which remained relatively high during subsidence of the plateau, possibly in the Miocene (Exon *et al.*, 1975). It consists of numerous north-northeast-trending fault-blocks of mainly Middle Jurassic age. The gravity high in the northern part of the province is associated with shallow, possibly igneous basement. The Wombat Regional Gravity Complex (22) corresponds with the small Wombat plateau and several east to north-trending grabens and troughs along the northern margin of the Exmouth Plateau. Local gravity features within the province reflect the combined effect of variations in water depth and the relative elevation of basement within major fault-blocks. East-trending features within the southern part of the province are probably related to deep-seated Palaeozoic structures.

The Cuvier Regional Gravity Complex (20) encompasses the northwest and southwest margins of the Exmouth Plateau and part of the Cuvier Abyssal Plain. North and northwest-trending gravity ridges within it are attributed to upturned beds and relatively shallow continental basement along the Exmouth Plateau margins (Exon & Willcox, 1976). In some places, igneous intrusions contribute to the gravity ridges and give rise to intense magnetic anomalies. Along the northwest margin, the intrusions were probably emplaced during rifting and formation of the margin in the late Middle Jurassic. Intrusions on the southwest margin were probably emplaced in the Late Cretaceous along a transform fault (Veevers & Heirtzler, 1974), which may have developed along an old line of weakness within the continent, in the manner illustrated by Wilson (1965, Figure 6).

Western Margin

The Western Margin extends from the Cuvier Abyssal Plain to just south of the Naturaliste Plateau (Figure 2). The structure of this margin formed during the breakup of Gondwanaland commencing in the late Carboniferous with a 170 m.y. period of uplift, erosion and deposition of epiclastic sediments in rift valleys (Veevers & McElhinny, 1976). This produced a margin characterized by a series of north-northeast-trending and north-northwest-trending longitudinal ridges and troughs, forming the sub-basins of the Carnarvon and Perth Basins, respectively. The structural grain is clearly reflected in the gravity field by adjacent belts of positive and negative free-air anomalies that lie parallel to the continental margin trends. The trend of the gravity anomalies over the Wallaby and Naturaliste Plateaus suggests that these features, which are partially detached from the continental margin, also fit into this scheme for the development of the western margin.

In the early Cretaceous (130 m.y. B.P.) sea-floor spreading commenced about a northeast-trending ridge, and Greater India (Veevers *et al.*, 1975) separated from Antarctica/Australia along transforms such as that now defined by the Wallaby-Perth escarpment (Figure 3) (Veevers & Heirtzler, 1974). This was accompanied by local eruption of basalt on the continental margin, followed by a marginal marine transgression and then, finally, progradation of carbonates over a slowly subsiding margin since the Late Cretaceous (Veevers & Johnstone, 1974). The sea-floor spreading produced the ocean floors of the Cuvier and Perth Abyssal Plains; these are associated with negative free-air anomaly values on the gravity map.

The southern margin of the Naturaliste Plateau formed in a tectonic environment related to the separation of Antarctica and Australia commencing in the Late Paleocene (see p. 310).

Positive free-air anomaly values over the continental shelf and upper slope, and negative values at the base of the continental slope, are due in part to the free-air anomaly edge effect over the continental margin (Figure 1). On the continental shelf this has been highly modified by near-surface geology, and in several places onshore gravity provinces and trends extend to the upper continental slope. The most prominent gravity features are associated with basement highs such as the regional gravity high over the Bernier Platform. Regional gravity highs adjacent to the Perth Basin are related to offshore extensions of the Northampton and Naturaliste Blocks, and the Turtle Dove Ridge, all of which are Precambrian inliers or basement highs. Relative gravity lows correspond with the thick, faulted, Mesozoic sediments of the offshore Exmouth Sub-basin and the Abrolhos and Vlaming Sub-basins.

Slightly positive free-air anomalies over the Wallaby Plateau indicate that this feature is very close to isostatic equilibrium. More positive free-air anomaly values over the Naturaliste Plateau may indicate that slight subsidence is necessary for it to attain isostatic equilibrium.

The steep Bouguer anomaly gradient associated with the continental slope and the western and southern margins of the Naturaliste Plateau (Figure 4) is indicative of rapid crustal thinning in these areas. Bouguer anomaly values suggest that the crust under the Wallaby and Naturaliste Plateaus is about 8 km thinner than that under the adjacent

continental shelf (Branson, 1974). A crustal profile over the Naturaliste Plateau computed by Petkovic (1975a) from Bouguer anomaly values using assumed densities, and a standard crustal thickness of 31 km derived from the seismic refraction results of Mathur (1974), gave a crustal thickness of 22 km for the plateau and about 18 km for the trough between the plateau and the continental shelf.

The gravity field offshore from western Australia is characterized by three major belts of gravity provinces, which extend parallel to the continental margin. The most striking of these occurs at the foot of the continental slope and is a belt of free-air anomaly lows which comprises the Petrel (18) and Naturaliste (2) Regional Gravity Troughs. This belt is bounded to the east on the continental shelf and upper continental slope by several provinces which are characterized by free-air anomaly highs. To the west of the Petrel (18) and Naturaliste (2) Regional Gravity Troughs are provinces which have complex gravity contour patterns. The gravity platforms within these provinces generally correspond to marginal plateaus and the lows to areas of deep ocean floor.

The Hartog Regional Gravity High (17) and the Montebello Regional Gravity Ridge (23) cover part of the offshore Carnarvon Basin. Contour trends in both provinces are well-defined north-northeasterly, parallel to structural trends in the Carnarvon Basin. The eastern part of the Hartog Regional Gravity High (17) covers the offshore Gascoyne Sub-basin. A north-northeast-trending gravity high within the province is probably related to a basement high which was partly revealed by an aeromagnetic survey (Geophysical Associates Pty Ltd, 1966). This basement high, lying west of Carnarvon, has been called the Bernier Platform (Geary, 1970) (Figure 3), and may delineate the western margin of the Carnarvon Basin in this area. The size of the gravity high indicates that the Bernier Platform may extend further to the north and south than has been previously thought.

The two pronounced gravity highs within the Geraldton Regional Gravity High (16), and the gravity ridge in the east of the Leeuwin Regional Gravity High (3), correspond to basement highs and inliers of Precambrian rocks. The northernmost high within the Geraldton Province is associated with the mid-Proterozoic granulites of the Northampton Block; its shape suggests an extension of the granulites north of the Hardabut Fault, and a west to northwest extension offshore (the 'Easter Ridge') (Figure 3). The northwest-trending southernmost high is associated with the Turtle Dove Ridge, formed of uplifted Precambrian basement (Jones & Pearson, 1972). The north-trending Beagle Ridge, which is a Precambrian basement high that merges with the Turtle Dove Ridge, has very little gravity expression on the Gravity Map of Australia. This may be partially due to the lack of control in the gravity contours in the zone between the marine and land data sets. The northwest-trending gravity trough within the Geraldton Province is associated with the depocentre of the Abrolhos Sub-basin. The shape of the gravity contours indicates that the sub-basin is an off-shoot of the Perth Basin and that its depocentre is connected to the Perth Basin rather than trending south-southwest between the Turtle Dove and Beagle Ridges as indicated by Jones & Pearson (1972). The prominent north-trending gravity ridge within the Leeuwin Regional Gravity High (3) is associated with the late Proterozoic granulites and gneisses of the Naturaliste Block. The areal extent of the ridge suggests that the block extends offshore for large distances to the north, west and south of its onshore exposure. The inferred offshore extension of the Dunsborough Fault, which defines the eastern margin of the Naturaliste Block, as shown on the Tectonic Map of Australia and New Guinea (Geological Society of Australia, 1971) and reproduced in Figure 3, is based on the offshore continuation of high frequency magnetic anomalies associated with the eastern margin of the Naturaliste Block (BMR, 1976b). The only evidence for the offshore Dunsborough Fault on the gravity map is a slight westward displacement of the gravity ridge associated with the Naturaliste Block. The continuity of the gravity ridge to the north suggests that rocks similar to those of the Naturaliste Block

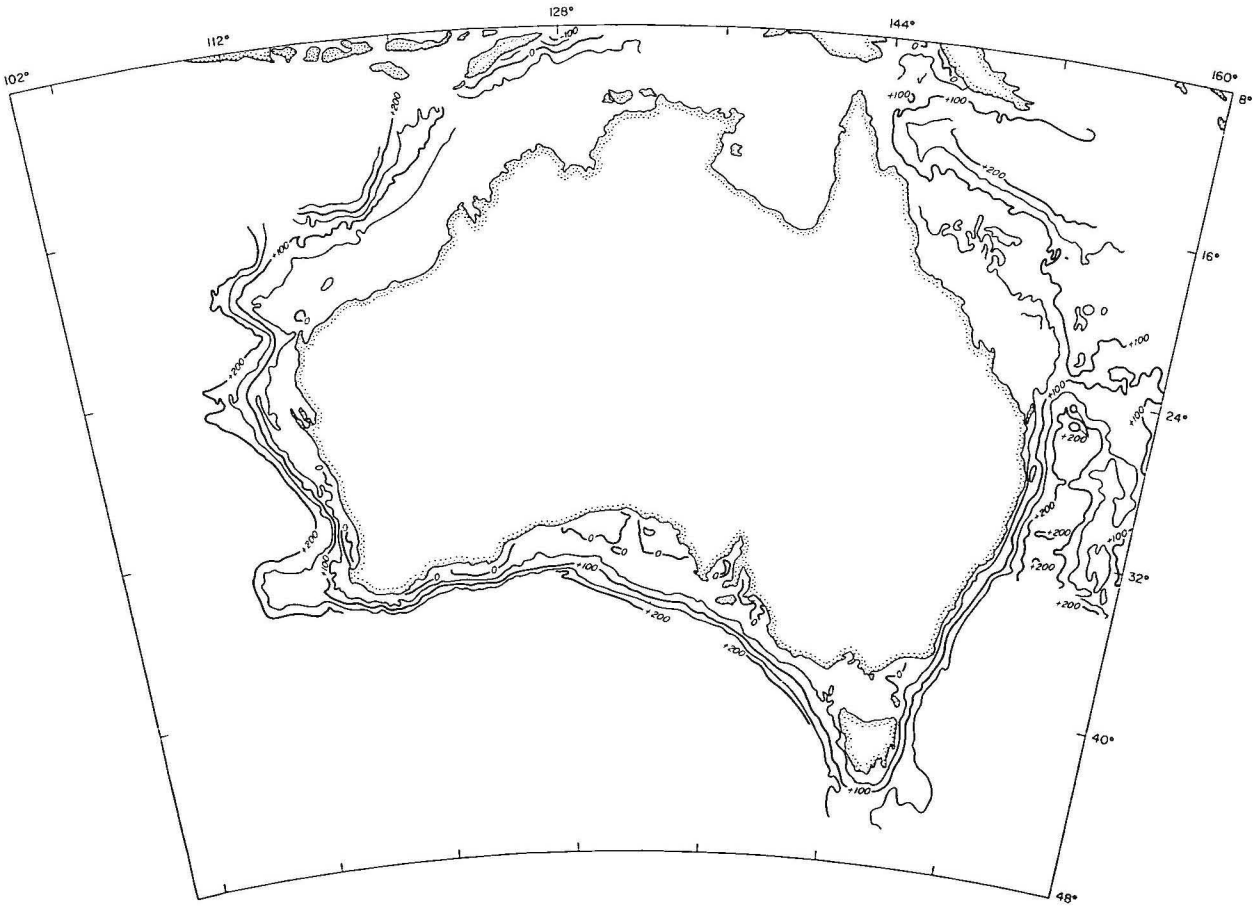

Figure 4. Marine Bouguer anomalies (Bouguer density 2.2 t.m^{-3}).

occur at shallow depth to the north of the fault. There is some indication of this on BMR seismic lines in the area. An interpretation which explains the apparent conflict between the magnetic and gravity results is that onshore the Dunsborough Fault has placed magnetic Proterozoic rocks against Mesozoic and Permian sediments in the Bunbury Trough; however, offshore magnetic Proterozoic rocks lie against non-magnetic Proterozoic rocks.

The Geraldton (16) and Leeuwin (3) Regional Gravity Highs are separated by a northwest-trending saddle, which connects the Perth Regional Gravity Low (4) with the Petrel Regional Gravity Trough (18). The contour closure within the saddle area east of Perth is probably the gravity expression of the Cretaceous-Tertiary Vlaming Sub-basin. The apparent continuity of trend of the possible transform fault delineated by the Wallaby-Perth scarp (Veevers & Heirtzler, 1974), with the saddle in the free-air anomalies east of Perth and the gravity low associated with the Bunbury Trough, suggests that the negative free-air anomalies may define the old line of weakness within the continent responsible for initiating the transform fault during rifting.

The Petrel (18) and Naturaliste (2) Regional Gravity Troughs extend along the base of the continental slope adjacent to deep ocean floor, and across the saddles separating the continental shelf from marginal plateaus. Part of the negative free-air anomaly expression of the provinces is related to the gravity edge effect of the continental slope, particularly where the provinces lie adjacent to the deep ocean floor. The provinces are associated with a strong Bouguer anomaly gradient, indicating westward crustal thinning. The northeast-trending portion of the Petrel Regional Gravity Trough (18) contains two units which culminate in closures of the −40 mGal contour. The northern unit is associated with the Montebello Trough (see Northwest Margin), and the southern unit extends over the base of the continental slope in the north and the saddle between the continental shelf and the Wallaby Plateau in the south. The gravity expression of the Naturaliste Regional Gravity Trough (2), and those sections of the Petrel Regional Gravity Trough (18) adjacent to marginal plateaus, is due partly to the rapid change in water depth and partly to an increase in the thicknesses of sediments in these areas.

The Wallaby Regional Gravity Complex (19) mainly covers the Wallaby Plateau. An examination of seismic sections reveals that the variation in the gravity values throughout the province is generally related to basement depth.

The Naturaliste Regional Gravity Platform (1) covers most of the Naturaliste Plateau. The northern, western and southern margins of the province are associated with strong Bouguer anomaly gradients indicating rapid crustal thinning. The main features within the province are two gravity highs having a free-air anomaly magnitude greater than +30 mGal. They correspond with bathymetric highs but may, in part, represent the effect of basement highs (P. J. Cameron & P. Petkovic, unpublished data.)

Southern Margin

The southern margin extends from 115° to 143°E. Northwest to northeast-trending structures onshore occur mostly within the Proterozoic Yilgarn and Gawler Blocks, and as flanking mobile belts. The gravity anomalies indicate that some of these features extend at least to the edge of the continental shelf and probably underlie the Eyre and Ceduna Terraces. The Adelaide Geosyncline consists of Upper Proterozoic and Cambrian sequences capped by Tertiary sediment, extends southwards across the coast and then follows a southwest trend on the continental shelf.

The Early Cretaceous-Tertiary Great Australian Bight and Otway Basins contain up to 10 000 m of sediment deposited during the formation of the continental margin. Extensive block-faulting roughly parallel to the coast occurred at the end of the Early Cretaceous. This led to the formation of elongated troughs, in which Late Cretaceous and Early Paleocene fluvio-deltaic sediment was deposited, together with shallow marine sediment resulting from brief incursions of the sea (Willcox, 1974; Bouef & Doust, 1975; Denham & Brown, 1976; Willcox, in press). Sea-floor spreading commenced in the Late Paleocene (Weissel & Hayes, 1972) but was not a synchronous event along the entire margin—marine influence appears to have spread from the west.

The preponderance of positive free-air anomalies on the continental shelf, although partly due to edge effect (Figure 1), indicates that slight subsidence must take place to achieve isostatic equilibrium. The short wave-length of the anomalies, and the thin sediment cover, averaging about 500 m, is interpreted as indicating a source largely within the Proterozoic crystalline basement, although the gravity effects of the Polda Trough and a basement ridge along the southern edge of the Eyre Terrace are also evident. A regional gravity low corresponds with the Ceduna Terrace, and results from the thick sedimentary sequence and great depth of basement in the Great Australian Bight Basin. Gravity troughs also occur over the Bremer Basin (Cooney *et al.*, 1975) and the Otway Basin, but are not as well-developed.

The Bouguer anomalies show gradients across the margin of between 1 and 3 mGal/km, caused by crustal thinning. Crustal profiles over the Eyre and Ceduna Terraces have been computed by Willcox (in press) from filtered gravity values, using assumed densities, and a standard crustal thickness consistent with that derived from seismic refraction surveys onshore (Doyle & Everingham, 1964). These profiles indicate that 30 km of crust underlies the continental shelf, 22-28 km under the terraces, and that the transition from crust of typically continental to typically oceanic thickness occurs under the continental rise. However, the continental rise in this region is up to 200 km wide and is underlain by block-faulted structures and unconformities which appear to correlate with those on the Ceduna Terrace (Bouef & Doust, 1975; Willcox, in press).

The free-air anomaly field over the southern margin may be divided into four major bands of gravity features roughly parallel to the coast. These comprise relatively short wavelength, largely positive, features over the continental shelf, upper part of the continental slope, and the Eyre Terrace; gravity platforms over the Ceduna Terrace and offshore Otway Basin; a pronounced free-air anomaly trough along the foot of the continental slope; and a marginal free-air anomaly ridge of about 40 mGal amplitude over the continental rise south of the Eyre Terrace.

In the west of the region, the well-defined Albany Regional Gravity Ridge (7) overlies the continental shelf. A comparison with the adjacent gravity features indicates that it is probably associated with amphibolite facies rocks within an offshore portion of the Proterozoic Albany-Fraser Province which flanks the Yilgarn Block. These amphibolites also give rise to the Fraser Regional Gravity Ridge (10), whereas Proterozoic sediments and granites within the Province give rise to regional gravity lows. Edge effect at the continental margin contributes about +30 mGal to the Albany Regional Gravity Ridge (7).

The Eyre Regional Gravity Complex (69) corresponds to an area of shallow, probably Proterozoic, basement which generally lies beneath only 200 to 500 m of Eucla Basin sediment. A gravity ridge along part of its southern edge is caused by a basement ridge and by edge effect (Figure 1). Most of the adjacent Nullarbor Regional Gravity Shelf (70) also corresponds to the Eucla Basin, although the sediments are somewhat thicker. In its southeast corner, a salient in the gravity contours indicates that the Denman Basin, which consists of 1500 m of sediment ranging in age from Proterozoic to Tertiary (Scott & Speer, 1969; Thompson, 1970), extends offshore for about 25 km.

The intense north-trending D'Entrecasteaux Regional Gravity Ridge (73) lies on the margin of the Gawler Block (Geological Society of Australia, 1971) and appears to be an offshore extension of a gravity ridge within the Woorong Regional Gravity Complex (71). It corresponds to an area of intense magnetic anomalies of up to 2000 nT amplitude, which have a source just below a thin blanket of Quaternary sediment. This feature may be caused by ultrabasic rocks or a mineralized zone flanking the Gawler Block (Willcox, in press).

The east-trending Investigator Regional Gravity Trough (75) corresponds with a trough in the magnetic basement (Geological Society of Australia, 1971). These features are expressions of the fault-bounded Polda Trough, a Jurassic or Early Cretaceous rift in the Gawler Block; the Trough contains about 2500 m of sediment (Smith & Kamerling, 1969; Target, 1971).

Gravity features within the Kangaroo Regional Gravity Complex (78) are attributed largely to density contrasts within the Gawler Block which lies beneath a veneer of sediment. North-trending contours in St. Vincent's Gulf, and east-trending contours near Kangaroo Island, reflect the structure of the Adelaide Geosyncline and Cambro-Ordovician sediments of the Kanmantoo Trough on its southeast flank. The southwest edge of the gravity province corresponds with the Cygnet Fault west of Kangaroo Island, and with a steep fault-controlled shelf-break south of Kangaroo Island, giving rise to a large edge effect.

The Ceduna Terrace Regional Gravity Shelf (74) and the southern part of the Gambier Regional Gravity High (83) are attributed to the Great Australian Bight and Otway Basins, respectively. Both basins comprise 6000-10 000 m of Lower Cretaceous to Tertiary sediment overlying Precambrian and/or Palaeozoic basement (Bouef & Doust, 1975; Willcox, in press). The pre-Upper Cretaceous sequence is extensively block-faulted and uplifted blocks flank the southern margin of both basins, contributing to the marginal gravity ridges.

Free-air anomaly lows within the Eltanin Regional Gravity Trough (87) are partly caused by edge effect (Figure 1). However, a free-air anomaly low of −100 mGal 350 km southwest of Esperance, may be related to the 2000-3000 m of probable Cretaceous and Tertiary sediment in the Bremer Basin (Cooney *et al.*, 1975). The linear free-air anomaly trough south of the Eyre Terrace corresponds with a band of major faults along the northern edge of the continental rise which is up to 200 km wide in this area.

A free-air anomaly ridge occurs 20-40 km beyond the continental slope south of the Eyre Terrace and extends westward for at least 500 km. The ridge lies within a region which on seismic profiles appears to be composed of subsided continental crust; however, its source is not apparent. Intrusions within an aborted rift or along a major fault which was formed during the rifting of Australia and Antarctica may explain this gravity feature.

Inflections of the Eltanin Regional Gravity Trough (87), particularly just east and west of the Ceduna Terrace and between the Eyre (69) and Albany (7) gravity provinces, may be related to zones of weakness in the basement which led to formation of transform faults in the Southern Ocean.

Tasmania and Tasman Sea

The Tasmania and Tasman Sea region is considered to extend from just northwest of Tasmania, around the southeast Australian continental margin to the northern end of the Tasman Basin (Figure 2). The continental margin differs markedly from that in other regions of Australia in that it is very narrow, averaging about 50 km in width. Much of the region consists of deep ocean floor which was formed during two stages of rifting and sea-floor spreading.

The Tasman Sea evolved by sea-floor spreading about a northwest-trending ridge between 80 and 60 m.y. ago and resulted in the separation of the Lord Howe Rise/New Zealand Plateau from Australia (Hayes & Ringis, 1973). This process produced the structurally complex north Tasman Basin, bounded to the east by the north-trending Dampier Ridge and the enclosed Middleton and Lord Howe Basins (Figure 2). The complex structure is reflected in the gravity map by a very complicated free-air anomaly pattern over the north Tasman Basin.

The western continental margin of Tasmania and the Tasmania Ridge developed as a result of Antarctica separating from Australia. The initial breakup commenced in the Middle Jurassic with the formation of rift valleys (Veevers & McElhinny, 1976). The onset of sea-floor spreading in the Late Paleocene (55 m.y. B.P.) led to the formation of the Southern Ocean and this process continues to the present day (Weissel & Hayes, 1972). North-trending gravity ridges in the north Tasman Basin are associated with chains of guyots and seamounts. These may have formed during the northward movement of the Indian-Australian plate over a fixed mantle hot spot as Australia and Antarctica separated (Vogt & Conolly, 1971).

The two adjacent belts of gravity provinces which are parallel to the continental margin are formed by free-air anomaly highs over the continental shelf and upper continental slope, and free-air anomaly lows over the lower continental slope and adjacent deep ocean floor. This gravity pattern is mainly due to the free-air anomaly edge effect over the steep continental margin (Figure 1). Offshore extensions of structures and basins, such as the Sydney Basin, generally have no appreciable affect on the gravity ridge over the continental shelf.

Free-air anomaly values over the north Tasman Basin and the Tasmania Ridge average about zero, indicating that these features are in isostatic equilibrium. Steep Bouguer anomaly gradients across the continental margin and western margin of the Tasmania Ridge imply rapid crustal thinning into the adjacent ocean basins. An increase in Bouguer anomaly values over the Dampier Ridge indicates crustal thickening under this feature.

The most prominent features of the gravity field offshore from southeast Australia are two belts of related gravity provinces which extend parallel to the continental margin and two north-trending gravity ridges in the north Tasman Basin. Much of the remainder of the region has a complex gravity expression.

The belt of provinces covering the continental shelf and upper continental slope is made up of the West Tasmanian (86), East Tasmanian (90) and Gladstone-Eden (96) Regional Gravity Ridges. The north-northwest-trending West Tasmanian Regional Gravity Ridge (86) contains two units formed by closures of the +20 mGal contour. The northern unit covers the King Island High, and is probably related to shallow late Precambrian basement of the Rocky Cape Geanticline. This interpretation is consistent with the results of an aeromagnetic survey in the area (Finney & Shelley, 1966). The southern unit may correspond to an offshore extension of the Cambrian Dundas Trough. The unit is associated with high magnetic intensity values and its eastern margin extends over scattered outcrops of ultrabasic rocks onshore. This suggests that at least part of the gravity expression of the unit may be related to ultrabasic bodies within the Dundas Trough (Fraser *et al.*, in prep).

The East Tasmanian Regional Gravity Ridge (90) consists of three main units. The southern unit, which has a complex gravity expression, corresponds to a bathymetric feature, the Tasmania Ridge. The variation of free-air anomaly values within the unit is closely related to the rugged bathymetry of this part of the ridge. Bouguer anomaly gradients associated with the unit indicate gradual crustal thinning from Tasmania to the ridge, and rapid crustal thinning across the western margin of the ridge. The central unit is a free-air anomaly high, which covers the continental shelf and upper slope off south and southeast Tasmania. At least part of this gravity high may be the expression of dolerite bodies; these intruded the Permo-Triassic sediments of the Tasmania Basin extensively during the Jurassic. The northern unit is a free-air anomaly high covering the continental shelf and upper slope northeast of Tasmania. It is not associated with positive magnetic anomalies similar to those that occur over igneous bodies on the lower continental slope in this area (Cameron & Pinchin, 1974). There is some indication on seismic lines in the area that the gravity high may correspond to a non-magnetic basement high near the shelf-break.

The variation in free-air anomaly values and associated strong Bouguer anomaly gradient across the adjacent Gladstone-Eden Regional Gravity Ridge (96) and Hamme Regional Gravity Trough (97), reflects the rapid transition from continental to oceanic-type crust across the continental margin in this area. The Sydney, Clarence-Moreton and Maryborough Basins have no appreciable affect on gravity values within the Gladstone-Eden Regional Gravity Ridge (96). A 10-20 mGal increase in the magnitude of the free-air anomaly values north of 33°S corresponds to the boundary

between the Permo-Triassic Sydney Basin and the Silurian to Permian New England Geosyncline.

The west-northwest-trending gravity low within the Hamme Regional Gravity Trough (97) east of Bass Strait is related to the Bass Canyon. The more poorly defined gravity low within the Hamme Province, north of 24°S, corresponds with the Cato Trough. The Bouguer anomaly ridge associated with the province in this area probably indicates crustal thinning beneath the Cato Trough (Mutter, 1974).

The gravity highs forming the north-trending Tasmantid (98) and Lord Howe (100) Regional Gravity Ridges are associated with basaltic guyots and seamounts of the Tasmantid and Lord Howe Island seamount chains, respectively. The complex pattern of gravity highs at the northern end of the Tasmantid Regional Gravity Ridge (98) is related to reefs on the eastern margin of the Cato Trough, and bathymetric highs of the rugged Mellish Rise.

Free-air anomaly values within the Dampier Regional Gravity Complex (99) are closely related to bathymetry; gravity lows on its western margin correspond to the Tasman Basin, gravity highs in the centre of the province correspond to the Dampier Ridge, and gravity lows on its eastern margin correspond to the Middleton and Lord Howe Basins. The gravity highs in the centre of the province are associated with a Bouguer anomaly depression which reflects crustal thickening under the Dampier Ridge. Many local contour closures within the Dampier Regional Gravity Complex (99) correlate with maxima and minima of basement relief (Symonds, unpublished data). For instance, gravity highs over the Dampier Ridge generally correspond with positive magnetic anomalies and basement highs, indicating that at least part of the Dampier Ridge probably consists of basic igneous rocks (Symonds, 1973).

The Cascade Regional Gravity High (91) corresponds to a bathymetric feature, the Cascade Plateau. It is separated from the Tasmanian continental shelf by a bathymetric trough which is associated with negative free-air anomaly values of the Hamme Regional Gravity Trough (97). A local high within the cascade province is formed by closure of the zero milligal contour and corresponds with a bathymetric feature, which is either a basement high or intrusion.

Coral Sea and Gulf of Papua

The Coral Sea and Gulf of Papua region extends north from the southern margin of the Marion Plateau to the coast of Papua New Guinea (Figure 2). The region contains three large marginal plateaus, the Marion, Queensland and Eastern Plateaus, and a small enclosed ocean basin, the Coral Sea Basin. The tectonic development of the northeastern margin of Australia is still in doubt; it is not possible to ascertain whether the Coral Sea Basin resulted from sea-floor spreading, as no ridge or identifiable magnetic lineation pattern has yet been found. On the basis of Deep Sea Drilling Project results in the Coral Sea, Taylor (1975) suggested that continental break-up occurred in the Early Eocene along the trend of the Coral Sea Basin. This may be reflected in the gravity map by a west-northwest trending gravity high in the centre of the Basin.

The gravity field of much of offshore northeast Australia is relatively smooth, and is characterized by large areas of positive free-air anomaly values over the continental shelf and the marginal plateaus. The continuity of positive free-air anomaly values from the Australian continental shelf across Torres Strait to Papua New Guinea probably indicates continuity of Tasman Geosyncline-type Palaeozoic basement across the area. Similarity of the trends of gravity highs over the Marion and Queensland Plateaus to structural trends within the Palaeozoic geosyncline onshore supports the interpretation that the basement rocks of these plateaus are part of the Tasman Geosyncline (subdivided in Figure 3 into the New England and Lachlan Geosynclines).

Negative free-air anomaly values associated with the Queensland, Townsville and Moresby Troughs are the result of the combined effects of thick sediments, bathymetry, and the gravity edge effect over the continental margin.

The free-air anomalies over the marginal plateaus average about +20 mGals suggesting that some subsidence is necessary if they are to attain isostatic equilibrium. The zero average free-air anomaly over the Coral Sea basin indicates that this feature is in isostatic equilibrium. A strong Bouguer anomaly gradient over the northern margin of the Queensland Plateau implies rapid crustal thinning across the margin. A gravity crustal profile computed by Falvey (1972) showed that the crust thinned from 25 km on the Plateau to about 10 km in the Coral Sea Basin. The lack of Bouguer anomaly expression over the Queensland and Townsville Troughs suggests that there is no crustal thinning beneath them and thus they are probably supported by the crust.

The main features of the free-air gravity field of the Coral Sea and Gulf of Papua region are a regional gravity high over the Australian continental shelf and Torres Strait; gravity platforms containing weak northwest trends over the Queensland and Marion Plateaus; and gravity troughs over the Queensland, Townsville and Moresby Troughs.

The offshore part of the Cape York Regional Gravity High (120) covers the continental shelf north of Cairns, Torres Strait, and part of the Gulf of Papua. Onshore it extends over parts of the Coen Inlier, the Hodgkinson Basin and the Laura Basin. Free-air anomaly highs along the eastern margin of the province are probably due, at least in part, to the edge effect over the continental margin. Onshore, Fraser *et al.* (in prep.) have attributed the high Bouguer anomaly level to Proterozoic metamorphic rocks and granites of the Coen Inlier at depth throughout the province. However, this does not appear to be the case as the western margin of the gravity high corresponds to the eastern edge of the Coen Inlier, and most of the province overlies features such as the Laura Basin, which is thought to have a basement of predominantly low-grade Middle Palaeozoic metasediments, Upper Permian granites and Permian sediments (Sedimentary Basins Study Section, 1974). of the northern Tasman Geosyncline. High free-air anomaly values within the Cape York Province may be due to the presence of relatively dense rocks within this part of the Tasman Geosyncline. The areal extent of the province indicates that Tasman Geosyncline-type basement may underly the shelf between Cape York and Papua New Guinea.

The large areas of mainly positive free-air anomaly values which cover the Queensland and Marion Plateaus are called the Willis (104) and Swain (106) Regional Gravity Platforms. Gravity highs within the provinces exhibit weak northwest trends and have been interpreted as being due to both intra-basement density changes and basement relief (Mutter, 1974; in press; Falvey & Taylor, 1974). The trend of the gravity highs is similar to the trend of structures in the onshore Palaeozoic Tasman Geosyncline and thus supports the interpretation that the basement rocks of the Queensland and Marion Plateaus are part of the Tasman Geosyncline (Falvey & Taylor, 1974; Mutter, 1974). The northern margin of the Queensland Plateau is associated with a strong west-northwest trending Bouguer anomaly gradient. This is related to rapid crustal thinning across the margin from about 25 km on the Queensland Plateau to about 10 km in the Coral Sea Basin (Falvey, 1972).

The west-northwest-trending Papua Regional Gravity Complex (103) covers the Eastern Plateau and much of the Coral Sea Basin. Falvey & Taylor (1974) have interpreted the negative free-air anomaly values on the southern margin of the province as being due in part to the gravity edge effect over the margin of the Queensland Plateau, and in part to about 1-2 km of rift related sediments underlying the base of the plateau slope. The elongate, west-northwest-trending gravity high in the centre of the Coral Sea Basin may mark the oceanic crustal axis (extinct spreading ridge?) (Falvey and Taylor, 1974, p. 124). A gravity high in the west of the Papuan Regional Gravity Complex (103) corresponds closely with the bathymetry of the Eastern Plateau (Eastern Fields Fan, Mutter, 1975). Local gravity highs have a weak northeast trend and may be related to intra-basement density changes and Palaeozoic basement relief in a similar manner to highs within the Willis Regional Gravity Platform (104).

The Barrier Regional Gravity Trough (105) wraps around the western and southern margins of the Willis Regional Gravity Platform (104). Its northwest-trending limb corresponds to the Portlock Trough, Osprey Basin and Queensland Trough, and the east-trending limb to the Townsville Trough. The gravity low at the northern end of the province formed by closure of the −20 mGal contour is partly an edge effect at the base of the continental slope, but there is also a strong negative contribution from thick sediments within the Portlock Trough and Osprey Basin (Mutter, 1975). Gravity lows over the Queensland and Townsville Troughs are caused by the combined effects of thick sediments, bathymetric variations, and edge effects over the continental slope. Both of these graben-type features have little or no Bouguer anomaly expression, which indicates that they are probably not compensated by crustal thinning.

The west-northwest-trending Moresby Regional Gravity Trough (102) is parallel to the southern margin of Papua New Guinea and the Louisiade Archipelago. Although gravity lows within the province are at least partly due to the gravity edge effect at the base of the slope and bathymetry, there is also a strong gravity component from near-surface geology. Mutter (1975) has interpreted the cause of the deep free-air anomaly low in the west of the province as being a very thick sediment fill within the Moresby Trough, that he considers to be an offshore extension of the Aure Trough. More positive free-air anomaly values in the centre of the Moresby Regional Gravity Trough (102) are associated with the Papuan Plateau.

The triangular-shaped Coral Sea Regional Gravity High (101) corresponds to an area of intermediate water depth (2-3.5 km) on the eastern margin of the Coral Sea Basin. Terrill (1975) suggests that this area, which is called the Louisiade Rise, has a similar basement structure to the Queensland Plateau and by analogy is also underlain by continental-type crust.

Acknowledgements

Several members of the Seismic, Gravity and Marine Section, BMR, have contributed to this paper in the form of unpublished records and informal discussions. We are particularly indebted to A. R. Fraser and D. Denham for critically reviewing the draft manuscript.

Drafting of the figures was carried out by L. Hollands.

References

ANFILOFF, W., MURRAY, A., BARLOW, B. C., DENHAM, D., & SANDFORD, R., 1976—Compilation and production of the 1976 1:5 000 000 gravity map of Australia. *BMR Journal of Australian Geology and Geophysics* **1,** 273-6.

AUDLEY-CHARLES, M. G., CARTER, D. J., & MILSON, J. S., 1972—Tectonic development of Eastern Indonesia in relation to Gondwanaland dispersal. *Nature,* **239,** 35-9.

BMR, 1976a—Gravity Map of Australia, scale 1:5 000 000. *Bureau of Mineral Resources, Australia, Canberra.*

BMR, 1976b—Magnetic Map of Australia, scale 1:2 500 000. *Bureau of Mineral Resources, Australia, Canberra.*

BOTT, M. H. P., 1971—THE INTERIOR OF THE EARTH. Edward Arnold, London.

BOUEF, M. G., & DOUST, H., 1975—Structure and development of the southern margin of Australia. *APEA Journal,* **15,** 33-43.

BRANSON, J. C., 1974—Structures of the western margin of the Australian continent. *Oil and Gas Journal,* **20,** 24-35.

CAMERON, P. J., & PINCHIN, J., 1974—Geophysical results from offshore Tasmania. *Bureau Mineral Resources, Australia—Record* **1974/98** (unpublished).

CHALLINOR, A., 1970—The geology of the offshore Canning Basin, Western Australia. *APEA Journal,* **10,** 78-90.

CHAMALAUN, F. H., LOCKWOOD, K., & WHITE, A.,—The Bouguer gravity field of eastern Timor. *Tectonophysics,* **30,** 241-259.

COONEY, P. M., EVANS, P. R., & EYLES, D., 1975—Southern margin of Australia; *in* VEEVERS, J. J. (Editor), *Deep Sea Drilling in Australasian Waters, Challenger Symposium, Sydney,* 26-7.

DENHAM, J. I., & BROWN, B. R., 1976—A new look at the Otway Basin. *APEA Journal,* **16,** 91-8.

DOYLE, H. A., & EVERINGHAM, I. B., 1964—Seismic velocities and crustal structure in Southern Australia. *Journal of the Geological Society of Australia,* **11,** 141.

EXON, N. F., WILLCOX, J. B., & PETKOVIC, P., 1975—A preliminary report on the regional geology of the Exmouth Plateau. *Bureau Mineral Resources, Australia—Record* **1975/158** (unpublished).

EXON, N. F., & WILLCOX, J. B., 1976—Mesozoic outcrops on the continental slope off Exmouth, Western Australia. *BMR Journal of Australian Geology and Geophysics,* **1,** 205-209.

FALVEY, D. A., 1972—The nature and origin of marginal plateaux and adjacent ocean basins off Northern Australia. *Unpublished Ph.D. thesis, University of New South Wales.*

FALVEY, D. A., & TAYLOR, D. J., 1974—Queensland Plateau and Coral Sea Basin: structural and time stratigraphic patterns. *Bulletin of the Australian Society Exploration Geophysicists,* **5,** 123-6.

FALVEY, D. A., & VEEVERS, J. J., 1974—Physiography of the Exmouth and Scott Plateaux, Western Australia, and adjacent northeast Wharton Basin. *Marine Geology,* **17,** 21-59.

FINNEY, W. A., & SHELLEY, E. P., 1966—Tasmania aeromagnetic survey. *Bureau Mineral Resources, Australia—Record* **1966/139** (unpublished).

FITCH, T. J., 1972—Plate convergence, transcurrent faults, and internal deformation adjacent to South East Asia and Western Pacific. *Journal of Geophysical Research,* **77,** 4432-60.

FRASER, A. R., 1976—Gravity features and their nomenclature. *BMR Journal of Australian Geology and Geophysics,* **1,** 351-3.

FRASER, A. R., DARBY, F., & VALE, K. R., (in prep)—A qualitative analysis of the results of the reconnaissance gravity survey of Australia. *Bureau Mineral Resources, Australia—Report.*

GAPOSCHKIN, E. M., & LAMBECK, K., 1971—Earth's gravity field to sixteenth degree and station coordinates from satellite and terrestrial data. *Journal of Geophysical Research,* **76,** 4855-83.

GARSON, M. S., & KRS, M., 1976—Geophysical and geological evidence of the relationship of Red Sea transverse tectonics to ancient fractures. *Geological Society America Bulletin,* **87,** 169-81.

GEARY, J. K., 1970—Offshore exploration of the southern Carnarvon Basin. *APEA Journal,* **10,** 9-15.

GEOLOGICAL SOCIETY OF AUSTRALIA, 1971—Tectonic Map of Australia and New Guinea, 1:5 000 000, *Sydney.*

GEOPHYSICAL ASSOCIATES PTY LTD, 1966—Permit to explore 235H. Western Australia, airborne magnetometer survey. *Bureau Mineral Resources, Australia—Petroleum Search Subsidy Act Report* (unpublished).

GLICKEN, M., 1962—Eotvos corrections for a moving gravity meter. *Geophysics,* **27,** 531-33.

HAYES, D. E., & RINGIS, J., 1973—Seafloor spreading in the Tasman Sea. *Nature,* **243,** 454-8.

HEIRTZLER, J. R., VEEVERS, J. J., *et al.* 1973—Deep Sea Drilling Project, leg 27 in the Eastern Indian Ocean. *Geotimes,* **18,** 16-17.

HOGAN, A. P., & JACOBSON, E. P., 1976—Geophysical results from the continental margin of northwest Australia. *Bureau Mineral Resources, Australia—Record* **1975/101** (unpublished).

JONES, B. F., 1969—Timor Sea gravity, magnetic and seismic survey, 1967. *Bureau Mineral Resources, Australia—Record* **1969/40** (unpublished).

JONES, D. K., & PEARSON, G. R., 1972—The tectonic elements of the Perth Basin. *APEA Journal,* **12,** 17-22.

LAWS, R., A., & KRAUS, G. P., 1974—The regional geology of the Bonaparte Gulf—Timor Sea area. *APEA Journal,* **14,** 77-94.

MATHUR, S. P., 1974—Crustal structure in southwestern Australia from seismic and gravity data. *Tectonophysics,* **24,** 151-82.

MUTTER, J. C., 1974—Geophysical Results from the Coral Sea: Continental Margin Survey report. *Bureau of Mineral Resources, Australia—Record* **1974/116** (unpublished).

MUTTER, J. C., 1975—A structural analysis of the Gulf of Papua and northwest Coral Sea Region. *Bureau Mineral Resources, Australia—Report* **179.**

MUTTER, J. C., (in press)—The Queensland Plateau. *Bureau Mineral Resources, Australia—Bulletin.* **179.**

PETKOVIC, P., 1975a—Origin of the Naturaliste Plateau. *Nature,* **253,** 30-3.

PETKOVIC, P., 1975b—Geophysical Results from the southwest margin. *Bureau Mineral Resources, Australia—Record,* **1975/180** (unpublished).

POWELL, D. E., 1976—The geological evolution and hydrocarbon potential of the continental margin off northwest Australia. *APEA Journal,* **16,** 13-23.

SCOTT, A. F., & SPEER, G. W., 1969—Mallabie No. 1 well completion report, Outback Oil Company, N.L. *Bureau Mineral Resources, Australia—Petroleum Search Subsidy Acts Report* **69/2013** (unpublished).

SEDIMENTARY BASINS STUDY SECTION, 1974—Summary of Phanerozoic sedimentary basins of Australia and adjacent regions, 1974. *Bureau Mineral Resources, Australia—Record* **1974/178** (unpublished).

SMITH, E. R., 1966—Timor Sea/Joseph Bonaparte Gulf marine gravity and seismic 'Sparkarray' survey, Northwest Australia 1965. *Bureau Mineral Resources, Australia—Record* **1966/72** (unpublished).

SMITH, R., & KAMERLING, P., 1969—Geological framework of the Great Australian Bight. *APEA Journal,* **9,** 60-6.

SYMONDS, P. A., 1973—The structure of the north Tasman Sea. *Bureau Mineral Resources, Australia—Record* **1973/167** (unpublished).

TARGET (EXPLORATION N.L.), 1971—Polda Basin 2 marine seismic survey. *Bureau Mineral Resources, Australia—Petroleum Search Subsidy Acts Report* **71/355** (unpublished).

TAYLOR, L. W. H., 1975—Depositional and tectonic patterns in the western Coral Sea; *in* L. A. FALVEY AND G. H. PACKHAM (Editors), Southwest Pacific Workshop. *Bulletin Australian Society Exploration Geophysicists,* **6,** 33-5.

TERRILL, A., 1975—Depositional and tectonic patterns in the northern Lord Howe Rise—Mellish Rise area. *Bulletin of the Australian Society of Exploration Geophysicists,* **6,** 37-9.

THOMAS, B. M., & SMITH, D. N., 1974—A summary of the petroleum geology of the Carnarvon Basin. *APEA Journal,* **14,** 66-76.

THOMPSON, B. P., 1970—A review of Precambrian and Lower Palaeozoic tectonics of South Australia. *Transactions of the Royal Society South Australia,* **94,** 193-222.

TILBURY, L. A., 1975—Geophysical results from the Gulf of Papua and Bismarck Sea. *Bureau Mineral Resources, Australia—Record* **1975/115** (unpublished).

VEEVERS, J. J., 1976—Early Phanerozoic events on and alongside the Australian-Antarctic Platform. *Journal of the Geological Society Australia,* 23 (2), 183-206.

VEEVERS, J. J., & HEIRTZLER, J. R., 1974—Tectonic and paleogeographic synthesis of leg 27; *in* VEEVERS, J. J., HEIRTZLER, J. R., *et al., Initial Reports of the Deep Sea Drilling Project,* **27,** *Washington, U.S. Government Printing Office.*

VEEVERS, J. J., HEIRTZLER, J. R., *et al.,* 1974—*Initial reports of the Deep Sea Drilling Project,* **27,** *Washington, U.S. Government Printing Office.*

VEEVERS, J. J., & JOHNSTONE, M. H., 1974—Comparative stratigraphy and structure of the Western Australian margin and the adjacent deep ocean floor; *in* VEEVERS, J. J., HEIRTZLER, J. R., *et al., Initial Reports of the Deep Sea Drilling Project,* **27,** *Washington, U.S. Government Printing Office,* 571-85.

VEEVERS, J. J., POWELL, C. McA., & JOHNSON, B. D., 1975—Greater India's place in Gondwanaland and in Asia. *Earth Planetary Science Letters,* **27,** 383-7.

VEEVERS, J. J., & MCELHINNY, M. W., 1976—The separation of Australia from other continents. *Earth-Science Reviews,* **12,** 139-59.

VOGT, P. R., & CONOLLY, J. R., 1971—Tasmantid Guyots, the age of the Tasman Basin, and motion between the Australian plate and the mantle. *Bulletin of the Geological Society of America,* **82,** 2577-84.

WARRIS, B. J., 1973—Plate tectonics and the evolution of the Timor Sea, northwest Australia. *APEA Journal,* **13,** 13-8.

WATT, C. J., 1976—Geophysical results from the Timor Trough. *Bureau Mineral Resources, Australia—Record* **1976/14** (unpublished).

WEISSEL, J. K., & HAYES, D. E., 1972—Magnetic anomalies in the southeast Indian Ocean; *in* Hayes, D. E. (Editor), Antarctic Oceanology II, The Australian-New Zealand Sector, *American Geophysical Union, Antartic Research Series,* **19,** 165-96.

WHITWORTH, R., 1969—Marine geophysical survey of the Northwest Continental Shelf, 1968. *Bureau Mineral Resources, Australia—Record* **1969/99** (unpublished).

WILLCOX, J. B., 1974—Geophysical results from the Great Australian Bight. *Bureau Mineral Resources, Australia—Record* **1974/147** (unpublished).

WILLCOX, J. B., in press—The Great Australian Bight: a regional interpretation of the gravity and magnetic fields and of seismic profiles. *Bureau Mineral Resources, Australia—Report* **201.**

WILSON, J. T., 1965—A new class of faults and their bearing on continental drift. *Nature,* **207,** 343-7.

A selected bibliography on Australian gravity

O. Terron, W. Anfiloff, F. J. Moss, and P. Wellman

Introduction

This bibliography mainly contains reports of those major surveys used to construct the 1976 1:5 million gravity map of Australia. The bibliography is listed in alphabetical order, and the list is numbered consecutively. Figure 1 relates the reference number to the area covered by each report. Most reports give the survey method, logistic information, the gravity meter number and its calibration details, the datum of horizontal coordinates, vertical coordinates and gravity, the accuracy of the reduced position and gravity data, a Bouguer anomaly map, and a description and geological interpretation of this map.

Also included are selected publications on the progress of gravity mapping, on the establishment and refinement of a national gravity reference network of base stations to define datum and scale, and of the use of the mapped gravity anomalies in the definition of geological structure and in geodetic studies.

A comprehensive bibliography of gravity in Australia has been prepared, and it is planned to make this available shortly.

1. ALLIANCE OIL DEVELOPMENT AUST. N.L., 1967—Scopes gravity survey (PEL 52) New South Wales, 1967. *Petroleum Search Subsidy Act unpublished company report* (BMR file number 66/4826).
2. AMERICAN OVERSEAS PETROLEUM LTD., 1963—Blackall-Augathella gravity survey, Queensland, Australia, 1963. *Petroleum Search Subsidy Act unpublished company report* (BMR file number 63/1907).
3. AMERICAN OVERSEAS PETROLEUM LTD., 1966—Tibooburra-Louth gravity survey (65/4818) and PEL 203 gravity survey (66/4824) New South Wales, Australia, 1965/66. *Petroleum Search Subsidy Act unpublished company report* (BMR file number 65/4818).

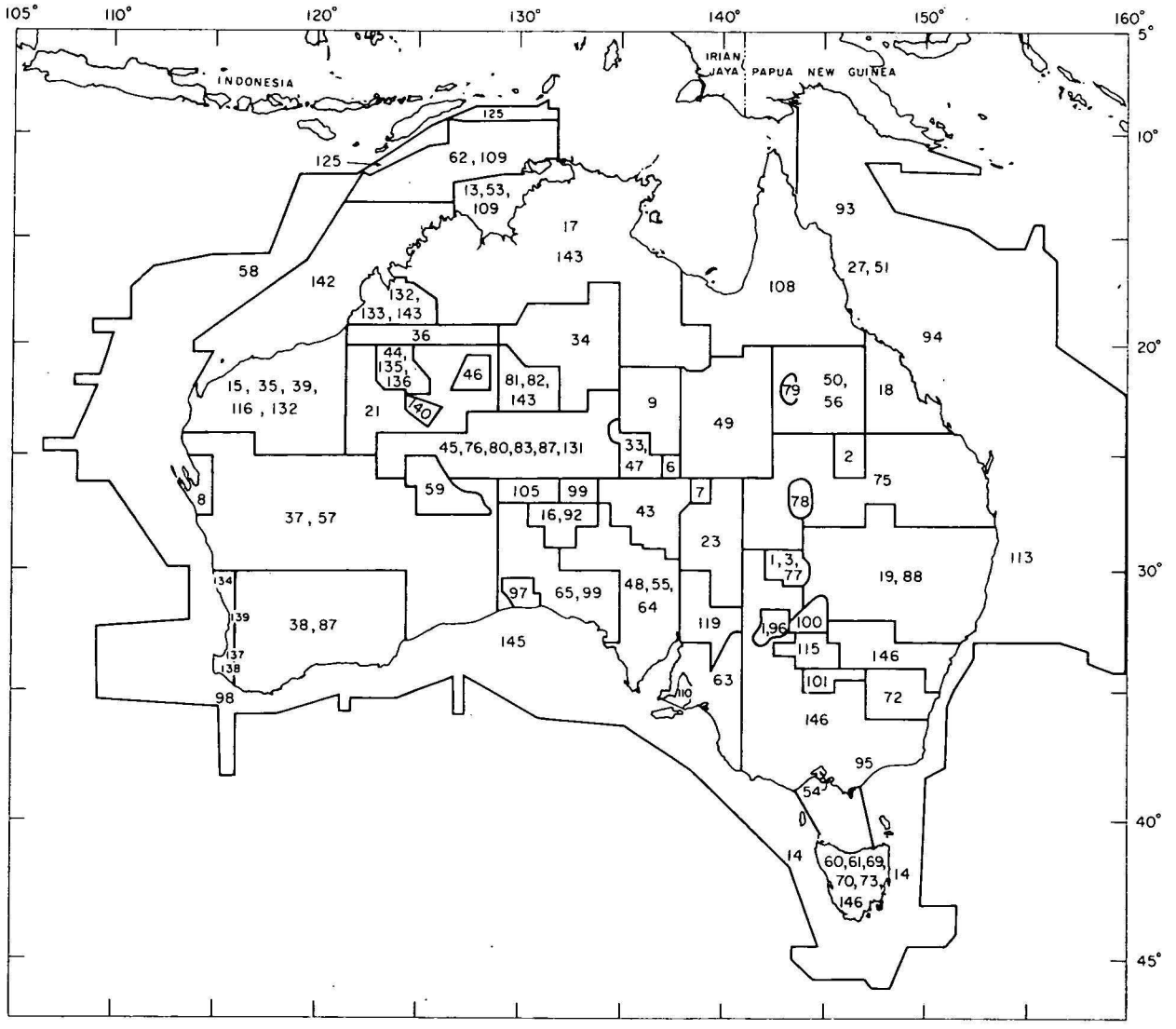

Figure 1. Key to reports on major gravity surveys.
The numbers are those of the bibliography listing.

4. ANFILOFF, W., BARLOW, B. C., MURRAY, A. S., DENHAM, D.,& SANFORD, R., 1976—Compilation and production of the 1976 Gravity Map of Australia. *BMR Journal of Australian Geology & Geophysics*, **1**, 273-6.

5. ANGLO-PERSIAN OIL COMPANY, 1930—The oil exploration work in Papua and New Guinea conducted by the Anglo-Persian Oil Company on behalf of the Government of the Commonwealth of Australia. 1920-1929. *HMSO, London*. 4 volumes.

6. ASSOCIATED FRENEY OIL FIELDS, 1961—Simpson Desert (south) gravity survey, 1961. *Petroleum Search Subsidy Act unpublished company report* (BMR file number 62/1917).

7. AUSTRALIAN PETROLEUM LTD., 1962—Alton Downs gravity survey, Birdsville—Lake Frome gravity survey, 1962. *Petroleum Search Subsidy Act unpublished company report* (BMR file number 62/1929).

8. BAWEWA OIL & MINING N.L., 1970—Murchison-Gascoyne helicopter gravity survey P. E. 226H, Western Australia, 1970. *Petroleum Search Subsidy unpublished company report* (BMR file number 70/326).

9. BARLOW, B. C., 1966—Georgina Basin reconnaissance gravity survey using helicopters, N.T. and Qld. 1960-1961. *Bureau of Mineral Resources Australia—Record* **1966/147** (unpublished).

10. BARLOW, B. C., 1968—National Report on gravity in Australia, January 1963 to December 1966. *Bureau of Mineral Resources, Australia—Record* **1968/21** (unpublished).

11. BARLOW, B. C., 1970—National Report on gravity in Australia, July 1965 to June 1970. *Bureau of Mineral Resources, Australia—Record* **1970/62** (unpublished).

12. BELLAMY, C. J., LODWICK, G. D., & TOWNSEND, D. G., 1971—The gravity reductions, storage and retrieval system used by BMR, *Bureau of Mineral Resources, Australia—Record* **1971/7** (unpublished).

13. BIGG-WITHER, A. L., 1963—Compilation and review of the geophysics of Bonaparte Gulf Basin, 1962. *Bureau of Mineral Resources, Australia—Record* **1963/165** (unpublished).

14. CAMERON, P. J., & PINCHIN, J., 1974—Geophysical results from offshore Tasmania. *Bureau of Mineral Resources, Australia—Record* **1974/98** (unpublished).

15. CHAMBERLAIN, N. G., DOOLEY, J. C., & VALE, K. R., 1954—Geophysical exploration in the Carnarvon (N.W.) Basin, Western Australia. *Bureau of Mineral Resources, Australia—Record* **1954/44** (unpublished).

16. CONTINENTAL OIL COMPANY OF AUSTRALIA LTD., 1967—Eastern Officer Basin seismic and gravity survey OEL 28, South Australia, 1967. *Petroleum Search Subsidy Act unpublished company report* (BMR file number 67/11163).

17. DALY, J., & LANGRON, W. J., 1963—Darwin-Katherine region reconnaissance survey, Northern Territory, 1959. *Bureau of Mineral Resources, Australia—Record* **1963/28** (unpublished).

18. DARBY, F., 1968—North Bowen Basin gravity survey, Queensland 1963. *Bureau of Mineral Resources, Australia—Report* **1968/138** (unpublished).

19. DARBY, F., 1969—Reconnaissance helicopter gravity surveys, northern NSW and southern Qld, 1968. *Bureau of Mineral Resources, Australia—Record* **1969/109** (unpublished).

20. DARBY, F., 1970—Barometric heighting—An assessment of the accuracy achieved during reconnaissance gravity surveys in Australia. *Bureau of Mineral Resources, Australia—Record* **1970/89** (unpublished).

21. DARBY, F., & FRASER, A. R., 1969—Reconnaissance helicopter gravity survey, WA, 1968. *Bureau of Mineral Resources, Australia—Record* **1969/37** (unpublished).

22. DARBY, F., & VALE, K. R., 1969—Progress of the reconnaissance gravity survey of Australia. *Economic Committee for Asia and the Far East* (ECAFE) *Conference*, Canberra, Australia, 1969.

23. DELHI AUSTRALIAN PETROLEUM LTD., 1964—Strzelecki Creek and Lake Gregory helicopter gravity surveys South Australia, 1964. *Petroleum Search Subsidy Act unpublished company report* (BMR file number 64/4811).

24. DOOLEY, J. C., 1959—National Report on gravity in Australia and Australian Territories, May, 1959. *Bureau of Mineral Resources, Australia—Record* **1959/97** (unpublished).

25. DOOLEY, J. C., 1965—A common gravity datum and calibration lines for independent survey in Australia. *Economic Committee for Asia and the Far East* (ECAFE) *Conference*, Tokyo, Japan, 1965.

26. DOOLEY, J. C., 1965—Australian gravity network adjustment, 1962. *Bureau of Mineral Resources, Australia—Report* **72.**

27. DOOLEY, J. C., 1965—Gravity surveys on the Great Barrier Reef and adjacent coast, north Queensland, 1954-1960. *Bureau of Mineral Resources, Australia—Report* **73.**

28. DOOLEY, J. C., 1965—National Report on gravity in Australia January 1962 to June 1965. *Bureau of Mineral Resources, Australia—Record* **1965/162** (unpublished).

29. DOOLEY, J. C., 1965—Regional gravity surveys in Australia. *APEA Journal* **5**, 139-142.

30. DOOLEY, J. C., 1976—Variation of crustal mass over the Australian region. *BMR Journal of Australian Geology & Geophysics*, **1.**

31. DOOLEY, J. C., & BARLOW, B. C., 1976—Gravimetry in Australia, 1819-1976. *BMR Journal of Australian Geology & Geophysics*, **1.**

32. DOOLEY, J. C., MCCARTHY, E., KEATING, W. D., WILLIAMS, L. W., & MADDERN, C. A., 1961—Pendulum measurements of gravity in Australia, 1950-51. *Bureau of Mineral Resources, Australia—Bulletin* **46.**

33. FLAMINGO PETROLEUM CORPORATION, 1960—Allambi gravity survey, Northern Territory, 1960. *Petroleum Search Subsidy Act unpublished company report* (BMR file number 62/1914).

34. FLAVELLE, A. J., 1965—Helicopter gravity survey by contract, Northern Territory and Queensland 1965. *Bureau of Mineral Resources, Australia—Record* **1965/212** (unpublished).

35. FLAVELLE, A. J., 1974—Canning Basin gravity surveys, 1953-62. *Bureau of Mineral Resources, Australia—Record* **1974/181** (unpublished).

36. FLAVELLE, A. J., & GOODSPEED, M. J., 1962—Fitzroy and Canning Basin reconnaissance gravity survey, Western Australia, 1952/60. *Bureau of Mineral Resources, Australia—Record* **1962/105** (unpublished).

37. FRASER, A. R., 1973—Reconnaissance helicopter gravity survey, W.A. 1971-72. *Bureau of Mineral Resources, Australia—Record* **1973/130** (unpublished).

38. FRASER, A. R., 1974—Reconnaissance gravity survey of the southwest of Western Australia 1969. *Bureau of Mineral Resources, Australia—Record* **1974/26** (unpublished).

39. FRASER, A. R., 1974—Reconnaissance gravity survey of the northwest of Western Australia, 1969. *Bureau of Mineral Resources, Australia—Record* **1974/27** (unpublished).

40. FRASER, A. R., in preparation—Gravity surveys of Western Australia and the west of South Australia. *Bureau of Mineral Resources, Australia—Bulletin.*

41. FRASER, A. R., 1976—Gravity provinces and their nomenclature. *BMR Journal of Geology & Geophysics*, **1**, 351-3.

42. FRASER, A. R., DARBY, F., & VALE, K. R., in preparation—A qualitative analysis of the results of the reconnaissance gravity survey of Australia. *Bureau of Mineral Resources, Australia—Report.*

43. FRENCH PETROLEUM COMPANY (AUSTRALIA) PTY LTD., 1963—Dalhousie gravity survey, South Australia, 1963. *Petroleum Search Subsidy Act unpublished company report* (BMR file number 63/1911).

44. FRENCH PETROLEUM COMPANY (AUSTRALIA) PTY LTD., 1967—Jarmura gravity survey, 1967. *Petroleum Search Subsidy Act unpublished company report* (BMR file number 67/4832).

45. FROELICH, A. J., & KRIEG, E. A., 1969—Geophysical-geologic study of the northern Amadeus Trough, Australia. *Bulletin of the American Association of Petroleum Geologists*, **53**, 1978-2004.

46. GEOSURVEYS OF AUSTRALIA LTD, & HUCKATHON NZ OILS LTD., 1964—Stansmore Ranges gravity survey, Western Australia 1964. *Petroleum Search Subsidy Act unpublished company report* (BMR file number 64/4807).

47. GEOSURVEYS OF AUSTRALIA LTD., 1961—Andado (Finke area) gravity survey, Northern Territory, 1961. *Petroleum Search Subsidy Act unpublished company report* (BMR file number 62/1904).

48. GERDES, R. A., 1972—A helicopter gravity survey of the Gawler Platform. *Department of Mines, South Australia, Geological Survey-Mining Review.* **133**, 137-147.

49. GIBB, R. A., 1967—Western Queensland reconnaissance gravity survey, 1957-1961. *Bureau of Mineral Resources, Australia—Report* **129.**

50. GIBB, R. A., 1968—North Eromanga and Drummond Basin gravity surveys, Queensland 1959-1963. *Bureau of Mineral Resources, Australia—Report* **131.**

51. GOODSPEED, M. J., & WILLIAMS, L. W., 1959—Preliminary report on underwater gravity survey, Great Barrier Reef area, Thursday Island to Rockhampton. *Bureau of Mineral Resources, Australia—Record* **1959/70** (unpublished).

52. GRUSHINSKY, N. P., & SAZHINA, N. B., 1941—The gravitational field and the geoid of Australia. *Journal of the Geological Society of Australia.* **18**, 183-199.

53. GULF OIL SYNDICATE, 1964—Bonaparte Gulf gravity survey, Western Australia, 1959. *Petroleum Search Subsidy Act unpublished company report* (BMR file number 47).

54. GUNSON, S., & WILLIAMS, L. W., 1965—Gravity surveys of Port Phillip Bay and adjacent areas, Victoria, 1957-8. *Bureau of Mineral Resources, Australia—Record* **1965/64** (unpublished).

55. HALL, J. Mc. G., & TOWNSEND, I. J., 1969—Helicopter gravity survey of areas marginal to the western Great Artesian Basin. *Department of Mines, South Australia, Geological Survey-Mining Review.* **130**, 70-9.

56. HARRISON, P. L., ANFILOFF, W., & MOSS, F. J., 1971—Galilee Basin seismic and gravity survey, Queensland 1971. *Bureau of Mineral Resources, Australia—Report* **175.**

57. HARRISON, P. L., & ZADOROZNYJ, I., in preparation—Officer Basin W.A. seismic and gravity survey, 1972. *Bureau of Mineral Resources, Australia—Report* **191.**

58. HOGAN, A. P., & JACOBSEN, E. P., 1975—Geophysical results from the continental margin of northwest Australia. *Bureau of Mineral Resources, Australia—Record* **1975/101** (unpublished).

59. HUNT OIL COMPANY, 1963—Final report Lennis-Breaden gravity surveys, Officer Basin, Western Australia, 1963. *Petroleum Search Subsidy Act unpublished company report* (BMR file number 63/1900).

60. JOHNSON, B. D., 1972—Crustal structure studies in Tasmania. *Ph.D. Thesis, University of Tasmania, Hobart* (unpublished).

61. JOHNSON, B. D., 1974—Analysis of the regional gravity field of Tasmania using orthoganilized trigonometric functions. *Geophysical Journal of the Royal Astronomical Society*, **36**, 285-94.

62. JONES, B. F., 1969—Timor Sea gravity, magnetic and seismic survey, 1967. *Bureau of Mineral Resources, Australia—Record* **1969/40** (unpublished).

63. KENDALL, G. W., & SEEDSMAN, K. R., 1964—Reconnaissance seismic refraction and gravity surveys in the northern portion of the Murray Basin in South Australia, 1963. *Department of Mines, South Australia, Geological Survey-Mining Review.* **120**, 5-16.

64. KERR-GRANT, C., 1951—Geophysical survey of parts of counties Gawler, Stanley and Daly. *Department of Mines, South Australia, Geological Survey-Mining Review* **91**, 164-7.

65. KERR-GRANT, C., & PEGUM, D. M., 1954—Gravity survey in the northeastern portion of the Nullarbor Plain and adjacent areas. *Department of Mines, South Australia, Geological Survey—Report* **GS200.**

66. LANGRON, W. J., 1966—National Report on gravity in Australia, January 1960 to December 1962. *Bureau of Mineral Resources, Australia—Record* **1966/108** (unpublished).

67. LANGRON, W. J., 1966—Regional gravity traverses, northern Australia, 1959-1963. *Bureau of Mineral Resources, Australia—Record* **1966/123.** (unpublished).

68. LAUDON, T. S., 1968—Land gravity survey of the Solomon and Bismarck Islands, *in* KNOROFF, L., DRAKE, C. L., & HART, P. J., (Editors), THE CRUST AND UPPER MANTLE IN THE PACIFIC AREA, 279-95 *American Geophysical Union, Washington, D.C.*

69. LEAMAN, D. E., & SYMONDS, P. A., 1975—Gravity survey of north eastern Tasmania. *Department of Mines, Tasmania, Geological Survey—Paper* **2.**

70. LEAMAN, D. E., SYMONDS, P. A., & SHIRLEY, J. E., 1973—Gravity survey of the Tamar region, northern Tasmania. *Department of Mines, Tasmania, Geological Survey—Paper* **1.**

71. LEPISTO, P. S., 1964—Interim report, east New Guinea land gravity survey. *United States Army Map Service, Far East.*

72. LODWICK, G. D., & FLAVELLE, A. J., 1968—Helicopter gravity training survey, A.C.T. and southern N.S.W. 1966. *Bureau of Mineral Resources, Australia—Record* **1968/85** (unpublished).

73. LONGMAN, M. J., LEAMAN, D. E., & SYMONDS, P. A., 1971—Gravity survey of the Tertiary Basins. *Department of Mines, Tasmania, Geological Survey Bulletin*, **51.**

74. LONSDALE, G. F., 1962—Great Artesian Basin reconnaissance gravity survey using helicopters, Qld 1961. *Bureau of Mineral Resources, Australia—Record* **1962/14** (unpublished).

75. LONSDALE, G. F., 1965—Southern Queensland contract reconnaissance gravity survey using helicopters, 1964. *Bureau of Mineral Resources, Australia—Record* **1965/251** (unpublished).

76. LONSDALE, G. F., & FLAVELLE, A. J., 1968—Amadeus and South Canning Basins gravity survey, Northern Territory and Western Australia 1962. *Bureau of Mineral Resources, Australia—Report* **133.**

77. L. H. SMART OIL EXPLORATION CO. LTD., 1961—Urisino-Tongo gravity survey, north-western New South Wales, 1961. *Petroleum Search Subsidy Act unpublished company report* (BMR file number 62/1920).

78. L. H. SMART OIL EXPLORATION CO. LTD., 1963—Report on a gravity survey in the Conbar area 99P, Queensland, 1963. *Petroleum Search Subsidy Act unpublished company report* (BMR file number 63/1902).

79. MAGELLAN PETROLEUM (N.T.) PTY. LTD., 1959—North Winton, 1959. *Petroleum Search Subsidy Act unpublished company report* (BMR file number 62/1909).

80. MAGELLAN PETROLEUM (N.T.) PTY. LTD., 1965—Missionary Plain seismic and gravity survey, oil permits 43 and 56, Northern Territory, 1965. *Petroleum Search Subsidy Act unpublished company report* (BMR file number 65/11013).

81. MAGELLAN PETROLEUM (N.T.) PTY. LTD., 1968—Ngalia Basin gravity survey OP 165, Northern Territory, 1968. *Petroleum Search Subsidy Act unpublished company report* (BMR file number 68/3051).

82. MAGELLAN PETROLEUM (N.T.) PTY LTD., 1970—Ngalia Basin regional gravity survey, OP 165, Northern Territory, 1970. *Petroleum Search Subsidy Act unpublished company report* (BMR file number 70/704).

83. MAGELLAN PETROLEUM (N.T.) PTY. LTD., 1970—Mt Rennie-Ooraminna seismic and gravity survey, 1966. *Petroleum Search Subsidy Act unpublished company report* (BMR file number 66/11074).

84. MARSHALL, C. E., & NARAIN, H., 1954—Regional gravity in the eastern and central of the Commonwealth. *Sydney University, Department of Geology and Geophysics—Memoir* **1954/2.**

85. MATHER, R. S., 1969—The free air geoid for Australia. *Geophysical Journal of the Royal Astronomical Society,* **18,** 499-516.

86. MATHER, R. S., BARLOW, B. C., & FRYER, J. E., 1971—A study of the Earth's gravitational field in the Australian region; *in* Communications from Australia to section V IAG, XV General Assembly, IUGG, Moscow 1971. *University of New South Wales, Sydney, Unisurv. rep.* **22,** 1-41.

87. MATHUR, S. P., 1976—Relation of Bouguer anomalies to crustal structure in central and southwestern Australia. *BMR Journal of Australian Geology & Geophysics,* **1,** 277-86.

88. MCINTYRE, J. I., 1972—Gravity values at bench marks along main roads in New South Wales. *Geological Survey of New South Wales—Report* **GS1972/440** (unpublished).

89. MILSOM, J. S., 1973—Papuan ultramafic belt: gravity anomalies and the emplacement of ophiolites. *Bulletin of the Geological Society of America,* **84,** 2243-58.

90. MILSOM, J. S., 1973—The gravity field of the Papuan Peninsula. *Geologie en Mijnbouw,* **52,** 13-20.

91. MURRAY, A. S., 1974—The Australian National gravity repository computer system. *Bureau of Mineral Resources, Australia—Record* **1974/68** (unpublished).

92. MURUMBA OIL N.L., 1970—Eastern Officer Basin helicopter gravity survey PEL 10 and 11, South Australia, 1970. *Petroleum Search Subsidy Act unpublished company report* (BMR file number 70/134).

93. MUTTER, J. C., 1974—Marine geophysical survey of the Bismarck Sea and Gulf of Papua, 1970. A structural analysis of the Gulf of Papua and northwest Coral Sea region. *Bureau of Mineral Resources, Australia—Report* **179.**

94. MUTTER, J. C., 1975—The Queensland Plateau. *Bureau of Mineral Resources, Australia—Bulletin* **179.**

95. NEUMANN, F. J. G., 1974—BMR gravity surveys, Gippsland Basin, Vic 1948-61. *Bureau of Mineral Resources, Australia—Record* **1974/160** (unpublished).

96. NEW SOUTH WALES OIL & GAS COMPANY N. L., 1969—Blantyre Basin detailed gravity survey no. 1, PEL 163, New South Wales, 1969. *Petroleum Search Subsidy Act unpublished company report* (BMR file number 69/3029).

97. OUTBACK OIL COMPANY N.L., 1965—Eucla Basin gravity survey (OEL 33), South Australia, 1965. *Petroleum Search Subsidy Act unpublished company report* (BMR file number 65/4819).

98. PETKOVIC, P., 1975—Geophysical results from the southwest margin. *Bureau of Mineral Resources, Australia—Record* **1975/180** (unpublished).

99. PETTIFER, G. R., and FRASER, A. R., 1974—Reconnaissance helicopter gravity survey, SA, 1970. *Bureau of Mineral Resources, Australia—Record* **1974/88** (unpublished).

100. PLANET EXPLORATION COMPANY PTY LTD., 1963—East Darling helicopter gravity survey, New South Wales, 1963. *Petroleum Search Subsidy Act unpublished company report* (BMR file number 63/1905).

101. PLANET EXPLORATION COMPANY PTY LTD., 1968—Murrumbidgee gravity survey, PELA 233, PELA 236, N.S.W., 1968. *Petroleum Search Subsidy Act unpublished company report* (BMR file number 68/3032).

102. RADESKI, A. M., 1962—Regional gravity survey, central and northern Australia, 1959. *Bureau of Mineral Resources, Australia—Record* **1962/6** (unpublished).

103. REID, M. A., 1961—Broken Hill district regional gravity survey using Cessna aircraft, 1960. *Bureau of Mineral Resources, Australia—Record* **1961/93** (unpublished).

104. REISZ, E. J., MOSS, F. J., 1971—Regional marine geophysical surveys in the Australian area. *Bureau of Mineral Resources, Australia—Record* **1971/119** (unpublished).

105. ROWAN, I. S., 1968—Regional gravity survey of Mann and Woodroffe 1:250 000 sheet area. *Department of Mines, South Australia, Geological Survey-Mining Review,* **126,** 71-79.

106. SHIRLEY, J. E., 1964—A gravity survey of Papua and New Guinea. *Ph.D. Thesis, University of Tasmania, Hobart,* (unpublished).

107. SHIRLEY, J. E., 1966—Pendulum gravity measurements in Australia, 1964. *Bureau of Mineral Resources, Australia—Record* **1966/162.** (unpublished).

108. SHIRLEY, J. E., & ZADOROZNYJ, I., 1974—Reconnaissance helicopter gravity survey, northern Queensland, 1966. *Bureau of Mineral Resources, Australia—Record* **1974/140** (unpublished).

109. SMITH, E. R., 1966—Timor Sea/Joseph Bonaparte Gulf marine gravity and seismic 'spark array' survey, NW. Aust. 1965. *Bureau of Mineral Resources, Australia—Record* **1966/72** (unpublished).

110. SPRIGG, R. G., & STACKLER, W. F., 1965—Submarine gravity surveys in St. Vincent Gulf and Investigator Strait, South Australia, in relation to oil search in Australia. *APEA Journal,* **5,** 168-178.

111. ST. JOHN, V. P., 1967—The gravity field in New Guinea. *Ph.D. Thesis, University of Tasmania,* (unpublished).

112. ST. JOHN, V. P., 1970—The gravity field and structure of Papua New Guinea. *APEA Journal,* **10,** 41-55.

113. SYMONDS, P. A., in preparation—Geophysical results from the Tasman Sea. *Bureau of Mineral Resources, Australia—Record.*

114. SYMONDS, P. A., & WILLCOX, J. B., 1976—The gravity field of offshore Australia. *BMR Journal of Australian Geology & Geophysics,* **1,** 303-14.

115. TEXAM OIL CORPORATION, 1965—Ivanhoe helicopter gravity survey, New South Wales, 1965. *Petroleum Search Subsidy Act unpublished company report* (BMR file number 64/4809).

116. THYER, R. F., 1951—Gravity reconnaissance (1950), N.W. Basin, Western Australia. *Bureau of Mineral Resources, Australia—Record* **1951/69.** (unpublished).

117. THYER, R. F., 1963—Geophysical exploration—Australia. *Geophysics,* **28,** 273-305.

118. TILBURY, L. A., 1975—Geophysical results from the Gulf of Papua and Bismarck Sea. *Bureau of Mineral Resources, Australia—Record* **1975/115** (unpublished).

119. TUCKER, D. H., & BROWN, F. W., 1973—Reconnaissance helicopter gravity survey in the Flinders Range, South Australia 1970. *Bureau of Mineral Resources, Australia—Record* **1973/12** (unpublished).

120. VALE, K. R., 1962—Reconnaissance gravity surveys, using helicopters for oil search in Australia. *Bureau of Mineral Resources, Australia—Record* **1962/130** (unpublished).

121. VALE, K. R., 1965—Progress of the reconnaissance gravity survey of Australia. *Bureau of Mineral Resources, Australia—Record* **1965/197.** (unpublished).

122. VALE, K. R., TURPIE, A., & WHITWORTH, R., 1969—Offshore reconnaissance geophysical techniques. *Bureau of Mineral Resources, Australia—Record* **1969/138** (unpublished).

123. WALKER, D. G., & HASTIE, L. M., 1962—Two methods of gravity traversing with helicopters. *Bureau of Mineral Resources, Australia—Record* **1962/134** (unpublished).

124. WATTS, M. D., 1969—Sepik River helicopter gravity survey, T.P.N.G. 1968. *Bureau of Mineral Resources, Australia—Record* **1969/124** (unpublished).

125. WATT, C. J., 1976—Geophysical results from the Timor Trough. *Bureau of Mineral Resources, Australia—Record* **1976/14** (unpublished).

126. WELLMAN, P., 1974—National Report on gravity in Australia, July 1970 to June 1974. *Bureau of Mineral Resources, Australia—Record* **1974/114** (unpublished).

127. WELLMAN, P., 1976—The gravity field of the Australian basement. *BMR Journal of Australian Geology & Geophysics*, **1**, 287-90.

128. WELLMAN, P., 1976—Gravity trends and the growth of Australia. *Journal of the Geological Society of Australia*, **23**, 11-4.

129. WELLMAN, P., 1976—Regional variation of gravity and isostatic equilibrium of the Australian crust. *BMR Journal of Australian Geology & Geophysics*, **1**, 297-302.

130. WELLMAN, P., BOULANGER, Yu. D., BARLOW, B. C., SHCHEGLOV, S. N., & COUTTS, D. A., 1974—Australian and Soviet gravity surveys along the Australian calibration line. *Bureau of Mineral Resources, Australia—Bulletin* **161.**

131. WELLS, A. T., 1963—Helicopter traverses in the Gibson Desert, Western Australia. *Bureau of Mineral Resources, Australia—Record* **1963/59** (unpublished).

132. WEST AUSTRALIAN PETROLEUM EXPLORATION PTY. LTD., 1956—Carnarvon and Canning Basin gravity survey. *Unpublished company report.* *

133. WEST AUSTRALIAN EXPLORATION PETROLEUM PTY. LTD., 1962—Laurel Downs-Virgin Hills gravity survey, 1962. *Petroleum Search Subsidy Act unpublished company report* (BMR file number 62/1928).

134. WEST AUSTRALIAN PETROLEUM EXPLORATION PTY. LTD., 1962—Dongara-Mullewa gravity survey, Perth Basin, Western Australia, 1962. *Petroleum Search Subsidy Act unpublished company report* (BMR file number 62/1925).

135. WEST AUSTRALIAN PETROLEUM EXPLORATION PTY. LTD., 1963—Joanna Springs gravity survey, 1963. *Petroleum Search Subsidy Act unpublished company report* (BMR file number 63/1908).

136. WEST AUSTRALIAN PETROLEUM EXPLORATION PTY. LTD., 1963—Sahara gravity survey, 1963. *Petroleum Search Subsidy Act unpublished company report* (BMR file number 63/1910).

137. WEST AUSTRALIAN PETROLEUM EXPLORATION PTY. LTD., 1963—Augusta-Moora, 1963. *Petroleum Search Subsidy Act unpublished company report* (BMR file number 62/1935).

138. WEST AUSTRALIAN PETROLEUM EXPLORATION PTY. LTD., 1963—Augusta-Moora gravity survey, 1963. *Petroleum Search Subsidy Act unpublished company report* (BMR file number 62/1935).

139. WEST AUSTRALIAN PETROLEUM EXPLORATION PTY LTD., 1963—Central Perth Basin, 1963. *Petroleum Search Subsidy Act unpublished company report* (BMR file number 62/1935).

140. WEST AUSTRALIAN PETROLEUM EXPLORATION PTY. LTD., 1965—South-east Kidson helicopter gravity survey, Western Australia, 1965. *Petroleum Search Subsidy Act unpublished company report* (BMR file number 65/4814).

141. WHALEN, C. T., 1966—The Western Pacific calibration line survey, 1964-65. *United States Air Force, ACCS OPLAN 503, Phase Report* **3.**

142. WHITWORTH, R., 1969—A marine geophysical survey of the northwest Continental Shelf of Australia, 1968. *Economic Committee for Asia and the Far East* (ECAFE) *Conference, Canberra, Australia.*

143. WHITWORTH, R., 1970—Reconnaissance gravity survey of parts of Northern Territory and Western Australia, 1967. *Bureau of Mineral Resources, Australia—Record* **1970/15** (unpublished).

144. WHITWORTH, R., 1974—Marine and land gravity reconnaissance survey of Australia. *Australian National Committee for Antarctic Research, Committee on Geodesy and Geophysics*, Canberra, July 1974.

145. WILLCOX, J. B., 1974—The Great Australian Bight: A regional interpretation of the gravity and magnetic fields and seismic profiles. *Bureau of Mineral Resources, Australia—Report* **201.**

146. ZADOROZNYJ, I., in preparation—Reconnaissance helicopter gravity survey, New South Wales, Victoria, Tasmania and South Australia 1973/74. *Bureau of Mineral Resources, Australia—Report.*

147. ZADOROZNYJ, I., & COUTTS, D. A., 1973—Central highlands helicopter gravity survey, New Guinea, 1970. *Bureau of Mineral Resources, Australia—Record* **1973/14** (unpublished).

* Data held by Government of Western Australia.

BMR Journal of Australian Geology & Geophysics, 1 (1976), 321-333

The Cahill Formation—host to uranium deposits in the Alligator Rivers Uranium Field, Australia*

R. S. Needham and P. G. Stuart-Smith

All the uranium deposits of the Alligator Rivers Uranium Field of Australia, which between them contain a quarter of the world's reasonably assured uranium resources, are strata-bound within the Cahill Formation. Three of the four economic deposits are more or less conformable within a lower member near the base of the formation, which contains carbonate and carbonaceous rocks. The formation forms a poorly exposed but continuous folded belt, 5 km or more wide, over an area of about 15 000 square kilometres. Exposure is sparse, the rocks are generally deeply weathered, and knowledge of the stratigraphy of the unit is based largely on the results of shallow stratigraphic drilling.

Quartzo-feldspathic and micaceous metasediments are the dominant rock types in the Cahill Formation as a whole, and they have been metamorphosed to the amphibolite grade (staurolite-almandine subfacies). The unit appears to unconformably overlie the Archaean-Lower Proterozoic granite-gneiss-migmatite Nanambu Complex and the Lower Proterozoic psammo-pelitic Mount Partridge Formation, and is overlain, in places unconformably, by the Fisher Creek Siltstone. It grades into the migmatite-gneiss-granite terrain of the Nimbuwah Complex in the north-east.

The formation is a facies equivalent of the Koolpin Formation (host to uranium mineralization in the South Alligator Valley uranium field) to the south, and, in places, was separated from it during deposition by a basement high of Mount Partridge Formation.

The carbonate-carbonaceous sequence was probably deposited under shallow near-shore shelf conditions, along with considerable admixed terrigenous material. The upper part of the formation represents a period of transgression over the shelf. Uranium was concentrated under reducing conditions which developed locally in many places within the carbonate shelf. Subsequent concentration and reconstitution took place a number of times, the main period being during 1800 m.y. regional metamorphism and deformation. Mobilization of uranium away from the carbonate-carbonaceous sequence took place only under high temperature and pressure conditions such as those attending formation of the Nimbuwah Complex, where the metal was relocated in favourable low pressure structures.

Introduction

This paper describes a recently recognized sequence of rocks which contains the major uranium deposits of the Alligator Rivers Uranium Field, about 200 km east of Darwin in the Northern Territory of Australia (Figure 1). The stratigraphy, metamorphism and structure of the sequence are described, and the genesis of the uranium contained in the sequence is discussed in the light of this information. The name proposed for the sequence is the Cahill Formation, which replaces the informal 'Koolpin Formation equivalent' which was used prior to sufficient data being obtained to indicate the need to define a new stratigraphic unit.

The proven reserves of the field are about 335 000 tonnes of U_3O_8, which represents about 25 percent of the western world's reasonably assured reserves recoverable at less than $US30/lb. These reserves are contained in the ore bodies of Jabiluka, Ranger 1, Koongarra, and Nabarlek (Figure 1).

The field is occupied mostly by Archaean to Lower Proterozoic metasedimentary and igneous rocks, which underlie extensive sand plains between the coast and the Arnhem Land Plateau (Figure 1). They are weathered, poorly exposed, and are covered by up to 100 m of Mesozoic and Cainozoic deposits which are thicker nearer the coast. Although exposures of the Archaean and Lower Proterozoic rocks are extremely rare, a reasonable construction of solid geology is possible by use of scattered exposure, photo-interpretation, scout and exploration drilling, and aeromagnetic interpretation (Figure 2). Air-photo trends in areas of thin superficial cover allow continuation of strike directions between scattered outcrop and, most significantly, indicate a geological continuity between the Jabiluka, Ranger 1, and Koongarra deposits. Similar host-rock geology and continuity of aeromagnetic trends between the deposits are additional pointers to a common stratigraphic position for them. Rotary-percussion drilling along three traverses across this stratigraphic zone in unmineralized areas near Jabiru, Koongarra, and Mount Basedow (Figure 3) proved that a stratigraphic unit is continuous between the deposits, and provided data on which the definition of this unit, known as the Cahill Formation, is largely based. Detailed results of the drilling are given by Stuart-Smith & Hone (1976).

Regional geology

The geology of the Alligator Rivers Uranium Field was summarized by Needham *et al.* (1974). A comprehensive account of the regional geology is given by Smart *et al.* (1976). Generalized regional geology is shown in Figure 2, and generalized stratigraphy is given in Table 1. The uranium field lies in the northeast corner of the Pine Creek Geosyncline (Figure 1), and contains an Archaean to Lower Proterozoic mantled gneiss dome (the Nanambu Complex) overlain by amphibolite-grade Lower Proterozoic metasediment (the Mount Partridge and Cahill Formations, and the Fisher Creek Siltstone), some of which are transitional into Nanambu Complex gneiss. In the extreme northeast of the region the metasediments grade into a large late Lower Proterozoic migmatite complex (the Nimbuwah Complex), which was the focus of regional metamorphism and deformation about 1800 m.y. ago (Page & Needham, in prep.). The Lower Proterozoic rocks are intruded by pre and post-deformation basic igneous rocks (the Zamu Complex, as numerous sills later folded with the enclosing rocks; and the Oenpelli Dolerite, as an extensive series of lopolith-like basins and attendant dykes), and by early Carpentarian

* Paper presented at 25th International Geological Congress, Sydney, August 1976

anatectic granites developed during formation of the Nimbuwah Complex (the Jim Jim, Tin Camp, and Nabarlek Granites). All these rocks are overlain with marked unconformity in the east and southeast of the uranium field by extensive Carpentarian (1800-1400 m.y.) plateau sandstone with interbedded volcanics (the Kombolgie Formation).

Cahill Formation

The delineation of a continuous sequence of metasedimentary rocks from the South Alligator Valley uranium field north into the Alligator Rivers Uranium Field, with which uranium mineralization is almost exclusively associated, is the most economically significant result of the recent work. In the South Alligator Valley, this group of rocks was named the Koolpin Formation by Walpole (1962). The name now proposed for this group in the Alligator Rivers Uranium Field is the Cahill Formation; during the recent work it has been referred to informally as 'Koolpin Formation equivalent'. The results described in this paper have indicated sufficient lithofacies differences (Table 2) to require the creation of a new stratigraphic unit, and have enabled formal definition of Cahill Formation as a separate although correlative unit of the Koolpin Formation. The name is derived from Mount Cahill, in the centre of the uranium field at 12°52′S, 132°42′E (Figure 2).

The Cahill Formation is confined largely to the Alligator River 1:250 000 Sheet area. Scattered exposures, airphoto trends, aeromagnetic interpretation, and widely spaced scout drillholes have allowed approximate delineation of the distribution of the unit under Cainozoic cover, and indicate an apparent thickness of about 5 km. The formation extends to near the Mount Partridge Range in the south, and is covered by Cretaceous sediments of Cobourg Peninsula in the north. The most northerly occurrence known is in a drillhole 68 km northwest of Nabarlek (Hughes, 1973). The drillhole intersected Cahill Formation rocks after passing through 58 m of Cretaceous sediments. The western extent of the formation is not clear. The formation grades laterally into Koolpin Formation under Cainozoic deposits probably in the vicinity of the South Alligator River—Jim Jim Creek confluence. To the east the formation is largely covered, with marked regional unconformity, by Carpentarian rocks. It strikes east in the Myra Falls Inlier, curves north in an arc in the vicinity of Nabarlek and thence strikes west and north to Cooper Creek, where it grades into a migmatite terrain.

Stratigraphy

The Cahill Formation consists of a partly carbonate-carbonaceous lower part transitionally overlain by a more psammitic upper part, which are informally referred to here as lower and upper members. Both contain orthoamphibolite which in places has a relict igneous texture, and is believed to be in the main metamorphosed Zamu Com-

	Unit	Lithology	Remarks, relationships	Age (Page & Needham, in prep.)
	MESOZOIC AND CAINOZOIC SEDIMENTS			
			Unconformity	
CARPENTARIAN	*Kombolgie Formation*	Sandstone, basalt, conglomerate, minor siltstone, tuffaceous siltstone.	Largely undeformed plateau sandstone overlies older units with angular unconformity. Unconformity plane highly irregular in places.	
			Marked regional unconformity	
	Oenpelli Dolerite	Porphyritic and olivine dolerite, ophitic gabbro, granophyre and syenite.	Differentiated dolerite intruded as a series of lopoliths. Undeformed.	About 1720 m.y.
	Nabarlek, Tin Camp, and Jim Jim Granites	Altered coarse biotite granite.	Probably anatectic granites derived from centre of Nimbuwah Complex.	About 1800 m.y.
	Nimbuwah Complex	Lit-par-lit gneiss and schist, biotite gneiss, hornblende gneiss, granodioritic migmatite, gneiss.	Zoned migmatite complex formed at the focus of 1800 m.y. orogenesis. Outer margins were probably mostly South Alligator Group.	1800-1840 m.y.
			Regional deformation and metamorphism	
	Zamu Complex	Metadolerite, amphibolite.	Differentiated dolerite intruded as sills, mostly into South Alligator Group.	
PROTEROZOIC	*Fisher Creek Siltstone*	Quartz-mica schist, mica schist.	Transitionally overlies Cahill Formation.	
SOUTH ALLIGATOR GROUP			*Local unconformity*	
	Cahill Formation	Micaceous and feldspathic schist, quartz schist, quartzite, marble, para-amphibolite, calc-silicate rock, carbonaceous schist.	Correlates with Koolpin Formation (see Table 2) from which it was partially separated during deposition by hills of Mount Partridge Formation.	
LOWER GOODPARLA GROUP			*Gentle folding?*	
	Mount Partridge Formation	Sandstone, quartzite, arkose, siltstone, conglomerate.	Deposited on and marginal to Archaean granite mass, and later (1800 m.y.) partly accreted to it to form Nanambu Complex.	
ARCHAEAN TO LOWER PROTEROZOIC	*Nanambu Complex*	Leucocratic and pegmatoid gneiss, quartz-feldspar, schist mica schist, migmatite, granite, minor quartzites.	Mantled gneiss dome containing granitic Archaean core and accreted Lower Proterozoic sediments, mostly Mount Partridge Formation.	2520-1800 m.y.

Table 1. Summary of stratigraphy of the Alligator Rivers Uranium Field
(some minor intrusive units omitted).

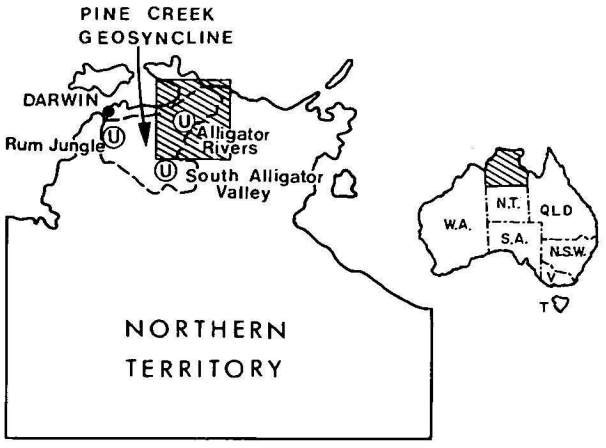

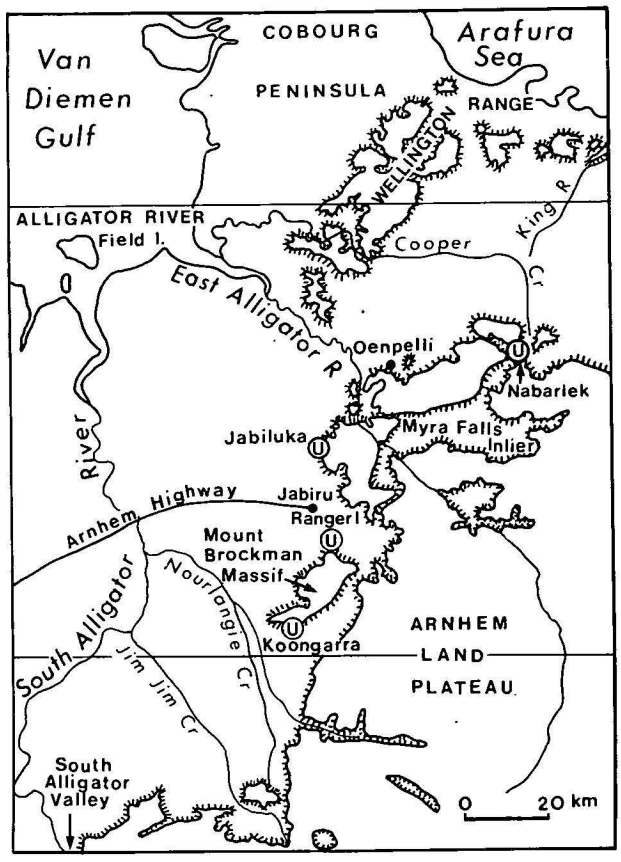

Figure 1. Locality map.

plex dolerite (Smart *et al.*, 1976). The type section of the formation is based on the Jabiru drill traverse (Figure 3).

Lower member

The lower member is a sequence of interbanded pyritic carbonaceous mica schist, chloritized feldspathic quartzite and quartz schist, para-amphibolite and calc-silicate rock. with lenses of massive dolomite up to 250 m thick. The unit contains uranium mineralization in the area, and is distinguished from the overlying member by the presence of carbonate and carbonaceous schist. It ranges in thickness from 300 to 600 m, and is characterized by numerous sharp changes in rock type. Along the Mount Basedow traverse, pyritic carbonaceous amphibole-mica schist is predominant, whereas along the Jabiru traverse chlorite-

	KOOLPIN FORMATION (terrigenous sediment rare)	CAHILL FORMATION (terrigenous sediment dominant)	
		West of East Alligator River	East of East Alligator River ('resisters')
PELITES	minor pyritic siltstone pyritic carbonaceous siltstone	mica schist feldspathic schist pyritic carbonaceous mica schist ± amphibole	carbonaceous quartz schist
QUARTZITES		mica-quartz schist quartz sandstone and conglomerate (minor) quartz–feldspar gneiss feldspar–quartz schist quartz schist feldspathic quartzite	feldspathic quartzite, mica quartzite, amphibole quartzite
CARBONATES	dolomite	para–amphibolite calc–silicate rock marble	calc–silicate rock marble

NIMBUWAH COMPLEX
gneiss, schist, migmatite, granite

Table 2. Rock types of the Cahill and Koolpin formations

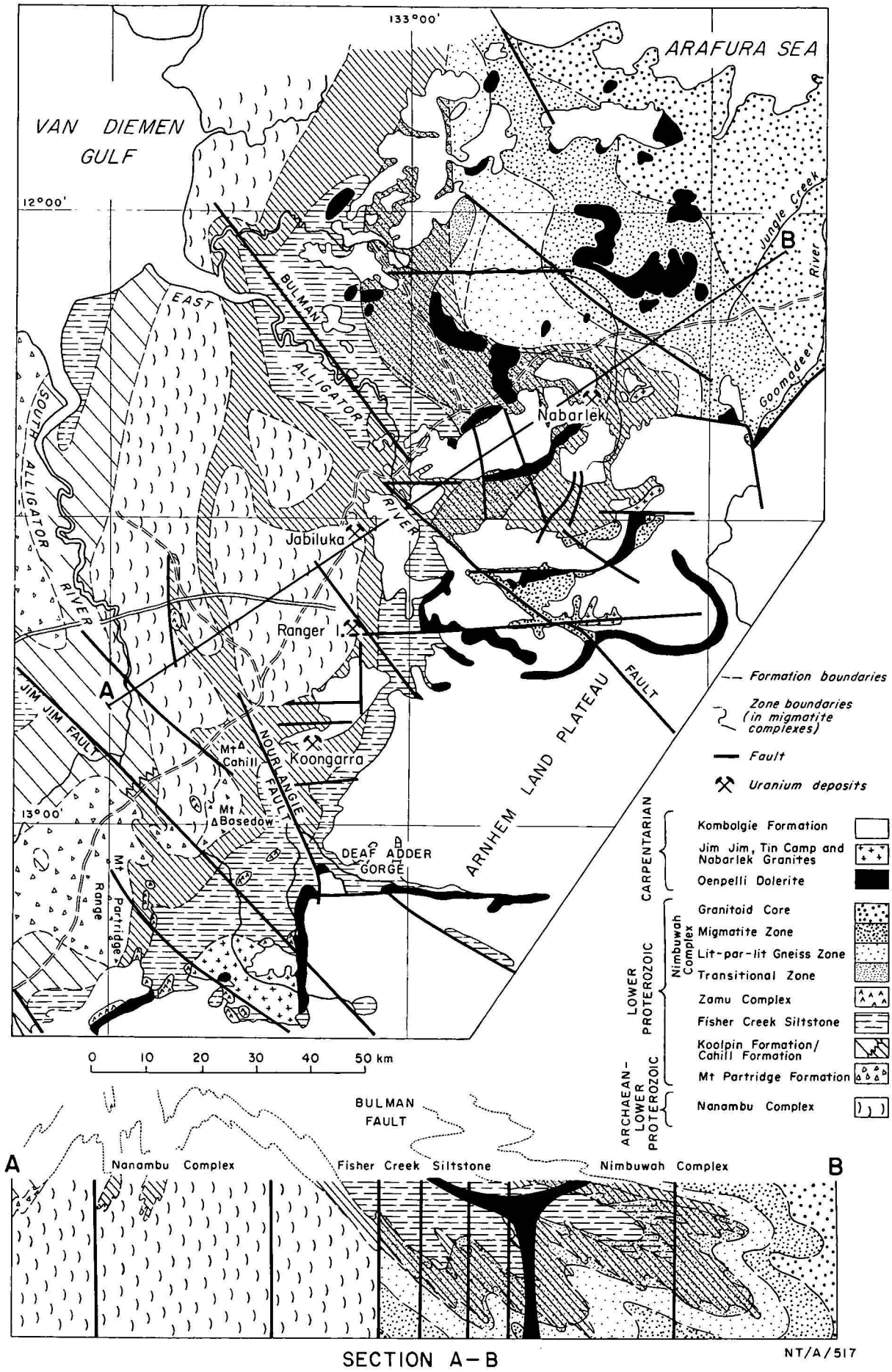

Figure 2. Generalized solid geology of the Alligator Rivers Uranium Field.

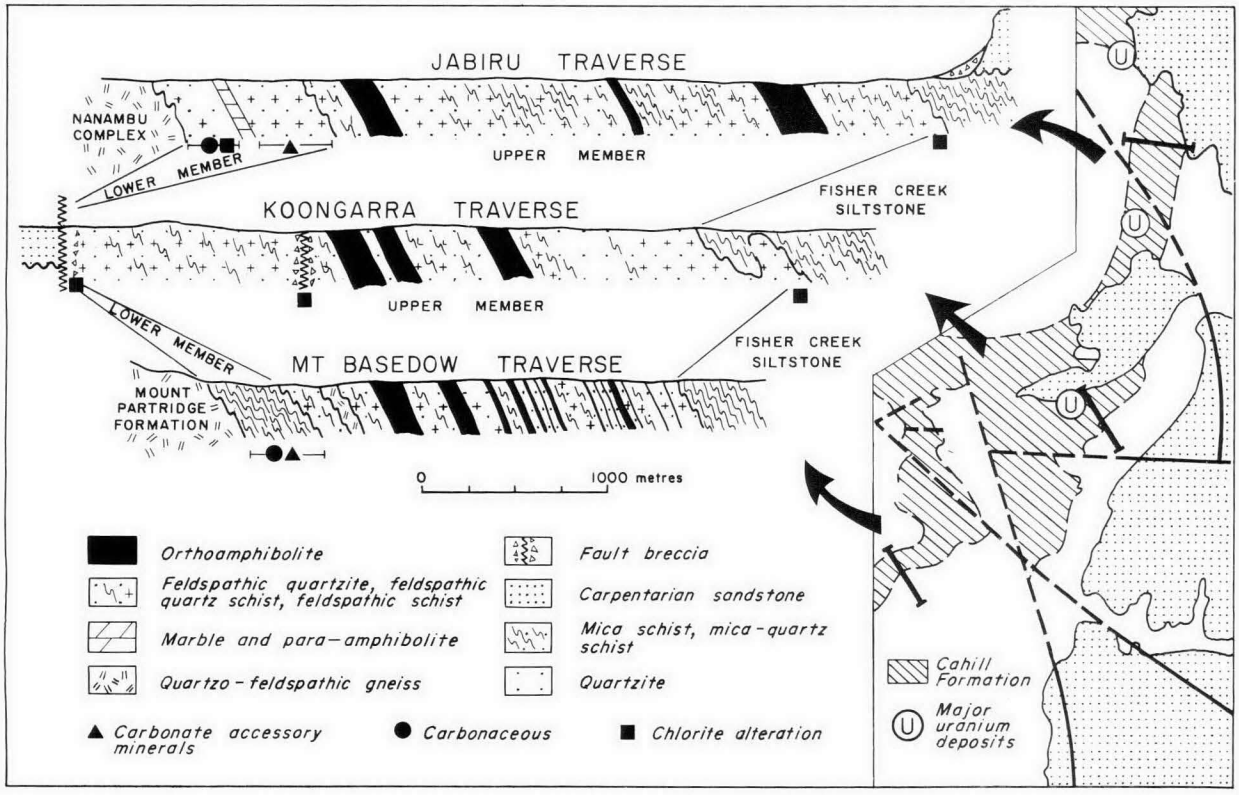

Figure 3. BMR drill traverse sections in Cahill Formation.

dolomite schist, chloritized amphibole-feldspar-quartz schist and carbonaceous schist are common. The lower member was not intersected along the Koongarra traverse, owing to folding and displacement of the Lower Proterozoic sequence across a major reverse fault which coincides with the eastern scarp of the Mount Brockman massif. Preliminary interpretation of geochemical analyses (Stuart-Smith, unpublished data), suggests that the lower member can be distinguished generally from the upper member by lower Co and Pb, and higher F, values. Within the formation, carbonaceous rocks have the highest U, Zn, Ni and S values.

Carbonaceous rocks. Carbonaceous schist forms low rubbly ferruginized outcrops that are indistinguishable from non-carbonaceous schist of the Cahill Formation. The fresh rock identified in drillholes consists of fine-grained foliated carbon, quartz, and minor disseminated pyrite, pyrrhotite, and quartz-rich bands. Fine-grained graphite is present along sheared foliation and crenulation cleavage surfaces (Figure 8). The carbonaceous schist of the Mount Basedow traverse also contains phlogopite (Figure 9), and in places tremolitic amphibole, accessory scapolite, epidote, and carbonate minerals, which suggest that the rock was derived from a magnesium carbonate-bearing sediment similar to the pyritic carbonaceous dolomitic shale and siltstone found throughout the central and western parts of the Pine Creek Geosyncline.

Marble, calc-silicate rock and para-amphibolite. Marble throughout the Alligator Rivers Uranium Field is unique to the lower member of the Cahill Formation. The most common variety is massive crystalline carbonate which ranges in composition from calcitic dolomite to magnesite (Needham, 1976). It crops out as discontinuous ridges, up to 10 m high, of iron-stained vuggy, cherty rock with rare, usually columnar, possible algal structures (Figure 4). Near-surface and surface silicification and ferruginization are common; fresh crystalline magnesian dolomite has been intersected less than 10 m below an outcropping ridge of ferruginous silicified dolomite near Nanambu Creek (Needham, 1976). Only two exposures of fresh carbonate are known (one is a dolomite marble 8 km southwest of Ranger 1, and the other a tremolite-dolomite-marble 18 km southwest of Nabarlek (Figure 10)). Both are adjacent to the prominent escarpment which marks the edge of the Carpentarian plateau sandstone, suggesting that these outcrops

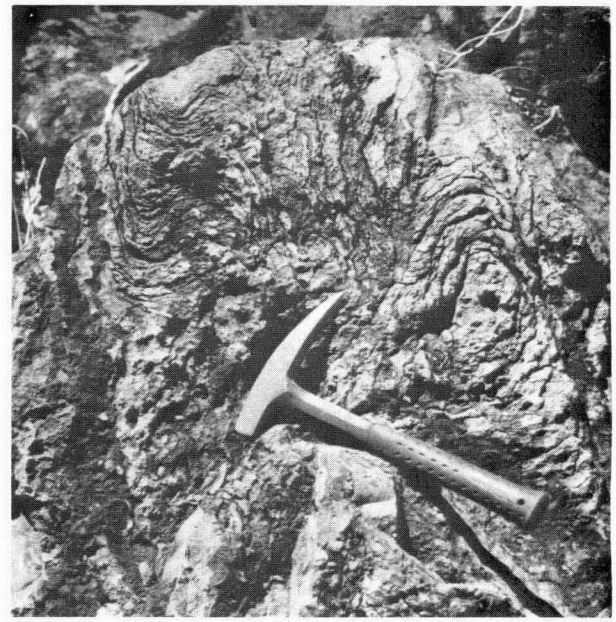

Figure 4. Columnar algal? structures in ferruginized silicified dolomite. Cahill Formation lower member. 12°35′S 132°37′E.

Figure 5. Interbedded fine cross-bedded quartzite and schist. A typical exposure of Cahill Formation upper member quartzite, 1.5 km northwest of Mount Cahill.

have been exhumed by scarp retreat since the period of ferruginization and silicification, which probably took place in early Tertiary times. Other carbonate-rich rocks within the lower member are muscovite-quartz-chlorite-dolomite schist, quartz-tremolite-diopside gneiss, and para-amphibolite (Figure 12).

Calc-silicate rock is known to crop out only in the eastern part of the Myra Falls Inlier, and consists of alternating lenses rich in hornblende and quartz, and containing diopside and feldspar as well.

Steeply dipping layers of thinly banded magnetite-calcite-biotite - hornblende - diopside - quartz schist occur in a banded sequence of mica schist and feldspathic schist near the northwest end of the Mount Basedow traverse, and represent an intermediate stage in the transformation of a sediment to a para-amphibolite. Mineralogical banding in the para-amphibolite is distinct, and probably reflects compositional banding typical of that found in thinly bedded dolomitic marls. In contrast, ortho-amphibolite is homogeneous in composition, widespread in occurrence, thicker (up to 600 m), and generally lacks distinct mineralogical banding.

Other rock types. The non-carbonaceous and non-carbonate rocks of the lower member are similar to the mica schist, feldspathic quartzite, and quartz schist of the upper member. However, accessory amphibole and sphene in some feldspathic quartzite of the lower member reflect the carbonate affinity of the rocks of that member; these accessories are not present in the upper member.

Upper member

The upper member conformably overlies and grades into the lower member, and is composed of interlayered feldspathic quartz schist, feldspathic schist, feldspathic quartzite, and minor mica schist and quartzo-feldspathic gneiss. Its gradational boundary with the overlying Fisher Creek Siltstone is marked by an increase in the proportion of mica schist, and a change in magnetic response (Horsfall & Wilkes, 1975). The thickness of the sequence ranges up to 2500 m or more along the Jabiru traverse; the apparent thickness of about 2500 m for only part of the upper member along the Koongarra traverse is a result of repetition by folding and faulting.

Exposure of the upper member is poor and confined to low discontinuous ridges or rubbly rises of quartzite, (some of which also contain schist (Figure 5)). The quartzites are indistinguishable from those in the Nanambu Complex and Mount Partridge Formation. The ridges are best developed south of Mount Cahill; in this area the member is characterized by a smooth white photo-pattern on aerial photographs. Other rock types which crop out in this area are clayey quartz sandstone, banded and cross-bedded fine-grained sandstone, quartz-pebble conglomerate, banded hematite rock, and hematite-quartz breccia (Needham & Smart, 1972).

Quartzo-feldspathic rocks. The quartzo-feldspathic rocks of the member are composed of quartz + feldspar + muscovite ± biotite/chlorite; accessory apatite, tourmaline, magnetite and garnet, and rare calcite and clinozoisite. They are medium-grained, foliated, banded, or, rarely, massive rocks. The absence of mineral elongation and shearing generally distinguishes them from Nanambu Complex quartzo-feldspathic rocks (Needham & Smart, 1972).

Macroscopic and microscopic banding is common, and probably relates to original compositional layers in the parent sedimentary rock. Phyllosilicates form thin planar folia along which the rock readily parts, defining its schistosity. The rocks are cut by minor veins of quartz and tourmaline-quartz-alkali feldspar.

Mica and mica-quartz schist. These rocks are typically composed of quartz + biotite/chlorite + muscovite + feldspar ± garnet ± iron oxides, and are distinguished from feldspathic quartzite, feldspathic quartz schist, and feldspathic schist only by their greater proportion of mica and low feldspar content (less than 10 per cent). The mica schist is intimately associated with quartz-feldspar schist, and commonly forms thin bands in it. Strongly kinked, highly micaceous bands in the mica schist contain boudins and fold noses of quartz and feldspar.

Porphyroblasts of almandine and magnetite are common (Figure 14), and magnetite is generally altered to hematite. Staurolite and kyanite are rare, and have been found only along the Mount Basedow traverse where, together with almandine and titano-magnetite, they form porphyroblasts up to 1 cm across. Hematite forms small hexagonal plates parallel to the foliation, and replaces magnetite octahedra. Banding within the staurolite and kyanite schist is intensely kinked and folded.

The upper member is probably a metamorphosed sequence of well-bedded feldspathic arenite and siltstone, minor conglomerate, and thin bands of pelite. The high proportion of Fe and Al-bearing silicates in the schists of the member suggests that they may represent metamorphosed iron-rich pelites. Staurolite and kyanite schist is a common rock type in the overlying Fisher Creek Siltstone, but can be readily distinguished from Cahill Formation rocks by its lack of magnetite, except along the Mount Basedow traverse.

Metamorphism

The metamorphic grade of the Lower Proterozoic metasediments ranges from the staurolite-almandine subfacies of the amphibolite facies in most parts of the area to the sillimanite-almandine-orthoclase subfacies within the migmatite terrain of the Nimbuwah Complex (Smart *et al.*, 1976). Rare amphibole schist interbedded with meta-arkose of the Mount Partridge Formation in the southwest of the region suggests that amphibolite-grade metamorphism pervades the Lower Proterozoic metasediments throughout the uranium field.

Almandine is found in most rock types in the Cahill Formation, but is more abundant in mica schist. Kyanite is found only with staurolite, indicating that the metamorphic grade does not reach the kyanite-almandine subfacies (Winkler, 1967). The rarity of staurolite, and abundance of potassium feldspar in Cahill Formation schist, contrast with the mineralogy of Fisher Creek Siltstone schist, and indicate a relative abundance of alkalis in the parent sediments of the Cahill Formation.

Retrograde metamorphism has resulted in chloritization of ferro-magnesian minerals and sericitization of feldspars. Garnet, biotite, and amphibole commonly show complete or partial alteration to chlorite; chloritized haloes surrounding small quartz veins are common in all rock types (Figure 13).

The Lower Proterozoic rocks have also undergone ferromagnesian metasomatism. This alteration is most pervasive in the lower member, where rocks are depleted in Na and enriched in Mg (Stuart-Smith, unpublished data), and chlorite has replaced feldspar in feldspathic quartzite, to give rise to quartz-chlorite schist. Chloritization is particularly intense in some sheared and brecciated schists of the lower member near the contact with the Nanambu Complex, suggesting that chloritization followed cataclastic deformation. However, the association of chlorite with the sheared Nanambu Complex/Cahill Formation contact, and also with the unconformable Cahill Formation/Fisher Creek Siltstone contact (Figure 3), suggests that stratigraphic and structural breaks are the main loci of chloritization, providing channelways for Fe and Mg-rich fluids.

Hematitization is widespread, and is associated with chlorite alteration, particularly in areas of uranium mineralization. Hematite is a common vein-filling mineral, also replaces ferromagnesian minerals, and forms pseudomorphs after magnetite.

Relationships with other units

The base of the Cahill Formation is not exposed, and, where intersected by drilling, is in sheared contact with the underlying rocks. The Cahill Formation appears to be contiguous with the Nanambu Complex and Mount Partridge Formation, as the regional strike within these three formations is generally parallel, which suggests that the Cahill Formation lies conformably on older rocks. However, the Cahill Formation appears to overstep the Mount Partridge Formation in places to directly overlie Archaean granite of the Nanambu Complex (for example 4 km southeast of Jabiluka). Consequently we infer that the Cahill Formation unconformably overlies older units, (as does the correlative Koolpin Formation southwest of the uranium field) but this relationship has been obscured by the 1800 m.y. metamorphic and depositional event.

The formation is transitional upwards into a monotonous sequence of quartz meta-siltstone and quartz-mica schist which comprise the Fisher Creek Siltstone. Convergence of, and discontinuity between, two sets of air-photo trends coincide with the position of the Cahill Formation/Fisher Creek Siltstone contact on the Koongarra traverse, and indicate local unconformity between the two formations. The break in the pattern of air-photo trends has enabled accurate projection of the contact between the two formations under Cainozoic cover from this traverse north to the Mount Brockman massif, and southwest to the Nourlangie Fault (Figure 2).

Northeast of the East Alligator River the Lower Proterozoic metasediments grade into gneiss, migmatite, and granite of the Nimbuwah Complex, but 'resister' rock types (Read 1944, quoted in Mehnert, 1968, p. 298) remain evident almost as far northwest as Nabarlek, and indicate that partly granitized Cahill Formation forms a large proportion of the outer parts of the Nimbuwah Complex (Table 2). The gradational granitization of Cahill Formation rock types is best studied in the Myra Falls Inlier, where quartzite, marble, calc-silicate rock, and carbonaceous schist 'resisters' (mapped as Cahill Formation) crop out within incipiently differentiated schist ('Transitional Zone') and lit-par-lit gneiss ('Lit-par-lit Gneiss Zone') mapped as Nimbuwah Complex (Needham, *et al.*, 1974).

There are two zones of transition between the Cahill Formation and the Koolpin Formation. One is at the southern end of the Mount Partridge Range, and the other is inferred to be in the area of the South Alligator River and Jim Jim Creek confluence under extensive flood plain sediments (Figure 2). The most obvious difference between the two formations is the absence of chert bands, nodules, and boudins in the Cahill Formation, which characterize the pelitic rocks of the Koolpin Formation. The coincidence of one of the zones of transition with the Mount Partridge Range suggests that the Mount Partridge Formation may have formed a positive relief feature during the early part

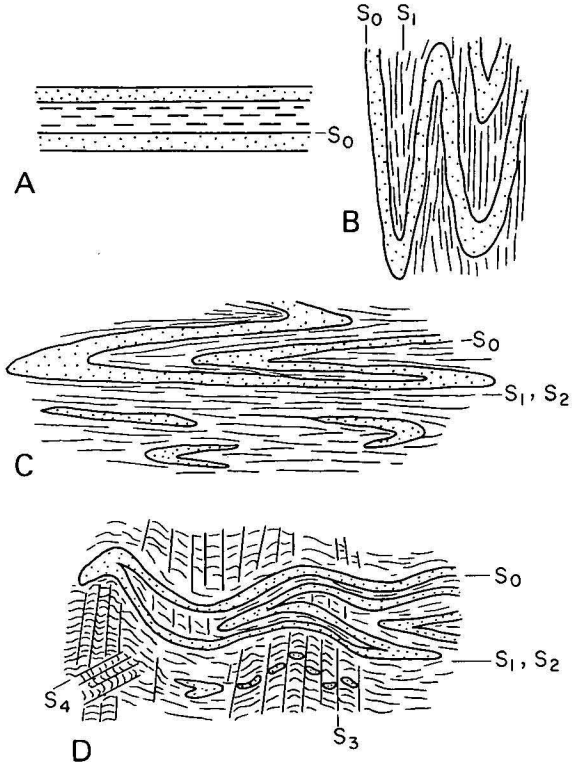

A Undeformed sedimentary sequence, bedding S_0

B Isoclinal folding ?, penetrative axial plane foliation S_1, greenschist to amphibolite facies metamorphism

C Isoclinal folding, penetrative axial plane foliation S_2, transposition of S_0 and S_1, amphibolite facies metamorphism

D Open to tight folding, axial plane crenulation cleavage S_3 and crenulation cleavage S_4, amphibolite facies metamorphism

Figure 6. Deformational history of Cahill Formation rocks.

of the South Alligator Group deposition, thereby forming a partial barrier between areas of Cahill and Koolpin sedimentation. The contrast in rock type assemblages in the two formations indicates different environments of deposition, even though the common carbon/carbonate component suggests a broad lithofacies similarity (Table 2). There may also have been a partial barrier between the two formations near the South Alligator River and Jim Jim Creek confluence; this is suggested by the proximity of Mount Partridge Formation, as an anticlinal spur, to the Nanambu Complex in this area (Figures 2, 7).

Structure and tectonic history

Owing to lack of exposure, our knowledge of the structure of the formation is based almost entirely on small-scale structures evident in drill core, on aerial photo trends, and on the regional distribution of the unit. Microstructures reveal at least four phases of deformation (Figures 6, 15), probably all related to the 1800 m.y. period of deformation and metamorphism.

Mineralogical and textural banding form the oldest preserved foliation (S_0), and are probably original bedding. S_1 foliation is produced by the parallel growth and alignment of phyllosilicates at a shallow angle (less than 10°) to S_0. These two foliations are rarely preserved in the mica schist, but are dominant features of the quartzo-feldspathic schist.

Intense isoclinal folding transposed S_0 and S_1, and with recrystallization of the phyllosilicates produced the dominant schistosity (foliation S_2). Relict isoclinal fold noses are preserved in the more competent quartz-rich bands. Almandine and magnetite porphyroblasts show deformed, rotational, and crosscutting textures indicating their development before, during, and after this phase of deformation.

Foliation S_3—axial plane to tight, angular, and rarely isoclinal folds—was produced by recrystallization of phyllosilicates and development of crenulation cleavage, which rarely transposed older foliations.

Large unstrained mica and idiomorphic kyanite and staurolite porphyroblasts cut across the S_3 foliation, and indicate a probable temperature increase associated with hydrostatic pressure after the development of that foliation. These minerals deflect a later set of poorly developed kinks (S_4) that are not related to major recrystallization or folding. The degree of apparent deformation locally differs substantially over even a small area, but generally the intensity increases towards the Nimbuwah Complex (Smart *et al.*, 1976). The apparent thickness of the formation differs with structural orientation; in most parts it is about 5 km, but it appears to be more than 20 km in the Koongarra area and in the Myra Falls Inlier as a result of changes in dip and repetition of the unit about horizontal fold axes. The style and orientation of folds and faults have been governed largely by basement configuration (the Archaean core of the

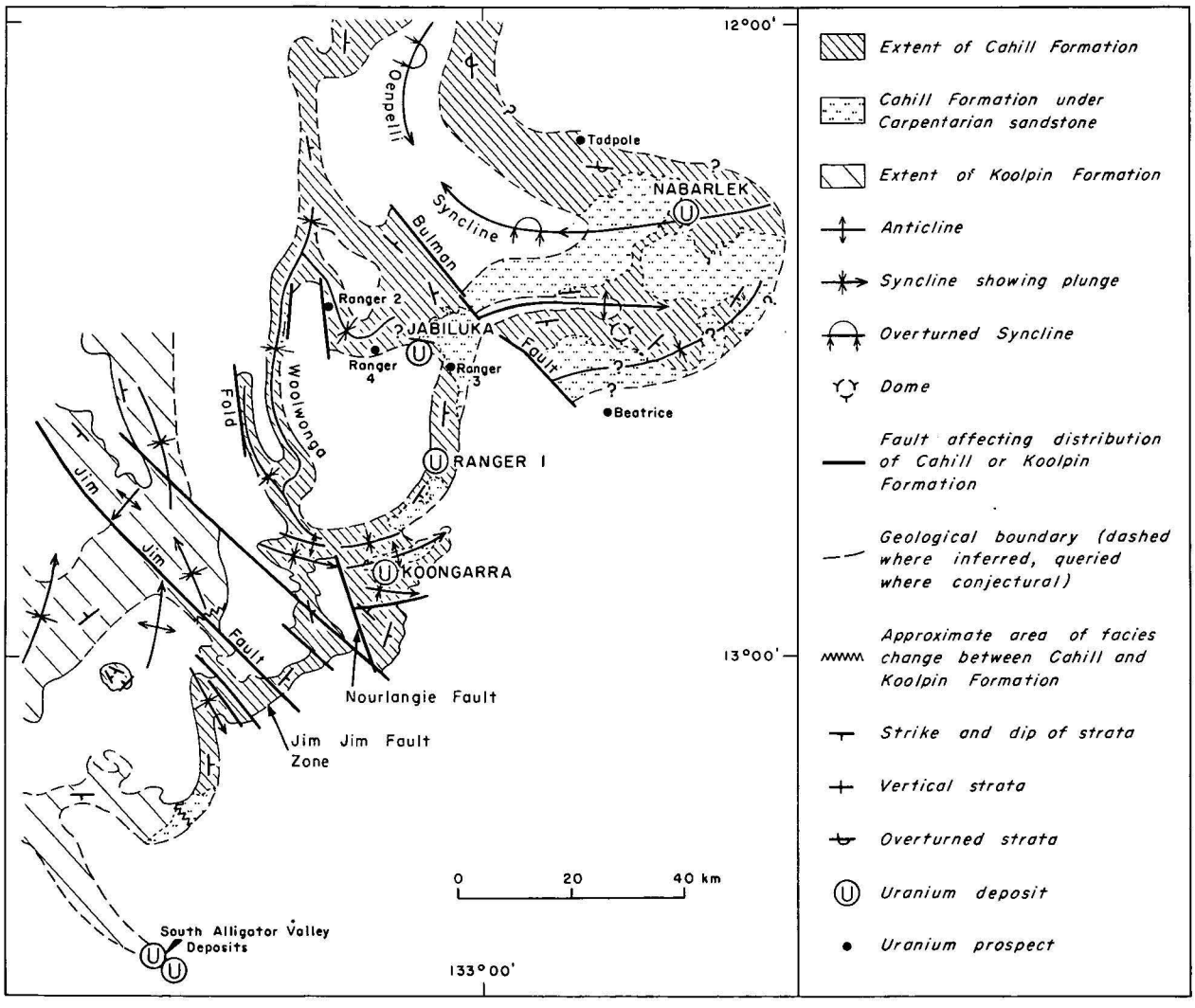

Figure 7. Major structural elements of Cahill Formation, and distribution of uranium ore bodies and prospects.

Nanambu Complex), and development of the Nimbuwah migmatite complex.

The first phase of deformation recognizable in the Alligator Rivers region was east-west compression which gently folded Mount Partridge Formation strata, and resulted in the unconformable relationship between this unit and the Koolpin and Cahill Formations. The S_1 foliation, parallel to bedding, probably developed during this event, and is best preserved in the rocks of the Mount Partridge Formation. Local unconformity between the Cahill Formation and the Fisher Creek Siltstone suggests that similar minor activity took place at times throughout the remainder of Lower Proterozoic sedimentation.

After sedimentation, diapiric growth of the Nimbuwah Complex in the northeast of the region caused marginal overfolding and intense isoclinal folding of the sedimentary pile accompanied by amphibolite-facies regional metamorphism. The Oenpelli Syncline is a large overturned basinal syncline formed by marginal overfolding along the southwest flank of the complex (Figures 2, 7). The Cahill Formation occupies parts of both the southwest and northeast limbs of the structure, but is known in the northeast limb only by the occurrence of 'resister' quartzite ridges in a migmatite terrain. The centre of the structure is filled with partly granitized Fisher Creek Siltstone. The attitude of the syncline (overturned outwards from the migmatite complex) suggests that the complex formed by upward and outward diapiric growth, involving movement of a mobile mass of granitized material over less granitized material, much as for the migmatite diapirs described by Haller (1956, p. 162).

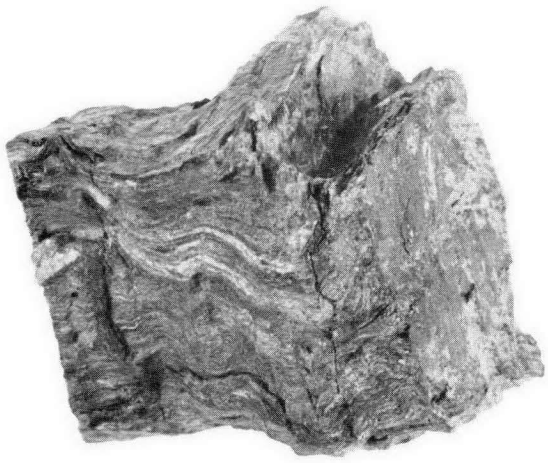

Figure 8. Crenulated pyritic carbonaceous quartz schist with graphite on fracture and schistosity surfaces. Cahill Formation lower member. x 1.

During this period of deformation, a block of Archaean granitic material was reactivated and partly migmatized, and had leucocratic gneissic material, probably derived from Mount Partridge Formation, accreted to it to form the Nanambu Complex (Page & Needham, in prep.). The Cahill Formation was draped around it to form a complex refolded synclinal structure known as the Woolwonga Fold. The isoclinal fold axes were similarly controlled, being concentrically arranged around the Archaean block (Figure 7).

A strong foliation (S_2) developed parallel to the axial plane of these folds, and gave rise to the dominant regional schistosity. During the formation of the Nimbuwah Complex, complex small-scale cross-folding with axial plane crenulation cleavage (S_3), developed in the less

Figure 9. Carbonaceous (dark grey) mica-quartz schist with pervasive S^2 crenulation cleavage and large phlogopite porphyroblasts. Cahill Formation lower member. Plane-polarized light x 5.

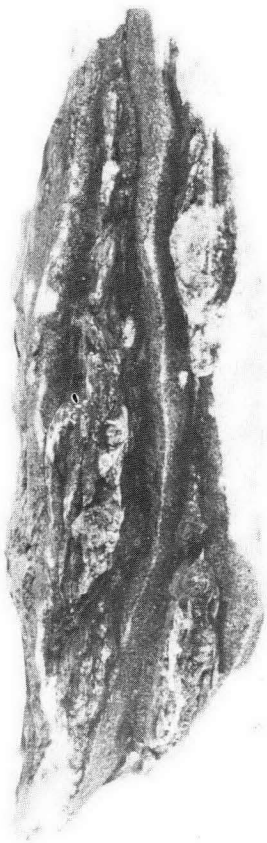

Figure 10. Layered tremolite-dolomite-marble from a 'resister' within the Nimbuwah Complex migmatite terrain. Cahill Formation lower member. x ½.

competent rock types. This may have been related to further movements of the migmatite and Archaean granite masses, and to the intrusion of anatectic granites as the grade of metamorphism reached its peak after the formation of S_3. Biotite which grew during the development of S_3 has yielded a K-Ar isotopic age of about 1800 m.y., and dates the climax of late Lower Proterozoic tectonism in the Alligator Rivers region.

Faulting was probably mostly contemporaneous with S_2. Faults are usually long and linear, and have vertical or dip-slip displacements, which in many places developed parallel to northwest-trending S_2 axial planes. They are in the main quartz or quartz-breccia filled, and the adjacent country rocks are sheared. The Jim Jim Fault Zone is a 10 km wide zone of intense shearing and step-faulting, bounded on the northeast by the Jim Jim Fault. Other major faults in the area may be similarly complex. Several of the major faults show displacements up to 70 m for the latest movements affecting the overlying Carpentarian strata, but otherwise the area has been essentially stable since the late Lower Proterozoic.

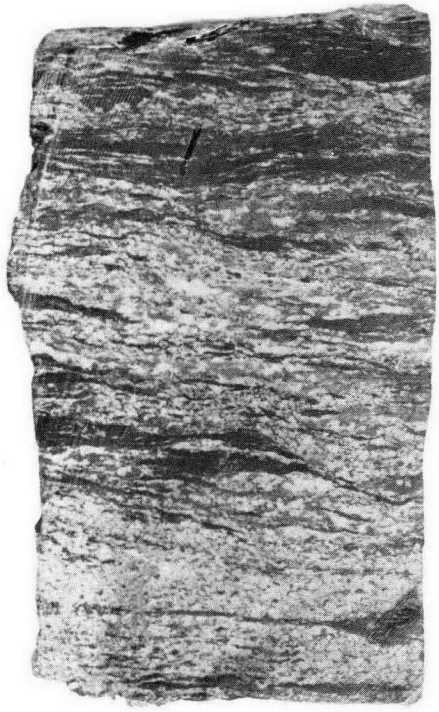

Figure 11. Banded muscovite-quartz-chlorite-dolomite schist. Dark bands are chlorite, and white mineral is dolomite. Cahill Formation lower member. x 1.

Depositional environment

A broad concept of palaeoenvironment can be postulated by comparison with concepts put forward for the Rum Jungle area, which has many geological features in common with the Alligator Rivers region.

Weak tectonic activity marked the end of Mount Partridge Formation sedimentation. This activity resulted in doming in the extreme southwest of the Alligator Rivers region, which divided subsequent sedimentation into at least two basins. Cahill Formation sediments were deposited northeast of the area of uplift in a basin which was possibly periodically interconnected with areas of contemporaneous sedimentation south, west, and north of the area of doming, represented by the Koolpin and Golden Dyke Formations.

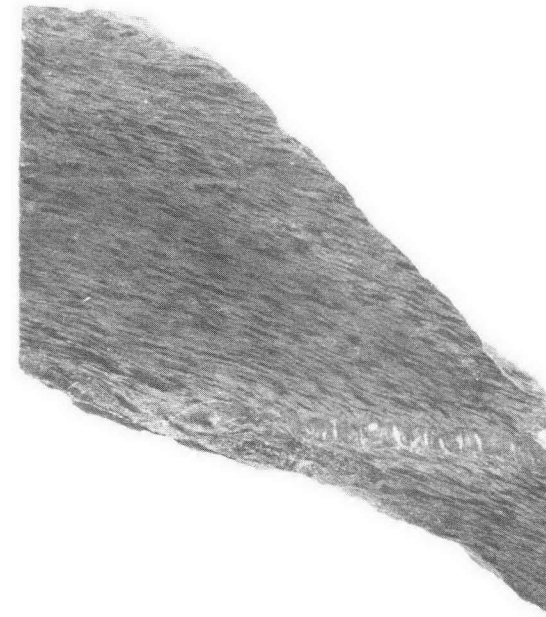

Figure 12. Para-amphibolite; lenticles are biotite replacing garnet. Cahill Formation lower member. x 1.

Carbonate-carbonaceous assemblages typify the sediments deposited within these basins, but the different form of the carbonate rocks, and the relative proportions of carbonate, carbonaceous, and terrigenous rock types in each basin indicates in each case differences in depositional environment. The Golden Dyke Formation contains carbonaceous rocks with subordinate carbonate, as extensive sheets generally less than 1 m thick, which predominate over minor terrigenous sediment. Lenses and beds of carbonate range from less than 20 m to over 300 m thick in the Koolpin Formation where carbonaceous and carbonate rocks are exclusive. In the Cahill Formation carbonate is present predominantly as sharply lenticular bodies up to 250 m thick and there is minor carbonaceous rock, but terrigenous material is dominant. Roberts (1973) concluded that Golden Dyke Formation dolomite in the Rum Jungle area was deposited in a shallow marine evaporitic environment; however, the absence of evaporitic minerals, and the association between dolomitic and terrigenous sediments, suggest a low initial salinity. We envisage the Cahill Formation carbonate was deposited under similar conditions.

Widespread stromatolites in all of the Pine Creek Geosyncline carbonate rocks suggest that algae were common in the depositional environment of these rocks. Algae which depend on photosynthesis are restricted to the euphotic zone, i.e. less than 120 m in clear tropical water, and so it seems likely that the Cahill Formation carbonate accumulated in a shelf environment. The proximity of the older Nanambu Complex to the base of the Cahill Formation, and the common presence of feldspar in most of the clastic rocks, suggest that the formation was deposited near-shore.

Carbonaceous sediments which are interbedded with the carbonate rocks were most probably deposited in restricted reducing environments in depressions within the generally oxygenated carbonate/terrigenous sediment environment. The source of the carbon was most probably organic detritus derived from nearby algal bioherms, which was deposited with different amounts of fine terrigenous sediment as a foetid ooze.

The quartzite and quartz schist of the upper member represent a gradual transgression over the shelf. The

contribution of biological processes to sedimentation following transgression was insignificant, owing to either the fast rate of deposition, or deepening of the water/sediment interface to below the photic zone, or both. When Cahill Formation sedimentation ceased the transgression of clastic sedimentation over the shelf was probably complete.

Uranium ore genesis

The primary uranium ore of the Jabiluka, Ranger 1, Koongarra and Nabarlek deposits is uraninite, mostly pitchblende, found as both disseminated and massive (colloidal and vein-type) forms (Rowntree & Mosher, 1976; Eupene *et al.*, 1976; Foy & Pederson, 1976; Anthony, 1976). The orebodies are generally conformable tabular to basin-shaped bodies except Nabarlek, which is a cigar-shaped transgressive vein. All are associated with quartz-chlorite schist and massive chlorite rock, and to a lesser degree (in all but Nabarlek) also with carbonaceous schist. In some places carbonaceous horizons are associated with above-average uranium grades. Primary mineralization at Ranger 1 is also found in chert, and at Nabarlek in micaceous schist. Massive carbonate is known adjacent to, or nearby, the Jabiluka, Ranger 1 and Koongarra deposits, and in each case its distribution is mutually exclusive to that of uranium. All the orebodies contain disseminated sulphides, and in Jabiluka and Ranger 1 the concentration of gold is related to that of uranium.

Three methods of formation have been proposed by various workers for the Alligator River uranium deposits. These methods—syngenetic, epigenetic and supergene —are reviewed by Dodson *et al* (1974). Lateral and vertical proximity of the deposits to the regional unconformity at the base of the Carpentarian suggests at first glance the possibility of supergene concentration, but the relevance of the unconformity to mineralization has decreased as mapping and exploration has progressed (Dodson *et al.*, 1974; Ryan *et al.*, 1976). It is now generally accepted that thinner superficial cover over Lower Proterozoic rocks near the escarpment at the edge of the Carpentarian units has facilitated successful airborne and ground exploration in these areas, relative to areas where Cainozoic cover is thicker. Therefore we do not consider it necessary to enter into a discussion on the possibility of supergene formation of the ore.

Throughout the Pine Creek Geosyncline uranium is almost invariably found in association with carbonaceous assemblages. It follows that as most carbonaceous strata in the Pine Creek Geosyncline are deposited in association with carbonate rocks, in many places the distribution of uranium and carbonate is similar. Their mutual exclusion apparent in the Alligator Rivers orebodies, however, underlines their extrinsic relationship.

In the Alligator Rivers Uranium Field all major and most minor uranium mineralization is strata-bound in the Cahill Formation, and is generally near the base of the formation where carbonaceous strata are common. This association demonstrates that carbon may have played a role in the location of uranium, and is an important clue to the method of ore genesis.

Carbon may have fixed uranium in reducing conditions either during diagenesis from surface and interstitial waters, or under similar chemical conditions after lithification from connate and circulating ground waters. In either case, the size and grade of the Alligator Rivers deposits suggest that additional factors were involved in the accumulation of such rich orebodies.

Each of the major deposits is associated with one or a number of dislocation structures, and ferromagnesian alteration of country rock is common in the mineralized areas. Stratigraphic and structural breaks may have provided pathways for mineralizing and metasomatizing fluids, thus explaining the association of both chloritization and uranium mineralization with unconformities and faults. However, this has not resulted in any significant movement of uranium away from the lower part of the Cahill Formation, and underlines the essential nature of the uranium/carbon relationship. For instance, whereas chloritization is associated with both the Nanambu Complex/Cahill Formation and Cahill Formation/Fisher Creek Siltstone unconformities, uranium is associated only with the lower stratigraphic break.

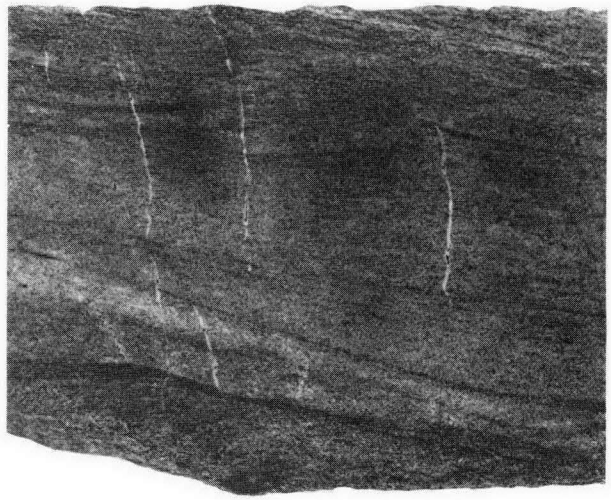

Figure 13. Feldspathic quartzite with chlorite alteration of biotite (pale grey areas) surrounding quartz veinlets. Chaill Formation upper member. x 1.

The complex mineragraphy of the primary uranium minerals and the occurrence of several varieties of chlorite in some of the orebodies indicate that solution and re-deposition of these minerals took place a number of times, each event probably increasing the concentration of these minerals. The ages of these events are reflected in the isotopic ages obtained from uranium in the region (1880, 1700, 900-800 m.y.—Hills & Richards, 1976). The 1880 m.y. concentration coincides approximately with late Lower Proterozoic regional metamorphism, migmatization, and deformation, and was probably the main concentrating event. Certainly the absence of any substantially younger metamorphic mineral ages in the Lower Proterozoic rocks of the region indicates that subsequent concentrations were low-temperature events.

The Nabarlek deposit is an extremely high-grade, massive, transgressive vein of pitchblende, and is markedly different from the other stratabound orebodies. The absence of a carbon association suggests that higher pressure and temperature conditions which pervaded this area (nearer, as it is, to the 1800-m.y. orogenic centre represented by the core of the Nimbuwah Complex) resulted in uranium being transported by hydrothermal solutions away from its original (carbonaceous?) position in the rock pile, and its being re-deposited in a favourable dilatational structure.

Insufficient evidence exists to choose emphatically between syngenetic and epigenetic origins for the Alligator Rivers uranium deposits. However, the importance of the uranium/carbon association is clear, and, together with the palaeoenvironmental model we propose, strongly suggests that the orebodies were formed partly syngenetically. The

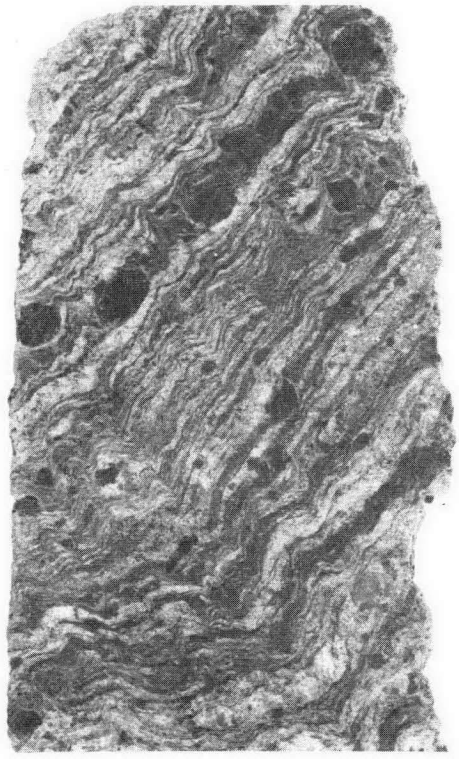

Figure 14. Crenulated banded garnet-mica-quartz schist, typical of Cahill Formation upper member and Fisher Creek Siltstone. Dark grey mineral, about 2 mm diameter, is magnetite. x 1.

Figure 15. Strongly deformed mica-quartz schist of Fisher Creek Siltstone shows a complex deformational history: compositional layering (S^0) is isoclinally folded and virtually parallel to the axial plane (S^2), which is openly folded by crenulation cleavage S^3. Black flecks in extreme bottom left are magnetite. x 1.

veinlets of pitchblende could represent epigenetic enrichment of the amorphous syngenetic protore, and the uranium contained in the epigenetic fluids may have been derived from the Cahill Formation or from other Lower Proterozoic and Archaean rock units. The massive vein deposit of Nabarlek represents extreme hydrothermal processes of ore formation operating under high pressure/temperature conditions.

The ultimate source of the uranium, prior to its being located in the Cahill Formation, was therefore the older Archaean and Lower Proterozoic rocks. Six samples of Nanambu Complex gneiss and granite analysed by Wilkes (1975) averaged 5 ppm uranium (average value for granite and gneiss is 3.5—Bowie, 1970). If this value is regarded as an average for the Nanambu Complex, then the amount of uranium contained in the Alligator Rivers Uranium Field deposits (335 000 tonnes U_3O_8) could conceivably have been derived from 21 440 million m^3 of Nanambu Complex rocks. Spread over the present-day surface area of the Complex, this volume represents a vertical thickness of about 20 m. Chemical and physical processes could have removed uranium from a 20 m layer of Nanambu Complex, and transported the element via surface or groundwater to areas of Cahill Formation deposition.

Acknowledgements

We wish to thank the following companies for information which has helped considerably in the construction of a regional geological framework; in particular we are grateful for the many valued discussions we have had from 1971-5 with their field geologists. Noranda (Australia) Ltd., Geopeko Ltd., Queensland Mines Ltd., Pancontinental Mining Ltd., Project Mining Corporation, Ocean Resources N.L., Australia and New Zealand Exploration, Esso Minerals Ltd., Pechiney (Australia) Exploration P/L.

P. G. Smart (1971-5) and A. L. Watchman (1972-4) have contributed significantly to this work in both field work and preparation of maps and progress reports. Dr John Ferguson is thanked for his helpful criticism during the preparation of this manuscript. The figures were drawn by Sue Davidson, Geological Drawing Office, BMR.

References

ANTHONY, P. J., 1976—Nabarlek uranium deposit; *in* ECONOMIC GEOLOGY OF AUSTRALIA AND PAPUA NEW GUINEA. Volume **1**—Metals, 304-308. *Australasian Institute of Mining and Metallurgy, Melbourne.*

BOWIE, S. H. U., 1970—World uranium deposits; *in* Symposium on Uranium exploration geology. *International Atomic Energy Agency, Vienna,* 22-23.

DODSON, R. G., NEEDHAM, R. S., WILKES, P. G., PAGE, R. W., SMART, P. G., & WATCHMAN, A. L., 1974—Uranium mineralization in the Rum Jungle—Alligator River province, Northern Territory, Australia *in* FORMATION OF URANIUM ORE DEPOSITS, 551-568 *International Atomic Energy Agency, Vienna.*

EUPENE, G. S., FEE, P. H., & COLVILLE, R. G., 1976—Ranger 1 uranium deposits; *in* ECONOMIC GEOLOGY OF AUSTRALIA AND PAPUA NEW GUINEA, Volume **1**—Metals, 308-317, *Australasian Institute of Mining and Metallurgy, Melbourne.*

FOY, M. F., & PEDERSON, C. P., 1976—Koongarra Uranium deposit; *in* ECONOMIC GEOLOGY IN AUSTRALIA AND PAPUA NEW GUINEA, Volume **1**—Metals, 317-321, *Australasian Institute of Mining and Metallurgy, Melbourne.*

HALLER, J., 1956—Probleme der Tiefentektonik, Bauformen im Migmatit—Stockwerk der ost-grönlandischen Kaledoniden. *Geologische Rundschau,* **45,** 159-167.

HILLS, J. H., & RICHARDS, J. R., 1976—Pitchblende and Galena Ages in the Alligator Rivers Region, Northern Territory, Australia. *Mineralium Deposita*, **12**, (4).

HORSFALL, K. R., & WILKES, P. G., 1975—Aeromagnetic and Radiometric Survey of Cobourg Peninsula, Alligator River and Mount Evelyn (part) 1:250 000 Sheet Areas Northern Territory 1971-1972. *Bureau of Mineral Resources, Australia—Record* **1975/89** (unpublished).

HUGHES, R. J., 1973—Stratigraphic drilling, Cobourg Peninsula 1:250 000 Sheet area, N.T., 1973. *Bureau of Mineral Resources, Australia—Record* **1973/196** (unpublished).

MEHNERT, K. R., 1968—MIGMATITES AND THE ORIGIN OF GRANITIC ROCKS. *Elsevier, Amsterdam.*

NEEDHAM, R. S., 1976—BMR Rotary-percussion and Auger Drilling in the Cahill and East Alligator 1:100 000 Sheet areas, Alligator Rivers Region, 1972-3. *Bureau of Mineral Resources, Australia—Record* **1976/43** (unpublished).

NEEDHAM, R. S., & SMART, P. G., 1972—Progress report, Alligator River Party, N.T. 1971. *Bureau of Mineral Resources, Australia—Record* **1972/1** (unpublished).

NEEDHAM, R. S., SMART, P. G., & WATCHMAN, A. L., 1974—A Reinterpretation of the Geology of the Alligator Rivers Uranium Field, N.T. *Search*, **5**, 397-399.

PAGE, R. W., & NEEDHAM, R. S., in preparation—Isotopic dating and evolution of Archaean and Proterozoic rocks in the Alligator Rivers Uranium Field, Northern Territory, Australia.

ROBERTS, W. M. B., 1973—Dolomitization and the Genesis of the Woodcutters Lead-Zinc Prospect, Northern Territory, Australia. *Mineralium Deposita*, **8**, 35-56.

ROWNTREE, J. C., & MOSHER, D. V., 1976—Jabiluka uranium deposits; *in* ECONOMIC GEOLOGY OF AUSTRALIA AND PAPUA NEW GUINEA, Volume 1—Metals, 321-326, *Australasian Institute of Mining and Metallurgy, Melbourne.*

RYAN, G. R., EUPENE, G. S., & FRAZER, W. J., 1967—Alligator Rivers type uranium deposits. *Australian and New Zealand Association for the Advancement of Science, 47th Congress, Hobart*, Section **3** (abstract).

SMART, P. G., WILKES, P. G., NEEDHAM, R. S., & WATCHMAN, A. L., 1976—Geology and Geophysics of the Alligator Rivers Region; *in* ECONOMIC GEOLOGY OF AUSTRALIA AND PAPUA NEW GUINEA, Volume 1—Metals, 285-301 *Australasian Institute of Mining and Metallurgy, Melbourne.*

STUART-SMITH, P. G., in preparation—Preliminary interpretation of geochemical analyses of the Cahill Formation and other Lower Proterozoic rock units, Alligator Rivers Uranium Field, Northern Territory. *Bureau of Mineral Resources, Australia—Record.*

STUART-SMITH, P. G., & HONE, I. G., 1976—Shallow stratigraphic drilling in the Cahill and Jim Jim 1:100 000 Sheet areas, Alligator Rivers region, N.T. *Bureau of Mineral Resources, Australia—Record* **1975/79** (unpublished).

WALPOLE, B. P., 1962—Mount Evelyn, N.T. 1:250 000 Geological Series. *Bureau of Mineral Resources, Australia—Explanatory Notes* **SD/53-5.**

WILKES, P. G., 1975—Results of radiometric surveys in the Alligator River and Cobourg Peninsula area of the Northern Territory. *Proceedings of the Australian Institute of Mining and Metallurgy Conference, South Australia*, June 1975, 495-512.

WINKLER, H. G. F., 1967—PETROGENESIS OF METAMORPHIC ROCKS. Springer-Verlag, Berlin.

The freshwater lens on Home Island in the Cocos (Keeling) Islands

G. Jacobson

Groundwater resources have been investigated on Home Island, in the Cocos (Keeling) Islands, Indian Ocean, to assess the prospects of developing a reticulated water supply and sewerage system for the settlement there. Home Island is part of the South Keeling atoll and contains a lens of fresh groundwater overlying sea water. Measurements of water-levels in existing wells, and levelling with respect to mean tide-level, indicate that theoretically the freshwater lens is up to 19 m thick, and averages about 15 m over an area of about 30 hectares. Allowing for tidal fluctuations and for periods of drought, the sustainable yield of the aquifer would be about 200 000 litres per day. Recommendations have been made for the development of the aquifer by pumping from infiltration galleries; pumping should reduce the lens thickness by no more than half if saltwater contamination is to be avoided.

The Cocos (Keeling) Islands Territory is in the Indian Ocean, 2800 km northwest of Perth. The Territory consists of two coral atolls about 24 km apart. The smaller atoll, North Keeling Island, is uninhabited and difficult of access. The larger atoll, the South Keeling Islands (Figure 1), consists of 26 islands surrounding a central lagoon; two of the islands are inhabited. An Australian settlement on part of the West Island has a population of about 100. Apart from the Australian-owned land on West Island, the remainder of the islands are owned by Mr John Cluniés-Ross, and form a coconut plantation. The only other permanent settlement is the village on Home Island, which has a population of about 500—mainly Malays.

Lenses of fresh groundwater are commonly developed on small oceanic islands owing to the lower density of freshwater derived from precipitation, compared with the underlying salt water. In the South Keeling atoll freshwater lenses are developed on Home Island, Horsburgh Island, West Island, and South Island (Figure 1). On smaller islands such as Direction Island, there is no freshwater. The minimum width of island to sustain a freshwater lens is about 400 m.

The groundwater resources of the Cocos Islands were investigated during December 1975. The main object of the investigation was a hydrogeological assessment of the Home Island freshwater lens to determine the feasibility of using groundwater for a proposed reticulated water supply and sewerage scheme for the village. At present groundwater forms virtually the entire water supply of Home Island; there are only a few supplementary rainwater tanks. Details of 108 wells on Home Island were recorded during the investigation, including depth, elevation of water table, and electrical conductivity of the water. The wells are generally 0.8-1.2 m in diameter, 1.5-2.5 m deep, and are lined with brick or concrete. Abstraction of groundwater is mainly by bucket; only three wells are fitted with electric pumps and storage tanks.

General geology

The Cocos Islands are coral atolls formed on a volcanic seamount rising from a depth of 5000 m (Jongsma, 1976). Bathymetry shows that the seamount is one of a series trending approximately northeast from the Ninety East Ridge to Christmas Island. The volcanic nature of the seamount has been indicated by a magnetic survey of the South Keeling atoll in 1946 (Chamberlain, 1960), which revealed a magnetic anomaly of about 250 gammas in vertical intensity; the extent of the anomaly coincides approximately with the atoll. Additional evidence is afforded by volcanic pebbles dredged from the sea-floor west of the Cocos Islands (Bezrukov, 1973).

The islands were visited by Charles Darwin during the voyage of H.M.S. 'Beagle' in 1836. Darwin (1842) described the formation of the islands as follows:

'The islets on the reef are first formed between two hundred and three hundred yards from its outer edge, through the accumulation of a pile of fragments, thrown together by some unusually strong gale. . . . Those on the south-east and windward side of the atoll, increase solely by the addition of fragments on their outer side. . . . The highest part of the islets (excepting hillocks of blown sand, some of which are thirty feet high) is close to the outer beach . . . and averages from six to ten feet above ordinary high-water mark. From the outer beach the surface slopes gently to the shores of the lagoon. . . . The fragments beneath the surface are cemented into a solid mass, which is exposed as a ledge projecting some yards in front of the outer shore and from two to four feet high.'

A cross-section showing some of the atoll features is given in Figure 2. The present investigation has confirmed that the reef flat—Darwin's projecting ledge—does in fact extend beneath Home Island as a hardpan of cemented coral fragments, 0.4-1.0 m thick. The hardpan is both overlain and underlain by coarse coral sand (Figure 3).

Darwin based his subsidence theory of atoll formation largely on observations made in the Cocos Islands. He considered that the upgrowth of reefs continues as the seamounts that support them subside.

'The facts stand thus;—there are many large tracts of ocean, without any high land, interspersed with reefs and islets, formed by the growth of those kinds of corals which cannot live at great depths; and the existence of these reefs and low islets, in such numbers and at such distant points, is quite inexplicable, excepting on the theory, that the bases on which the reefs first became attached, slowly and successively sank beneath the level of the sea, whilst the corals continued to grow upwards.'

Darwin's theory has been borne out by much of the deep drilling and geophysical probing done on various atolls. The thickness of coral underlying the Cocos Islands is not known; it may be of the order of 1000 m.

Hydrology

At the meteorological station on West Island the mean annual rainfall for the period 1901-1973 was 2009 mm, with a recorded minimum of 1100 mm in 1918, and a maximum of 3288 mm in 1942. The months of February to July are generally the wettest, and September to November the driest.

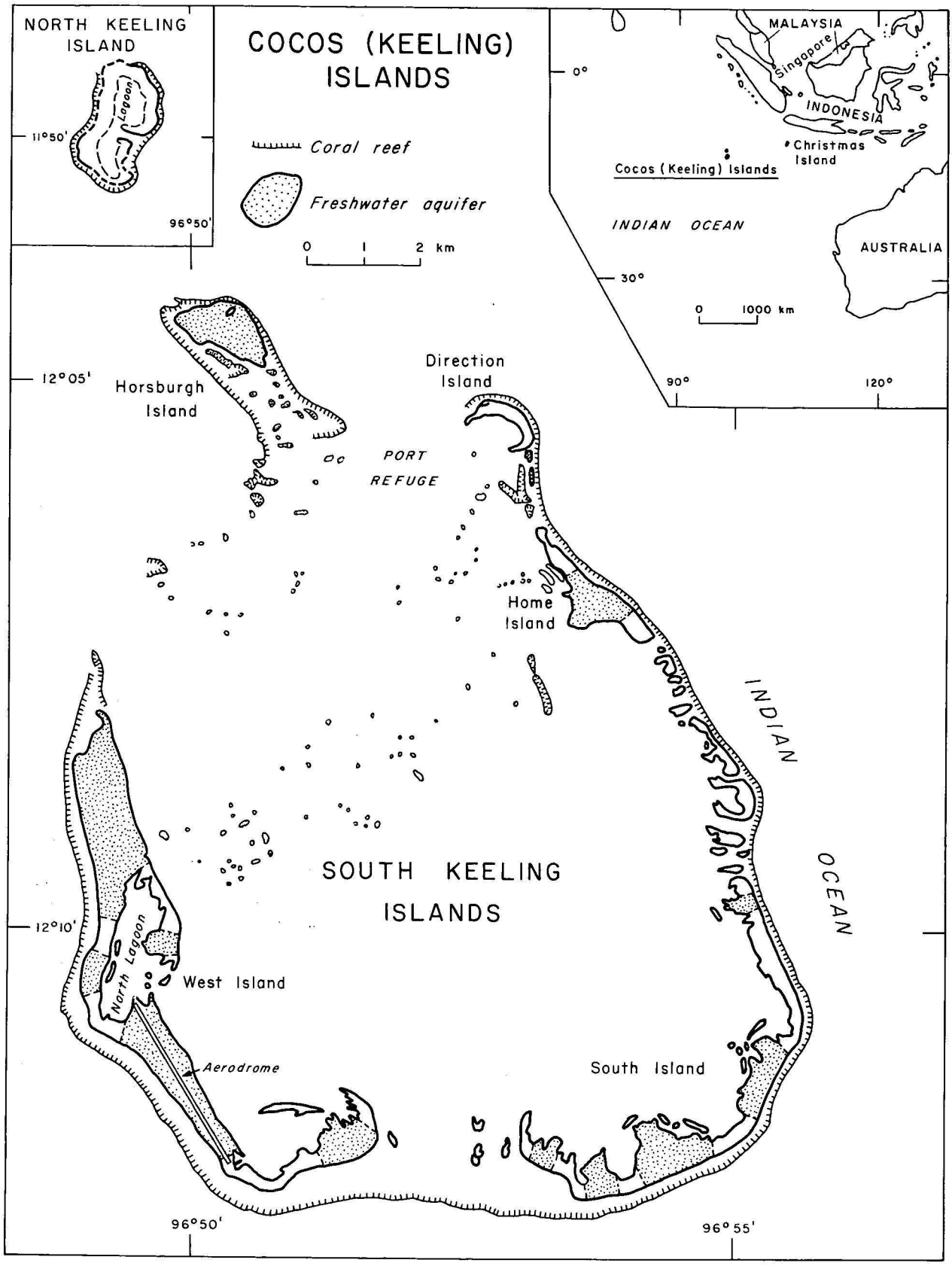

Figure 1. Groundwater aquifers in the Cocos (Keeling) Islands.

Of the 66 years for which complete records are available, 13 years had recorded rainfall below 1500 mm, that is less than 75 percent of the mean. Drought periods with less than 100 mm of rain in 3 months have been recorded in 18 separate years.

No surface runoff was observed during the present investigation although 114 mm of rain was recorded in one day.

With negligible runoff, the water balance of Home Island is:

rainfall = recharge to groundwater aquifer + evapotranspiration losses.

No data are available for evapotranspiration losses, which are a significant factor in the analysis of sustainable yield of the aquifer. An estimated loss of 1500 mm annually has been used in the present investigation, based on experimental work done on Christmas Island by the Land Resources Division of the British Ministry of Overseas Development. The Christmas Island study was concerned with coconut plantations having a tree density of 250 to the hectare (J. D. Mather, personal communication).

With a mean annual rainfall of 2000 mm and assuming evapotranspiration of 1500 mm, the effective recharge to the groundwater aquifer would be 500 mm in a year of average rainfall.

Theory of the freshwater lens

The theory of the freshwater lens on an oceanic island is illustrated in Figures 4, 5 and 6. The freshwater lens floats on salt water; the approximate depth of the freshwater/salt-water interface assuming static conditions is given by the Ghyben-Herzberg relation (Herzberg, 1901). In Figure 4, from Archimedes Principle,

$$\frac{\rho_f}{\rho_s - \rho_f} h_f$$

where h_s is the depth of the interface below mean sea level, h_f is the height of the water table above sea level, ρ_s is the salt-water density, and ρ_f is the freshwater density. Assuming the density of the salt-water to be 1.025 g/cm^3, the Ghyben-Herzberg relation indicates that the depth of the interface below mean sea level is about 40 times the height of the water-table above mean sea level.

The freshwater lens is, however, a dynamic system. Groundwater in the lens flows into the surrounding and underlying sea water, with a transition zone of diffusion (Figure 5) at the freshwater/salt-water interface (Cooper, 1959; Kohout, 1960). The thickness of the transition zone is affected by the continuous reciprocative movement of the lens caused by ocean tides. In the long term the effective recharge to the lens is balanced by the outflow into the sea

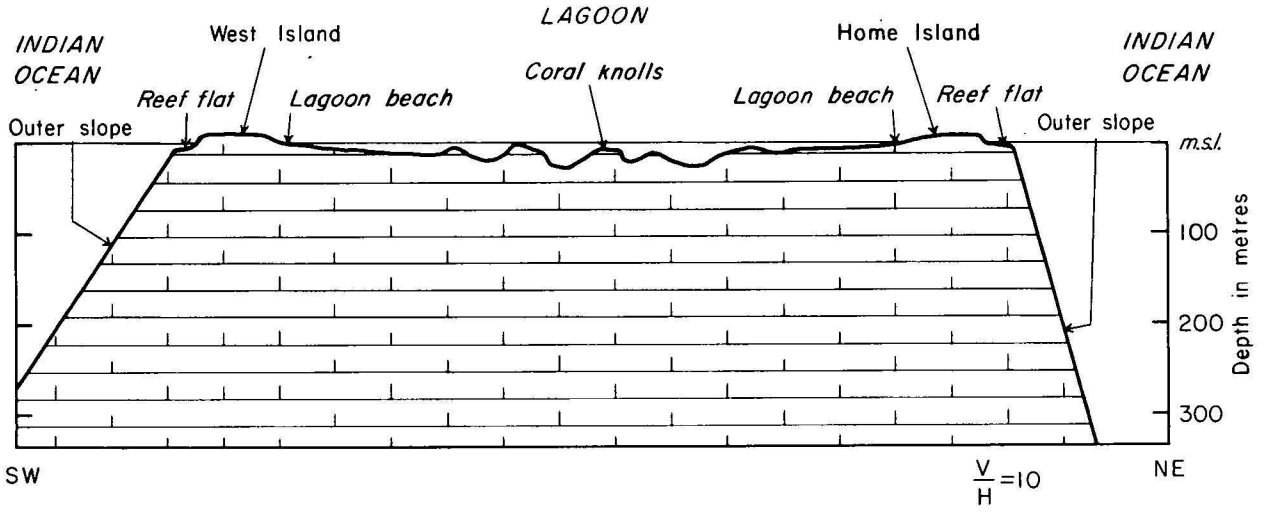

Figure 2. **Cross-section through the South Keeling Islands showing atoll features.**

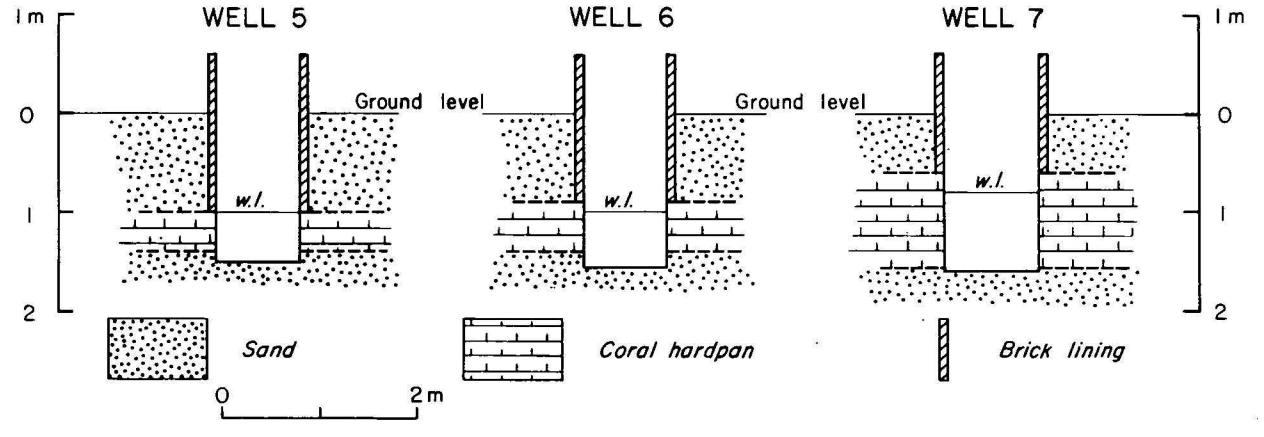

Figure 3. **Home Island: typical well sections.**

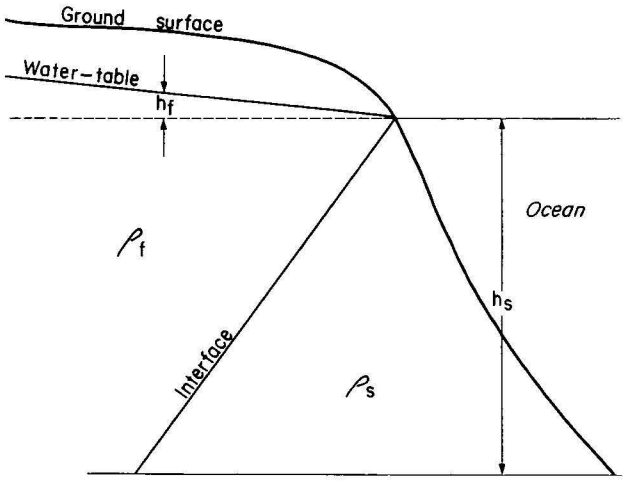

Figure 4. Diagram to illustrate Ghyben-Herzberg relation (after Walton, 1970).

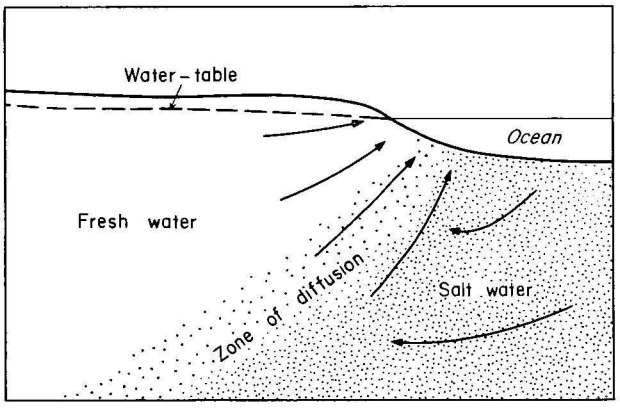

Figure 5. Circulation of saltwater from sea to zone of diffusion and back to sea (after Cooper, 1959).

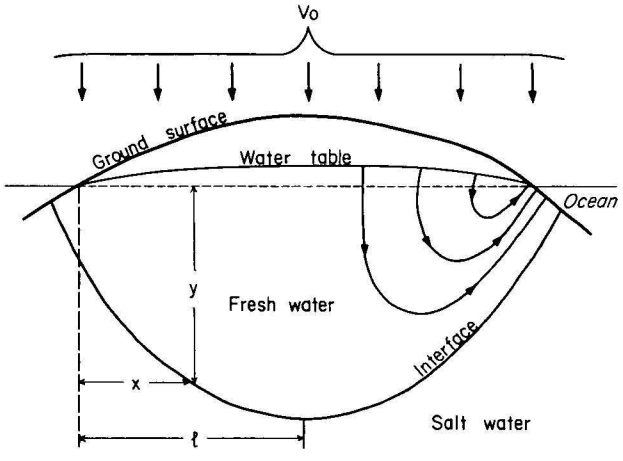

Figure 6. Flow pattern beneath an oceanic island (after Henry, 1964).

(Mather, 1975). Groundwater abstraction will result in a reduction in this outflow, leading to the establishment of a new equilibrium position of the freshwater/salt-water interface. Groundwater abstraction can thus be considered equivalent to a reduction in effective recharge.

Henry (1964) considered the freshwater lens as a dynamic system incorporating parameters such as the width of the island, the hydraulic conductivity, and the rate of recharge. Figure 6 is a diagrammatic sketch of the flow pattern beneath an oceanic island. The approximate relation between the coordinates of the interface is (Henry, op cit.):

$$\frac{y}{l} = \sqrt{\frac{V_o}{k_1}\left[\frac{2x}{l} - \left(\frac{x}{l}\right)^2\right]}$$

where y is the depth below sea level to the interface, x is the horizontal distance from the shore, l is half the width of the island, V_o is the rate of uniform recharge per unit area, and

$$k_1 = \bar{k}\,\frac{\rho_s - \rho_f}{\rho_f}$$

where $\bar{k}$ is the hydraulic conductivity.

For a particular lens, Mather (1975) has pointed out that most of these parameters are constant, and therefore the depth below sea level to the freshwater/salt-water interface is proportional to the square-root of the rate of uniform recharge per unit area, i.e.

$$y \propto \sqrt{V_o}.$$

Assuming that abstracting groundwater from the lens is equivalent to reducing the vertical recharge, then changes in the equilibrium position of the interface can be predicted.

The freshwater lens on Home Island

Water levels in the Home Island wells were measured with respect to mean tide level on 11-12 December 1975. The datum mean tide-level was determined by gauging for 24 hours at an observation point on the Home Island wharf, and is an approximation to mean sea level at the time of the survey. Determinations of monthly mean sea level at the CSIRO tide gauge on West Island have shown a variation of up to 0.52 m over three years (Figure 7).

Lens thickness

Water-table elevations are shown in Figure 8. Because of the tidal fluctuation of water levels meaningful water-table contours cannot be constructed. At the three wells where observations over a full tidal range were made, the thickness of the freshwater lens is estimated by the Ghyben-Herzberg relation as follows:

Well No.	*Distance from lagoon (m)*	*Water-table elevations (cm above mean tidal level)*	*Minimum lens thickness (m)*	*Average lens thickness (m)*
2	40	17-34	7	10
1	90	23-39	9	12
48	190	36-61	14	19

The average thickness of the freshwater lens ranges from 10 to 19 m, with an average of about 15 m in the Home Island settlement. In two of the wells the water-table was below mean tide level; the significance of this is not clear.

Tidal fluctuations in groundwater levels were monitored in three wells (Figure 9). The fluctuations in groundwater levels had an amplitude of about 25 percent of the tidal amplitude in the lagoon, and a lag of 1-2 hours. Fluc-

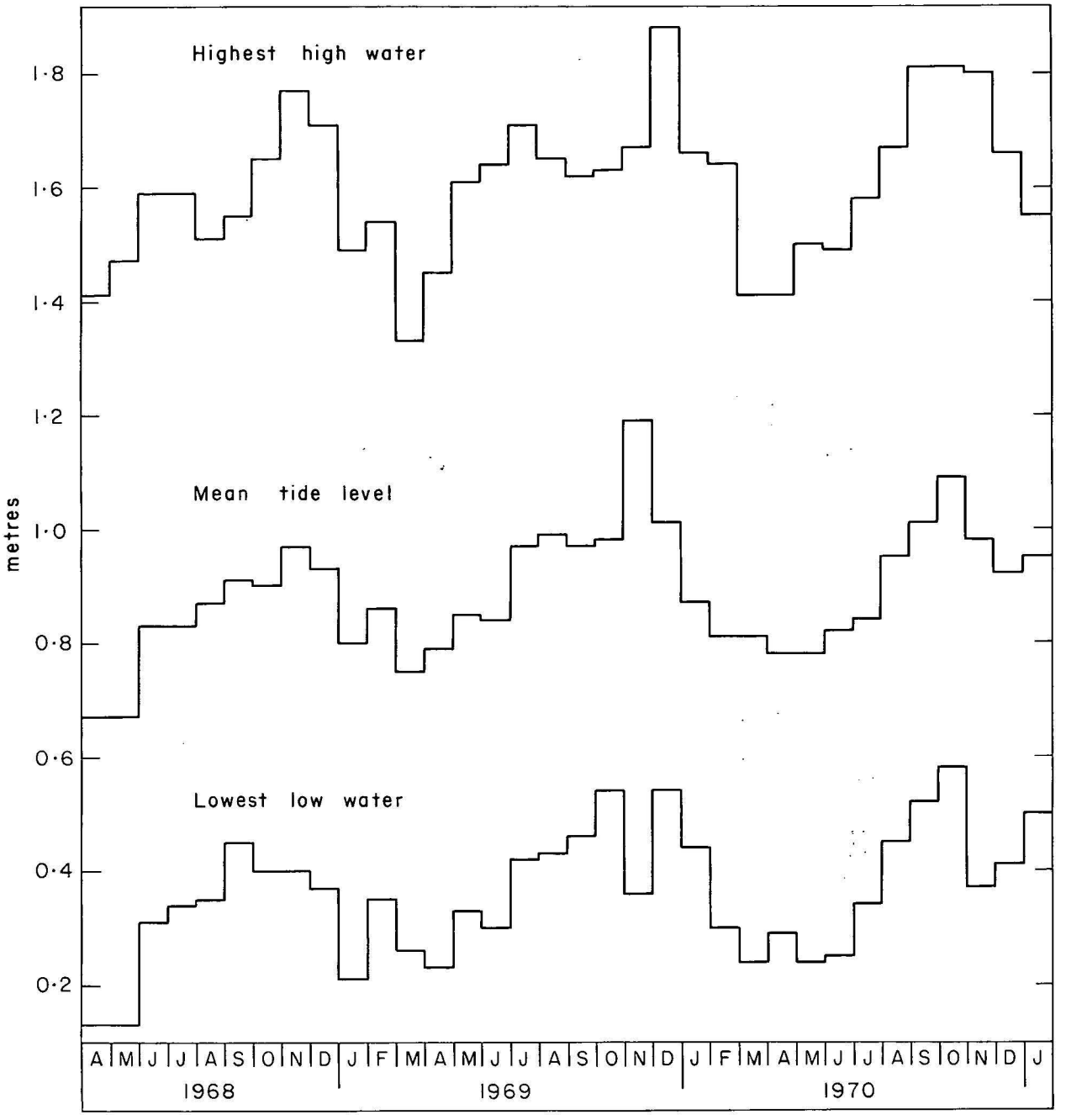

Figure 7. Monthly tide levels in the South Keeling lagoon, West Island.

tuations in groundwater level are slightly greater away from the lagoon side of Home Island, and have a reduced lag. The marked tidal fluctuations observed in the wells indicate that there is a wide zone of diffusion at the freshwater/salt-water interface.

The tidal fluctuations indicate high hydraulic conductivity and suggest that the thickness of the lens may well be less than that calculated by the Ghyben-Herzberg relation. The thickness will need to be checked by geophysical surveys or drilling before long-term development of the aquifer is undertaken.

Water quality

Contours of electrical conductivity (Figure 8) show that most of the Home Island settlement has good quality groundwater (600-1000 microsiemens/cm). There is an area of more saline, but still potable, groundwater (2000 microsiemens/cm) in the northeast of the settlement, and two other areas of 1200-1400 microsiemens/cm.

A salinity gradient was observed in some of the wells, with fresher water on top. The effect of tidal fluctuation on salinity was not investigated.

Subsequent chemical analyses of groundwater samples (Table 1) show that electrical conductivity as measured in the laboratory in microsiemens/cm at 25°C is related to the total dissolved solids content in milligrams per litre by a factor of about 0.54. Electrical conductivity measured in the laboratory was generally about 20 percent higher than the field values.

Figure 10 is a Piper trilinear diagram showing the ionic composition of several samples of Home Island groundwater. It is generally a bicarbonate water with ap-

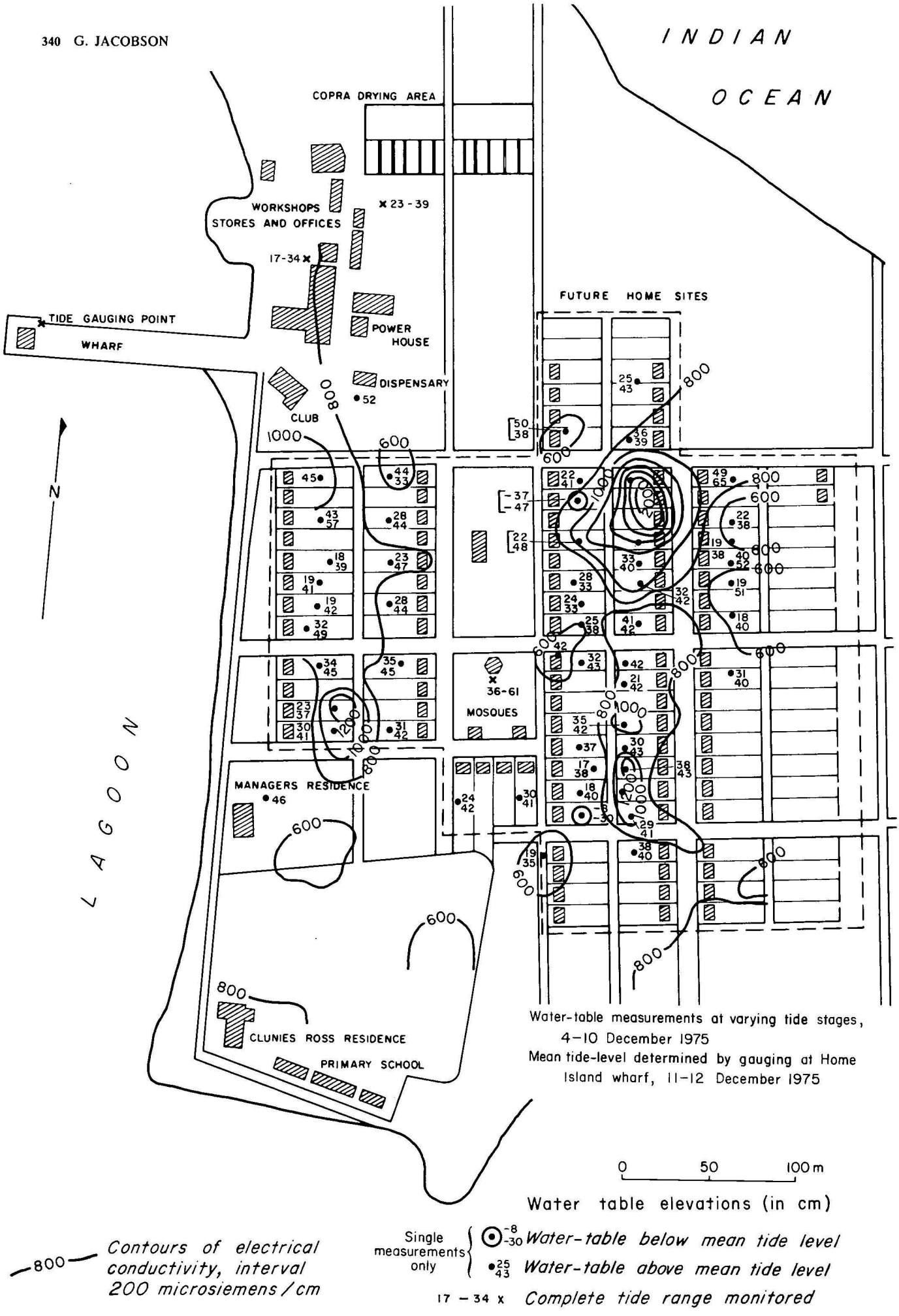

Figure 8. **Home Island: water-table elevations and groundwater quality.**

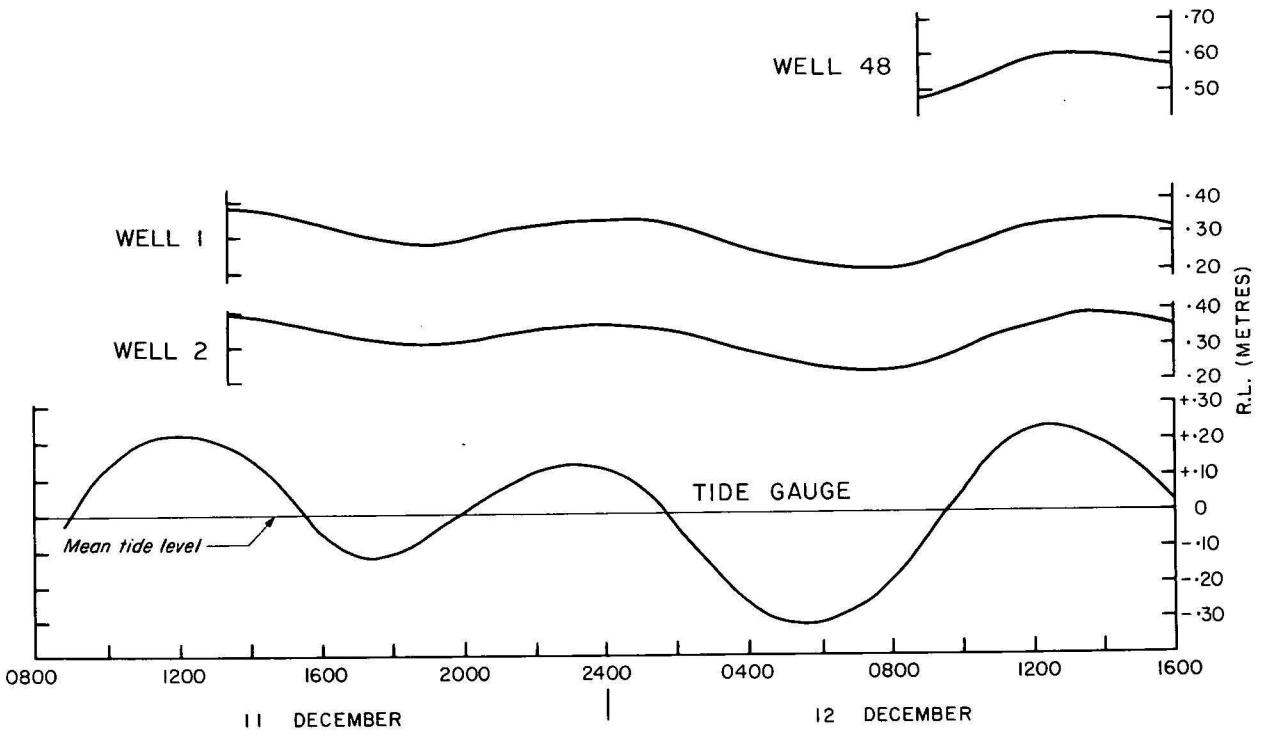

Figure 9. Home Island: Tidal fluctuations in groundwater levels, 11-12 December, 1975.

preciable chloride in the more saline samples. Sodium and calcium are the dominant cations. The trend in ionic composition towards that of sea water indicates slight salt-water contamination in some of the wells, which may be close to the transition zone of diffusion. The water is hard for domestic use with total hardness ranging from 264 to 488 mg/l.

The relatively high nitrate content of some groundwater samples probably indicates pollution from animal refuse. Four out of nine samples analysed had nitrate contents above 45 mg/l which, by most public health standards, is the maximum safe limit for avoiding possible toxic effects in infants.

Sustainable yield

The sustainable yield of the Home Island lens without contamination by salt water has been estimated using Mather's (1975) analysis, which is based on the proportionality relationship between depth to the interface and the square-root of the rate of uniform recharge per unit area.

Table 2 is based on this relationship, and shows calculated changes in the equilibrium position of the interface with a reduction in effective recharge because of pumping. It assumes that the freshwater lens on Home Island can be considered as an equilibrium system resulting from an effective recharge of 500 mm annually.

Well no.	*Ca*	*Mg*	*Na*	*K*	*HCO_3*	*SO_4*	*Cl*	*NO_3*	E. C. *(micro-siemens /cm)*	*T.D.S.*	*Total Hardness as $CaCo_3$*	*pH*
1*	103	12	42	16	397	37	37	0	813	442	307	7.7
6*	90	24	65	27	346	24	109	39	981	547	323	7.7
11*	86	18	83	71	305	49	138	62	1190	657	289	7.9
26*	118	47	230	211	631	101	398	65	2549	1481	488	7.9
29*	99	13	21	5	338	14	30	20	691	368	301	7.7
42*	127	34	112	144	495	75	227	103	2007	1065	457	7.7
52*	99	15	55	54	372	33	106	25	1012	569	309	7.8
3‡	86	12	—	—	—	—	—	1	—	310	264	8.5 Fluoride 0.3 mg/l, Boron 0.1 mg/l
66‡	61	13	—	—	—	—	—	56	—	350	266	7.9 Fluoride 0.3 mg/l, Boron less than 0.1 mg/l

Table 1. Chemical analyses of groundwater samples (mg/l)

* Analysis by AMDEL, Adelaide. ‡ Analysis by Government Chemical Laboratories, Perth. E.C. Electrical conductivity, measured in the laboratory

Original depth to interface assuming annual recharge of 500 mm (m below M.S.L.)	*Estimated depth to interface (m) if pumping reduces recharge to*			*Estimated depth to interface (m) after a 3 year drought if annual recharge is reduced to*			*Estimated depth to interface (m) after a 5 year drought if annual recharge is reduced to*		
	400 mm	*300 mm*	*200 mm*	*400 mm*	*300 mm*	*200 mm*	*400 mm*	*300 mm*	*200 mm*
20	18	15	13	15	12	10	14.5	11.5	9.5
15	14	12	10	11	9	7	10.5	8.5	6.5
10	9	8	6	6	5	3	5.5	4.5	2.5
5	4.5	4	3	1.5	1	0	1	0.5	*

Table 2. Effect on freshwater/salt water interface of pumping from the lens

* negative value, indicating that there would be no freshwater layer.

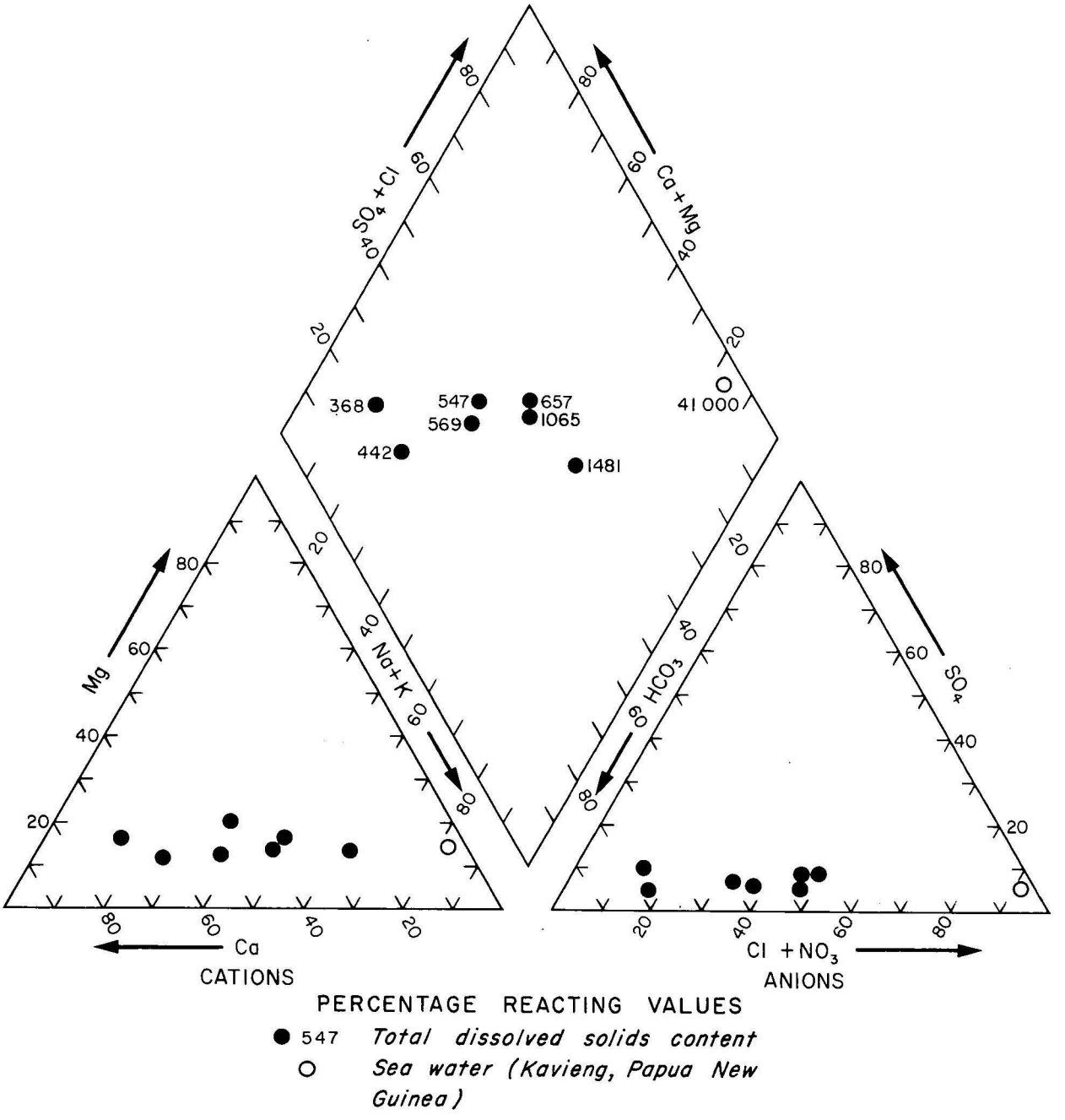

Figure 10. Home Island: Ionic composition of groundwater.

Rainfall statistics show that the worst series of drought years recorded on Home Island was 1961-5. Three successive years had rainfall averaging 30 percent below the mean, and, over the five years, rainfall averaged 21 percent below the mean. If the three-year drought reduced the effective annual recharge by 30 percent from 500 to

350 mm, then over the three-year period there would be a total deficit of 450 mm. Assuming a specific yield of 15 percent for the aquifer, then 450 mm of groundwater would be stored in 3 m of aquifer thickness. The effects of the three-year drought on the position of the interface are shown in Table 2.

Similarly, the five-year drought would reduce the effective annual recharge by 21 percent from 500 to 395 mm, with an accumulated deficit of 525 mm over five years. Assuming a specific yield of 15 percent then 525 mm of groundwater would be stored in 3.5 m of aquifer thickness. The effects of the five-year drought on the position of the interface are shown in Table 2.

A substantial rise and fall of the freshwater lens on Home Island is attributable to the tides, and is the major control on the width of the transition zone of diffusion. Pumping is expected to reduce the natural hydraulic flow in the aquifer, and consequently increase the width of the transition zone. In order to maintain conditions in the transition zone as steady as possible, pumping should be carried out at a constant rate and continuously so that a new set of equilibrium conditions are set up. The rate of pumping should be such that the thickness of the freshwater lens is maintained at more than half the original thickness.

Recommended abstraction rates for lenses of varying thickness, allowing for a five-year drought and maintaining half of the original lens thickness can be derived from Table 2. For an original lens thickness of 15 m, the effective annual recharge necessary would be 250 mm. This would leave 250 mm of rainfall available for extraction, which is equivalent to 6850 litres per day per hectare.

Over an area of 30 hectares on Home Island, the sustainable yield would be about 200 000 litres per day.

Abstraction of groundwater

The present system of abstraction by buckets from wells ensures careful water usage and minimal risk of saltwater intrusion. The settlement water supply could be improved at little cost by increasing rainwater storage capacity.

If development of the aquifer is undertaken for a reticulated water supply and sewerage system, then abstraction points are best sited where the lens is thickest. Where the lens is less than 10 m thick it will not be capable of long-term development. The distribution of abstraction points and the optimum pumping rates have to be determined by pumping tests.

Drawdown should be minimized; infiltration galleries are preferable to dugwells for this reason. The aquifer could possibly be developed by a field of four galleries each drawing from 7.5 hectares with a steady pumping rate of 2000 litres per hour. Inverts of the galleries should be above the calculated base of the lens when it attains its new equilibrium position.

Large-scale development of the aquifer will require careful control and monitoring to avoid salt-water intrusion, especially in view of the substantial tidal fluctuations in the lens, and the variations in monthly mean tide level. Maintenance of the water-supply system will be necessary and the people will have to be educated not to waste water.

Abstraction by pumping from galleries will lower the water-table by as much as 25 cm, and depending on the state of the tide many of the existing dugwells may go dry. Measures might need to be taken to prevent the disposal of refuse in the existing dugwells, and avoid further pollution of the aquifer. For the same reason, a sewage outfall if constructed should be taken to the ocean.

Acknowledgements

The investigation was carried out for the Department of Administrative Services in collaboration with engineers of the Department of Construction who investigated the feasibility of a water supply and sewerage scheme. I am grateful for assistance from Mr K. Campbell with the field work. The Army's 5th Field Survey Squadron, Karrakatta, Western Australia gave me survey information. Chemical analyses of water samples were done by AMDEL in Adelaide; the CSIRO Division of Fisheries and Oceanography, Cronulla, New South Wales, supplied tide-gauge data; and the Bureau of Meteorology supplied rainfall statistics. The figures were drawn by Sue Davidson and Rex Bates, Geological Drawing Office, BMR.

References

BEZRUKOV, P. L., 1973—Principal scientific results of the 54th cruise of the R. V. Vitian in the Indian and Pacific Oceans (Feb-May 1973). *Oceanology*, **13**, 761-6.

CHAMBERLAIN, N. G., 1960—Cocos Islands magnetic survey, 1946. *Bureau of Mineral Resources, Australia—Record* **1960/124** (unpublished).

COOPER, H. H., 1959—A hypothesis concerning the dynamic balance of freshwater and salt water in a coastal aquifer. *Journal of Geophysical Research* **64**, 461-7.

DARWIN, C., 1842—ON THE STRUCTURE AND DISTRIBUTION OF CORAL REEFS. *London, Smith, Elder.*

HENRY, H. R., 1964—Interfaces between salt water and freshwater in coastal aquifers; *in* Sea water in coastal aquifers. *United States Geological Survey Water Supply Paper* **1613-C**, 35-70.

HERZBERG, B., 1901—Die Wasserversorgung einiger Nordseebäder. (The water supply on parts of the North Sea coast). Journal für Gasbeleuchtung und Beleuchtungsarten, sowie für Wasserversorgung, Munich, **44**, 815-9, 842-4.

JONGSMA, D., 1976—Review of geology and geophysics of the Cocos Islands and the Cocos Rise. *Bureau of Mineral Resources, Australia—Record* **1976/38** (unpublished).

KOHOUT, F. A., 1960—Cyclic flow of salt water in the Biscayne aquifer of southeastern Florida. *Journal of Geophysical Research*, **65**, 2133-41.

MATHER, J. C., 1975—Development of the groundwater resources of small limestone islands. *Quarterly Journal of Engineering Geology*, **8**, 141-50.

WALTON, W. C., 1970—GROUNDWATER RESOURCE EVALUATION. *New York, McGraw-Hill.*

A sandstone breccia, formed by quasi-liquid deformation, from the Amadeus Basin, Northern Territory

J. M. Kennard

A prominent sandstone breccia crops out in the Pacoota Sandstone, Western MacDonnell Ranges, Northern Territory. The breccia occurs as discontinuous lenses which grade laterally, through incipient breccia and disrupted sandstone beds, into the enclosing sandstone sequence. This sequence consists of interbedded well-sorted silicia-cemented and poorly sorted friable quartzose sandstones; these two sandstone types also constitute, respectively, the clasts and matrix of the breccia. The clasts are rectangular (joint-bounded) and broken rectangular in shape, ranging up to 1 m in length. The matrix is predominantly massive, but convolute bedding is locally present. Similar sandstone breccias are known from three other localities in the region, all at the same stratigraphic level within the Pacoota Sandstone.

Petrographic data indicate that the clast sandstone was cemented and strained prior to brecciation, whilst the matrix sandstone retained a largely cohesionless state and failed in a quasi-liquid manner. It is concluded that the brecciation occurred *in situ* at a considerable depth in a sedimentary pile, and resulted from the rotation and fragmentation of joint blocks of silica-cemented sandstone in the interbedded mobile matrix sandstone. Pore-water pressures are thought to have played an important role in the mobilization of the matrix sandstone.

A prominent sandstone breccia crops out within the basal 10 m of the Pacoota Sandstone at Finke Gorge, Western MacDonnell Ranges, Northern Territory, and is particularly well exposed in the cliff face immediately behind the Glen Helen Tourist Camp (Figure 1). On aerial photographs the breccia is seen to continue along strike for up to 700 m. The breccia was initially described by Mawson & Madigan (1930) and Madigan (1932), but has since received little attention apart from a brief mention by Prichard & Quinlan (1962) and Ranford *et al.*, (1965). Collectively, these brief accounts have proposed three separate origins for the breccia; a sedimentary conglomerate, a tectonic crush breccia and a sedimentary slump breccia. This paper presents the results of a detailed study of this unusual sandstone breccia, and examines the problem of its origin.

Geological setting

The Pacoota Sandstone is an extensive Cambro-Ordovician marine sequence of well-sorted quartzose sandstone with thinly interbedded siltstone (Wells *et al.*, 1970). This sequence conformably overlies the Cambrian Goyder Formation, a marine sequence of poorly sorted quartzose sandstone, siltstone, dolomite and limestone (Wells *et al.*, op cit.). The contact between these two units is gradational, so that the sandstone breccia which crops out at the base of the Pacoota Sandstone actually occurs in the lithological transition zone where well-sorted quartzose sandstone is interbedded with poorly sorted quartzose sandstone. In the Finke Gorge area, the Pacoota Sandstone forms a prominent strike ridge and dips vertically or very steeply to the south. This ridge forms part of the extensive MacDonnell Ranges which represent the upfolded northern margin of the Amadeus Basin.

Similar breccias, also from the base of the Pacoota Sandstone, were noted by Ranford *et al.*, (1965, p. 24) at two localities to the south (Figure 1); one near Illamurta Yard, and the other on the west bank of the Finke River where it cuts the James Ranges 'A' Anticline. A fourth minor occurrence of similar breccia was observed by the author at Pattalindama Gap, 4 km south of the Areyonga Native Settlement.

Description of outcrop

The breccia occurs as discontinuous lenses within an interbedded sequence of cross-bedded, white silicified sandstone and minor brown ferruginous sandstone. The lenses are about 20 cm to 12 m thick, and up to 100 m long. The

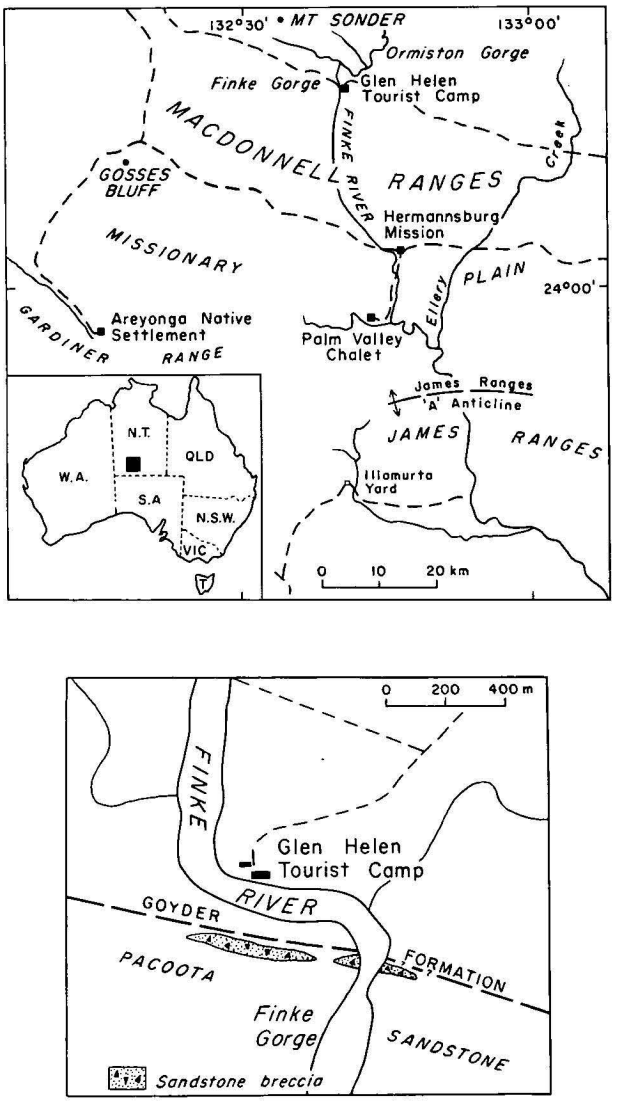

Figure 1. Locality map with enlarged segment showing the distribution of the sandstone breccia at Finke Gorge.

Figure 2. Disrupted bed of white sandstone within the interbedded white and brown sandstone sequence, Finke Gorge. The bed has been disrupted along joint and bedding planes, and this has caused a slight deformation (convolution) of the lamination in the overlying brown sandstone.

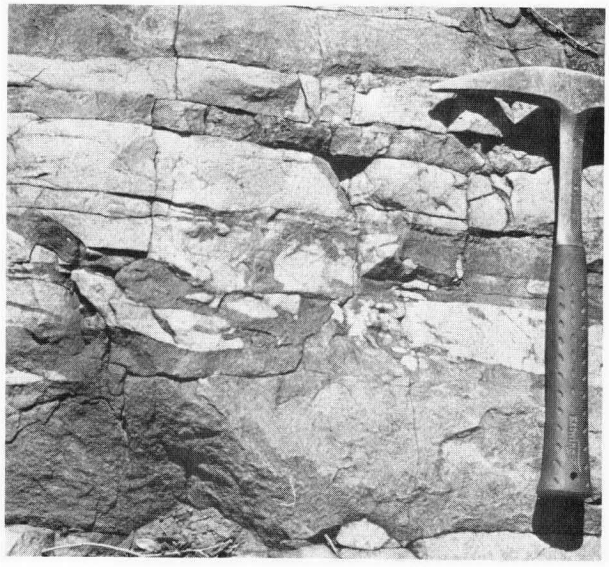

Figure 3. Disrupted white sandstone beds and incipient breccia, Finke Gorge.

Figure 5. Sandstone breccia, Finke Gorge.

Figure 4. Small breccia lens enclosed within interbedded white and brown sandstones, Finke Gorge. The breccia to the left of the hammer abuts a joint bounded, white sandstone bed, and contains clasts (rotated blocks and slabs) thought to have been derived from that bed.

Figure 6. Convolute bedding developed in brown (matrix) sandstone which grades laterally into breccia lenses, Finke Gorge.

upper and lower contacts of the breccias are sharp and planar, predominantly conformable with the enclosing sandstone sequence. Locally, however, the breccias partially abut joint faces of white sandstone. The lateral contacts of the breccias are generally irregular, and there is a complete gradation from interbedded white and brown sandstone, to disrupted beds and isolated slabs of white sandstone, to incipient breccias and small breccia lenses (Figures 2, 3, 4). These in turn amalgamate into the larger breccia lenses.

The breccia consists of variable-sized angular clasts of cross-bedded, silicifed, white sandstone set in a matrix of slightly friable brown sandstone (Figure 5). The sandstone composing the clasts and matrix are lithologically indistinguishable from the enclosing white and brown sandstones respectively. The clasts range from less than 1 cm to 1 m in length, and are typically rectangular or broken rectangular in shape. A well-developed stratification parallels and undoubtedly controls their rectangular shape. In places the clasts are closely packed and form a framework, in others they 'float' in the brown matrix sandstone. The matrix sandstone is largely structureless, but irregular convolute bedding is locally present where clasts are sparse (Figure 6).

Petrography

Breccia clasts

The clasts consist of well to moderately well sorted, fine to medium-grained quartz sandstone (Figures 7, 8). The framework consists of rounded to subrounded quartz together with minor amounts (<1%) of well-rounded tourmaline, zircon, ?epidote, and rare feldspar. The quartz grains are predominantly monocrystalline undulatory quartz, and grain contacts are frequently crushed and sutured. Interstices are filled, or rarely only partially filled, with a quartz cement which occurs as overgrowths in optical continuity with the grains. Fine detrital matrix material is absent.

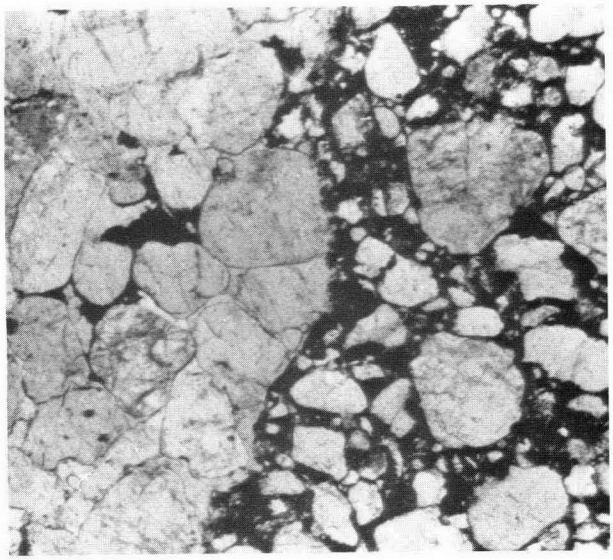

Figure 7. Contrasting textural maturity of a white sandstone clast (left-hand side) and the brown matrix sandstone. The black interstitial material of the matrix sandstone consists of iron stained silt and clay, whereas the interstices of the white sandstone clast are 'clean' and filled by a quartz cement. Note the broken quartz grains at the margin of the clast. (BMR Slide 75500122C X 40).

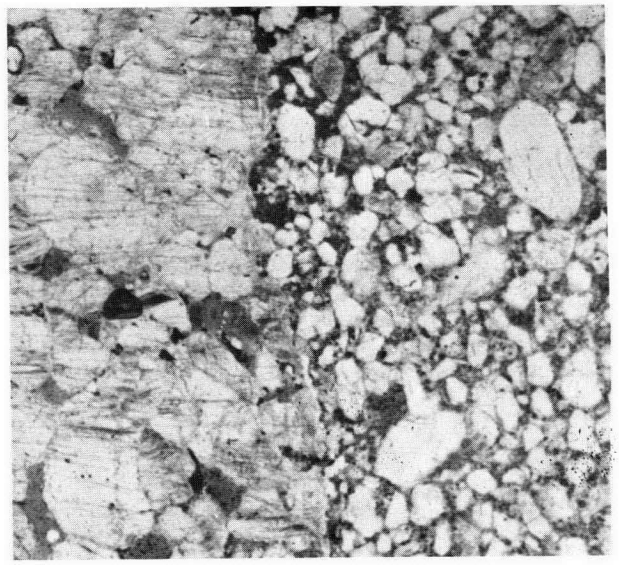

Figure 8. Strain lamellae within a sandstone clast (left-hand side). Lamellae extend throughout both the grains and the quartz cement of the clast, but stop sharply at the clast/matrix contact. (BMR Slide 75500122E, X 30).

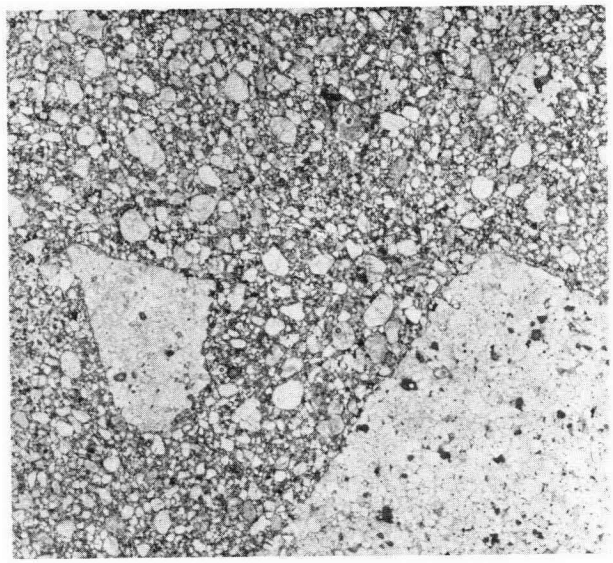

Figure 9. Sandstone clasts bounded by linear margins (forming rectangular shaped clast) and irregular margins (right hand margin of the clast on the left). Note the marked contrast in grain sorting between the matrix and clast sandstones. (BMR Slide 75500122D X 6.5).

Many clasts exhibit parallel trains of inclusions (strain lamellae) that extend throughout both grains and overgrowths. In all determinable cases the lamellae parallel bedding traces within each clast. As the orientation of the clasts varies within the breccia, so does the orientation of lamellae. This implies that the white sandstone was cemented and strained prior to its fragmentation and incorporation in the breccia.

The clast margins are linear or irregular (Figure 9). Linear margins cut across both grains and grain overgrowths, and the quartz at the clast margin in finely fractured parallel to that margin. The linear margins commonly define rectangular-shaped clasts and are thought to represent original joint surfaces. Irregular margins, however, are defined and directly controlled by the shape of the constituent quartz grains of the clasts. These margins

represent fractures which have selectively followed paths of relatively weak interstitial quartz cement, and grains have been plucked intact from the margin of the clast.

Breccia matrix

The matrix is composed of poor to very poorly sorted quartzose sandstone (Figures 7, 8). The average grainsize of the larger detrital quartz fraction is 0.1-0.2 mm, but there is a complete range from a maximum of 0.75 mm down to silt-size material. Quartz grains are mainly sub-angular, but many rounded, fractured rounded grains (some with fractured overgrowths) and angular grains are present. Minor framework constituents include rounded tourmaline, zircon and ?epidote. Quartz silt and detrital argillaceous material make up 2-15 percent of the sandstone, and a prominent but weak iron-oxide cement is present. Strain lamellae are rarely developed in individual grains, and are randomly oriented from grain to grain. The plasma of the sandstone, fines plus cement, notably lacks an orientation fabric.

Some of the silt-size and larger quartz grains of the matrix sandstone have most likely resulted from the diminution and plucking-off of grains from the white sandstone clasts during brecciation (e.g. the broken rounded grains and the grains with broken quartz overgrowths). The presence of detrital argillaceous material, however, suggests that most of the silt is probably of normal detrital origin.

Origin

Mawson and Madigan (1930) initially proposed that the breccia represents a coarse conglomerate, but as indicated by Madigan (1932), the angular and monomictic nature of the clasts and the fact that they are indistinguishable from the host sandstone sequence, suggests an *in situ* brecciation. Madigan favoured a crush tectonic origin for the breccia, a proposal later supported by the senior author in Prichard & Quinlan (1962, p. 29). The junior author, however, believed that the breccia was formed by 'slumping before the beds were lithified'. With the discovery of similar breccias at the same stratigraphic level, but at widely scattered localities (Ranford *et al.*, 1965), the sedimentary control on the formation of the breccia was firmly established. These authors supported the proposal of a slump origin. Although the term slump is now generally applied to 'a landslide characterized by shearing and rotary movement of a generally independent mass of rock or earth along a curved slip surface' (Margaret Gary *et al.*, 1972) the author considers that Prichard & Quinlan (1962), and Ranford *et al.*, (1965), applied the term to the breccia at Finke Gorge in the sense of a ?downslope flow or slide of a mass of sediment shortly after its deposition on an underwater slope. This is the sense defined by Challinor (1962), and referred to here as 'slump-like'.

The present author discounts a tectonic origin for the breccia since, in addition to the established stratigraphic control on the formation of the breccia, the orientation of strain lamellae varies from clast to clast (hence straining preceded rather than caused brecciation), and the matrix of the breccia completely lacks a tectonic (e.g. sheared) fabric. Whilst in many regards the breccia shows an affinity to 'slump-like' deposits and mass-flow (Dott, 1963) or sediment gravity flow (Middleton & Hampton, 1973) deposits, collectively referred to here as 'mass-flow' deposits, the following features peculiar to the breccia require further discussion and explanation:

1. The matrix of the breccia is composed of sandstone. Most 'mass-flow' deposits are characterized by a prevalent pelitic matrix (Dott, 1963; Abbate *et al.*, 1970), but some sandy matrix deposits do occur (Leitch, 1969; Dott, 1963). The brown matrix sandstone has locally retained disturbed sedimentary structures (convolute bedding), but otherwise original sedimentary structures have been completely destroyed. Thus failure of the matrix involved a loss of grain cohesion and occurred by means of a grain-by-grain flow, i.e. quasi-liquid deformation of Elliott (1965).

2. The clasts and matrix of the breccia both consist of quartzose sandstone. The clasts and matrix of 'mass-flow' deposits are characterized by a marked contrast in competence at the time of brecciation, and this is typically expressed by a marked contrast between clast and matrix lithologies, such as sandstone and mudstone respectively. The breccia at Finke Gorge, however, has only a subtle distinction between clast and matrix lithologies; both consist of quartzose sandstone and differ only in textural maturity and cementation history. Hence any contrast in competence of the two sand/sandstone types at the time of brecciation was due to the control exerted by textural maturity on cementation.

3. Brecciation occurred *in situ* and involved minimal horizontal and vertical displacements. Individual beds of white sandstone can be traced from the enclosing sandstone sequence into disrupted beds, isolated slabs, rotated blocks and finally scattered clasts. Furthermore, the enclosing sandstone sequence is not disturbed above or below the individual breccia lenses or the whole breccia horizon. Hence the horizontal translation of material evident in 'mass-flow' deposits (typically downslope over considerable distances) did not occur during the formation of this breccia.

4. Brecciation apparently did not occur at or near the sedimentation surface, but rather occurred at a considerable depth in a sedimentary pile. The white sandstone composing the clasts of the breccia was cemented (lithified) and strained prior to disruption and, as indicated by the parallelism of strain lamellae and bedding traces, this straining resulted from vertical compression, i.e. lithostatic loading.

5. The distribution of the breccia is locally controlled by, and many clasts are bounded by, joint surfaces. Again this implies that the white sandstone was competent prior to disruption, and fragmentation was in part controlled by joint patterns developed in the white sandstone.

Conclusion

An *in situ* disruption of a buried interlayered sand/sandstone sequence is indicated for the breccia; a disruption caused by quasi-liquid deformation of the brown sand layers. The process envisaged is similar to that of the forceful injection of clastic sandstone dykes. The following model is proposed for the genesis of the breccia.

(a) White and brown sands were deposited under alternating conditions of depositional environment and/or source material, so that a sequence of interbedded mature and immature quartz sands resulted.

(b) Initial shallow burial of the sediments was accompanied by selective diagenetic quartz cementation of the highly permeable white sands by the circulation of siliceous groundwaters, whilst the less permeable immature brown sands retained a largely cohesionless state.

(c) Lithostatic loading and compaction of the sedimentary sequence resulted in the straining of the now competent white sandstone beds.

(d) The interlayered competent/incompetent sequence was inherently unstable and eventually failed. The mechanism which triggered this failure is not known. The

incompetent brown sands suffered a complete loss of cohesion and failed by a grain-by-grain flow, whilst the competent white sandstone beds failed in a brittle manner and broke into rectangular joint blocks. Rotation and translation of these blocks in the mobile matrix resulted in further fracture and diminution of the white sandstone to form clasts ranging in size from 1 m slabs to individual grains.

(e) Late-state cementation by iron oxide selectively occurred in the previously uncemented matrix sandstone.

The ability of the brown sands to fail in a quasi-liquid manner at such an advanced stage in the burial history of the sediments is poorly understood, but it is suggested that pore-water content may have played an important role. Pore waters would be expected to be a significant component of the porous immature sands and, due to lack of permeability and to capping by the impermeable cemented white sandstones, the water could not escape as overburden pressures increased with burial. Pore-water pressure may have finally approached hydrostatic pressures, destroying grain cohesion. Expanding-lattice clay minerals, capable of assisting failure by expulsion of interlayered water (Powers, 1967) were not detected in the breccia matrix by XRD techniques.

Acknowledgements

I wish to thank A. T. Wells for helpful discussions during field observations and throughout the study, and Dr K A. W. Crook for many useful suggestions. I am grateful to Drs A. R. Jensen, N. F. Exon and G. E. Wilford for their comments and criticism of the manuscript.

References

ABBATE, E., BORTOLOTTI, V., & PASSERINI, P., 1970—Olistostromes and olistoliths. *Sedimentary Geology*, **4**, 521-557.

CHALLINOR, J., 1967—A DICTIONARY OF GEOLOGY. 3rd edition. *Oxford University Press.*

DOTT, R. H., 1963—Dynamics of subaqueous gravity depositional processes. *Bulletin of the American Association of Petroleum Geologists*, **47**, 104-128.

ELLIOT, R. E., 1965—A classification of subaqueous sedimentary structures based on rheological and kinematical parameters. *Sedimentology*, **5**, 193-209.

GARY, Margaret, MCAFEE, R. (Jr), WOLF, C. L. (Editors), 1972—GLOSSARY OF GEOLOGY. *American Geological Institute, Washington, D.C.*

HAMPTON, M. A., 1972—The role of subaqueous debris flows in generating turbidity currents. *Journal of Sedimentary Petrology*, **42**, 775-793.

LEITCH, E. C., 1969—Mass-movement phenomena in an Upper Carboniferous greywacke-argillite sequence in north-east N.S.W. *New Zealand Journal of Geology and Geophysics*, **12**, 156-171.

MADIGAN, C. T., 1932—The geology of the Western MacDonnell Ranges, Central Australia. *Quarterly Journal of the Geological Society of London*, **88**, 672-711.

MAWSON, D., & MADIGAN, C. T., 1930—Pre-Ordovician rocks of the MacDonnell Ranges (Central Australia). *Quarterly Journal of the Geological Society of London*, **86**, 415-429.

MIDDLETON, G. V., & HAMPTON, M. A., 1973—Sediment gravity flows: mechanics of flow and deposition; *in* Middleton G. V., & Bouma, A. H. (Editors), TURBIDITES AND DEEP-WATER SEDIMENTATION. *Pacific Section SEPM, Los Angeles, California*, 1-38.

POWERS, M. C., 1967—Fluid release mechanisms in compacting marine mudrocks and their importance in oil exploration. *Bulletin of the American Association of Petroleum Geologists*, **51**, 1240-1254.

PRICHARD, C. E., & QUINLAN, T., 1962—The geology of the southern half of the Hermannsburg 1:250 000 Sheet. *Bureau of Mineral Resources, Australia—Report* **61.**

RANFORD, L. C., COOK, P. J., & WELLS, A. T., 1965—The geology of the central part of the Amadeus Basin, Northern Territory. *Bureau of Mineral Resources, Australia—Report* **86.**

WELLS, A. T., FORMAN, D. J., RANFORD, L. C., & COOK, P. J., 1970—Geology of the Amadeus Basin, Central Australia. *Bureau of Mineral Resources, Australia—Bulletin* **100.**

BMR Journal of Australian Geology & Geophysics, 1 (1976), 350-352

Gravity provinces and their nomenclature

A. R. Fraser

Gravity features have been defined and named by the various authors who have interpreted the results of land and marine reconnaissance gravity surveys in Australia. In general, two classes of feature have been identified—gravity provinces and gravity units. A gravity province is a region where the gravity field is characterized by uniformity of some property, such as contour trend, gravity level, or degree of contour disturbance, which distinguishes it from neighbouring provinces. A gravity unit is a subdivision of a province. Neighbouring units are again distinguished from each other by differences in contour trend, gravity level, or degree of contour disturbance—but on a smaller scale.

Many gravity features were originally defined from the results of individual reconnaissance surveys in isolated areas and have been shown to be inconsistent with the regional gravity pattern after more extensive coverage has been obtained. Land and marine gravity coverage is now virtually complete, and an attempt has now been made to rationalize gravity province boundaries and names over the whole of Australia and its continental margins. In all, 125 provinces have been defined and named. It is recommended that authors make use of the names when discussing regional gravity features.

Introduction

As a first step towards analysing and interpreting contoured gravity data, it is often convenient to divide the contour pattern into discrete regions of differing gravity characteristics. This helps to clarify the overall contour pattern and emphasize significant but less obvious features of the gravity field. It also simplifies the task of describing gravity features, their inter-relationship, and their correlations with geological or tectonic elements.

The method has been used consistently by the several authors who have contributed to the interpretation and reporting of the results of reconnaissance gravity surveys in Australia. In general two classes of feature have been defined and named—gravity provinces, and gravity units. A gravity province is a region where gravity field is characterized by uniformity of at least one property, such as contour trend, gravity level, or degree of contour disturbance, which distinguishes it from neighbouring provinces. A gravity unit is a subdivision of a province. As in provinces, but on a smaller scale, neighbouring units are distinguished from each other by differences in contour trend, gravity level, or degree of contour disturbance.

Gravity nomenclature

The names of gravity features are derived from physiographic features, towns, railway stations, homesteads, geophysical survey vessels and map sheet names, generally in that order of preference. A descriptive term such as high, low, complex, ridge, trough, shelf or platform is included in the name to describe the nature of the gravity feature. The basic form for the name of a gravity province is **proper name 'Regional Gravity' descriptive name,** e.g. Carnarvon Regional Gravity Complex. The basic form for the name of a gravity unit is **proper name 'Gravity' descriptive name,** e.g. Onslow Gravity Low.

Rationalization of gravity provinces

There have been inconsistencies in the way that gravity provinces have been defined. Different authors have used slightly different criteria in drawing boundaries, and many features defined from the results of individual reconnaissance surveys were shown to be inconsistent with the regional gravity pattern when more extensive coverage was obtained. For instance, interpreters studying small areas may have defined 'highs' and 'lows' which later, in a more regional context, were shown to be only local features within a complex or a shelf.

As the gravity coverage was built up, attempts were made to rationalize the province and unit boundaries on a broad scale, to formalize the nomenclature, and to summarize the geological interpretations of gravity features. This has been done by Vale (1965), Darby & Vale (1969) and Fraser, Darby & Vale (in prep.) for gravity coverage on land, and by Symonds & Willcox (1976) for gravity coverage offshore. With reconnaissance gravity coverage of the Australian region now virtually complete, this paper presents a map showing gravity provinces over the whole of Australia and its continental margins (Fig. 1) and lists the names proposed for the provinces (Table 1).

It is recommended that authors make use of province names when discussing regional gravity features.

References

DARBY, F. & VALE, K. R., 1969—Progress of the reconnaissance gravity survey of Australia. *Bureau of Mineral Resources Australia. Record* **1969/110** (unpublished).

FRASER, A. R., DARBY, F., & VALE, K. R., in preparation—A qualitative analysis of the results of the reconnaissance gravity survey of Australia. *Bureau of Mineral Resources Australia. Report* (in press).

SYMONDS, P. A. & WILCOX, J. B., 1976—The gravity field of offshore Australia—a brief description. *BMR Journal of Australian Geology & Geophysics*, **1**

VALE, K. R., 1965—PRogress of the reconnaissance gravity survey of Australia. *Bureau of Mineral Resources, Australia—Record* **1965/197** (unpublished).

1. Naturaliste Regional Gravity Platform
2. Naturaliste Regional Gravity Trough
3. Leeuwin Regional Gravity High
4. Perth Regional Gravity Low
5. Avon Regional Gravity High
6. Porongorup Regional Gravity Low
7. Albany Regional Gravity Ridge
8. Narembeen Regional Gravity Shelf
9. Rason Regional Gravity Low
10. Fraser Regional Gravity Ridge
11. Balladonia Regional Gravity Complex
12. Yeo Regional Gravity Shelf
13. Carey Regional Gravity Complex
14. Austin Regional Gravity Complex
15. Erabiddy Regional Gravity High
16. Geraldton Regional Gravity High
17. Hartog Regional Gravity High
18. Petrel Regional Gravity Trough
19. Wallaby Regional Gravity Complex
20. Cuvier Regional Gravity Complex
21. Exmouth Regional Gravity Ridge
22. Wombat Regional Gravity Complex
23. Montebello Regional Gravity Ridge
24. Carnarvon Regional Gravity Complex
25. Teano Regional Gravity Low
26. Ashburton Regional Gravity Ridge
27. Fortescue Regional Gravity Complex
28. Barrow Regional Gravity Low
29. Anketell Regional Gravity Ridge
30. South Canning Regional Gravity Low
31. Angas Regional Gravity High
32. Pedestal Regional Gravity Low
33. Tanami Regional Gravity Complex
34. Ord Regional Gravity Depression
35. Springvale Regional Gravity Ridge
36. Fitzroy Regional Gravity Complex
37. Munro Regional Gravity Platform
38. Scott Regional Gravity Complex
39. D'artagnan Regional Gravity High
40. Browse Regional Gravity Low
41. Kimberley Regional Gravity Platform
42. Cartier Regional Gravity Shelf
43. Timor Regional Gravity Low
44. Sahul Bank Regional Gravity Ridge
45. Bonaparte Regional Gravity Complex
46. West Arafura Regional Gravity Platform
47. Wangites Regional Gravity Ridge
48. Mary Regional Gravity Shelf
49. Oenpelli Regional Gravity Complex
50. Arnhem Regional Gravity Platform
51. Elcho Regional Gravity High
52. Dunmara Regional Gravity Low
53. Tipperary Regional Gravity Low
54. Victoria Regional Gravity Shelf
55. Buchanan Regional Gravity Platform
56. Pellew Regional Gravity High
57. McArthur Regional Gravity Shelf
58. Georgina Regional Gravity Shelf
59. Lander Regional Gravity Low
60. Willowra Regional Gravity Ridge
61. Yuendumu Regional Gravity Low
62. Papunya Regional Gravity Ridge
63. Amadeus Regional Gravity Low
64. Olga Regional Gravity Ridge
65. Petermann Regional Gravity Low
66. Blackstone Regional Gravity Ridge
67. Officer Regional Gravity Low
68. Wanna Regional Gravity Low
69. Eyre Regional Gravity High
70. Nullarbor Regional Gravity Shelf
71. Woorong Regional Gravity Complex
72. Wilgena Regional Gravity Low
73. D'Entrecasteaux Regional Gravity Ridge
74. Ceduna Terrace Regional Gravity Shelf
75. Investigator Regional Gravity Trough
76. Gairdner Regional Gravity High
77. Aroona Regional Gravity Complex
78. Kangaroo Regional Gravity High
79. Hawker Regional Gravity Complex
80. Muloorinna Regional Gravity Ridge
81. Barrier Regional Gravity Ridge
82. Darling Regional Gravity Low
83. Gambier Regional Gravity High
84. Murray Regional Gravity Complex
85. Melbourne Regional Gravity High
86. West Tasmanian Regional Gravity Ridge
87. Eltanin Regional Gravity Trough
88. Bass Regional Gravity Platform
89. Mersey Regional Gravity Complex
90. East Tasmanian Regional Gravity Ridge
91. Cascade Regional Gravity High
92. LaTrobe Regional Gravity Low
93. Lachlan Regional Gravity Complex
94. Namoi Regional Gravity Ridge
95. New England Regional Gravity Low
96. Gladstone-Eden Regional Gravity Ridge
97. Hamme Regional Gravity Trough
98. Tasmantid Regional Gravity Ridge
99. Dampier Regional Gravity Complex
100. Lord Howe Regional Gravity Ridge
101. Coral Sea Regional Gravity High
102. Moresby Regional Gravity Trough
103. Papuan Regional Gravity Complex
104. Willis Regional Gravity Platform
105. Barrier Regional Gravity Trough
106. Swain Regional Gravity Platform
107. Coastal Regional Gravity Complex
108. Bourke Regional Gravity High
109. Diamantina Regional Gravity Shelf
110. Illogwa Regional Gravity High
111. Cloncurry Regional Gravity High
112. Thompson Regional Gravity Low
113. Nebine Regional Gravity High
114. Roma Regional Gravity Low
115. Bowen Regional Gravity Low
116. Anakie Regional Gravity Ridge
117. Muttaburra Regional Gravity Ridge
118. Flinders Regional Gravity Low
119. Burdekin Regional Gravity Shelf
120. Cape York Regional Gravity High
121. Atherton Regional Gravity Low
122. Carpentaria Regional Gravity Platform
123. Mornington Regional Gravity High
124. Mitchell River Regional Gravity Complex
125. Weipa Regional Gravity Shelf

Table 1. Names of Gravity Provinces

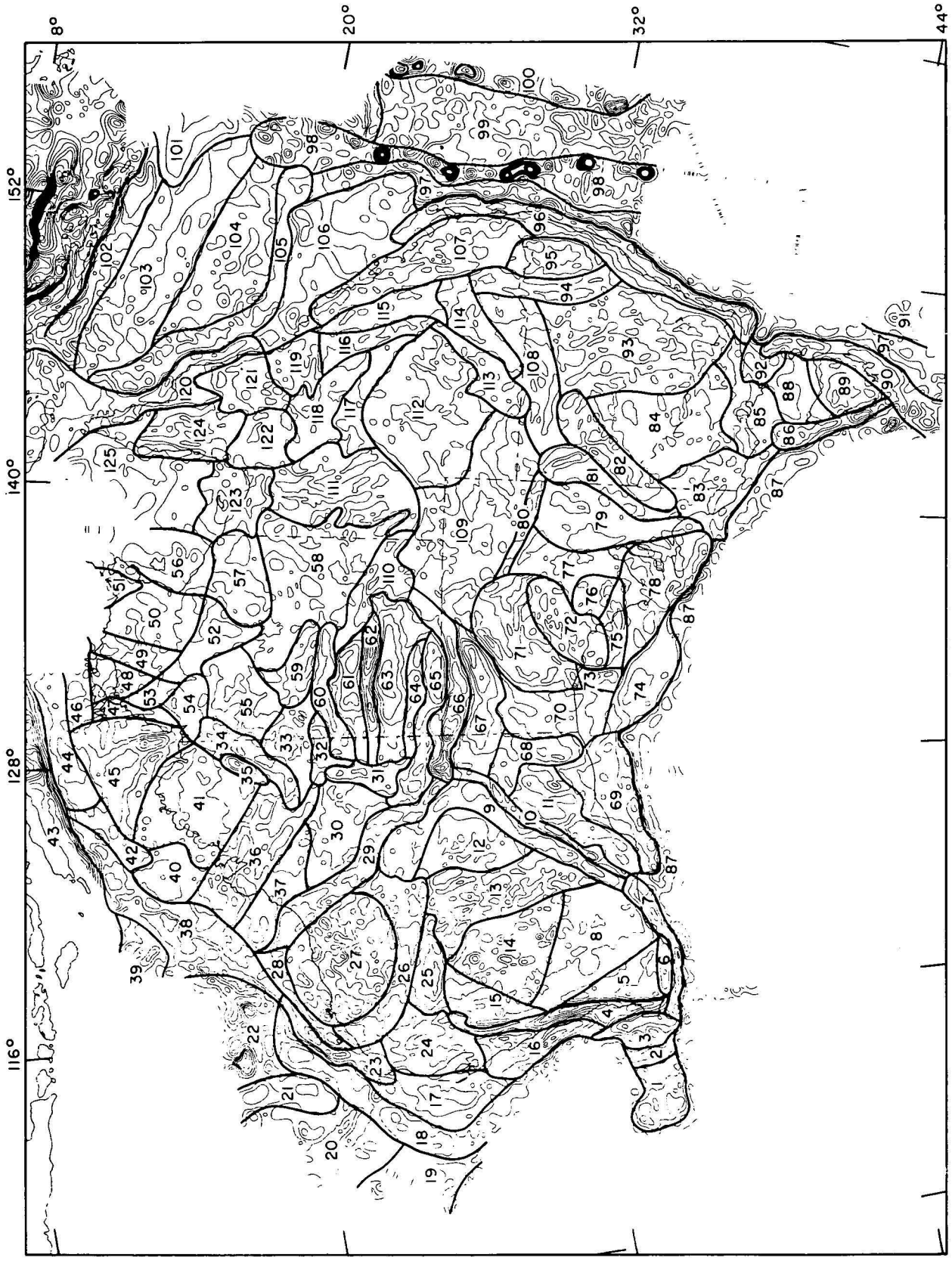

Figure 1. Gravity provinces on and around Australia.

BMR Symposium

These annual symposia stress work of relevance to industry. The Sixth Symposium will be held in Canberra in the Academy of Science Building on 3 and 4 May 1977. The program and registration form will be available from February 1977. Write to Director, (Attention Mrs E. Young), Bureau of Mineral Resources, P.O. Box 378, Canberra City, ACT 2601; or phone (062) 49 9615.

Crespin Commemorative Volume

Dr Irene Crespin has been associated with the Commonwealth Government since 1927. She joined BMR when it was founded in 1946. To mark her 80th birthday BMR will produce a commemorative volume, in bulletin form. The bulletin is compiled by D. J. Belford, and contains the following papers.

N. de B. Hornibrook
Late Cretaceous Forminifera from sediments associated with the Tangihua Volcanics, Northland, New Zealand.

J. W. Pickett
Conodont faunas from the Mt. Frome Limestone, near Mudgee, N.S.W.

J. M. Dickins
Relationship of *Mourlonia* and *Ptychompalina*, Upper Palaeozoic Gasteropoda.

A. N. Carter
Foraminifera from the Mitchellian Stage.

M. F. Glaessner
The oldest Foraminifera.

B. McGowran
Early Tertiary foraminiferal biostratigraphy in southern Australia progress report.

R. O. Brunnschweiler
Notes on the geology of eastern Timor.

P. J. Coleman
Reflections on outer Melanesian Tertiary larger Foraminifera.

E. C. Druce
Correlation of the Cambrian-Ordovician boundary in Australia.

E. M. Kemp
Microfossils of fungal origin from Tertiary sediments on the Ninetyeast Ridge, Indian Ocean.

D. J. Belford
The genus *Triplasia* (Foraminiferida) from the Miocene of Papua New Guinea.

P. G. Quilty
The Late Cretaceous—Tertiary section in Challenger No. 1 (Perth Basin): Details and implications.

R. W. Day
Onestia McLearn, an aberrant cardiacean bivalve from the Lower Cretaceous of Australia and Canada.

V. Scheibner
Some Cretaceous Foraminifera from Leg 26 of the DSDP in the Indian Ocean.

S. Shafik
Paleocene and Eocene Nannofossils from the Kings Park Formation, Perth Basin, Western Australia.

Contents

Notes

Centre pages

Free-air anomaly and gravity maps of Australia—in colour, 1:25,000,000

BMR Journal of Australian Geology & Geophysics Volume 1, (4)